GEOCHEMICAL AND PETROLOGICAL STUDIES OF SUPRACRUSTAL ROCKS OF BASTER CRATON AND ITS IMPLICATIONS TO CRUSTAL EVOLUTION

ABSTRACT
OF THE
THESIS
SUBMITTED FOR THE AWARD OF THE DEGREE OF
Doctor of Philosophy
IN
GEOLOGY

BY

HAMIDULLAH WANI

DEPARTMENT OF GEOLOGY
ALIGARH MUSLIM UNIVERSITY
ALIGARH (INDIA)

2008

GEOCHEMICAL AND PETROLOGICAL STUDIES OF SUPRACRUSTAL ROCKS OF BASTER CRATON AND ITS IMPLICATIONS TO CRUSTAL EVOLUTION

ABSTRACT

The Central Indian shield is a collage of two cratonic blocks, the northerly lying Bundlekhand block and the southerly lying Bastar block separated by Narmada-Son lineament or Central Indian Tectonic Zone (CITZ) running nearly east-west. The Bastar craton which is considered to be of Archean age contains granitoids and gneisses. These granitoids and gneisses form the basement for the Proterozoic supracrustal rocks. The supracrustal rocks of the Bastar craton can be conveniently divided into Older (Archean - Paleoproterozoic) supracrustals and Younger (Neoproterozoic) supracrustals. The Older supracrustals (Archean – Paleoproterozoic) are highly deformed and metamorphosed, while the younger supracrustals (Neoproterozoic) of the Bastar craton are undeformed and unmetamorphosed.

The Bastar craton consists of three major Archean - Paleoproterozoic and three Paleoproterozoic supracrustal groups. The Archean - Paleoproterozoic supracrustal groups are (i) the Bailadila Group, (ii) the Bengpal Group and (iii) the Sukma Group in the southern part of the craton, and Paleoproterozoic supracrustal groups are (i) the Sakoli Group, (ii) the Dongargarh Supergroup and (iii) the Sausar Group in the northern part of the craton. The younger supracrustal rocks occur in two major Neoproterozoic basins namely (1) the Chhattisgarh basin and (2) the Indravati basin (Bastar basin) within the Bastar craton.

Among these supracrustal rocks, the Paleoproterozoic metasedimentary rocks (metapelite, quartzite) of the Sakoli basin and the Sausar basin, and Neoproterozoic

unmetamorphosed sedimentary rocks (shale, sandstone) of the Chhattisgarh basin and the Indravati basin have been included in the present study.

The Sakoli Group is composed of supracrustal rocks including mostly metapelite and quartzite with basalt and rhyolite. The Sausar Group comprises of quartzite, pelite and carbonate associations containing stratiform manganese deposits which form the largest manganese reserves in India.

The Chhattisgarh and Indravati basins are two major intra-cratonic sedimentary basins of the Bastar craton containing the Neoproterozoic sediments. The basins are similar in their mixed siliclastic - carbonate lithology, absence of metamorphic overprinting and very low tectonic disturbance. The Chhattisgarh and Indravati basins consist of unmetamorphosed conglomerate, sandstone, shale, limestone, chert and dolomite. Origin of both the Paleoproterozoic and the Neoproterozoic cratonic basins, however, is still poorly constrained, though a riftogenic or intra-cratonic origin has been invoked for them.

Occurrence of rock formations in the Bastar craton ranging in age from the Paleoproterozoic to the Neoproterozoic make this region a unique terrain where geological processes operated for a long geological period which is most suited to understand the Proterozoic crustal evolution. The emphasis of the present work is to carry out petrological and geochemical studies of the Neoproterozoic rocks of the Chhattisgarh and Indravati basins of the Bastar craton to know the paleoweathering, source rock composition and tectonic setting. Geochemical studies of Paleoproterozoic metasedimentary rocks of the Sakoli and Sausar basins of the Bastar craton have also been carried out for comparison to know whether there was any change in paleoweathering, source rock composition and tectonic setting through the Proterozoic time in the Bastar craton.

Petrography of sandstones and geochemical studies of terrigenous sediments have long been used to determine the compositions of the provenance, to evaluate weathering processes and paleoclimate, to qualify the secondary processes such as hydraulic sorting, to model the tectonic setting of the basin and finally to trace the evolutionary history of mantle and crust.

In the absence of available geochemical data of the clastic rocks of the Bastar craton, comparison of the data have been made against the available geochemical data of North American Shale Composite (NASC), Upper Continental Crust (UCC), granite and gneiss of Bastar craton, mafic volcanic rocks of Bastar craton and Paleoproterzoic Kaapvaal pelites of the Kaapvaal craton whish share many common conditions with the Paleoproterozoic supracrustals of the Bastar craton.

Petrographic study reveals that the main framework grains of the Paleoproterozoic Sakoli and Sausar pelites are quartz, chlorite, muscovite, biotite, garnet and opaques. The Sakoli and Sausar quartzites are composed of quartz, muscovite, biotite and opaques. The mineralogy of pelites, quartzites and shales has been of less use than the mineralogy of sandstones in determining the provenance since many minerals in such rocks are formed during weathering, diagenesis and metamorphism. Keeping the above consideration in mind, only the Neoproterozoic sandstones of the Chhattisgarh basin and the Indravati basin have been investigated in detail in order to trace out their provenance and tectonic setting.

Modal analysis of the sandstones reveals that the main detrital framework mineral grains of the Chandarpur Group of the Chhattisgarh basin and the Tiratgarh Formation of the Indravati basin include quartz, potash feldspar, plagioclase, rock fragments (mainly chert), micas and heavy minerals. Sandstones of the Chandarpur Group and the Tiratgarh Formation of the Indravati Group are characterized by abundant quartz grains (82.22 % and 88.16 % on average, respectively). According to Folk's classification (Folk, 1980), the sandstones of the Chandarpur Group and the Tiratgarh Formation are mostly subarkoses, sublitharenites and quartzarenite. Quartz occurs mainly as monocrystalline quartz. Some of these have undulatory extinction. Polycrystalline quartz represented by recrystallized and stretched metamorphic quartz occurs in subordinate proportions. In majority of polycrystalline grains, subgrains with both straight and sutured contacts are common. Feldspar constitutes 1.87 % and 2.02 % on average of the framework grains of the Chandarpur Group and the Tiratgarh Formation respectively, and is dominated by microcline. However, plagioclase is also present in minor quantities in some samples. Rock fragments are very few and are dominated by sedimentary lithics (mainly chert). Heavy minerals are rare and are dominated by zircon. These sandstones are generally matrix free. Authigenic quartz, iron oxide and calcite are dominantly cementing material. Quartz cement occurs primarily as overgrowth around detrital grains.

On average, compositions of the Chandarpur Group become more mature in the Kansapathar Formation. The proportion of framework quartz increases from Lohardih Formation (Lower Formation of the Chandarpur Group) to the Kansapathar Formation (Upper Formation of the Chandarpur Group) stratigraphically at the expense of less robust constituents. The chemical data show that SiO_2 increases through time and all major oxides decreases progressively. The variation in modal abundances and the concentrations of CaO, Na_2O and K_2O indicate that alkalis are mainly controlled by the abundance and composition of feldspars. The sandstones are mature because of their low feldspar and negligible lithic fragment content.

Under microscope, the Neoproterozoic shales of the Chhattisgarh basin and the Indravati basin of the Bastar craton display compositional variation from that of typical shale to calcite rich shale. This is best depicted by the abundance of CaO in these shales. Therefore, this allows separation of shale samples into the calcareous shales (the Gunderdehi Formation of the Chhattisgarh basin) at >6 % CaO and the non-calcareous shales (the Tarenga Formation of the Chhattisgarh basin and the Jagdalpur Formation of the Indravati basin) at < 0.3 % CaO.

In comparison to NASC (North American Shale Composite), the non-calcareous shales show enrichment in $Fe_2O_3^t$ and K_2O while the calcareous shales show enrichment in CaO and MnO. The non-calcareous shales contain higher concentrations of the most major and trace elements (including REEs) compared to the calcareous shales. The exceptions are CaO, MnO, Sr and Br concentrations as they are higher in the calcareous shales compared to the non-calcareous shales. Plots of transition elements (Sc, V, Ni, Cr), LILEs and HFSEs (Cs, Nb, U and Zr) vs. Al_2O_3 and K_2O yield linear plots for both the calcareous and the non-calcareous shales. This may suggest that these elements in the calcareous and the non-calcareous shales are housed in the clay minerals. Sr correlates positively with CaO but not with Al_2O_3 or K_2O, thus indicating that Sr are housed in calcite rather than in clay minerals. However, elements like Ba, Y and Ta do not show linear trend against Al_2O_3 and K_2O indicating some accessory minerals other than clay minerals (e.g. allanite for Y and barite for Ba) controlling their abundance.

In contrast, the Paleoproterozoic pelites are characterized by lower SiO_2 (59 %) and higher $Fe_2O_3^t$ + MgO (10.41 %) compared to the non-calcareous shales (8.6 %) and NASC. Immobile elements like TiO_2 (0.75 %), Al_2O_3 (22.02 %) and $Fe_2O_3^t$ (8.62 %) are enriched in the pelites compared to the non-calcareous shales, calcareous shales and NASC. Mobile elements like Na_2O (0.5 % for the pelites and 0.2 % for the non-calcareous shales) and CaO (0.25 % for the pelites and 0.1 % for the non-calcareous shales) are strongly depleted in the pelites and the non-calcareous shales compared to NASC.

Relative to the Neoproterozoic calcareous and the non-calcareous shales, the Paleoproterozoic pelites are highly enriched in all transition elements especially in Cr (189 ppm), Ni (58 ppm), Sc (21 ppm) and V (100 ppm). In the pelites transition elements like Ni and Co show good positive correlation with Al_2O_3 or K_2O while Cr and Sc do not correlate with Al_2O_3 and K_2O. Most of the LILE and HFSE (e.g. Th, U, Rb, Sr) in pelites show good positive correlation against Al_2O_3 and K_2O indicating mica minerals (phyllosilicate) control on their contents.

In chondrite normalized REE plot (Sun and Mc Donough, 1989), both the calcareous and the non-calcareous shales show highly fractionated patterns with LREE enrichment having (La/Yb)n ratio of 18 for non-calcareous shales and 7 for the calcareous shales, flat HREE with (Gd/Yb)n ratio of 1.9 for the non-calcareous shales and 1.4 for the calcareous shales, and negative Eu anomaly (0.65 for the non- calcareous shales and 0.8 for the calcareous shales). The chondrite normalized LREE pattern of the pelite Sample No. DS-524 is also fractionated but less fractionated than that of the non-calcareous and calcareous shales with LREE enrichment having (La/Yb)n of 8.86 and flat HREE with (Gd/Yb)n of 1.83 and small negative Eu anomally (Eu/Eu* = 0.80).

The major element composition of the sandstones of all the three formations of the Chandarpur Group does not show much variation. In general the SiO_2 concentration is high (avg. 92.96 wt. %) in all the sandstones of the Chandarpur Group and the Tiratgarh Formation. On the sandstone classification schemes of the Heron (1988) and Pettijohn et al. (1972), the sandstones are mostly sublitharenite, subarkose and arenite.

Realtive to NASC, the sandstones and quartzites are depleted in major, trace elements including REE except for SiO_2, Na_2O, Co and Zr. Relative to the sandstones, quartzites have higher concentration of Al_2O_3, Na_2O and K_2O, Cr and Co. The transition elements (like Cr and Co) and the LILEs and HFSEs (like Rb, Cs, Sr, Th, U, Nb, Y and Zr) are higher in quartzites compared to sandstones.

Plots of transition elements (like Sc, Cr, Ni), LILEs and HFSEs (like U, Cs, Th, Rb, Ba and Ta) against Al_2O_3 and K_2O yield linear plots for both the sandstones and quartzites. However elements like Zr, Y, Nb do not show linear trend against Al_2O_3 and K_2O indicating some accessory minerals (e.g. allanite for Y, zircon for Zr) other than feldspar and mica to be controlling their abundance in the sandstones and the quartzites.

In chondrite normalized plot both the sandstones and the quartzites show highly fractionated REE patterns, with LREE enrichment having (La/Yb)n of 12.5 for sandstones and 12 for the quartzites, flat HREE patterns with (Gd/Yb)n of 1.56 for sandstones and 1.42 for the quartzites and a significant negative Eu anomaly (0.67 for the sandstones and 0.47 for the quartzites).

To identify the provenances and tectonic setting, the recalculated parameters of modal data were plotted on standard ternary diagrams given by Dickinson and Suczek

(1979). On the QmFLt, QtFL and QmPK plots, that the sandstone samples from all the three formations of the Chandarpur Group of the Chhattisgarh basin and the Tiratgarh Formation of the Indravati basin plot in the intra-cratonic field. On the SiO_2 vs. K_2O/Na_2O ratio diagram of Roser and Korsch (1986), all the Paleoproterozoic pelite and quartzite samples, and the Neoproterozoic sandstone and non-calcareous shale samples plot exclusively in the passive margin field (PM). The SiO_2/Al_2O_3 vs. K_2O/Na_2O plot of Maynard (1982) for the Paleoproterozoic pelite and quartzite samples, and the Neoproterozoic sandstone, calcareous and non-calcareous shale samples also suggest that the sediments were deposited in passive margin setting (except for the one pelite sample which falls in continental island arc field (CIA).

The geochemical tectonic setting discriminating parameters of Bhatia (1983), $Fe_2O_3^t$ + MgO, TiO_2, Al_2O_3/SiO_2, K_2O/Na_2O and Al_2O_3/ (CaO + Na_2O) of the sandstones and quartzite samples are comparable with that of passive margin (PM). The higher K_2O/Na_2O and Al_2O_3/(CaO+Na_2O) ratios of the non-calcareous shales and the pelite samples are also comparable with passive margin setting (PM).

On the Th - Sc - Zr/10 diagram all the sandstone samples of the Neoproterozoic Chhattisgarh basin and the Indravati basin plot near passive margin while the calcareous and the non-calcareous shale samples of the Chhattisgarh basin and Indravati basin plot near the active continental margin and continental arc fields. The pelite and quartzite samples of the Paleoproterozoic Sakoli and Sausar basins show a lot of scatter between active continental margin (ACM) and continental Island Arc (CIA). The wide scattering of the non-calcareous shale, pelite and quartzite samples between active continental margin and continental arc field on the Th-Sc-Zr/10 plot may be due effect of sorting.

Thus, it is inferred that intra-cratonic tectonic setting existed for both the Paleoproterozoic and the Neoproterozoic basins and in other words suggest stability of the Bastar craton during the Paleoproterozoic and the Neoproterozoic time. This study strengthens the stable intra-cratonic origin of these Paleoproterozoic and Neoproterozoic basins of the Bastar craton.

The enrichment of immobile elements like SiO_2, Al_2O_3, TiO_2, Rb and Ba and depletion of Na_2O, CaO and Sr in the studied samples especially in the Neoproterozoic non-calcareous shales and the Paleoproterozoic pelites suggests moderate to intense chemical weathering. The average CIA values of the Neoproterozoic non-calcareous shales (72.40) and the Paleoproterozoic pelites (79.06) are higher than that of NASC (57.12). Thus, CIA values of the Neoproterozoic non-calcareous shales and the Paleoproterozoic pelites suggest moderate to intense chemical weathering for these rock samples. Such an inference is also supported by the average trend of these sediments on A - CN - K diagram, which is defined by the chlorite and muscovite - illite end members. However, the average CIA values of the Paleoproterozoic quartzites (55.66) and the Neoproterozoic sandstones (67.50) are lower than the Paleoproterozoic pelites and the Neoproterozoic non-calcareous shales. The lower CIA values of the quartzites and sandstones probably do not reflect the general weathering conditions of the source region, but it may be due to sedimentary sorting effect. Moderate to intense chemical weathering of source rocks of the Paleoproterozoic pelites, and the Neoproterozoic non-calcareous shales and sandstones is also indicated by their high average plagioclase index of alteration values (PIA >80).

On the K_2O - $Fe_2O_3^t$ - Al_2O_3 ternary diagram most of the samples plot near NASC and some samples also plot between NASC and residual clays. The samples on this diagram fall along a trend defined by chlorite – illite and muscovite end members. Both the A – CN - K and $Fe_2O_3^t$ - K_2O - Al_2O_3 plots indicate moderate to intense chemical weathering in the provenance. This is further demonstrated by the ratios of K/Rb and Th/U ratios of the Paleoproterozoic pelites and quartzites, and the Neoproterozoic shales (both the non- calcareous shales and calcareous shales) and sandstones of the Bastar craton.

NASC normalized elemental concentrations of Paleoproterozoic pelites and quartzites, and Neoproterozoic shales and sandstones indicate that the sandstones, quartzites and shales (calcareous and non-calcareous shales) of the Bastar craton are depleted in mafic elements like Ni, Cr, Sc, $Fe_2O_3^t$, MgO, and TiO_2 while the

Paleoproterozoic pelites are enriched in mafic elements and show close similarity in these elements with the Paleoproterozoic Kaapvaal pelites of the Kaapvaal craton (derived from mafic source). This comparison indicates that the pelites were derived from a mafic source and the sandstones, quartzites and shales (calcareous and non-calcareous) were derived from a felsic source.

Most of the elemental concentrations of the Neoproterozoic sandstones are lower than those in NASC due to higher quartz content. The elemental concentrations of the Neoproterozoic calcareous shales are also lower than those in NASC due to calcite dilution. But when certain key trace elemental ratios like Eu/Eu*, Th/Sc, La/Sc, Th/Ni, Th/Cr, La/Ni and La/Cr of these quartz rich sandstones and of the calcareous shales have been plotted for quartz rich sandstones against SiO_2 (wt. %) and for the calcareous shales against CaO (wt. %), it is found that these elemental ratios are not much affected in the calcareous shales by calcite dilution and in sandstones by higher quartz content.

Certain key elemental ratios (incompatible/compatible) like Th/Sc, La/Sc, Th/Ni, Th/Cr, La/Ni and La/Cr of sandstones, shales, quartzites and pelite sample were normalized with those of the upper continental crust (UCC). It is observed that all the elemental ratios of the Neoproterozoic sandstones, shales (calcareous and non-calcareous shales) and the Paleoproterozoic quartzites are similar to UCC and show small deviation from UCC, suggesting all these rocks were derived from source similar to UCC. However, the Paleoproterozoic pelite sample show strong depletion in La/Sc, Th/Ni, Th/Cr, La/Ni and La/Cr ratios compared to UCC indicating a less differentiated source than UCC for the pelite.

The Ni-Cr and Th/Sc vs. Sc diagrams further suggest that Paleoproterozoic pelites were derived from mafic source and Neoproterozoic shales and sandstones and the Paleoproterozoic quartzites were derived from felsic source. The felsic sources were identified to be granite and gneiss of the Bastar craton.

The chondrite normalized REE diagram shows that REE patterns of the sandstones, the quartzites and the shales (calcareous and non-calcareous) are highly fractionated and there are no systematic variation in the REE patterns of the sandstones. quartzites and shales (calcareous and non-calcareous). The REE patterns and Eu/Eu* of the calcareous, non-calcareous shales and sandstones are similar to the granite (Eu/Eu* = 0.39) and the gneiss (Eu/Eu* =0.65) of the Bastar craton and do not match with the REE patterns of Archean mafic volcanic rocks of the Bastar craton. This further supports the felsic source for the Neoproterozoic sandstones and shales (calcareous and non-calcareous) of the Bastar craton.

In comparison to NASC, the pelite sample has lower REE abundances, and lower ratios of (La/Yb)n = 8.86 and (Gd/Yb)n = 1.83 and a small negative Eu anomaly (Eu/Eu* = 0.80). The REE pattern of the Paleoproterozoic pelite of the Bastar craton is clearly different from that of the Neoproterozoic sandstones, shales (calcareous and non-calcareous) and the Paleoproterozoic quartzites. The REE pattern of the pelite sample shows less fractionated trend than those of the sandstones, quartzites and shales (non-calcareous and calcareous).

The overall petrological and geochemical evidence indicates that the source rocks for the Neoproterozoic shales (calcareous and non-calcareous shales) and sandstones, and Paleoproterozoic quartzites were felsic in nature and the source rocks have been identified to be granite and gneiss of the Bastar craton. However, the source rocks for the Paleoproterozoic pelites have been identified to be the mafic volcanic rocks of the Bastar craton. The data also show petrological and geochemical similarities between the Neoproterozoic sandstones of the Chandarpur Group of the Chhattisgarh basin and the Tiratgarh Formation of the Indravati basin and thus indicate homogeneity in the source rock composition during the Neoproterozoic time and also indicate that the sediments for the Neoproterozoic Chhattisgarh and Indravati basins have been derived from similar sources i.e. granite and gneiss of the Bastar craton, and minor amount of detritus may have been derived from older sedimentary/metasedimentary successions of the craton which is consistent with petrography and paleocurrent studies. In contrast, the

Paleoproterozoic pelites and quratzites of the Sakoli and Sausar basins suggest heterogeneity in the source area. The Paleoproterozoic pelites of the Sakoli and Sausar Groups are enriched in mafic components while the Paleoproterozoic quartzites from the Sakoli and Sausar Groups are enriched in felsic components. This may be due to hydraulic sorting, as it sorts different source components into different grain size class. Thus, this is advantageous to use both pelites/shales and quartzites/sandstones, so as to delineate all source end members particularly the mafic end members and felsic end members respectively.

Thus, the present study shows that there is strong evidence to suggest a change in the upper crustal composition during Proterozoic in the Bastar craton and also there is ample evidence to suggest that the Paleoproterozoic exposed crust was less differentiated compared to the Neoproterozoic crust. The overall mineralogical and geochemical characteristics i.e. mixing of two end member source compositions exhibited by the Paleoproterozoic pelites (more mafic) and quartzites (felsic) relative to total felsic composition of the Neoptoterozoic shales and sandstones suggest that the composition of the source region of the Paleoproterozoic supracrustal rocks represented a transitional stage from mixed (mafic + felsic) in the Paleoproterozoic to entirely felsic in the Neoproterozoic in the unidirectional evolution of the Proterozoic continental crust of the Bastar craton. However, the geochemical characteristics do not indicate any change in tectonic setting from the Paleoproterozoic Sakoli and Sausar basins and the Neoproterozoic Chhattisgarh and Indravati basins of the Bastar craton. It is inferred that the intra-cratonic tectonic setting existed for both the Paleoproterozoic Sakoli and Sausar basins and the Neoproterozoic Chhattisgarh and Indravati basins and in other words suggest stability of the Bastar craton during the Paleoproterozoic and Neoproterozoic time. This study also strengthens the stable intra-cratonic origin of these Paleoproterozoic and Neoproterozoic basins of the Bastar craton using the petrology and geochemistry of the Paleproterozoic and the Neoproterozoic supracrustal rocks of the Bastar craton. The relationship among alkali and alkaline earth elements, CIA, PIA, Th/U and K/Rb ratios indicate that source area in the Bastar craton during the Proterozoic was affected by moderate to intense weathering history.

GEOCHEMICAL AND PETROLOGICAL STUDIES OF SUPRACRUSTAL ROCKS OF BASTER CRATON AND ITS IMPLICATIONS TO CRUSTAL EVOLUTION

THESIS

SUBMITTED FOR THE AWARD OF THE DEGREE OF

Doctor of Philosophy

IN

GEOLOGY

BY

HAMIDULLAH WANI

DEPARTMENT OF GEOLOGY
ALIGARH MUSLIM UNIVERSITY
ALIGARH (INDIA)

2008

DEPARTMENT OF GEOLOGY
ALIGARH MUSLIM UNIVERSITY
ALIGARH–202002

Telefax : (0571) 2700615
Internal : 3401
Fax AMU: +91-571-2700528

Ref. No. ....

Dated 18-11-08

CERTIFICATE

This is to certify that the work presented in this thesis, entitled **"Geochemical and Petrological Studies of supracrustal rocks of Baster Craton and its implications to crustal evolution"** has been carried out and completed by Mr. Hamidullah Wani under my supervision at the Department of Geology, Aligarh Muslim University, Aligarh. The research work presented here has not been submitted for any other degree at this or any other University.

I recommend that Mr. Hamidullah Wani be allowed to submit the thesis for the award of the degree of **Doctor of Philosophy** in **Geology** of the Aligarh Muslim University, Aligarh.

Dr. M. E. A. Mondal
Supervisor

ACKNOWLEDGEMENTS

First of all I would like to thank Almighty for bestowing me his kind blessings.

A special word of thanks goes to my supervisor Dr. M.E.A. Mondal who gave me the opportunity to be a Ph.D student of the Department of Geology, Aligarh Muslim University and to work and explore the problem of crustal evolution in my own country and also to enjoy the opportunity to live and experience the education of Aligarh Muslim University. My sincere thanks goes to him for trusting me, for intellectual support, for patience and for many pieces of advice from time to time. I also thank him for forcing me to be a researcher. I will always appreciate that. Thanks also for the enthusiasm and interest shown in my work. I appreciate his encouragement not to be afraid of any new challenge I may have in my future career.

I wish to thank the Chairman, Department of Geology, Aligarh Muslim University, Aligarh for providing the facilities during the period of this work.

I am thankful to Prof. M. Raza, Department of Geology for discussion and to Dr. A. H. M. Ahmad, Reader, providing me petrographic facilities in his sedimentary laboratory. Fruitful discussions with Dr M. Masroor Alam, Dr. S. H. Alvi, Dr. R. Umar, Dr. M. S. Khan, Dr. S. A. Rashid and Dr. Abdullah Khan are thankfully acknowledged.

Gratitude is expressed to Mr. R. Husain and Mr. Abdulli for preparing the thin sections and Dr. S. Ahmad for extending the geochemical laboratory facilities.

I wish to thank Department of Higher Education, J & K for the approval of leave to complete the work. Thanks are also due to Dr. T A Kawoos, Principal, Amar Singh College, Srinagar, for his supportive role granting me leave to complete the work. Thanks are also due to Dr. M. S. Bhat, Dr. A. M. Dar, Mr. Salim, Mr. K. A. Baba of A. S. College, for their encouragement and support at various stages during the study.

Special words of thanks go my M.Sc. classmates Aijaz, Shamim, R. A. Dar. A.H. Bhat and Abdullah. Dr. Faisal, Adnan, Waleed and Iyad for their love and affection.

I want to thank all my colleagues at the Department of geology at A.M.U especially Dr. Faroque, Salam Ranjeeta Devi and Ayaz for their support and friendship. I also want to thank all my friends especially Manzoor Ghatoo, Ashaq, Gulzar, Idris and Yaseen for their support. I also want to thank all my juniors Khanday, Akhtar, Bilal, Zahoor, Zubair, Shameem, Imran, Adil, Sajjad, Abiro, Fakhre and sajad for their cooperation and support to carry out my thesis.

My sincere thanks are due to Prof. M. W. Y. Khan, Head, School of Studies in Geology, Pt. R. S. University, Raipur for his logistic support and valuable discussion during the field survey.

The financial assistance received from the Scientific and Industrial Research Council of India (CSIR) in the form of JRF/NET Fellowship is gratefully acknowledged.

I wish to express sincere thanks to the Director, Wadia Institute of Himalayan Geology, Dehra Dun and Dr. N.K. Saini of Wadia Institute of Himalayan Geology for providing lab facilities during chemical analysis. I also want to thank Director NGRI and Dr. V. Balaram, Scientist-G of NGRI for providing lab facilities during chemical analysis.

Especial thanks are due to my sister Maqsooda, and my brother Dr. Shafi and my sister in law Sumaira for their constant encouragement and support while carrying out this work.

Last but not least I want to express my gratitude to my parents who always supported me. I thank them for the patience and the love that they always showered on me. **I dedicate this effort to them**.

Hamidullah Wani

CONTENTS

LIST OF FIGURES

Fig. No. **Page**

LIST OF TABLES

Chapter-I

INTRODUCTION

1. INTRODUCTION

Following cratonization of crystalline Archean crust, the Indian shield underwent diverse processes of tectonics, basin formation and crustal evolution during the prolonged span of 2000 Ma ranging from Paleoproterozoic to Neoproterozoic. The Proterozoic, standing midway between the Archean and Phanerozoic is of great significance in the evolution of the earth. By the dawn of this great eon the greater part of the continental crust of India had formed. The tremendous outbursts of volcanic and plutonic activity of the Archean had come to an end and were followed by a period of crustal deformation and thickening on a grand scale resulting in granulite grade metamorphism at depth and potash-rich granite magmatism at upper crustal levels. By Mesoproterozoic, the Indian shield, made up of the Archean granite - greenstone terrain and the more deeply buried crust of the granulite terrain had got welded to form a stable crust of continental dimensions. In India eight major suspect terranes are identified and delineated by Radhakrishna (1989), which were brought into juxtaposition and coalesced during different periods of earth history and formed the Indian continent. These are (i) Northern Bundelkhand Block (ii) Chotanagpur terrane (iii) Fold belts of Central India and Aravalli (iv) Marwar terrane (v) Eastern Ghat Mobile belt (vi) Himalayan Fold belt (vii) Gneiss - granulite belts of Tamilnadu and (viii) Southern Peninsular Block.

The peninsular India preserves an extensive record of Proterozoic successions which display extreme heterogeneity in stratigraphy, sedimentation pattern, metamorphism, deformation and magmatism. Radiometric age data from the mobile belt successions indicate that the history of deformed metasedimentary and metavolcanic successions with multiple episodes of deformation, metamorphism and magmatism extends mainly between 2500 - 1500 Ma, though events reflecting crustal perturbations in the peninsular India extended up to 1000 Ma and even up to Proterozoic – Phanerozoic boundary. Not withstanding the above, there is evidence of development of cratonic basins during the period between 1700 – 700 Ma on different Paleoproterozoic and Archean basements. The dominance of the orthoquartzite - shale - carbonate sequence indicates their generation on stable continental margins or within intracratonic basins (Condie, 1982). The basal groups of these basins can be classified as 'Assemblage II' of Condie (1982). This suggests that the early history of these basins involved lithospheric continental rifting with or without mantle activation. The basic igneous activity within these sequences and the Paleoproterozoic - Mesoproterozoic intrusions in their basements (Drury, 1984; Reddy and Ramakrishna, 1988) testify similar thermal activity in the crust associated with the development of these basins. Possibly, the Late Archean – Paleoproterozoic granitization event in the Peninsular shield (Radhakrishna and Ramakrishnan, 1988; Rao, 1985) also have contributed to the generation of these supracrustal intracratonic basins as has been postulated by Klein and Hsui (1987). Therefore, Precambrian supracrustal sequences are important for understanding the origin and evolution of the continental crust.

The Central Indian shield is a collage of two cratonic blocks, the northerly lying Bundlekhand block and the southerly lying Bastar block separated by Narmada-Son lineament or Central Indian Tectonic Zone (CITZ) running nearly east-west. The Bastar craton is bounded at the periphery by Mahanadi graben in the northeast, Godavari graben in the southwest, Satpura mobile belts in the north-northwest and Eastern Ghat mobile belts in the southeast (Fig. 1). The craton encompasses an area of about 215000 km^2

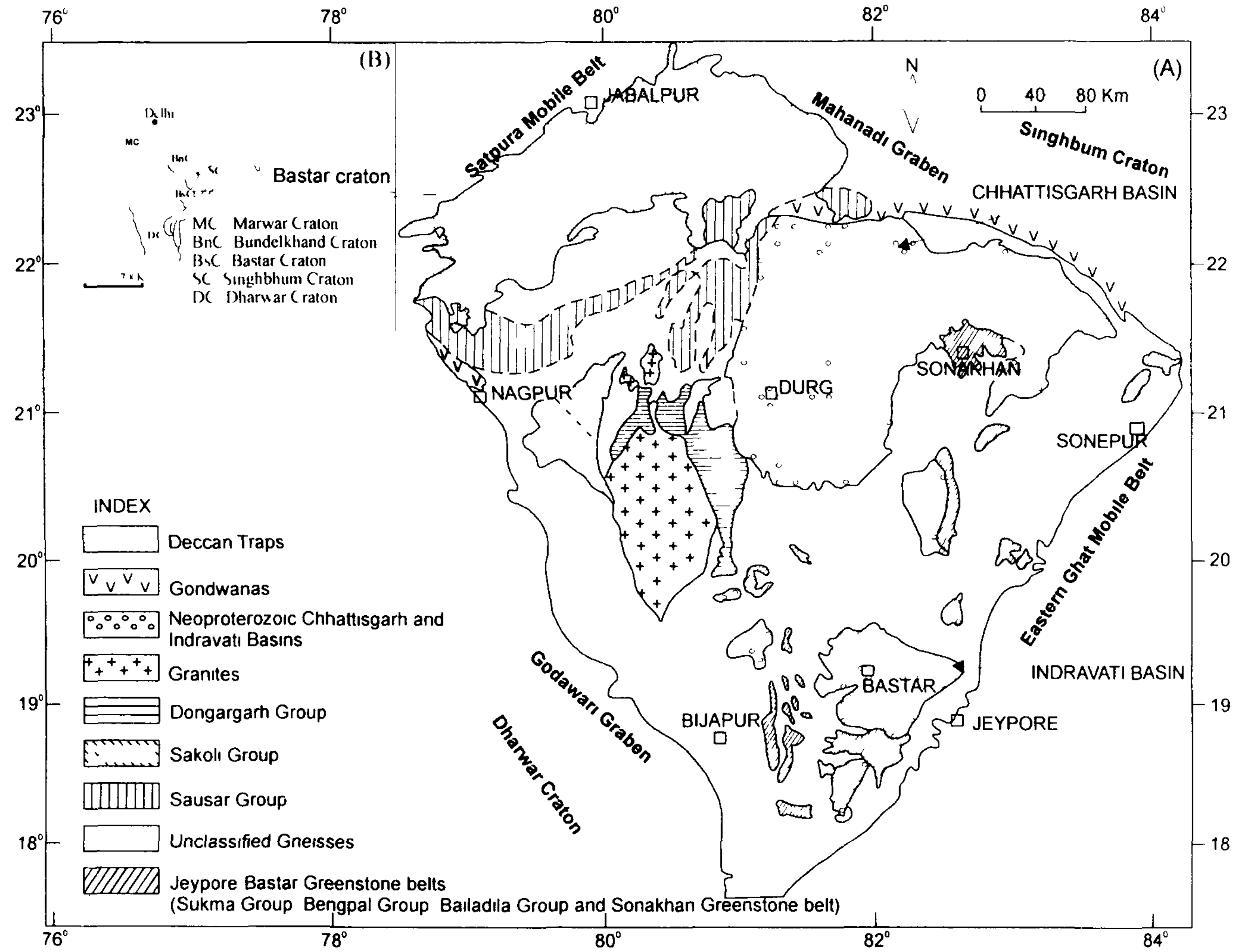

Fig. 1. (A) Geological map of the Bastar craton, Central Indian Shield showing locations of different Archean -Paleoproterozoic and Neoproterozoic sedimentary basins (Ramakrishnan, 1990), (B) Inset: Simplified Geological map of India showing major Archean cratons including Bastar craton (Radhakrishnan and Naqvi, 1986).

covering parts of Chhattisgarh, Madhya Pradesh, Maharashtra and Orissa in the Central India. Gneisses, granitoids, Proterozoic supracrustals (Paleoproterozoic and Neoproterozoic supracrustals) and basic intrusives make up the geology of the craton (Crookshank, 1963; Naqvi and Rogers, 1987; Prasad, 1990; Ramakrishnan, 1990). The granitoids and gneisses form the basement for the supracrustal rocks (Crookshank, 1963; Naqvi and Rogers, 1987; Prasad, 1990; Ramakrishnan, 1990). The supracrustal rocks of the Bastar craton can be conveniently divided into Older (Archean - Paleoproterozoic) supracrustals and Younger (Neoproterozoic) supracrustals. The difference between the two supracrustals is made based on the absence of intrusive granitoids in the younger ones and also that the older supracrustals are deformed and metamorphosed, whereas the younger supracrustals are undeformed and unmetamorphosed (Naqvi and Rogers, 1987).

1.1 THE OLDER (ARCHEAN - PALEOPROTEROZOIC) SUPRACRUSTAL ROCKS

The Bastar craton consists of three major Archean - Paleoproterozoic and three Paleoproterozoic supracrustal groups. The Archean - Paleoproterozoic supracrustal groups are (i) the Bailadila Group, (ii) the Bengpal Group and (iii) the Sukma Group in the southern part of the craton (Crookshank, 1963), and Paleoproterozoic supracrustal groups are (i) the Sakoli Group, (ii) the Dongargarh Supergroup and (iii) the Sausar Group in the northern part of the craton (Fermor, 1909) (Fig. 1).

The Paleoproterozoic basins which occur on the northern part of the Bastar craton in the proximity of the Central Indian Suture Zone (CISZ) have been mapped in detail (Naqvi and Rogers, 1987). Among these supracrustal rocks, Sausar and Sakoli Groups have been included in the present study. The supracrustal rocks in these basins are metasedimentary rocks interbedded with metabasalt and other volcanics (rhyolites). On the structural considerations, the Sakoli Group is considered to be older than the Sausar Group and is younger than the Amgaon Group (Sarkar and Saha, 1982). Sarkar et al. (1990a) consider the Sakoli and Sausar Groups as Paleoproterozoic on the basis of radiometric data of Ghosh et al. (1986) and Sarkar et al. (1988).

The Sakoli Group is composed of supracrustal rocks including mostly metapelite and quartzite with basalt and rhyolite. The Sausar Group comprises of quartzite, pelite and carbonate associations containing stratiform manganese deposits which form the largest manganese reserves in India (Bhowmik et al., 1997; Dasgupta et al., 1984).

1.2 THE YOUNGER (NEOPROTEROZOIC) SUPRACRUSTAL ROCKS

The younger supracrustal rocks occur in two major Proterozoic basins namely (1) the Chhattisgarh basin and (2) the Indravati basin (Bastar basin) within the Bastar craton as shown in Fig. 1. The younger supracrustal rocks consist of unmetamorphosed conglomerate, sandstone, shale, limestone, chert and dolomite.

The Chhattisgarh and Indravati basins are two major intracratonic sedimentary basins of the Bastar craton containing the Neoproterozoic sediments. The basins are similar in their mixed siliclastic - carbonate lithology, absence of metamorphic overprinting and very low tectonic disturbance. These sedimentary successions are believed to be younger than 1600 Ma (Kruezer et al., 1977), and, therefore, Neoproterozoic and are commonly designated as Purana successions in the Indian stratigraphy (Holland, 1907; Radhakrishna, 1987). Origin of both the Paleoproterozoic and Neoproterozoic cratonic basins, however, is still poorly constrained, though a riftogenic origin has been invoked for them (Chaudhuri et al., 2002; Naqvi and Rogers, 1987; Patrinabis Deb and Chaudhuri, 2002; Takashi et al., 2001).

1.3 PROBLEM STATEMENT

Either because of their presumed unfossiliferous character and the lack of important economic deposits, the study of the Proterozoic sedimentary basins (supracrustals) of the Bastar craton has not received as much attention as they deserve. The variety of sediments deposited in these sedimentary basins have sampled the continental crust of that period and therefore, act as a repository of evidence and clues regarding the composition of the continental crust, tectonic environment and the nature of weathering prevailing at the time of deposition of these rocks.

Most of the previous work on the Bastar craton has been carried out on geochemistry of Archean gneisses, granitoids, mafic dykes and mafic volcanic rocks (Hussain et al., 2004a, b, c; Hussain and Mondal, 2004; Mondal et al., 2006, 2007; Mondal, 2002; Mondal and Hussain, 2003; Sarkar et al., 1993; Srivastava, 2004), but the geochemistry of the overlying Proterozoic supracrustals have not been attended with a view to understand the provenance, paleoweathering and evolution of the early crust of the Bastar craton. Availability of a complete Proterozoic sedimentary record in the Bastar craton from Paleoproterozoic (e.g. the Sakoli and Sausar basins) to Neoproterozoic (e.g. the Chhattisgarh and Indravati basins) is the unique factor which makes this study very important. This sedimentary record is well preserved and the geological framework of the region has been worked out by earlier workers (e.g. Bandyopadhyay et al., 1995; Murthi, 1987; Naqvi and Rogers, 1987; Narayanswami et al., 1963; Ramakrishnan, 1987). The terrain is ideal not only for the studies on provenance, paleoclimate and tectonics but also to decipher the Proterozoic evolutionary history of the Bastar craton.

Most of the earlier works on cratonic supracrustals all over the world have been studied to mark the geochemical changes at Archean - Proterozoic boundary (Condie and Wrokienwicz, 1990; Taylor and McLennan, 1985). The geological studies of the sedimentary rocks from different parts of the world reveal that the Archean crust was enriched in Mg, Cr, Ni, Co and depleted in Th, U, Rb, K when compared with post-Archean and Phanerozoic crust. Although most of the rare earth element patterns of the sedimentary rocks are remarkably uniform with absolute abundances, the light rare earth element (LREE) enrichment and heavy rare earth element (HREE) depletion demarcates Archean from post-Archean. Significant enrichment of ratios like Ba/Sr, Rb/Sr, K/Na and depletion of Co/Th, Ni/Co, Zr/Y and Zr/Nb characterize the post-Archean crust (Gibbs et al., 1986). Some of these changes observed in the crustal rocks indicate a change in the composition of the upper crustal source from relatively mafic to felsic through time. This change probably marks the Archean - Proterozoic boundary and seems to be related with the widespread granitic magmatism during latter periods. However, the geochemical change during Proterozoic from Paleoproterozoic to Neoproterozoic has not been studied at large extent as has been studied for the Archean - Proterozoic boundary. Thus, present study not only reveals the nature of crust in the Proterozoic but also gives an opportunity to trace the geochemical changes through time from Paleoproterozoic to Neoproterozoic in the Bastar craton, Central Indian Shield.

The compositions of Archean - Proterozoic terrigenous clastic sedimentary rocks have often been used to infer crustal compositions, evolutionary growth of early continental crust and processes that prevailed on the surface of earth at the time of their deposition. Systematic differences have also been observed between the Archean and Proterozoic sedimentary rock record. These differences have often been interpreted as manifestation of change in tectono - magmatic system between these two eons.

Majority of well studied Archean sedimentary rocks are from greenstone belts, whereas those of Proterozoic age are mainly from continental marginal or intercratonic basins. Since the geological settings of deposition of these temporarily different sedimentary basins are different, it is quite possible that the differences in their compositions reflect the differences in geological setting rather than age. Thus, it may indicate that differences in composition may reflect tectonic sampling bias (Gibbs et al., 1986). A more judicious approach will be to study the sedimentary rocks of Archean-Proterozoic age from similar geological setting e.g., continental margin or intracratonic basins so as to mitigate the differences induced by contrast of geological setting (like greenstone belt and intracratonic setting). Any differences in compositions, thus obtained can be thought to reflect difference in tectono-magmatic events or crust-mantle interaction during Archean and Proterozoic. It is to be noted here that the Paleoproterozoic basins (Sakoli and Sausar Groups) as well as the Neoproterozoic basins (Chhattisgarh and Indravati basins) of the Bastar craton which are focus of the present study have been assigned similar tectonic setting i.e. rift-related or intracratonic basins by earlier workers (Chaudhuri et al., 2002; Naqvi and Rogers, 1987; Patranabis Deb and Chaudhuri, 2002; Takashi et al., 2001; Wani and Mondal, 2007).

Most of our present understanding regarding evolution of early continental crust is based on the petrographical, geochemical and isotopic composition of Precambrian sedimentary rocks. In India, attempts to apply geochemical data of Precambrian sedimentary rocks to understand crustal evolution, have not gathered much momentum, and as a result, Indian sedimentary rocks remain by and large unpresented in models proposed for crustal evolution. Some efforts have, however, been made in this direction recently (Bhat and Ghosh, 2001; Manikyamba et al., 2008; Paikaray et al., 2007; Rao et al., 1999; Raza et al., 2002) to understand Precambrian crustal evolution but in general petrological and geochemical studies of Proterozoic supracrustal rocks of the Bastar craton remain less studied.

1.4 PREVIOUS WORK

Considerable work has been done on the Bastar craton to document the regional distribution, stratigraphic positions and the geological characters of the Archean and Proterozoic supracrustals of the craton. Crookshank (1963) has done the legendary work on the craton through the systematic mapping of the southern Bastar and proposed the stratigraphic schemes for the supracrustals of the southern Bastar into three different series viz. Sukma, Bengpal and Bailadila series in the ascending order. Later, on the basis of the difference in geographical distribution, lithological associations, unconformable relationships and metamorphic grade, Ramakrishnan (1990) proposed a stratigraphic scheme of the Southern Bastar in greater detail.

The Bastar craton was believed to contain Archean components older than 3000 Ma like those of Dharwar and Singhbhum craton (Crookshank, 1963; Fermor, 1936).

Fermor (1936) considered the crystalline rocks of the Bastar craton as Archean in age and suggested temporal similarity with the oldest crustal rocks in the Singhbhum and Dharwar cratons. Sarkar et al. (1990a) have done the radiometric dating of the magmatic and also the non-magmatic rocks of the craton using Pb - Pb, Rb - Sr and K - Ar whole rock isochron dating techniques. They have proposed that the precursors of the gneisses were emplaced at ca. 3.6 Ga and 3.0 Ga and these were followed by a series of granitoid magmatism at ca. 2.6 Ga, 2.3 Ga, 1.8 Ga, 1.5 Ga and 0.8 Ga. Sarkar et al. (1993) have dated the gneisses that occur as enclaves in the southern Bastar within granitoids, which yielded a zircon U - Pb age of 3509 Ma. The granitoids that intruded the gneisses were also dated by them that yielded a zircon U - Pb age of 2480 Ma. Earlier Sarkar et al. (1990b) have dated the granite gneisses that occur as outcrop and the intrusive granitoids also following the Rb-Sr isochron dating techniques that yielded the ages of 3.0 Ga and 2.6 Ga respectively.

Overall, most of the earlier work on the Bastar craton has been carried out on geochemistry of the Archean gneisses, granitoids, mafic dykes and mafic volcanic rocks of the Bastar craton (Hussain et al., 2004a, b, c; Mondal et al., 2006, 2007; Sarkar et al., 1990b; 1993; Srivastava, 2004), but the geochemistry of the overlying Proterozoic supracrustal rocks have not been attended with a view to understand the provenance, paleoweathering and evolution of the early crust of the Bastar craton. Studies so far carried out on the supracrustals of the Bastar craton are mainly devoted to understand the stratigraphical, lithological framework and structural pattern of the supracrustal rocks but in general petrological and geochemical studies of supracrustal rocks of the Bastar craton remain sketchy and fragmentary.

The Paleoproterozoic Sakoli and Sausar basins of the Bastar craton have so far been studied mainly from the point of view of geology, structure, metamorphism and mineralization (Bandhopadyay et al., 1995; Bhowmik, et al., 1997; Dasgupta et al., 1984; Naqvi and Rogers, 1987; Narayanaswami et al., 1963; Roy and Bandyopadhyay, 1988, 1990; Roy et al., 1992; Takashi et al., 2001). However, the Neoproterozoic Chhattisgarh basin has so far been studied mainly from the point of view of lithostratigraphy, lithofacies and paleogeography (Das et al., 1992; Datta, 1998; Datta et al., 1999; Gupta, 1998; Jairam and Banerjee, 1978; Khan and Mukherjee, 1990; Moitra, 1995; Murthi, 1987, 1996; Patranabis Deb and Chaudhuri, 2002). Similar work has also been carried out by the previous workers on Indravati basin (Crookshank, 1963; Dutt, 1963; Murthi et al., 1984; Ramakrishnan, 1987, 1990).

1.5 GEOGRAPHY OF THE AREA

Bastar craton covers an area of about 2,15000 km^2 within $17.5^0N - 23.5^0N$ latitudes and $77.8^0E - 84.1^0E$ longitudes (Fig. 1). It occupies a large area in the central India covering parts of the states of Chhattisgarh, Madhya Pradesh, Maharashtra and Orissa. The topography of the terrain is very much rugged with isolated hills of gneissic and granitic rocks rising up to a maximum of 920m above the mean sea level. The quartz veins are projecting out as ledges and comprising the most spectacular landmass running at some places for several kilometers. The altitude of the terrain ranges around 400 - 500m above the mean sea level. Most of the study areas are accessible by motorable roads. Highways and railways interconnect important towns. Southern Railway, Raipur Vizainagaram branch, National Highway No.6 (Great Eastern Road) and National

Highway No. 23 run through the area. Mahanadi, Indravati, Dantewara and Jonk rivers constitute the major drainage systems of the terrain with almost a northerly flow of the rivers, which remain perennial throughout the year.

1.6 PURPOSE AND OBJECTIVES OF STUDY

Sedimentary rocks are the most abundant rock types on the surface of the earth. The terrigenous clastic sedimentary rocks preserve a record of their sources and consequently allow us to examine the nature and composition of the crust, sedimentary recycling, addition of the juvenile material from the mantle, unroofing and the climatic conditions. Petrographic and geochemical studies of terrigenous sediments have long been used to compute the crustal composition and to understand the weathering and climatic conditions (Arora et al., 1994; Bhat and Ghosh, 2001; Condie, 1993; Engel et al., 1974; Erikson et al., 1992; Fedo et al., 1997; Lee, 2002; Naqvi et al., 1972; Rao et al., 1999; Raza et al., 2002; Taylor and McLennan, 1981; Wronkiewicz and Condie, 1987, 1989, 1990; Zhang et al., 1998).

Sandstone petrography is widely considered to be a powerful tool for determining the origin and tectonic reconstructions of ancient terrigenous deposits (Anani, 1999; Blatt 1967; Critelli and Nilsen, 2000; Dickinson, 1970; Michaelsen and Henderson, 2000; Pettijohn et al., 1972). Sandstone mineralogical characterization of the basin fill is critical to any basin analysis and many studies have pointed to an intimate relationship between detrital sand compositions (i.e. bed rock compositions of sources) and tectonic setting (Dickinson and Suczek, 1979; Dickinson et al., 1983; Ingersoll, 1978). Sand composition is also sensitive to a complex set of factors involved in the clastic sediment system (e.g.

climate, relief, transport, diagenesis) which provide valuable information for paleoecological reconstructions (Johnson, 1993).

Geochemistry of clastic sedimentary rocks can best be used to determine the compositions of the provenance (McLennan et al., 1993), to evaluate weathering processes and paleoclimate (Fedo et al., 1995; Nesbitt and Young, 1982), to qualify the secondary processes such as hydraulic sorting (Cullers, 2000; McLennan et al., 1993), to model the tectonic setting of the basin (Bhatia, 1983; Bhatia and Crook, 1986; Roser and Korch, 1986) and finally to trace the evolutionary history of mantle and crust (Condie, 1993). Several trace elements like high field strength elements (HFSE), Th, Sc and rare earth elements (REE) are most suited for discriminations of provenance and tectonic setting because of their relatively low mobility during sedimentary processes and their short residence times in seawater (Taylor and McLennan, 1985). These elements probably are transferred quantitatively into clastic sediments during weathering and transportation, reflecting the signature of the parent materials and hence are expected to be more useful in discriminating tectonic environments and source rock compositions (Bhatia and Crook, 1986; Condie, 1993; McLennan, 1989).

In addition to inferring crustal compositions and the processes that operated on the surface of the earth, geochemical data of the sedimentary rocks have revealed systematic differences between the Archean and the Proterozoic sedimentary rock record. These differences have been interpreted as evidence of fundamental change in the crust mantle system between these two eons (Gibbs et al., 1986). Some of these changes observed in crustal rocks indicate a change in the composition of the upper crustal source from relatively mafic to felsic through time. This change has been in general considered to mark the Archean - Proterozoic boundary and seems to be related with the widespread granitic magmatism during latter periods (Taylor and McLennan, 1985). Gibbs et al. (1986) suggest that these transitions may be an artifact of a tectonic sampling bias, whereby the majority of the well studied Archean sediments coming from Archean mafic-rich greenstone belts and post-Archean samples largely coming from continental margin or intracratonic basins. The proposed study area provides excellent opportunity to trace the evolutionary history of crust in the central Indian shield from Archean to Proterozoic within a rather small geographic region.

The supracrustal rocks of the Bastar craton include both Paleoproterozoic metasedimentary rocks (quartzites, metapelites) and Neoproterozoic unmetamorphosed sedimentary rocks (sandstones, shales). Occurrence of rock formations in the Bastar craton ranging in age from Paleoproterozoic to Neoproterozoic make this region a unique terrain where geological processes operated for a long geological period which is most suited to understand crustal evolution. The emphasis of the present work is to carry out petrological and geochemical studies of the Neoproterozoic rocks of the Chhattisgarh and Indravati basins of the Bastar craton to know the paleoweathering, source rock composition and tectonic setting of these Neoproterozoic basins of Bastar craton. Geochemical studies of Paleoproterozoic metasedimentary rocks of the Sakoli and Sausar basins of Bastar craton have also been carried out for comparison to know whether there was any change in paleoweathering, source rock composition and tectonic setting through Proterozoic time in Bastar craton.

Data generated in this study from Paleoproterozoic and Neoproterozoic supracrustals are integrated with the available geochemical data of the basement gneisses, granitoids (Mondal et al., 2006) and mafic volcanic rocks (Srivastava, 2004) of the Bastar craton, so as to trace the crustal evolution history of the Bastar craton in particular and the central Indian shield in general. We have made a comparison of our data against the available geochemical data of North American Shale Composite (NASC) (Gromet et al., 1984), Upper Continental Crust (UCC) (Taylor and McLennan, 1985), and Paleoproterzoic Kaapvaal pelites of Transvaal and Venterdorp Supergroups of the Kaapvaal craton (Wronkiewicz and Condie, 1990).

The objectives of the work are as follows:

i) Field investigations to understand geological setting and collection of rock samples of quartzites and metapelites from the Paleoproterozoic Sakoli and Sausar basins, and sandstones and shales from the Neoproterozoic Chhattisgarh and Indravati basins of the Bastar craton.

ii) Petrographic analysis of the clastic rocks (especially sandstones of the Neoproterozoic Chhattisgarh and Indravati basins) with a view to understand the nature of provenance and tectonic setting.

iii) Geochemical analysis to generate high quality data comprising major and trace including rare earth elements of quartzites and metapelites of the Paleoproterozoic Sakoli and Sausar basins, and shales and sandstones of the Neoproterozoic Chhattisgarh and Indravati basins of the Bastar craton.

iv) To constrain the nature and composition of the Proterozoic crust from the petrographic and geochemical data of the Paleoproterozoic and the Neoproterozoic supracrustal rocks of the Bastar craton.

v) To constrain the source of the sedimentary sequence and to study whether there was any significant change in the location of the source areas and to decipher the paleoweathering conditions and paleoclimatic conditions prevailed during their deposition.

vi) To understand the tectonics of the basin of deposition of the sediments from the study of the Paleoproterozoic and the Neoproterozoic supracrustal rocks of the Bastar craton.

vii) To elucidate a model of crustal evolution of the Bastar craton in particular and central shield in general and the evolutionary trends from the Paleoproterozoic to the Neoproterozoic by comparing basement rock geochemistry with the geochemistry of the supracrustal rocks.

Chapter-II

GEOLOGICAL SETTING

2. GEOLOGICAL SETTING

Singhbhum, Dharwar and Bastar nuclei together constitute the Southern Peninsular Block (Radhakrishna, 1989). Towards north, the Bastar craton got accreted with the Bundelkhand craton along the east-northeast to west-southwest trending Narmada-Son Lineament, which together constitute the Central Indian Shield (Bandopadhyay et al., 1995). The Bastar craton is bounded at the periphery by Proterozoic mobile belts viz. Mahanadi graben in the northeast, Godavari graben in the southwest, Satpura mobile belt in the north-northwest and Eastern Ghat mobile belt in the southeast (Fig. 1).

The geology of the Bastar craton is very complex, as the craton represents a checkered history of evolution with contrasting petrological units of different ages, consisting of gneisses, granitoids, sedimentary supracrustals (Neoproterozoic), metasedimentary and metavolcanic supracrustals (Archean – Paleoproterozoic) and mafic dykes, which together constitute the bulk of the geology of the Bastar craton. The granitoids and gneisses form the basement for Proterozoic supracrustal rocks. The supracrustal rocks of the Bastar craton can be conveniently divided into older supracrustals (Archean – Paleoproterozoic) and younger supracrustals (Neoproterozoic).

The older supracrustals of Archaean - Paleoproterozoic age are highly deformed and metamorphosed sequences of sedimentary and volcanic rocks. The gneisses of the craton are of granitic compositions, which make up the basement for the supracrustal rocks of the craton. The gneisses are the most abundant rock type of the craton. The available radiometric data indicate that the granite-gneisses were emplaced at 3.0 Ga. However Sarkar et al. (1993) has reported the occurrences of an older suite of gneiss that yielded an age of 3.5 Ga. These older gneisses show trondhjemitic affinity and occur as enclaves over a much-limited area in the southern Bastar at and around Markampara. Granitoids, the second abundant rock units of the craton, are intrusive into the gneisses and into the older supracrustals as well.

2.1 OLDER SUPRACRUSTALS

The craton consists of three major Archean – Paleoproterozoic supracrustal groups viz. (i) the Bailadila Group, (ii) the Bengpal Group and (iii) the Sukma Group (Crookshank, 1963) in the southern part of the craton, and three Paleoproterozoic supracrustal groups viz. (i) the Sakoli Group, (ii) the Dongargarh Supergroup and (iii) the Sausar Group in the northern part of the Bastar craton near the proximity of the Central Indian Tectonic Zone (CITZ) (Fermor, 1909; Naqvi and Rogers, 1987). The CITZ has generally been interpreted as a suture between the northern and southern Indian shield. It is also considered that a widespread strong tectonothermal event took place during 1700 - 1500 Ma as well (Yadekar, 1990). Thus it is important to understand the geology around CITZ for considering the regional crustal processes before the East Gondwana Rodina assembly. The older supracrustal rocks are highly deformed and metamorphosed sequences of sedimentary and volcanic rocks. These rocks occur as co-folded enclaves within the basement gneisses. The general stratigraphic succession of the supracrustals of the Bastar craton is given in Table 1.

2.1.1 ARCHEAN - PALEOPROTEROZOIC SUPRACRUSTALS

Table 1. Stratigraphic successions of supracrustals of the Bastar craton (Naqvi and Rogers, 1987)

Nagpur, Bhandara, Chindwara (west of Chhattisgarh Basin)	Jeypore, Bastar (east, southeast and south of Chhattisgarh Basin)
Chhattisgarh and Indravati Basins	
----------Unconformity----------	
Sausar Group (~ 1600-900 Ma)	Bailadila Group (~ 2100 Ma)
Dongargarh Supergroup (~2462 Ma ~1367 Ma)	Bengpal Group (~2300 Ma)
Sakoli Group/ Sonakhan Group (~ 2500 Ma)	Sukma Group (~ 2500 Ma)
----------Basement Gneisses and Granitoids----------	

The rocks in these suites are mostly sandy, clayey and calcareous metasediments and mafic volcanic rocks and iron formations (Mukharya, 1975; Dutt et al., 1979). Ghosh et al. (1977) suggested that mafic lavas are the oldest rocks in the area and are succeeded upward by sedimentary rocks of the Sukma and Bengpal Groups. Crookshank (1963) correlated the supracrustal rocks with the Dharwar schist belts and shows considerable lithological resemblance of the supracrustal rocks with some parts of Dharwar belts and also with the iron ore series of the Singhbum craton. The geology of the southern Bastar is shown in Table 2.

2.1.2 SUKMA GROUP

The Sukma Group of supracrustals occur as enclaves of variable sizes and orientation in the gneisses that are occurring as outcrops to the west and northwest of Sukma, southeast of the Bailadila hills and near Bijapur. According to Crookshank (1963), the Sukma Group has five lithologic assemblages: biotite–cordierite gneiss, diopside-hornblende gneiss/pyroxene gneiss/diopside quartzite, hornblende schist, magnetite quartzite and grunerite schist and quartzite. Charnockites and other high-grade supracrustals of the Sukma Group are found in Bhopalpatnam and Kondagaon belts. The Sukma supracrustals show west-northwest trending first generation folds (F_1) associated with the main foliation and overprinted by the north-northeast trending second generation (F_2) folds. The third phase of deformation developed crenulation cleavages and northwest trending shear zones (Chaterjee, 1970). No stratigraphic sequence can be established because of isolation of the outcrops.

Table 2. Stratigraphy of the Southern Bastar craton (Crookshank, 1963)

Puranas (Neoproterozoic) (Unmetamorphosed Chhattisgarh and Indravati Basins)	Conglomerate/sandstone, limestone and shale
..........Unconformity..........	
Igneous rocks	Dolerite dykes, granite and pegmatite, charnokites, greenstone and granite gneiss
..........Unconformity..........	
Khondalites	(Position uncertain)
..........Unconformity..........	
Bailadila (Iron ore) Group	Banded hematite–quartzites, grunerite-quartzites and white quartzites
..........Unconformity..........	
Bengpal Group	Ferrugenous schists, schistose conglomerates, biotite hornblende-quartzites, shales slates. Slates, schists, phillites, grunerite-garnet-schists, magnetite-quartzites, garnet-biotite-gneiss with basaltic flows and tuffs. Sericite-quartzites, andaulisite-gneiss, banded magnetite-quartzites, grunerite schists, and quartzites with intercalated basalt flows.
..........Line of division uncertain..........	
Sukma Group	Silliminite-quartzites, grunerite-schists magnetite and diopside-quartzites, hornblende-schists, biotite corderite gneiss etc.

2.1.3 BENGPAL GROUP

The principal constituents of the Bengpal Group are andalusite-bearing gneisses and schists with biotite and muscovite. Silliminite and garnet occur at high metamorphic grades. Basaltic and tuffaceous rocks are abundant in the Bengpal sequence, in contrast to virtual absence of metavolcanic material in the Sakoli and Sausar Groups, west of the Chhattisgarh basin. The mafic rocks consist primarily of fine-grained hornblende and plagioclase.

The Bengpal Group is restricted to a narrow west-northwest trending belt with an average width of 10 km and a maximum width of 30 km. This belt is bounded to the north and south by the Indravati and Sukma basins respectively. The Bengpal Group is characterized by amygdular metabasalt with metagabbroic sills and dykes closely intercalated with andalusite schists and banded magnetite quartzite. The supracrustals of the group are highly deformed. South of the Bastar, horizontal shearing had produced mostly steep, north-northeast plunging overturned folds with axial planes dipping steeply east-northeast. To the west, the fold geometry changes to north-south trending non-plunging folds (Chatterjee, 1970).

2.1.4 BAILADILA GROUP

The Bailadila Group of supracrustals occurs in a north-south trending synclinorium with two synclines and intervening anticlines plunging north. The supracrustals are predominantly exposed in the Bailadila hills. These are composed of feldspathic quartzite at the base followed by phyllites and banded iron formations containing rich iron. The most abundant rock unit of the Bailadila sequence is the banded iron formation including banded hematite quartzite, banded hematite jasper. banded magnetite quartzite and jasper having bands and streaks of iron ores (Crookshank, 1963). Horizontal shearing in the Bailadila range has produced north-northeast plunging overturned folds with axial planes dipping east-northeast resulting from flexural slip folding. In the west of the Bailadila, the fold geometry changes to north-south trending non-plunging folds (Chaterjee, 1964).

2.1.5 RELATION OF SUKMA, BENGPAL AND BAILADILA

Division between the Sukma and Bengpal Groups is essentially based on the difference in metamorphic grade (Table 2). The Sukma Group is silliminite bearing and the Bengpal Group contains andaulisite. Crookshank (1963) regarded diopsidic quartzites and pyroxene gneiss as diagnostic of the Sukma Group. The Sukma and Bengpal Groups are severely deformed. In the south of the Bastar, Chatterjee (1970) found that horizontal shearing had produced mostly steep, NNE-plunging overturned folds with axial planes dipping steeply ENE. To the west, the fold geometry changes to N-S trending, non-plunging folds.

Relationships between the Sukma and Bengpal Groups, and the Bailadila (iron ore Groups) are controversial. Although the Bailadila Group appears, at some places, to overlie the other suites unconformably, it has also been proposed that quartzites at the base of the Bailadila Group are continuous with the Bengpal (Crookshank, 1963). The most abundant rock of the Bailadila sequence is banded hematite quartzite, which consists of roughly equal amounts of iron ore and quartz plus minor amphiboles of the manganesioriebeckite/reibeckite series (Chatterjee, 1969).

According to Chatterjee (1964), the Bailadila Group has been folded twice, with deformation less severe than that of the Sukma and Bengpal Groups. The major folds are asymmetric and open, with subhorizontal axes and axial planes dipping steeply eastward. The simple structure has been complicated by cross folding, which formed gentle flexures with steep axial planes.

2.2 PALEOPROTEROZOIC SUPRACRUSTALS

2.2.1 SAKOLI GROUP

The Sakoli Belt is located at the southern margin of the CITZ, and also, at the northern margin of the south Indian cratonic terrain (the Bastar craton). The Sakoli Group occurs in a large synclinorium west of the Chhattisgarh basin (Fig. 1). Lithologically, the volcano-sedimentary Sakoli Group comprises predominantly of metapelitic rocks (~ 80% by volume) (muscovite-quartz-garnet-biotite schists ± staurolite ± chlorite) with minor quartzite (Fig. 2A and B), arkose, conglomerate, banded iron formations, metamorphosed rhyolite, tuffs, epiclastic rocks, metabasalts and meta-ultramafic rocks (Bandopapadhyay et al., 1995). The Sakoli sediments show metamorphism of greenschist - lower amphibolite facies (Shastry and Dekate, 1984). The supracrustal sequence is composed of four formations (Table 3), viz., Gaikhuri, Dhabetekri, Bhiwapur and Pawni Formations from the oldest to the youngest (Bandhopadyay et al., 1995). The stratigraphic succession of the Sakoli Group of the Bastar craton is shown in Table 3.

The Sakoli Group of metamorphosed supracrustals has undergone two phases of deformation (Sengupta, 1965). The first phase has mainly produced isoclinal fold of the bedding plane (S_0) and axial plane schistosity (S_1). The second phase of deformation has

Fig. 2. Field photographs showing highly deformed Sakoli supracrustals near Sakoli (A) pelite (B) quartzite.

Table 3. Stratigraphic succession of the Sakoli Group of the Bastar craton (Bandyopadhay et al., 1995)

Formation	Lithology
Pawni Formation	Slate, phyllite, debris-flow deposits, meta-arkose sandstone, minor carbonaceous phyllite, ferruginous quartzite and BIF
Bhiwapur Formation	Metapelite (chloritoid-andalusite-garnet-staurolite schist), metarhyolite-rhyodacite and tuffs, minor metabasalt, metaexhalites (tourmalinite, chloritites etc.), sedex type Cu-Zn mineralization, Au and scheelite mineralization
Dhabetekri Formation	Metabasalt with minor metapelites, chert and metaultramafic rocks
Gaikhuri Formation	Conglomerate, gritty quartzite, metaquartzite, meta-arkose sandstone, minor carbonaceous phyllite, ferruginous quartzite and BIF
....	Unconformity...
Amgaon Gneissic Complex	Gneiss-migmatite, granitoids (with minor TTG), amphibolite, chromite-bearing metaultramafics, pre-Sakoli supracrustal assemblages of quartzite, kyanite and silliminite schist, calcsilicate rocks, marble, cordierite-gedrite-anthophyllite schist, garnet staurolite schist

folded both the S_0 and S_1 planes. First generation of folding was accompanied by development of schistosity and recrystallization of mica and quartz. Garnet was produced during the second phase of folding with staurolite and kyanite (Sengupta, 1965).

The Sonakhan Group of metamorphosed supracrustals occurs east of Chhattisgarh basin (Fig. 1). The supracrustals are composed mainly of quartzites, phyllites, mica schists, banded hematite quartzites, agglomerates and epidiorites. This Group is considered stratigraphically equivalent to the Sakoli Group.

2.2.2 DONGARGARH SUPERGROUP

The Dongargarh Supergroup of metamorphosed supracrustals occurs in north - northeast trending belt flanked by the Chhattisgarh basin and Sakoli synclinorium in the east and west respectively (Fig. 1). The belt is divided into Amgaon, Nandgaon and Khairagarh Groups (Sarkar et al., 1981) (Table 4). The Dongargarh Supergroup was regarded as part of the Sakoli Group in older classifications but is now considered as separate suite (Sarkar, 1983). The Tirodi gneiss separates the Dongargarh belt from the Sakoli and Sausar Groups.

The Amgaon Group is metamorphosed to amphibolite facies. The Amgaon Group is represented by psammitic metamorphites alternating with metabasic flows, which are represented by amphibolites and hornblende schists, feldspathic and other impure quartzite, quartz-sericite schist, hornblende-biotite-feldspar-quartz schists and garnet-epidote quartzite. These rocks have almost north-south strike and steep dip. Sarkar et al. (1981) proposed an Amgaon orogeny that occurred about 2300 Ma ago at which time granites and gneisses in the Amgaon suite were developed by syntectonic granitization.

Table 4. Stratigraphy of the Dongargarh Supergroup (Sarkar et al., 1981)

Dongargarh Supergroup

Khairagarh Group	Khairagarh orogenic phase (Ca. 900 Ma?) Mangikhuta Volcanics Karutola Formation Sitagota Volcanics (1367 Ma) (Intertrappean shale) (1686 Ma) Bortalao Formation Basal Shale (1524 Ma)
..........Unconformity..........	
Nandgaon Group	Dongargarh Granite (< Ca. 2200 Ma) Pitepani Volcanics Bijli Rhyolites (Ca. 2200 Ma)
....	
Amgaon Group	Amgaon orogeny, metamorphism and granitization (> Ca. 2300 Ma?) Quartz-sericite schist, feldspathic quartzite, garnet-epidote quartzite, quartz-feldspar biotite gneiss, hornblende schist and amphibolite.

The Nandgaon Group overlies unconformably by the Amgaon Group and is represented by Bijli rhyolite and Pitapani volcanics. The Bijli rhyolite has a total thickness of about 4500 m and contains rhyolites and rhyolitic conglomerates, sandstone, shale and tuffs. The suite contains inclusions of the Amgaon amphibolites and quartzites. The Pitepani volcanics are represented by andesitic and tholeiitic basalts and tuffs. Sarkar et al. (1981) suggested that the Bijli rhyolite is post-Sakoli in age. The Nandgaon Group and Dongargarh Granite are overlain by the Khairagarh Group. The Khairagarh Group is composed of sedimentary rocks (green sandy tuffs and tuffaceous sandstones, arkosic and lithic-wackes, arenites, shale, siltstones and conglomerates) and metavolcanics (basalts, tuffs and agglomerates) occurring in alternate layers. The sequence starts with a basal sedimentary formation.

The Dogargarh Supergroup has been affected by atleast three phases of complex and tight folding whose ages are mostly unknown. The first phase was originally designated as the Sakoli orogeny, but has been named as the Amgaon orogeny by Sarkar et al. (1981). It produced isoclinal folds in the Amgaon Group. The second phase affected the Bijli rhyolite and older rocks and has been designated as the Nandgaon orogeny. The third phase affected the Bartalao Formation and older rocks and is referred to as Khairagarh orogeny.

2.2.3 SAUSAR GROUP

The Paleoproterozoic Sausar Group is located along the southern margin of the CITZ in the Nagpur area, trending in the E-W to ENE-WSW direction making an arcuate belt of about 32 km wide and 210 km long. The Sausar Group is divided into six formations, in ascending order: Sitasaongi, Lohangi, Mansar, Chorbaoli, Junewani and Bichua Formations (Naryanaswamy et al., 1963; Bandyopadhyay et al., 1995) (Table 5). The orthoquartzite-corbonate association in the western part evidently indicates shallow water deposition in the basin margin under stable setting. Deeper water facies occur apparently towards Singbhum in the east, associated with ophiolites (Yedekar et al., 1990). The Sausar Group comprises of quartzite, pelite and corbonate associations (Fig. 3A and B), containing stratiform manganese deposits which form the largest manganese reserves in India (Dasgupta et al., 1984; Bhowmik et al., 1997) (Table 5). This group of rocks is characterized by virtual absence of volcanic rocks (Narayanaswamy et al., 1963). The Sausar Group shows evidence of three phases of deformation and four phases of metamorphism. Metamorphism of this group of rocks was roughly synchronous with the various stages of deformation. The first phase of deformation produced isoclinal folds, axial plane schistosity and mineral lineations. The second phase of deformation did not produce major structures but generated superfolds and crenulation cleavage while the third deformational phase formed open folds with steeply dipping axial planes (Sarkar et al., 1977). The stratigraphic succession is shown in Table 5.

2.2.4. AGE CONSIDERATIONS

In the Bastar area, the Bengpal Group is considered to be the oldest supracrustal sequence from stratigraphic evidence (Crookshank, 1963; Dutta et al., 1981). An unconformity separates the Bengpal from overlying the Bailadila sequence and in addition, a period of granitic activity, is believed to have intervened between two supracrustal sequences (Crookshank, 1963; Dutta et al., 1981). The latter view is

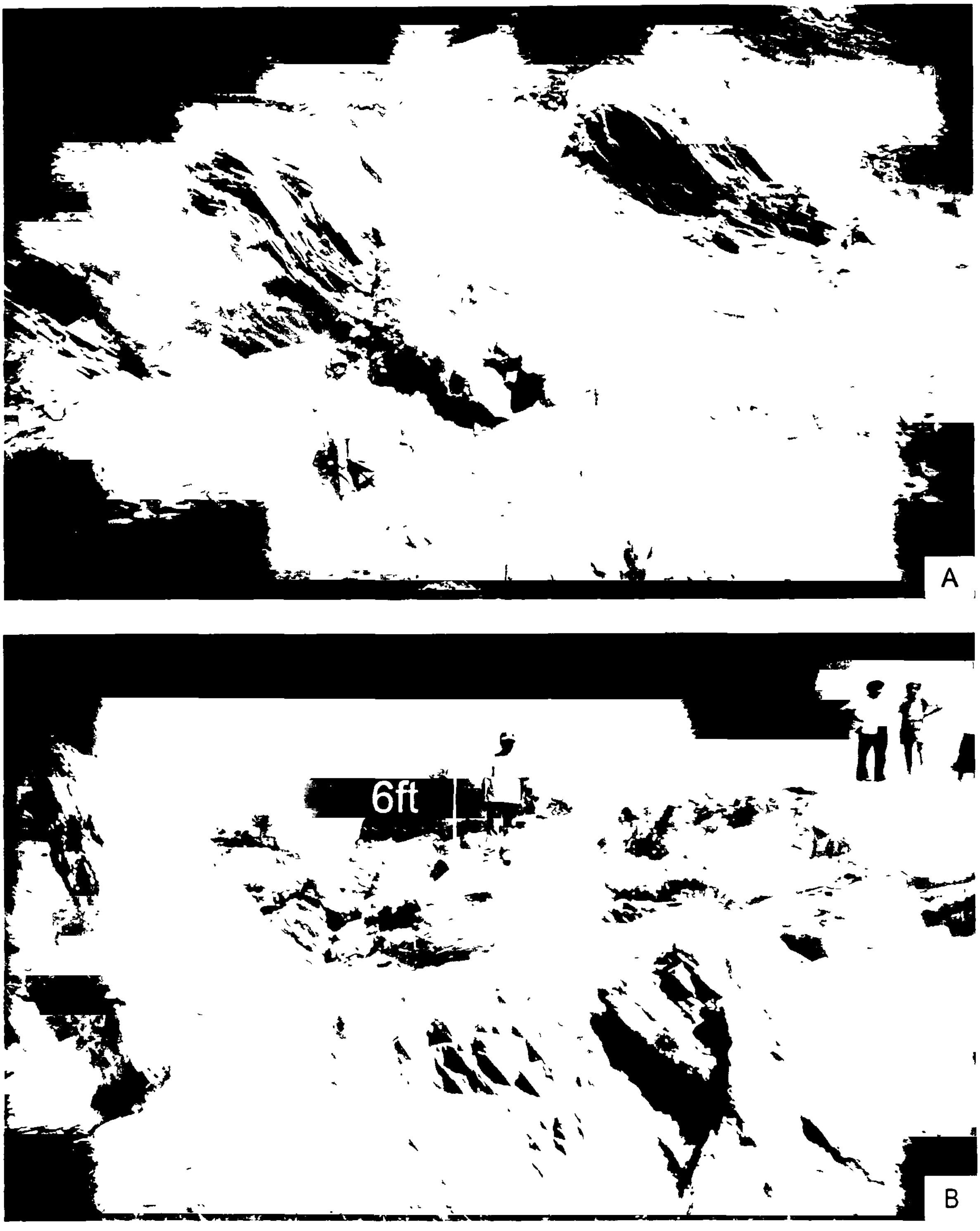

Fig. 3. Field photographs showing highly deformed Sausar supracrustals near Sausar (A) pelite (B) quartzite.

Table 5. Stratigraphic succession of the Sausar Group of the Bastar craton (Bandyopadhay et al., 1995, modified from Narayanswami et al., 1963)

Formation	Lithology
Bichua Formation	Dolomitic marble, calc-silicate gneiss-schist
Junewani Formation	Metapelite (mica schist), quartzite, granulite, biotite gneiss (reworked basement)
Chorbaoli Formation	Quartzite, feldspathic schists, gneisses, autoclastic quartz, conglomerate
Mansar Formation	Metapelite (mica schists and gneisses), graphitic schists, phyllite quartzite, major magnese deposits and gondite
Lohangi Formation	Calc-silicate schists and gneisses, marble, magnese deposits
Sitasaongi Formation	Quartz mica schists, feldspathic schists, mica gneiss, quartzite, conglomerate
Basement Gneiss	Biotite gneiss, amphibolite, calc-silicate gneiss, (Tirodi Gneiss) granulites, mica feldspathic schists

strengthened by the typical occurrence of the Bengpals as detached patches in the Central Indian Gneissic Complex (CIGC) and their granitised nature (Dutta et al., 1981). Both the Bengpal and Bailadila Groups show evidence of polyphase deformation, the effect of which is more severe in the older Bengpal rocks (Chatterjee, 1964).

The Nandgaon Group overlies unconformably by the Amgaon Group and is represented by the Bijli rhyolite and Pitapani volcanics. Sarkar et al. (1981) suggested that the Bijli rhyolite is post-Sakoli in age and presented an eight point Rb-Sr isochron age of 2160±25 Ma with an initial $^{87}Sr/^{86}Sr$ ratio of 0.7057±0.0015. The Nandgaon Group is intruded by the Dongargarh granite, which has a seven point Rb-Sr isochron age of 2270 Ma with an initial $^{87}Sr/^{86}Sr$ ratio of 0.7092±0.0054 (Sarkar et al., 1981).

The amphibolite grade pelites, psammopelites and volcanics of the Sakoli show imprints of two phases of folding and metamorphism (Sengupta, 1965; Sarkar et al., 1990a). The Sakoli Group shows strong imprints of two Proterozoic tectonothermal events (Sarkar et al., 1990a). The age of sedimentation of the Sakoli Group is, at least, pre-Bijili rhyolite (minimum age ca. 2.46 Ga) of the Nandgaon Group (Sarkar et al., 1990a). The pre-Bijili rhyolite status makes the Sakolis 2.5 Ga old.

Tripathi et al. (1981) consider the Sausar to be younger than the Nandgaon Group. The Sausar Group of rocks overlies granitic rocks of ca. 2360 Ma in the Malanjkhand area (Ghosh et al., 1986) and is therefore Paleoproterozoic.

2.3 YOUNGER SUPRACRUSTALS (NEOPROTEROZOIC)

The younger supracrustals comprise a great thickness of undeformed and unmetamorphosed sediments piled up unconformably over the Archean granite, gneiss and older supracrustals within eight Neoproterozoic basins including the major ones of the Chhattisgarh basin in the north-central part and the Indravati basin in the southern parts of the craton (Fig. 1). The unmetamorphosed supracrustals (Chhattisgarh Supergroup) contained within the major Chhattisgarh basin occupies about 35,000 km^2 area in the north-central parts of the craton and has a total thickness of 1500m. The supracrustals of the Indravati basin (Indravati Group) are lithologically similar to those of the Chhattisgarh basin. The size of the Indravati basin is quite small compared to the Chhattisgarh basin.

2.3.1 CHHATTISGARH BASIN

The Chhattisgarh basin occurs within an area of 35,000km^2, this is the third largest Neoproterozoic basin in the peninsular India. The Chhattisgarh Supergroup comprises of a thick succession of sandstone, shale and limestone (Naqvi and Rogers, 1987; Murthi, 1987, 1996; Das et al., 1992, 2001., Datta, 1998). The lower part of the succession is dominated by sandstone (Chandarpur Group), whereas limestone and shale dominate the upper part (Raipur Group). The shales are thinly bedded and are coloured in shades of yellow and pink and the limestones are dark grey and pink coloured with occasional stromatolitic structures (Tripathi et al., 1981).

The Chandarpur Group comprises of unmetamorphosed and gently dipping subhorizontal beds of sandstone with conglomerate and shale as subordinate constituents. The succession unconformably overlies gneisses, granitoids and the Sonakhan greenstone belt of the Archean basement complex (Table 6) (Fig. 4A). The Chandarpur Group is subdivided into three formations viz. Lohardih, Chaporadih and Kansapathar Formations.

Table 6. Lithostratigraphy of the Indravati basin and the Chhattisgarh basin (after Ramakrishnan, 1987; Murthi, 1987)

Indravati basin		Chhattisgarh basin (Chhattisgarh Supergroup)	
Indravati Group		Raipur Group	
		Tarenga Formation	Purple shale, and purple limestone
		Chandi Formation	Grey and pink limestone
		Gunderdehi Formation	Pink and purple shale/grey shale
		Charmuria Formation	Grey limestone/ White to buff clays
		............?....................................	
		Chandrapur Group	
Jagdalpur Formation	Calcareous Shales with purple and gray stromatolitic dolomite	Kansapathar Formation	White sandstone
Kanger Limestone	Purple limestone, grey limestone	Chopardih Formation	Reddish brown and olive green sandstone
Cherakur Formation	Purple shale with arkosic sandstone and chert pebble conglomerate, grit	Lohardih Formation	White pebbly sandstone
Tiratgarh Formation	Chitrakot sandstone member (quartz arenite)		
	Mendri sandstone member (subarkose and conglomerate)		

.... Unconformity..

Archean granites, gneisses and older supracrustals (Sonakhan greenstone belt).

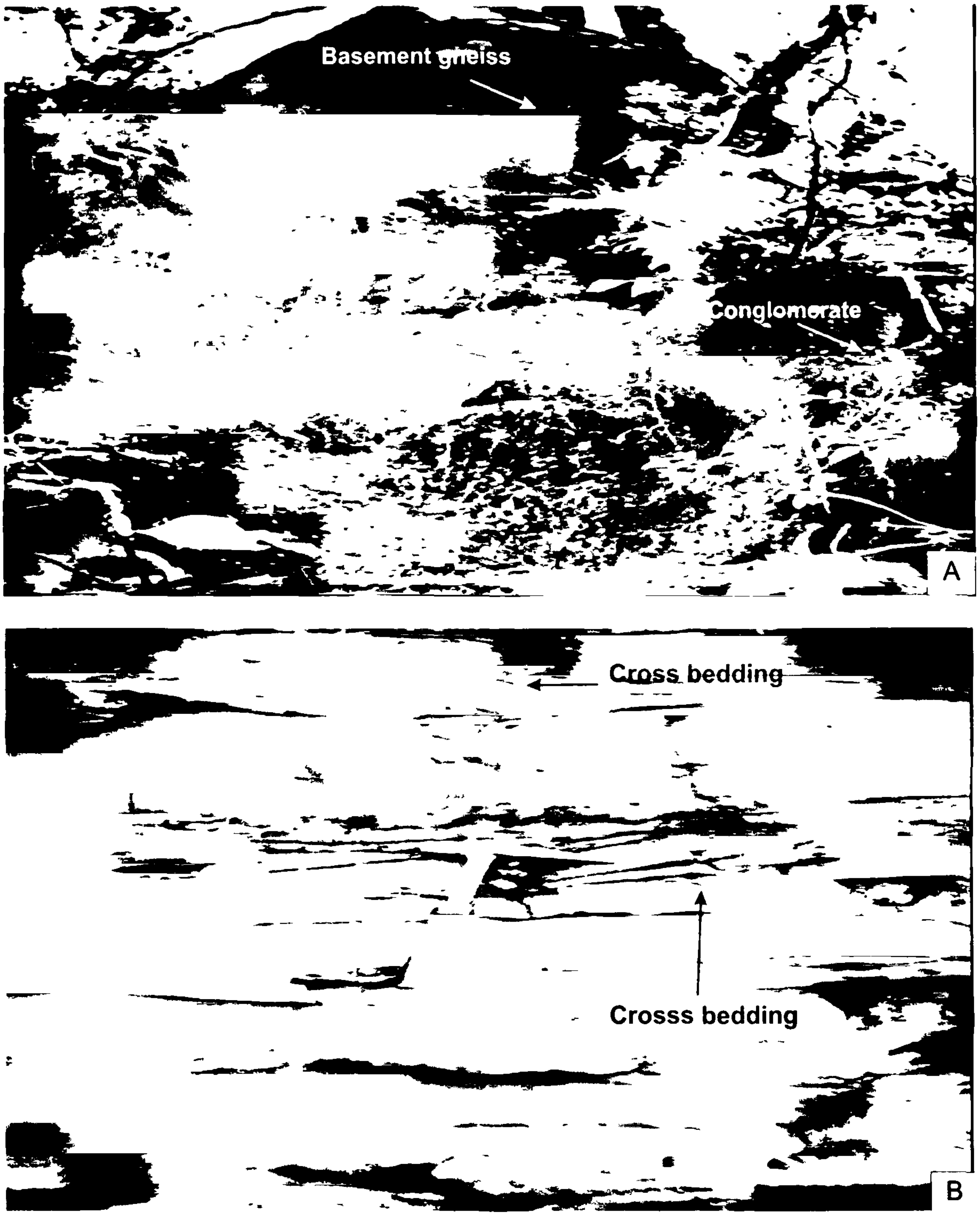

Fig. 4. Field photographs of the Chhattisgarh basin showing (A) contact between conglomerate/sandstone of the Lohardih Formation of the Chandarpur Group and Archean gneiss near Dhamtari and (B) cross-bedded sandstone of the Chopardih Formation, Chandarpur Group near Raipur.

arranged in ascending order of superposition (Datta, 1998; Murthi, 1987). The Chhattisgarh Supergroup is generally considered to have been deposited on stable shelf and is represented by minor conglomerates and sandstones which grade upward into a shale-carbonate assemblage. The crossbedded Chandarpur sandstone (Fig. 4B) represent sequence of shallow marine to intertidal environment (Datta, 1998; Patranabis Deb, 2004), while the Raipur Group points to a sub-tidal to inter- tidal environment (Murthi, 1987).

2.3.2 INDRAVATI BASIN:

The Indravati basin covers an area of 9000km^2 in Kanker-Bastar-Dantewara districts of the Chhattisgarh and Orrisa states. The Indravati Group of rocks unconformably overlies the Archean gneissic and granitic rocks. The Indravati Group comprises of basal sandstone (Tiratgarh Formation) (Fig. 5A and B) grading upwards into a conformable sequence of shale with sandstone (Cherakur Formation), horizontally laminated Kanger limestone and purple shales with stromatolitic dolomite (Jagdalpur Formation) in ascending order. The sediments of the Indravati basin are considered to have been deposited in shallow marine, near shore tidal flat or lagoonal environment (Ramakrishnan, 1987). The generalized stratigraphic sucession for the Indravati Group and Chhattisgarh Supergroup is given in Table 6.

2.3.3 AGE CONSIDERATIONS

The Chhattisgarh and the Indravati basins of the Bastar craton were considered as equivalent to the lower Vindhyans (Dutt, 1963; Kruezer, 1977; Murthi, 1987). Later

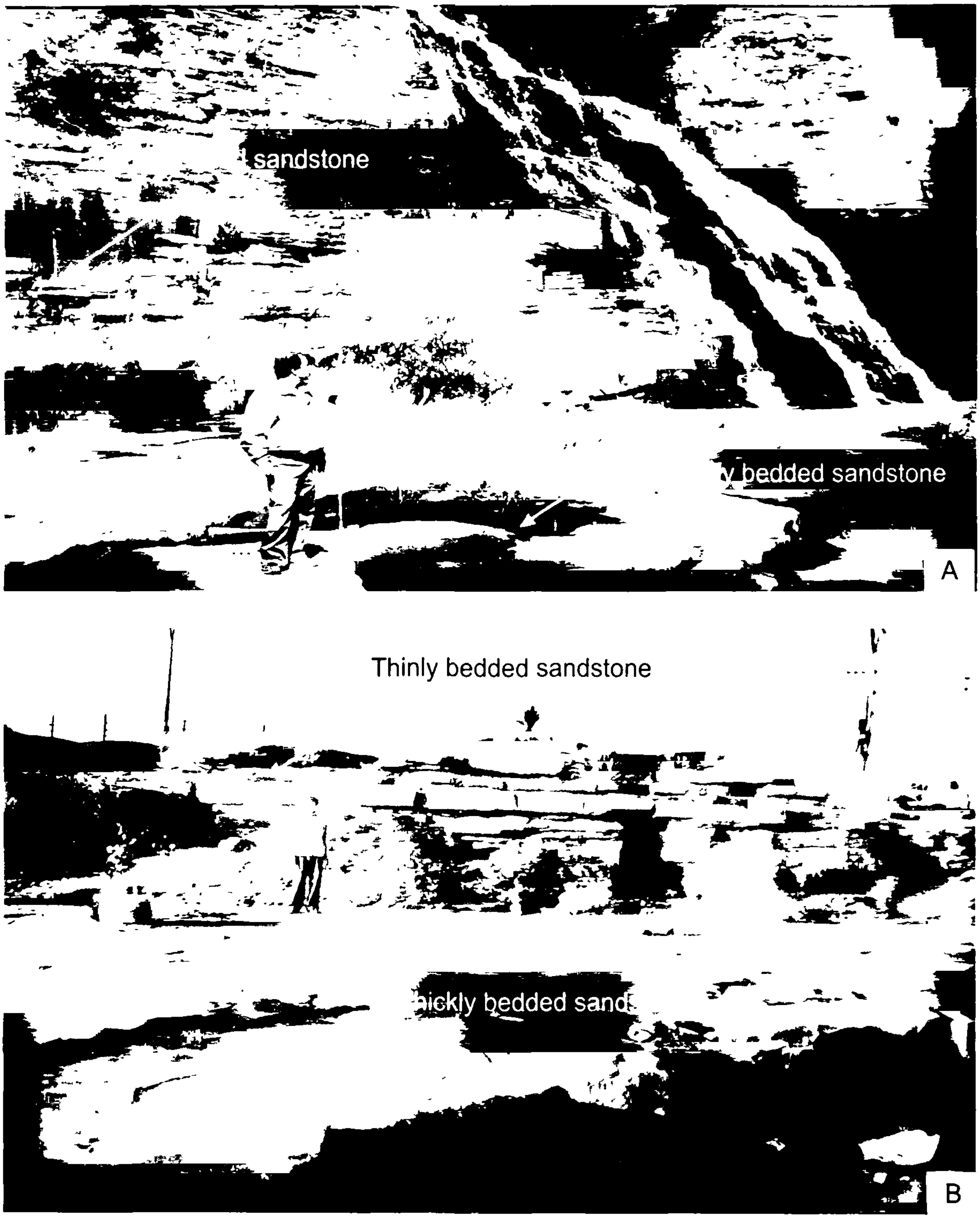

Fig. 5. Field photographs showing horizontally bedded Tiratgarh sandstone from the Indravati basin near (A) Tiratgarh waterfalls (B) Chitrakot water falls.

research revealed that the Chitrakot sandstone member (Tiratgarh Formation) of the Indravati basin can be compared with the Chopardih Formation (Chandarpur Group) of the Chhattisgarh Supergroup, which gives a K-Ar age of 700 - 750 Ma (Kruezer, 1977). This age data is also supported by the presence of stromatolites in limestones and dolomites of Machkot area, which correspond to late Riphean age (700 - 1100 Ma) as suggested by Walter (1976). Recent research revealed that the elevated $\delta^{13}C$ values of the Indravati carbonates and the Chhattisgarh carbonates are comparable with the Bander limestone unit of the Upper Vindhyan Supergroup (Maheshwari et al., 2005; Chakraborthy et al., 2002).

Chapter-III

PETROGRAPHY

3. PETROGRAPHY

Fresh samples of the Paleoproterozoic pelites and quartzites from the Sakoli and Sausar basins and the Neoproterozoic sandstones and shales from the Chhattisgarh and Indravati basins were collected from outcrops and mine exposures in the study area. Important sample locations are marked in Fig. 6. The samples were washed thoroughly to remove dust contamination. Thin sections were prepared for detailed petrographic studies.

3.1 PALEOPROTEROZOIC PELITES AND QUARTZITES

Petrographic study reveals that the main framework grains of the Paleoproterozoic Sakoli and Sausar pelites are quartz, chlorite, muscovite, biotite, garnet and opaques. The minerals that occur as major phases of these pelites include quartz, muscovite, biotite and chlorite. Opaques and garnet constitute the minor phases. The quartz and micas are typically elongated and aligned in a foliated fabric. Quartz in these pelites exhibits undulatory extinction. Quartz and mica makes bulk of the total mode of the pelites. The garnet and opaques together constitute minor amount of the total mode. Petrographically the Sakoli and Sausar pelites are similar with a difference that the Sakoli pelites are richer in quartz and the Sausar pelites in biotite.

The Sakoli and Sausar quartzites are composed of quartz, muscovite, biotite and opaques. Quartz, muscovite and biotite compose the bulk minerals for the Sakoli and Sausar quartzites, while garnet and opaques are present in minor amounts. Most of the micas and quartz have a preferred orientation. The quartz shows undulatory extinction.

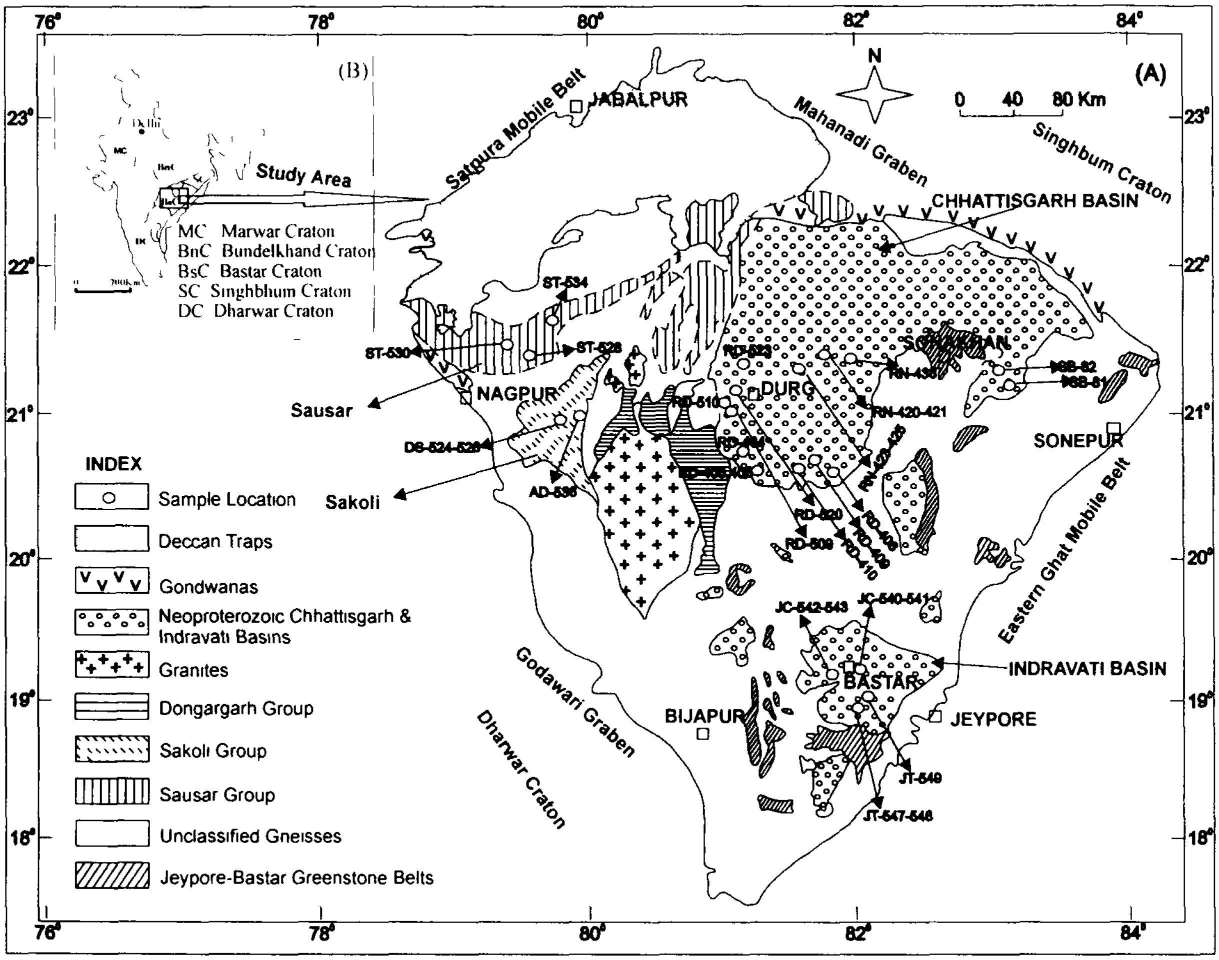

Fig. 6. (A) Geological map of the Bastar craton, Central Indian Shield (Ramakrishnan, 1990), showing locations of different Paleoproterozoic and Neoproterozoic sedimentary basins from which samples have been taken (B) Inset: Simplified Geological map of India showing major Archean cratons including the Bastar craton (Radhakrishnan and Naqvi, 1986). Numbers refer to sample locations.

The mineralogy of pelites, quartzites and shales has been of less use than the mineralogy of sandstones in determining the provenance since many minerals in such rocks are formed during weathering, diagenesis and metamorphism (Cullers, 2002). Keeping the above consideration in mind, only the Neoproterozoic sandstones of the Chhattisgarh basin and the Indravati basin have been investigated in detail in order to trace out their provenance and tectonic setting.

3.2 NEOPROTEROZOIC SANDSTONES

Sandstone petrography is widely considered to be a powerful tool for determining the origin and tectonic reconstructions of ancient terrigenous deposits (Blatt, 1967; Dickinson, 1970; Pettijohn et al., 1972). Sandstone mineralogical characterization of the basin fill is critical to any basin analysis and many studies have pointed to an intimate relationship between detrital sand compositions (bed rock compositions of sources) and tectonic setting (Dickinson and Suczek, 1979; Dickinson et al., 1983; Ingersoll, 1978). Sand composition is also sensitive to a complex set of factors involved in the clastic sediment system (e.g. climate, relief, transport, diagenesis) which provide valuable information for paleoecological reconstructions (Johnson, 1993).

The present petrological study of sandstones is focused mainly on the combined and comparative petrography of two sandstone successions viz. the Chandarpur Group and the Tiratgarh Formation which form lower parts of sedimentary successions of the the Chhattisgarh and Indravati basins respectively. The major emphasis of the present study is directed towards provenance studies and tectonic regime by the use of quantitative detrital modes, calculated from point counts of thin sections (Dickinson and

Suczek, 1979). The tectonic setting of the provenance apparently exerts primary control on sandstone compositions (Dickinson et al., 1983).

Twenty one sandstone samples were selected for modal analysis. Mineralogical composition of the sandstones was determined by modal analysis. Point counting was carried using the Gazzi-Dickinson method (Dickinson, 1970; Gazzi, 1966; Ingersoll et al., 1984). More than 500 points were counted for each thin section, using the maximum grid spacing to give full coverage of the slide. In a very few cases the thin sections were of poor quality and the grid spacing was reduced in order to obtain at least 500 counts. Some thin sections were stained to distinguish potash feldspar. The uncovered thin sections were first etched by hydrofluoric acid vapor and then dipped into freshly prepared saturated solution of sodium cobaltnitrite. Consequently, K-feldspars stained yellow making it easy to distinguish. The modal compositions of the sandstones of the Chandarpur Group of the Chhattisgarh basin and the Tiratgarh Formation of the Indravati basin are presented in Appendix-I.

The recalculated sandstone grain parameters used in this study are shown in Table 7. The sandstone classification as proposed by Folk (1980) has been followed in the present study. The sandstone modal analysis data were recalculated on a matrix free basis (Table 8) and was plotted in QFR diagram (Fig. 7) and other ternary diagrams given by Dickinson and Suczek (1979). Polycrystalline quartz (Qp) though not as durable as monocrystalline quartz (Qm) was placed at Q pole to obviate the problems of distinction between plutonic polycrystalline quartz and quartzite fragments. In the triangular diagrams constructed for delineating the tectonic setting of the provenance (Dickinson and Suczek, 1979), polycrystalline quartz was placed at rock fragment (RF) pole (in the

Table 7. Recalculated sandstone grain parameters used in this study (after Folk, 1980; Dickinson and Suczek, 1979)

QFR

Q = Total quartz grains (Qm + Qp) where
Qm = Monocrystalline quartz
Qp = Polycrystalline quartz
F = Total feldspar (P + K) where:
P = Plagioclase
K = K-feldspar
R = Total rock fragments including chert

QtFL

Qt = Total quartz grains (Qm + Qp) including chert where:
Qm = Monocrystalline quartz
Qp = Polycrystalline quartz
F = Total feldspar (P + K) where:
P = Plagioclase
K = K-feldspar
L = Total lithic fragments

QmFLt

Qm = monocrystalline quartz
F = Total feldspar (P + K) where:
P = Plagioclase
K = K-feldspar
Lt = Total lithic fragments including polycrystalline quartz (Qp)

QmPK

Qm = monocrystalline quartz
P = Plagioclase
K = K-feldspar

Table 8. Recalculated sandstone compositions of the Chandarpur Group, Chhattisgarh basin and the Tiratgarh Formation, Indravati basin of the Bastar craton

Sample	QFR			QmFLt			QtFL			QmPK		
No.	Q	F	R	Qm	F	Lt	Qt	F	L	Qm	P	K
Chandarpur Group (Chhattisgarh basin)												
Lohardih Formation												
RD-406	88.50	10.20	1.30	82.90	10.20	6.90	88.50	10.20	1.30	89.10	3.70	7.20
RD-420	76.20	4.50	19.30	74.90	4.50	20.60	95.50	4.50	0.00	94.30	4.00	1.60
RD-421	89.20	3.70	7.10	87.60	3.70	8.70	96.30	3.70	0.00	96.00	0.90	3.20
RN-438	89.10	3.80	7.00	85.50	3.80	10.70	96.20	3.80	0.00	95.70	1.30	3.00
RD-509	93.40	0.40	6.20	88.70	0.40	10.90	99.60	0.40	0.00	99.60	0.00	0.40
RD-523	88.80	6.30	4.90	82.00	6.30	11.70	92.80	6.30	0.90	92.90	1.90	5.20
Chopardih Formation												
RD-404	94.50	1.40	4.00	84.90	1.40	13.70	96.70	1.40	1.90	98.40	0.00	1.60
RN-423	95.90	0.00	4.10	90.30	0.00	9.70	100.00	0.00	0.00	100.0	0.00	0.00
RN-425	94.00	3.30	2.80	92.80	3.30	3.90	96.70	3.30	0.00	96.60	1.00	2.40
Kansapathar Formation												
RD-405	97.50	0.00	2.50	90.60	0.00	9.40	100.00	0.00	0.00	100.00	0.00	0.00
RD-408	97.70	1.60	0.80	93.70	1.60	4.70	98.40	1.60	0.00	98.40	0.60	1.00
RD-409	99.00	0.00	1.00	94.00	0.00	6.00	99.60	0.00	0.40	100.00	0.00	0.00
RD-410	97.60	0.00	2.40	80.90	0.00	19.10	99.80	0.00	0.20	100.00	0.00	0.00
RN-424	99.00	0.80	0.20	93.20	0.80	5.90	99.20	0.80	0.00	99.10	0.00	0 90
RD-510	95.20	0.00	4.80	87.20	0.00	12.80	97.70	0.00	2.30	100.00	0.00	0.00
RD-520	100.00	0.00	0.00	98.10	0.00	1.900	100.00	0.00	0.00	100.00	0.00	0.00
Indravati Group (Indravati basin)												
Tiratgarh Formation												
JC-541	93.10	6.90	0.00	3.40	6.90	89.70	93.10	6.90	0.00	33.30	11.10	55.60
JC-542	93.40	1.90	4.70	91.30	1.90	6.80	97.50	1.90	0.60	98.00	1.50	0.40
JC-543	99.50	0.00	0.50	93.40	0.00	6.60	99.50	0.00	0.50	100.00	0.00	0.00
JT-547	93.90	2.20	3.90	57.30	2.20	40.40	96.20	2.20	1.60	96.30	0.80	2.90
JT-548	94.00	0.00	6.00	88.10	0.00	11.90	99.70	0.00	0.30	100.00	0.00	0.00

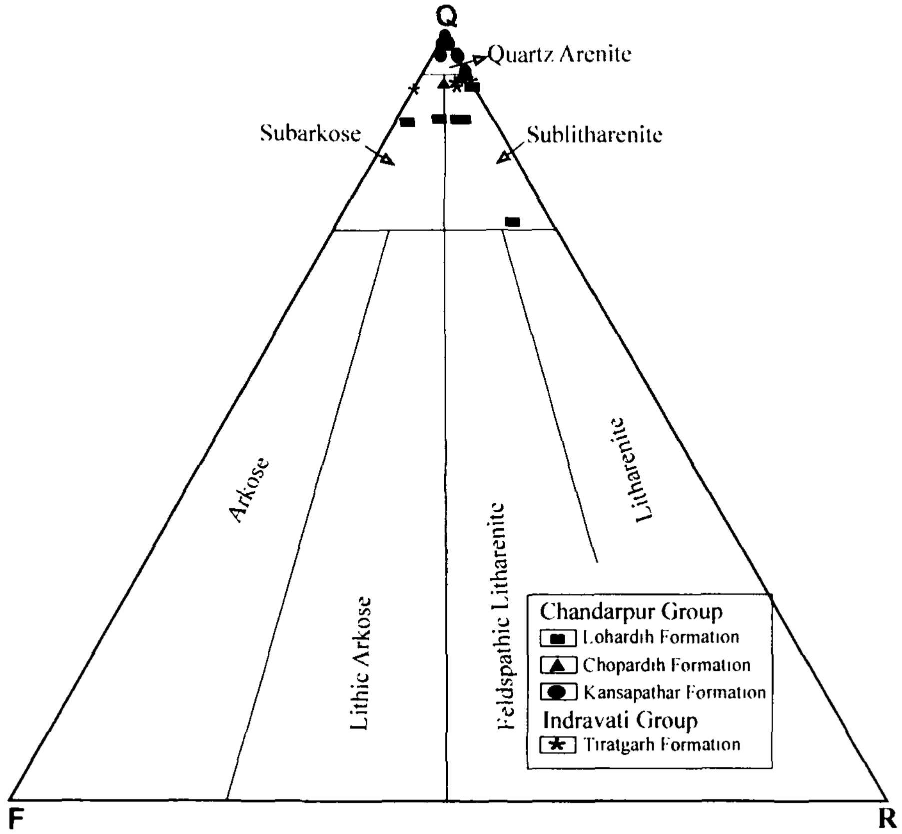

Fig. 7. QFR plot for the classification of sandstone samples from the Chandarpur Group of the Chhattisgarh basin and the Tiratgarh Formation of the Indravati basin (classification after Folk, 1980).

Lt pole of QmFLt plot of Dickinson and Suczek, 1979) and chert was also placed at rock fragment (RF pole) Lt pole as its origin can be unequivocally traced to a sedimentary source, though it was placed at the Q pole by several earlier workers (Blatt, 1967; Pettijohn et al., 1987). Klein (1963) argued that chert is less stable than quartz during transport and placed the chert fragment at the RF pole (Folk, 1980). The F-pole comprises all types of feldspar grains. For recognition of source rock lithology and tectonic setting of the provenance, the recalculated modal data were plotted on QtFL, QmFLt and QmPK triangular diagrams of Dickinson and Suczek (1979). In QtFL diagram, all quartzose grains were plotted together; the emphasis was on grain stability and consequently on weathering and relief in the provenance, transport mechanism, as well as composition of the source rock. In QmFLt diagram all lithic fragments were plotted together and emphasis was shifted towards the grain size of the rocks, because finer-grained rocks yield more lithic fragments in the sand-size range.

Modal analysis reveals that the main detrital framework mineral grains of the Chandarpur Group and the Tiratgarh Formation of the Indravati Group include quartz, potash feldspar, plagioclase, rock fragments especially chert, mica and heavy minerals. Sandstones of the Chandarpur Group and the Tiratgarh Formation are characterized by abundant quartz grains (82.22 % and 88.16 % on average, respectively). According to Folk's classification (Folk, 1980), the sandstones of the Chandarpur Group and the Tiratgarh Formation are mostly subarkoses, sublitharenites and quartzarenite (Fig. 7). Quartz occurs mainly as monocrystalline quartz. Some of these have undulatory extinction. Polycrystalline quartz represented by recrystallised and stretched metamorphic quartz occurs in subordinate proportions (Appendix I). In majority of polycrystalline grains, subgrains with both straight and sutured contacts are common. Stretched metamorphic quartz grains (Folk, 1980) are rare. Many of the quartz grains are stained and impregnated with the iron-oxide. Feldspar constitutes 1.87 % and 2.02 % on average of the framework grains of the Chandarpur Group and the Tiratgarh Formation respectively, and is dominated by microcline. However, plagioclase is also present in minor quantities in some samples (Appendix I). Rock fragments are very few and are dominated by sedimentary lithics especially chert and followed by metamorphic lithics mostly schist fragments. Heavy minerals are rare and are dominated by zircon. These sandstones are generally matrix free. Authugenic quartz, iron oxide and calcite are dominantly cementing material. Quartz cement occurs primarily as overgrowth around detrital grains.

3.3 CHANDARPUR GROUP (CHHATTISGARH BASIN)

3.3.1 LOHARDIH FORMATION

Lohardih Formation is dominated by quartz (70.91 % on average). Monocrystalline quartz is dominant type, averages 67.51 %. Feldspar content of this Formation exceeds that of any other unit documented here and the entire feldspar population averages 3.9 % for the sample set. Microcline dominates over plagioclase. Plagioclase/K-feldspar ratio (P/K ratio) averages 0.5. Most of the samples of the Lohardih Formation show little compaction and framework grains especially quartz (both well rounded quartz and angular quartz) are seen floating in carbonate cement (Fig. 8A and B). Some feldspar grains are replaced by carbonate cement through cracks and cleavages (Fig. 9A). The rock fragments are negligible in these sandstones and are made

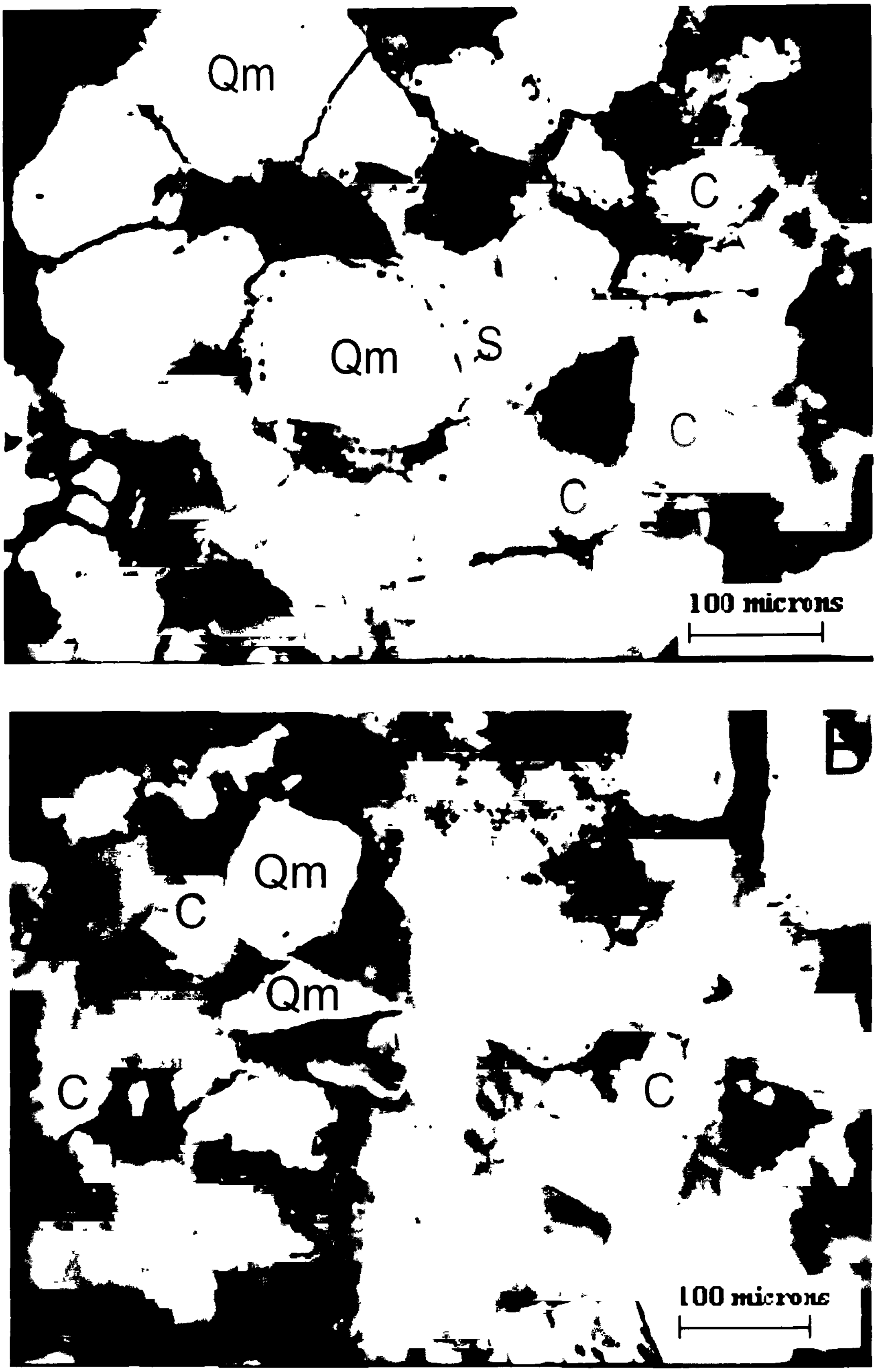

Fig. 8. Photomicrographs of sandstones of the Chandarpur Group, Chhattisgarh basin showing different types of mineral grains present. Qm - *monocrystalline* quartz, *S - silica* overgrowth, *C - calcite* cement. *(A) Lohardih* sandstone showing multicycle quartz grain floating in calcite cement and (B) Lohardih sandstone showing presence of well rounded and angular quartz grains floating in calcite cement.

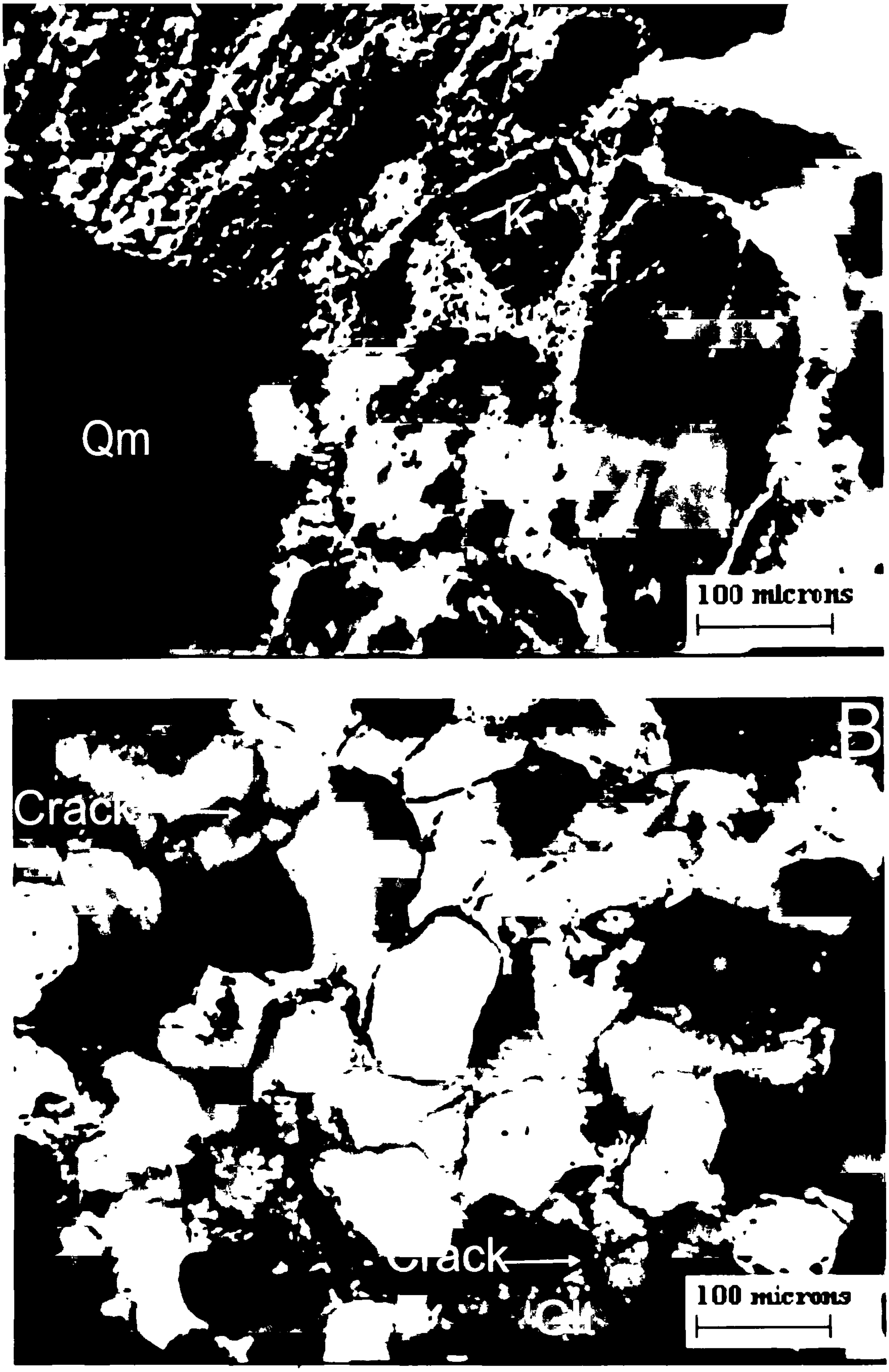

Fig. 9. Photomicrographs of sandstones of the Chandarpur Group, Chhattisgarh basin showing different types of mineral grains present. Qm - monocrystalline quartz , K - K-feldspar, Glt - glauconite, C - calcite cement. (A) Lohardih sandstone showing microcline replaced by calcite along twinning planes and (B) Chopardih sandstone showing presence of glauconite with cracks.

of chert and fine grained rock fragment, composed of quartz and mica. This stratigraphic unit has the highest representation of chert grains (5.02 % on average). Iron oxide is the dominant cement and occurs as isolated patches within interstitial spaces and as grain coating.

3.3.2 CHOPARDIH FORMATION

The Chopardih Formation is characterized high values of quartz (81.39 % on average). Monocrystalline quartz constitutes 76.59 % of the quartz. Polycrystalline quartz generally constitutes 4.8 % of quartz grains. Microcline dominates over plagioclase (P/K ratio averages 0.25) for the sample set. Glauconite pellets are very common in the Chopardih Formation (up to 11.28 %). Glauconite pellets commonly occur within interstitial spaces coated with ferrugenous materials. In thin sections the glauconites grains are generally olive green and show a weak green pleochroism (Fig. 9B). Many of the glauconitic grains display irregular surface cracks which taper inwards. Such cracks have previously been interpreted as either expansion cracks relating to differential mineral growth in the pellets (Odin and Morton, 1988), or as shrinkage cracks related to dehydration during the mineralogical evolution of glauconites (McRae, 1972). The cementing material is mostly silica cement (quartz overgrowth).

3.3.3 KANSAPATHAR FORMATION

This stratigraphic unit has the highest representation of quartz grains (average 94.38 %) for the entire basinal infill. The framework grains of the Kansapathar Sandstone Formation are composed dominantly of monocrystalline quartz and polycrystalline quartz with insignificant feldspar and rock fragments including chert which accounts 1.2 % on average. Stretched metamorphic quartz is very common among the polycrystalline quartz. The intergranular space is entirely filled by the quartz cement which constitutes about 2.34 % on average. An interlocking quartz mosaic is developed due to silica overgrowth on the grains (Fig. 10A and B). Quartz cement occurs primarily as overgrowth around quartz detrital grains, in optical continuity with cores. The overgrown rims are free of iron oxide stains, but are separated from the core by the sheath of iron oxide.

3.4 INDRAVATI GROUP (INDRAVATI BASIN)

3.4.1 TIRATGARH FORMATION

The Tiratgarh Formation is dominated by high values of quartz (88.16 % on average). Monocrystalline quartz is dominant quartz type (61.89 % on average) (Fig. 11A), but in some samples polycrystalline quartz dominates (Figs. 11B and 12A). K-feldspar dominates over plagioclase except in one sample (P/K ratio averages 0.37) and the entire feldspar population averages 2.02 % for all samples. The sandstones are mainly cemented by carbonate cement and silica cement. Some quartz grains are seen floating in carbonate cement. Heavy minerals and opaques are rare and are dominated by zircon and iron oxides respectively. Quartz cement occurs primarily as overgrowth around detrital quartz grains. Chert fragments are dominant over schist rock fragment (Fig. 12B).

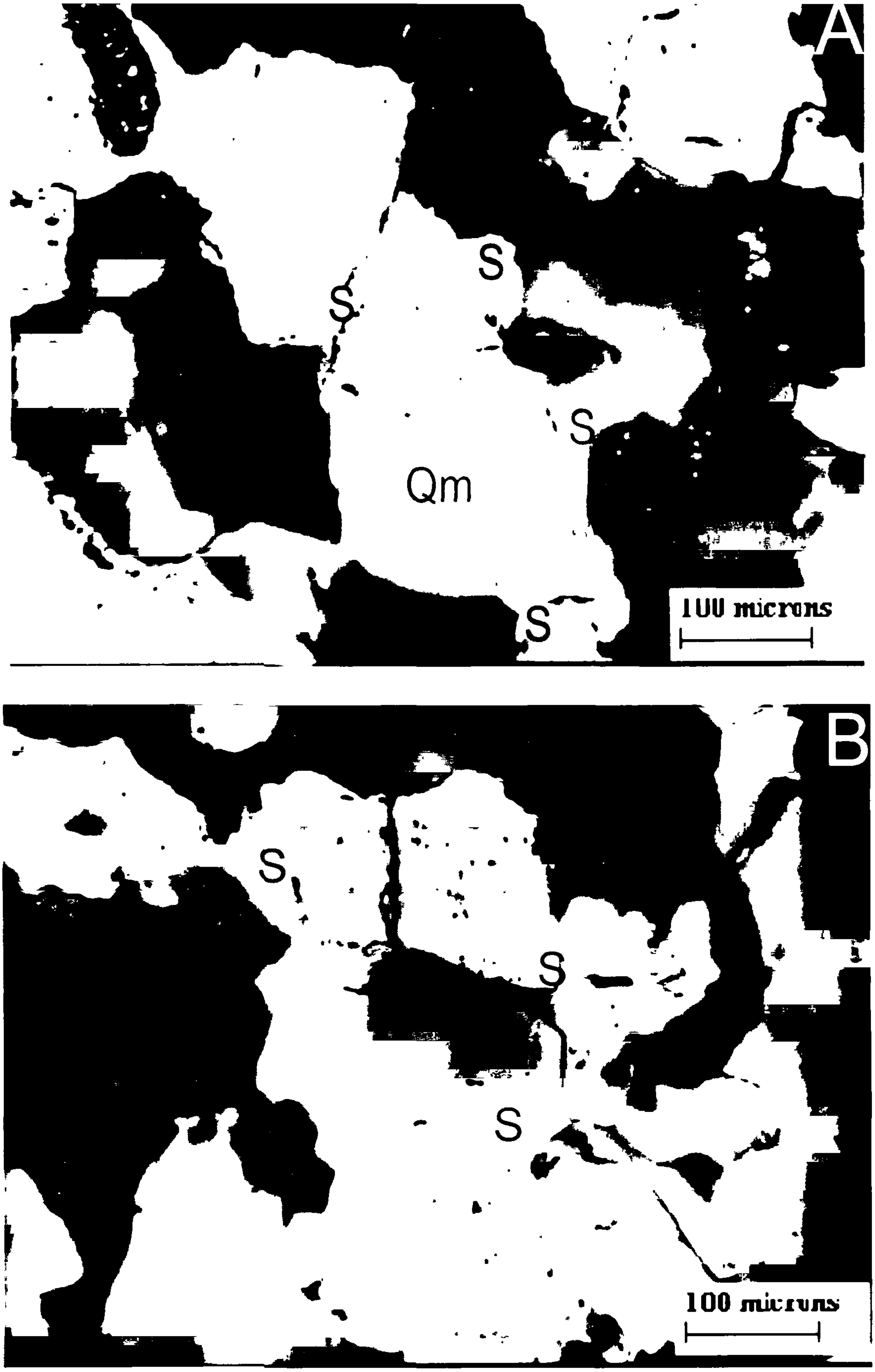

Fig. 10. Photomicrographs of sandstones of the Chandarpur Group, Chhattisgarh basin showing different types of mineral grains present. Qm - monocrystalline quartz, S - silica overgrowth. (A) and (B) Kansapathar sandstone showing advance stage of silica overgrowth.

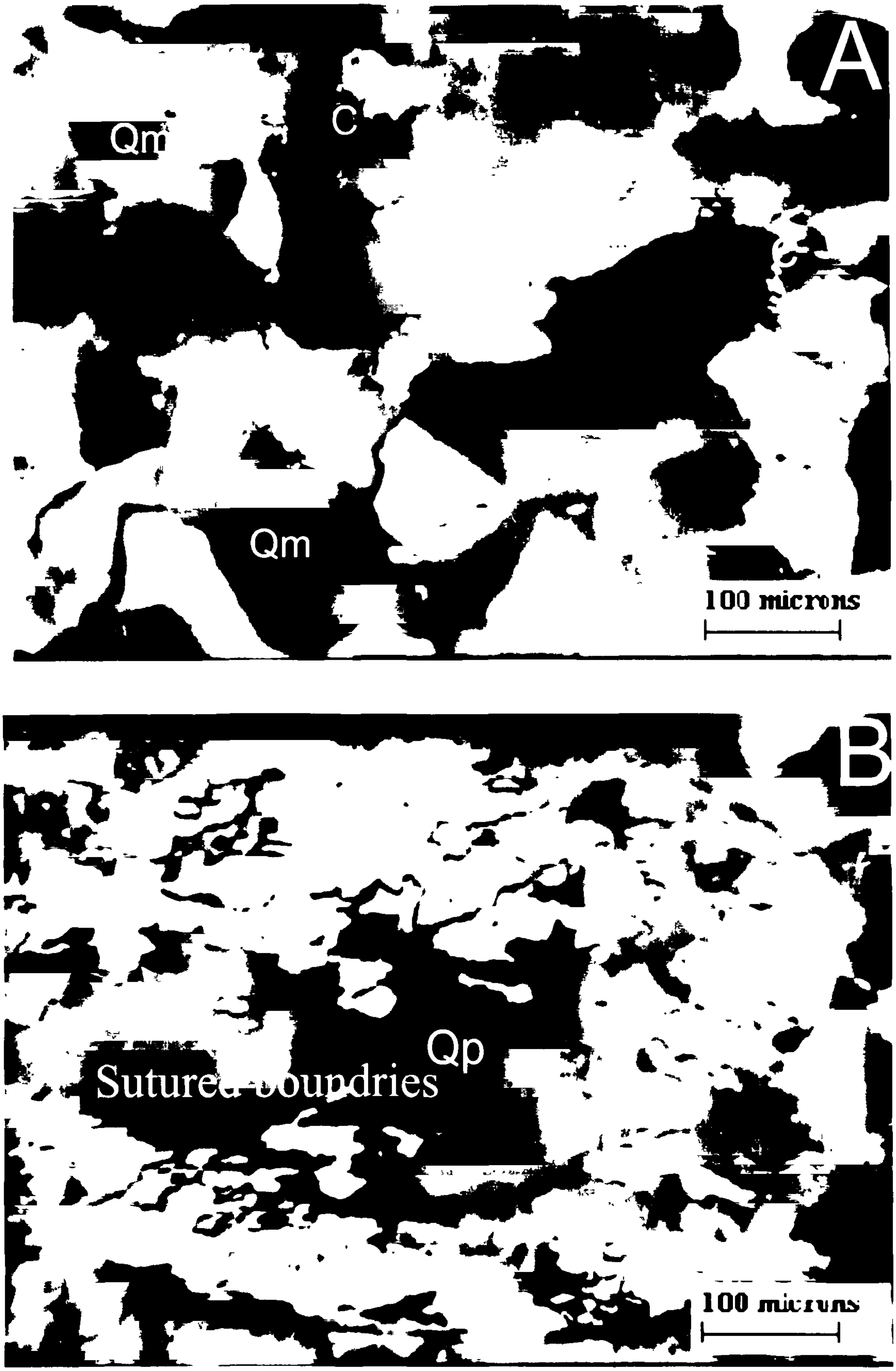

Fig. 11. Photomicrographs of sandstones of the Tiratgarh Formation, Indravati basin showing different types of mineral grains present. Qm - monocrystalline quartz, Qp - polycrystalline quartz and C - calcite cement, (A) Tiratgarh sandstone showing monocrystalline quartz grains cemented by calcite and (B) Tiratgarh sandstone showing polycrystalline quartz grain with semicomposite crystals with sutured contacts.

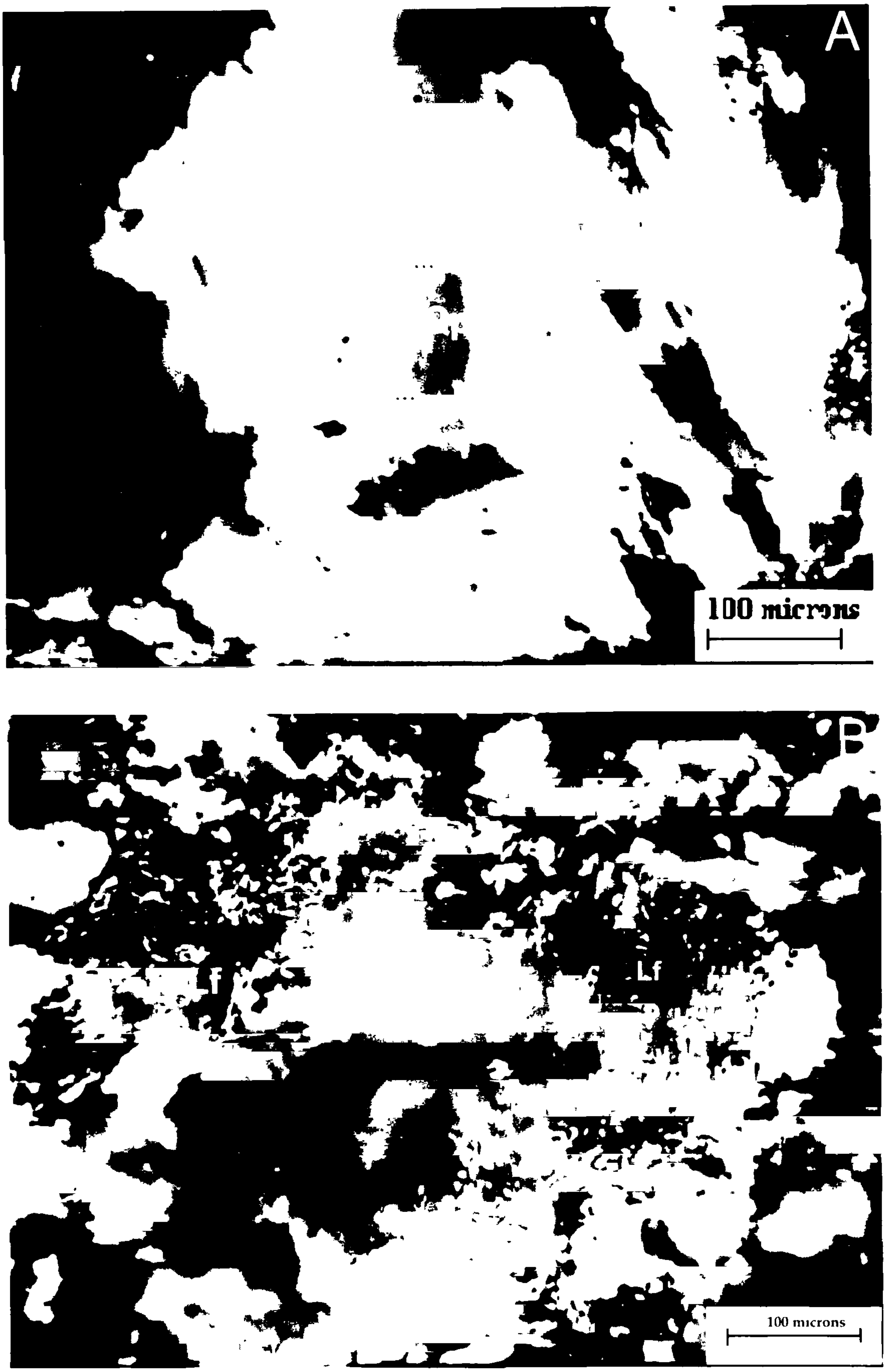

Fig. 12. Photomicrographs of sandstones of the Tiratgarh Formation, Indravati basin showing different types of mineral grains present. Qp - pollycrystalline quartz, Lf - lithic fragment (A) Tiratgarh sandstone showing polycrystalline quartz grain with highly stretched semicomposite crystals and (B) Tiratgarh sandstone showing metamorphic lithic fragments (schist fragments).

Chapter-IV

GEOCHEMISTRY

4. GEOCHEMISTRY

4.1 SAMPLING AND ANALYTICAL TECHNIQUES

Fresh samples (measuring about 6″x 4″) of the pelites, shales, sandstones and quartzites were collected from the outcrops. Locations of the samples are shown in Fig. 6. The rock samples have been collected from the Paleoproterozoic Sakoli and Sausar basins and the Neoproterozoic Chhattisgarh and Indravati basins of the Bastar craton with a view to observe spatial as well as stratigraphic variations. Extensive care has been taken to collect only the fresh samples from the outcrops. Prior to geochemical analysis, the rocks were studied under the microscope. Effects of alterations were observed in thin sections, and the samples which show least alteration effects, were opted for geochemical studies. After careful petrographic studies from the point of view of secondary alterations, and also for representation of maximum possible spatial and temporal variations of the clastic rocks, altogether twenty three samples were selected for geochemical analysis. Out of the twenty three samples, four pelite and three quartzite samples belong to the Bhiwapur Formation and the Pawni Formation of the Sakoli basin, and the Junewani Formation of the Sausar basin. Seven shale and five sandstone samples belong to the Gunderdehi Formation, the Tarenga Formation, the Lohardih Formation, the Chopardih Formation and the Kansapathar Formation of the Chhattisgarh basin, and two sandstone and two shale samples belong to the Tiratgarh Formation and the Jagdalpur Formation of the Indravati basin (Appendix II).

Rock samples were reduced to smaller size (~3cm) to observe any alteration. The chips were further crushed to yet smaller sizes (~2mm) then washed with distilled water and sun dried. These were then pulverized to ~200 mesh in agate mortar. Major elements were analyzed on WD-XRF (Siemens SRS 3000) at Wadia Institute of Himalayan Geology (WIHG), Dehradun. The accuracy (% RSD) for major oxide is less than 5 % and the precision is better than 1.5 % (Saini et al., 1998). Details of the analytic techniques, precision and accuracy of the machine are described by Saini et al. (1998). Trace elements including rare earth elements (REE) were analyzed on ICP-MS (Perkin Elmer Sciex ELAN DRC II) at National Geophysical Research Institute (NGRI), Hyderabad. The precision of ICP-MS trace and rare earth element (REE) data is < 5 % RSD for all the trace and rare earth elements. Details of the analytical techniques, accuracy and precision of the instrument are described by Balram et al. (1996). International standards like GSR-4 (sandstone), GSR-5 (shale), ASK-2 (schist), and JG-2 (quartzite) were used for calibration and testing of accuracy. Whole rock major and trace element data of the pelites, shales, sandstones and quartzites are presented in Appendix II.

4.2. GEOCHEMICAL CHARACTERISTICS

4.2.1. NEOPROTEROZOIC SHALES AND PALEOPROTEROZOIC PELITES

4.2.1.1 MAJOR ELEMENTS

The major element analysis of the Neoproterozoic shales of the Chhattisgarh and Indravati basins, and the Paleoproterozoic pelites of the Sakoli and Sausar basins of the Bastar craton are given in Appendix II. Under microscope, the Neoproterozoic shales of the Bastar craton display compositional variation from typical shale to calcite rich shale. This is best depicted by the abundance of CaO in these shales. Therefore, this allows separation of our shale samples into the calcareous shales (the Gunderdehi Formation of the Chhattisgarh basin) at >6 % CaO and the non-calcareous shales (the Tarenga

Formation of the Chhattisgarh basin and the Jagdalpur Formation of the Indravati basin) at < 0.3 % CaO. The calcareous shales have lower SiO_2 (43 %), Al_2O_3 (10 %) and $Fe_2O_3^t$ (3.3 %) content and higher CaO content (21 %), whereas the non-calcareous shales have higher SiO_2 (64 %), Al_2O_3 (17 %) and $Fe_2O_3^t$ (7.39 %) content and lower CaO content (0.1 %). The calcareous shales show large variations in Al_2O_3 content (7 % - 14.23 %) and in CaO content (6.84 % - 35 %). In these shales Al_2O_3 and K_2O content increases with the increase in SiO_2 content and decreases with the increase in CaO content, indicating clay minerals dominantly controling Al_2O_3, K_2O and SiO_2 contents and calcite controling the CaO content. The inverse linear trend of CaO against SiO_2 in the calcareous shales may indicate carbonate in these shales to be primary rather than secondary, because the influence of secondary carbonate should result in scatter on CaO – SiO_2 plot (Fig. 13) (Feng and Kerrich, 1990; Gu, 1994).

In comparison to NASC (North American Shale Composite; representative of continentally derived sediments) (Gromet et al., 1984), the non-calcareous shales show enrichment in $Fe_2O_3^t$ and K_2O and depletion in Na_2O and CaO. The non-calcareous shales also show concentrations of SiO_2, Al_2O_3, TiO_2, MnO and P_2O_5 similar to NASC. The calcareous shales show depletion in all major elements except for CaO and MnO relative to NASC and the depletion is most in SiO_2, Al_2O_3 and Na_2O (Appendix II).

In contrast, the Paleoproterozoic pelites are characterized by lower SiO_2 (59 %) and higher $Fe_2O_3^t$ + MgO (10.41 %) compared to the non-calcareous shales (8.6 %) and NASC. Immobile constituents like TiO_2 (0.75 %), Al_2O_3 (22.02 %) and $Fe_2O_3^t$ (8.62 %) are enriched in the pelites compared to the non-calcareous shales, calcareous shales and NASC. Mobile constituents like Na_2O (0.5 % for the pelites and 0.2 % for the non-calcareous shales) and CaO (0.25 % for the pelites and 0.1 % for the non-calcareous shales) are strongly depleted in the pelites and the non-calcareous shales compared to NASC, whereas the calcareous shales with reference to NASC are depleted only in Na_2O and not in CaO. K_2O is enriched in both the non-calcareous shales (5.5 %) and the pelites (4.8 %) than NASC. However, in the calcareous shales K_2O is lower (2.6 %) compared to the non-calcareous shales, pelites and NASC (Appendix II). The non-calcareous shales and pelites contain very low CaO concentration (<0.3 %), which can be expected to be present in feldspar minerals. Petrographic observation of thin sections also confirms the absence of carbonates and presence of minor amount of plagioclase minerals in these non-calcareous shales and pelites. The calcareous shales and the non-calcareous shales show lower TiO_2 values than do the pelites. The Jagdalpur shales have higher TiO_2 content among the non-calcareous shales and the calcareous shales.

Before we begin to understand how and when major and trace element monitor composition in detrital sedimentary rocks, we need to know which minerals control the element distribution and how the proportions of these minerals vary with lithological composition. One good approach to this problem is to look at a possible correlation between specific elements that monitor the relative abundances of specific minerals.

In the calcareous shales most of the major oxides (except CaO) show positive correlation with SiO_2, Al_2O_3 and K_2O indicating these elements are controlled by clay minerals (Figs. 13, 14 and 15). The plots of $Fe_2O_3^t$, K_2O and TiO_2 vs. Al_2O_3 and K_2O yield linear plots for the calcareous shales indicating all these elemental oxides are

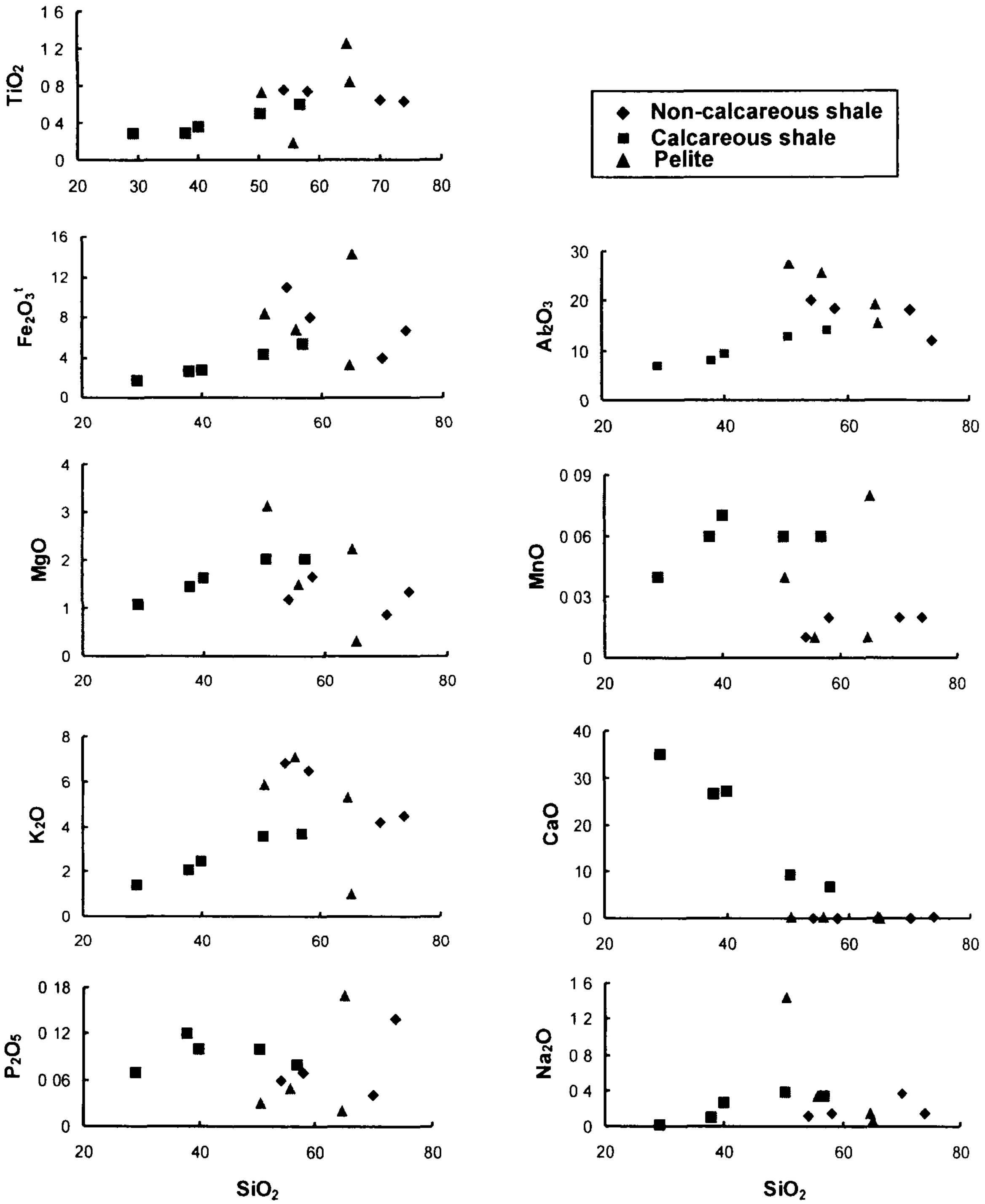

Fig. 13. Major oxides (wt. %) vs. SiO_2 (wt. %) for the non-calcareous shales and the calcareous shales of the Neoproterozoic Chhattisgarh and Indravati basins and the pelites of the Paleoproterozoic Sakoli and Sausar basins of the Bastar craton.

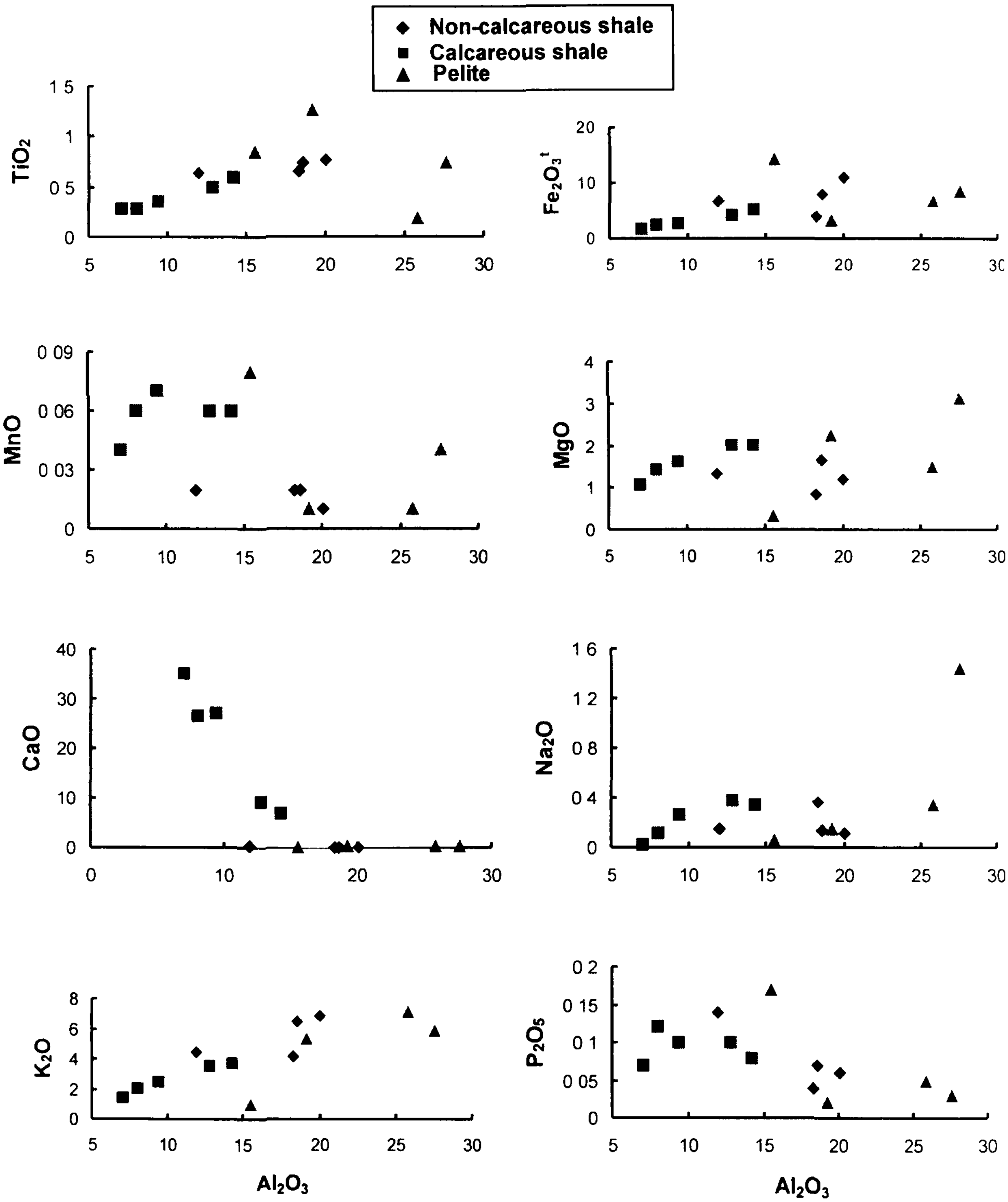

Fig. 14. Major oxides (wt. %) Vs. Al_2O_3 (wt. %) for the non-calcareous and calcareous shales of the Neoproterozoic Chhattisgarh and Indravati basins and the pelites of the Paleoproterozoic Sakoli and Sausar basins of the Bastar craton.

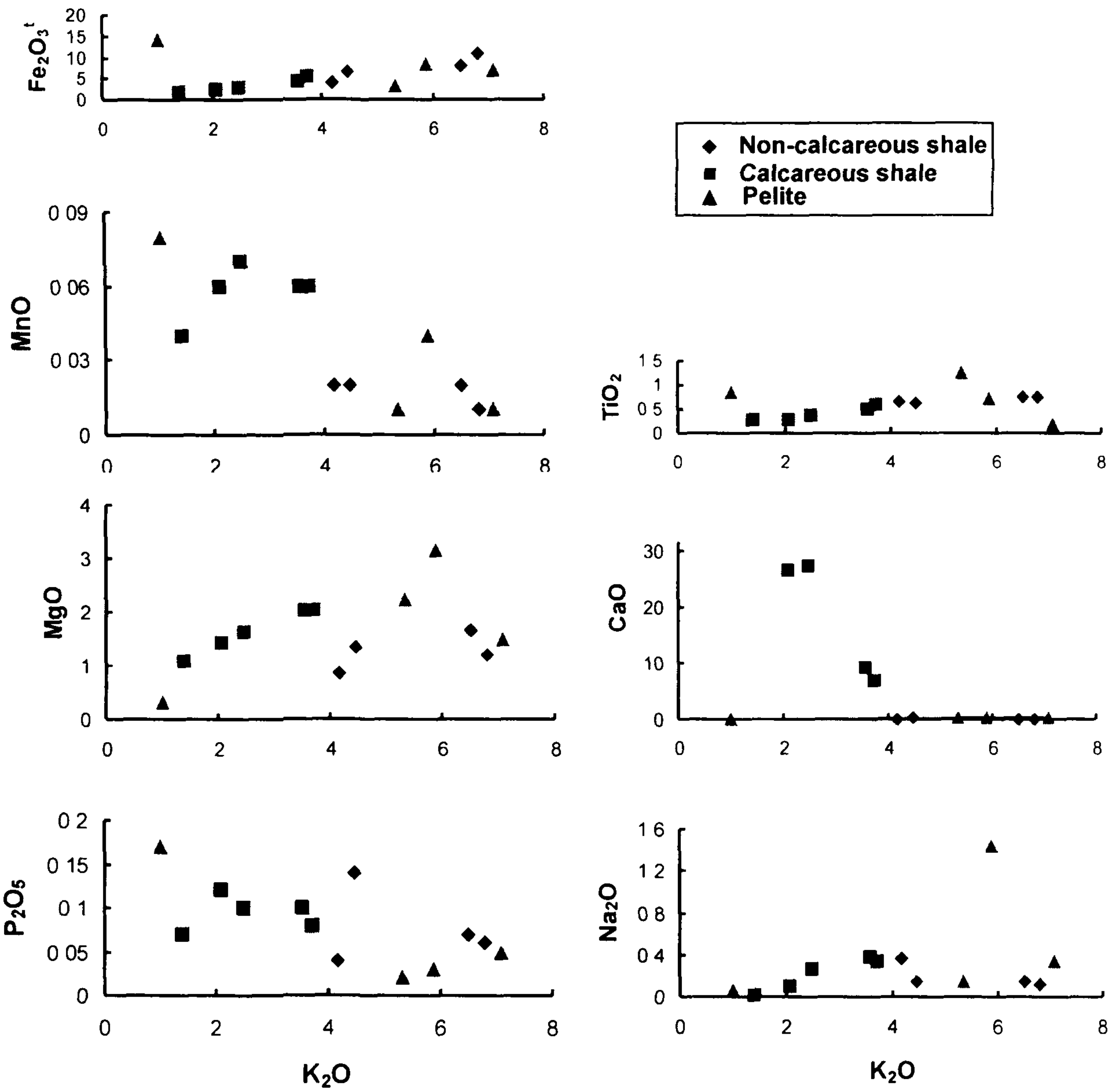

Fig. 15. Major oxides (wt. %) vs. K_2O (wt. %) for the non-calcareous shales and calcareous shales of the Neoproterozoic Chhattisgarh and Indravati basins and the pelites of the Paleoproterozoic Sakoli and Sausar basins of the Bastar craton.

incorporated into the clay minerals (Figs. 14 and 15). For the calcareous shales, CaO content decreases with the increase in Al_2O_3 content indicating CaO in the calcareous shales is controlled by calcite (Fig. 14) (Parekh et al., 1977; Cullers, 2002). In the non-calcareous shales and pelites $Fe_2O_3^t$, K_2O and TiO_2 also show linear trend against Al_2O_3, indicating all these elemental oxides are incorporated into the clay and mica minerals (Fig. 14).

The positive correlation of $Fe_2O_3^t$, MgO and TiO_2 with Al_2O_3 and K_2O in the calcareous shales, non-calcareous shales and pelites indicate clay-mica minerals (phyllosilicates) control on these elements (Figs. 14 and 15). This is suggested by linear trend between Al_2O_3 and K_2O (Fig. 14). All the non-calcareous shales, calcareous shales and pelites have low P_2O_5 and MnO contents. However, the calcareous shales have higher P_2O_5 and MnO content than the non-calcareous shales and pelites (Appendix II). The MnO and P_2O_5 do not show good positive correlation with either Al_2O_3 or K_2O (Fig. 14 and 15). This may suggest that mica and clay (phyllosilicates) fraction are not the only phases controlling these elements in the calcareous shales, non-calcareous shales and pelites. It is possible that minor accessory minerals like Fe-Ti oxides, sphene, apatite, epidote and monazite contain at least some of the Fe, Mg, Ti, Mn and P.

In the non-calcareous shales and pelites, SiO_2 shows negative correlation with Al_2O_3 (Fig. 13), indicating dilution of Al_2O_3 with increase in quartz content. The K_2O/Al_2O_3 ratio of sediments can be used as an indicator of original composition of ancient sediments. The K_2O/Al_2O_3 ratios for clay minerals and feldspars are different (0-0.3, 0.3-0.9 respectively, (Cox et al., 1995). The average K_2O/Al_2O_3 ratio for the calcareous shales varies from 0.19 to 0.27 and for the non-calcareous shales, it varies from 0.22 to 0.37. In most of the samples, the K_2O/Al_2O_3 ratios are close to the upper limit of the clay mineral range, which suggests illite to be dominant clay mineral in these shales.

4.2.1.2. TRACE ELEMENTS

Large ion lithophile elements such as Rb, Sr, Ba and Cs behave similarly to related major elements during weathering processes. Like K_2O, Rb and Cs will be incorporated into clays during chemical weathering. In contrast, CaO, Sr and Na_2O tend to be leached (Nesbitt et al., 1980). Ca, Na along with Rb and Cs are mainly controlled by feldspar, so depletion of Ca, Na, Rb and Cs in the samples may suggest depletion of feldspar in studied samples. The absence of feldspar can be explained either by (i) removal of feldspar by post-depositional dissolution or through weathering in the source area or (ii) by their depletion in the source rocks. Considering the higher concentrations of Rb and Cs in shales and pelites compared to CaO and Na_2O, the former seems more probable.

Most of the trace elements have higher concentration in the non-calcareous shales compared to the calcareous shales except for Sr and Ba (Appendix II). Plots of transition elements like Sc, V, Ni, Cr vs. Al_2O_3 and K_2O yield linear plots for both the calcareous and the non-calcareous shales (Fig. 16). This may suggest that these elements in the calcareous and the non-calcareous shales are housed in the clay minerals (Parekh et al., 1977, Cullers, 2002). When Rb and Sr are plotted against Al_2O_3 and K_2O in the calcareous shales, Rb shows a positive linear trend against Al_2O_3 and K_2O, whereas Sr shows a negative linear trend with Al_2O_3 and K_2O (Fig. 17). However, Sr in the calcareous shales shows a positive correlation with CaO (r = 0.82). This indicates Sr is housed in calcite and Rb is housed in clay minerals in the calcareous shales.

The other trace elements (LILEs and HFSEs) like Cs, Nb, U and Zr also show linear trend against Al_2O_3 and K_2O (Figs. 17 and 18). However, elements like Ba, Y and Ta do not show linear trend against Al_2O_3 and K_2O (Figs. 17 and 18) indicating some accessory minerals other than clay minerals (e.g. allanite for Y and barite for Ba) controlling their abundance.

Overall, the average concentrations of most of the trace elements are quite different in the calcareous shales compared to the non-calcareous shales. Those trace elements that are concentrated in clay minerals are higher in the non-calcareous shales compared to the calcareous shales. In contrast, those major and trace elements that are concentrated in calcite (CaO, Sr) are higher in the calcareous shales when compared with the non-calcareous shales. Most elemental concentrations decrease from non-calcareous shales to calcareous ones. This variation is presumably due to the fact that most elements are concentrated in clay minerals compared to calcite. When compared with NASC, both the calcareous and non-calcareous shales are depleted in transition elements like V, Ni, Cr and Co. However, the non-calcareous shales are enriched in other trace elements (large ion lithophile elements and high field strength elements) like Rb, Cs, Th, Ta and Nb, and show similar concentrations of Sc and Hf relative to NASC. On the other hand the calcareous shales are enriched in trace elements like Sr, Cs, Ba and Th, and show similar concentration of Sc and Th relative to NASC (Appendix II).

Relative to the Neoproterozoic calcareous and non-calcareous shales, Paleoproterozoic pelites are highly enriched in all transition elements especially in Cr

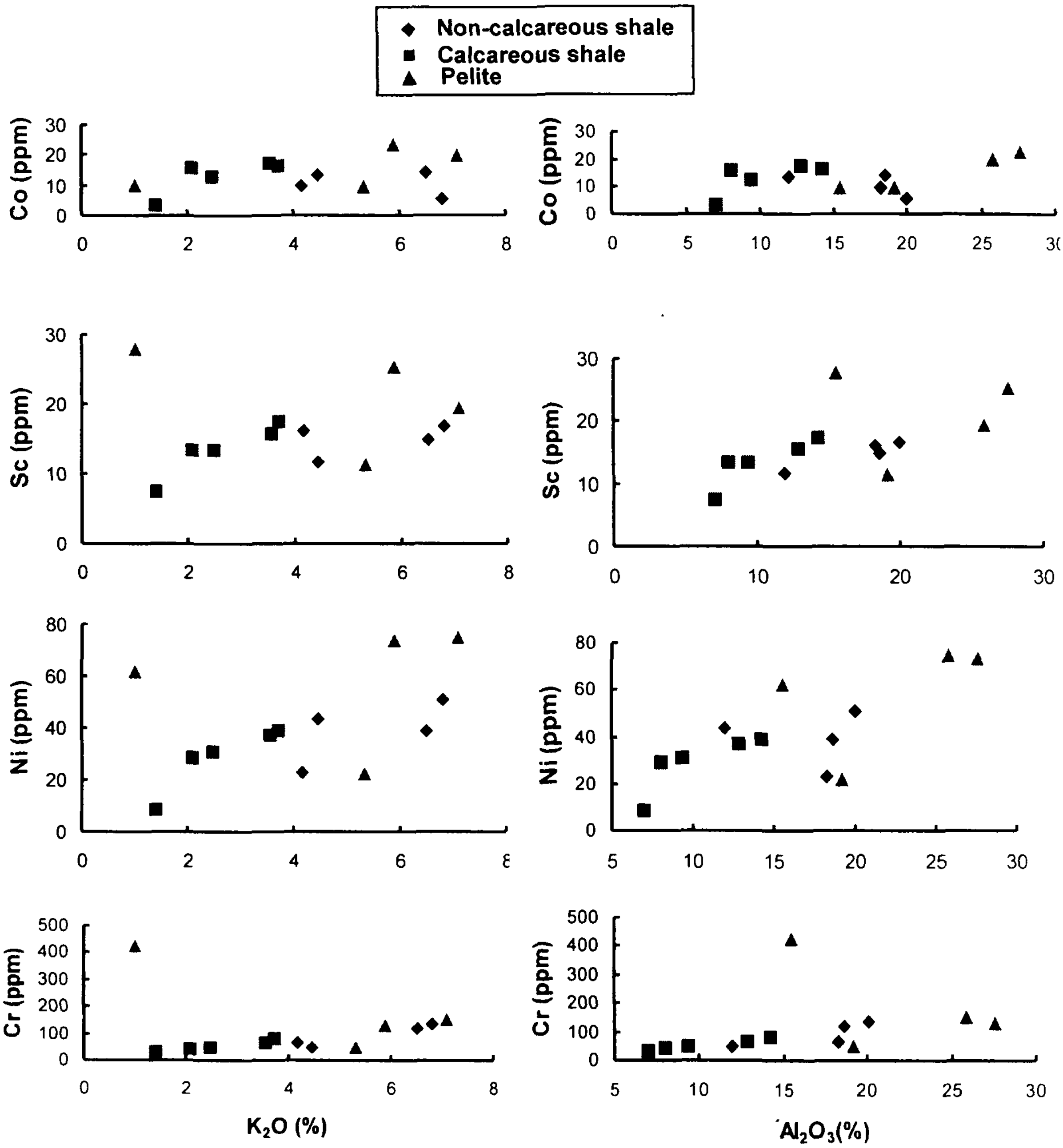

Fig. 16. Plot of transition elements vs. Al_2O_3 and K_2O for the non-calcareous shales and calcareous shales of the Neoproterozoic Chhattisgarh and Indravati basins and pelites of the Paleoproterozoic Sakoli and Sausar basins of the Bastar craton.

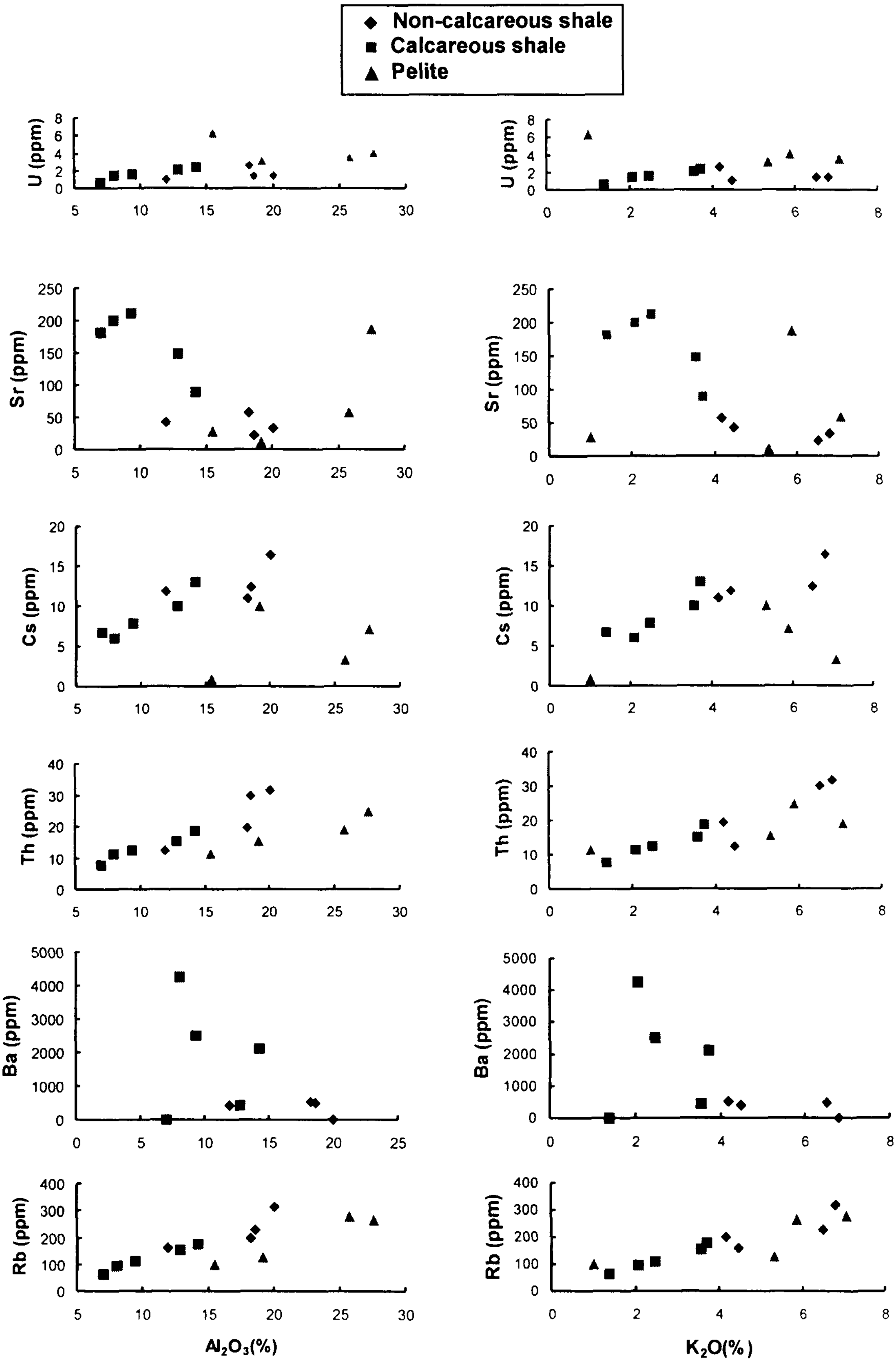

Fig. 17. Plot of large ion lithophile elements (LILE) vs. Al_2O_3 and K_2O for the non-calcareous shales and calcareous shales of the Neoproterozoic Chhattisgarh and Indravati basins and pelites of the Paleoproterozoic Sakoli and Sausar basins of the Bastar craton.

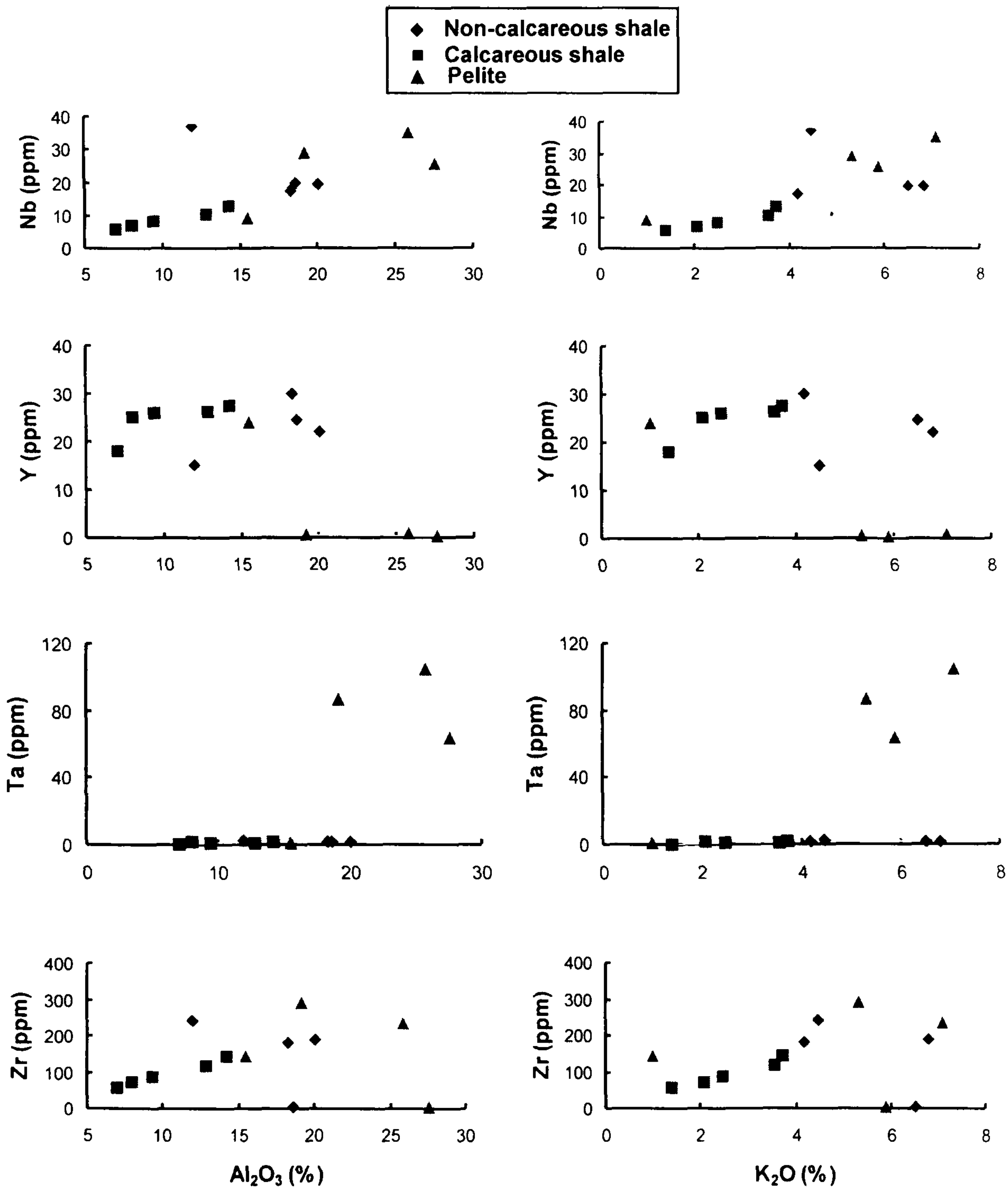

Fig. 18. Plot of high field strength elements (HFSE) vs. Al_2O_3 and K_2O for the non-calcareous shales and calcareous shales of the Neoproterozoic Chhattisgarh and Indravati basins and pelites of the Paleoproterozoic Sakoli and Sausar basins of the Bastar craton.

(189 ppm), Ni (58 ppm), Sc (21 ppm) and V (100 ppm) (Appendix II). In pelites transition elements like Ni and Co show good positive correlation with Al_2O_3 or K_2O while Cr and Sc do not correlate with Al_2O_3 and K_2O (Fig. 16). Average contents of LILE (except Sr and U) like Rb, Cs and Th of pelites are lower than those of the calcareous and the non-calcareous shales. The calcareous and the non-calcareous shales are enriched in LILE especially in Th compared to pelites, while pelites are enriched in HFSE like Zr, Hf, Nb compared to the calcareous and the non-calcareous shales. In comparison to NASC, pelites are enriched in transition elements like Sc, V, Ni and Cr. The pelites are also enriched in other trace elements like Rb, Nb, Cs, Ta, Th, U and depleted in Sr, Y, Zr, Hf relative to NASC (Appendix II). Most of the LILE and HFSE (e.g. Th, U, Rb, Sr) in pelites show good positive correlation against Al_2O_3 and K_2O indicating mica (phyllosilicate) control on their contents (Fig. 17 and 18).

4.2.1.3. RARE EARTH ELEMENTS (REE)

The sedimentary rocks preserve a record of the provenance and the processes of weathering (McLennan, 1989). Rare earth elements (REE) have very similar geochemical properties and are not easily fractionated during sedimentary processes and will not be affected to any great extent during a silicification episode (McLennan, 1989). The REEs are considered to be essentially uniform in abundances in fine grained clastic sedimentary rocks and are not significantly affected by weathering, diagenesis and most forms of metamorphism (Haskin et al., 1966; Nance and Taylor, 1977; Chaudhri and Cullers, 1979). The REEs are therefore very important in understanding crustal evolution. Total REE concentration ($\sum$REE) in the calcareous and the non-calcareous shales is variable with the highest mean value in the non-calcareous shales to be 263 ppm and the lowest mean value in the calcareous shales being 122 ppm. The ∑REE concentrations of the non-calcareous shales are higher than those of the NASC (183 ppm). The total REE concentration of the calcareous shales is very much lower than that of the NASC (Appendix II). The large differences in REE content between the calcareous and the non-calcareous shales may be due to the reason that REE normally reside in fine fraction (silt or clay) and it has also been inferred that the trivalent REE are readily accommodated in most clay-mica minerals (phyllosilicates) enriched with alumina and ferric iron (Cullers et al., 1987, Cullers, 1988). Therefore, the calcareous shales contains the lowest REE content due to its higher calcite content, while the non-calcareous shales contain the higher REE concentrations due to absence of calcite (Haskin et al., 1966). The moderate positive correlation between REEs and Al_2O_3, K_2O in the calcareous and non-calcareous shales (Fig. 19) suggests that clay and micas are important in hosting the REEs (Condie, 1991). Aluminum is the main constituent of the clay and mica minerals. It is now considered that the REE generally reside in minerals like zircon, monazite, allanite and apatite etc. (McLennan, 1989). The lack of good correlation between LREE and HREE with Zr in the non-calcareous shales (Fig. 16), suggests zircon does not control the REE abundances in the non-calcareous shales. However, in the calcareous shales Zr correlates positively with LREE and HREE indicating zircon control on REE in the calcareous shales (Fig. 19). In the calcareous and the non-calcareous shales LREE show linear trend with Th (Fig. 19), while HREE show linear trend with Y (Fig. 19), indicating monazite control for the LREE abundances and allanite control for the HREE. A negative or insignificant correlation is observed between P_2O_5 vs. LREE ($r = 0.27$ for the calcareous

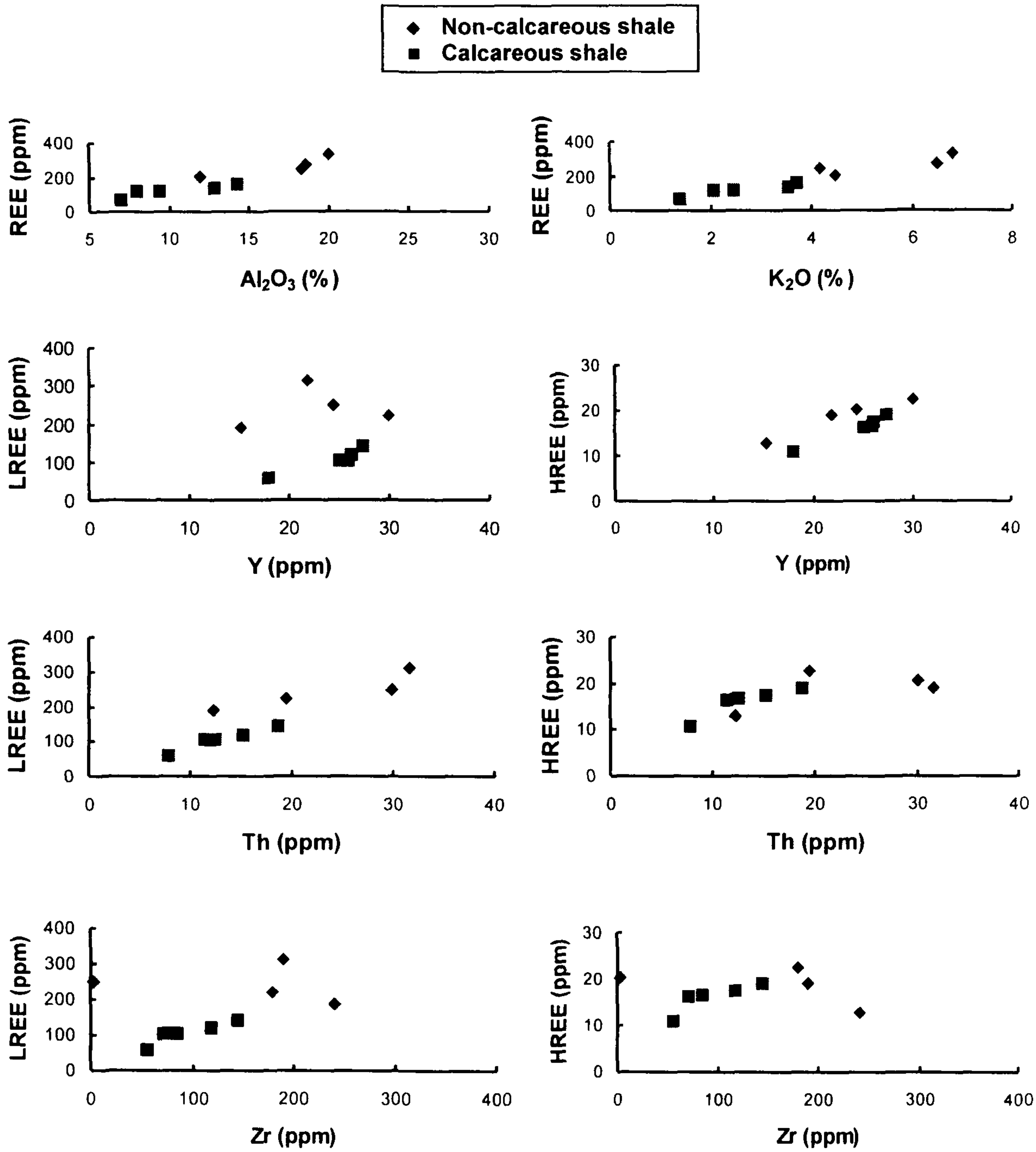

Fig. 19. Plot of REE vs. Al_2O_3 and K_2O and REE vs. Y, Th and Zr for the non-calcareous and calcareous shales of the Neoproterozoic Chhattisgarh and Indravati basins of the Bastar craton.

shales and r = 0.56 for non-calcareous shales) and HREE (r = 0.44 for the calcareous shales and r = -0.96 for the non-calcareous shales). This suggests that apatite is not controlling either LREE or HREE in the calcareous and the non-calcareous shales (Fig. 19).

In chondrite normalized REE plot (Sun and McDonough, 1989) (Fig. 20), both the calcareous and the non-calcareous shales show highly LREE enriched and flat HREE patterns with negative Eu anomaly. The non-calcareous shales have higher (La/Yb)n ratio (18) compared to the calcareous shales (7), while the (Gd/Yb)n ratio in both the non-calcareous and the calcareous shales do not show much variation (1.9 and 1.4, respectively). The calcareous and the non-calcareous shales also exhibit significant negative Eu anomaly (Eu/Eu* = 0.65 for the non-calcareous shales and 0.8 for the calcareous shales).

The chondrite normalized LREE pattern of the pelite sample no. DS-524 are also fractionated but less than that of the non-calcareous and calcareous shales (Fig. 20) with LREE enrichment (La/Yb)n = 8.86 and flat HREE (Gd/Yb)n = 1.83 and small negative Eu anomally (Eu/Eu* = 0.80).

In Figure 20, the REE patterns of the calcareous shales shows strong negative Ce anomaly (especially for the sample no. RD-512) compared to the non-calcareous shales. Ce may oxidize in sea water from the 3^{+} to the more insoluble 4^{+} oxidation state, but the other REEs are not oxidized. The Ce^{4+} in well oxygenated sea water may then be incorporated into marine sediment thus enriching the sediment in Ce relative to the other REE (Bellanca et al., 1997; German and Elderfield, 1990, Cullers, 2002). This process depletes seawater in Ce relative to the other REEs (Bellanca et al., 1997; German and

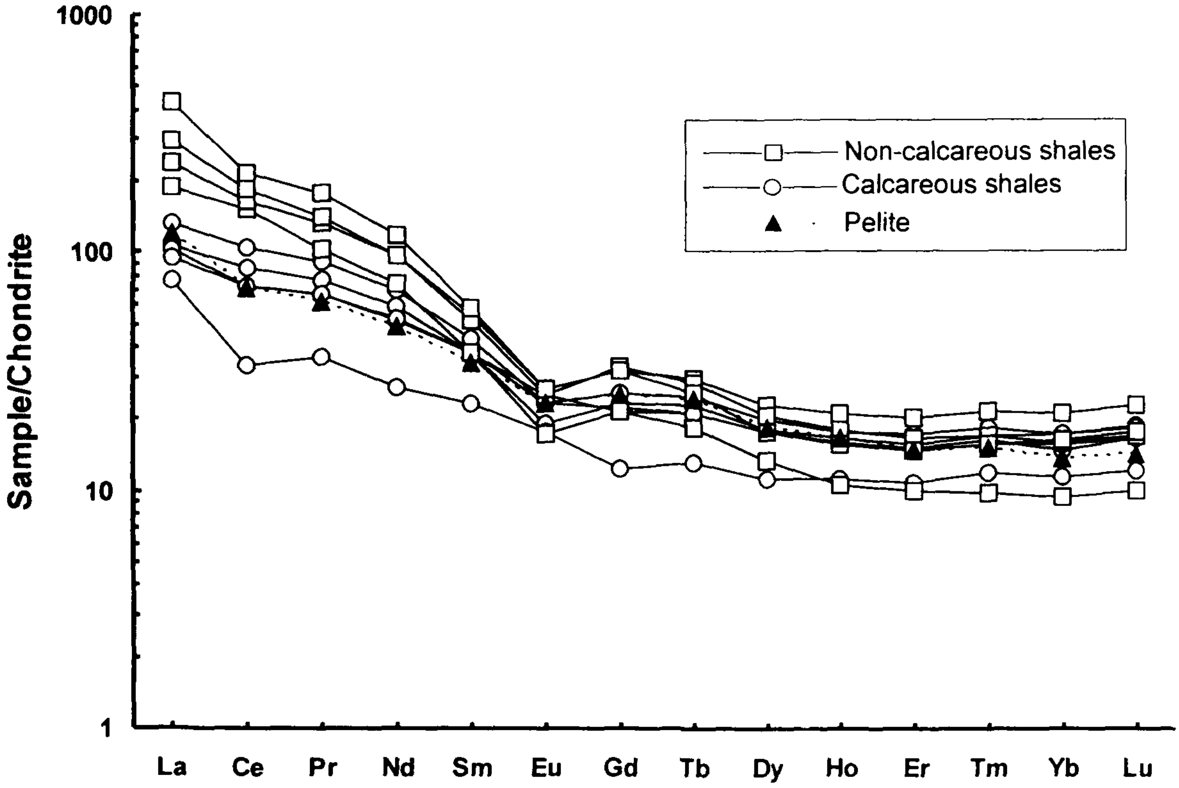

Fig. 20. Chondrite-normaized REE patterns for the non-calcareous and calcareous shales of the Neoproterozoic Chhattisgarh and Indravati basins, and a pelite sample of the Paleoproterozoic Sakoli basin of the Bastar craton.

Elderfield, 1990; Cullers, 2002). The Ce/Ce* has been used in sedimentary rocks to interpret the redox conditions in sea water at the time when the REE were incorporated into the marine sediment (German and Elderfield, 1990). The calcareous shales analyzed in this study contain lower average Ce/Ce* (0.86) than the non-calcareous shales (0.93). Present sea water is characterized by Ce/Ce* values of 0.4-0.7 (Elderfield and Greaves, 1982), whereas the average shales typically yield Ce/Ce* values of about 1.0 (Cox et al., 1995; Cullers and Berendsen, 1998). Therefore, the calcareous shales with the average Ce/Ce* value slightly lower than the non-calcareous shales and slightly higher than the present ocean water indicates suboxic conditions for the calcareous shales compared to the non-calcareous shales.

4.2.2. NEOPROTEROZOIC SANDSTONES AND PALEOPROTEROZOIC QUARTZITES

4.2.2.1. MAJOR ELEMENTS

The major element analysis of the Neoproterozoic sandstones of the Chhattisgarh and Indravati basins, and the Paleoproterozoic quartzites of the Sakoli and Sausar basins of the Bastar craton are given in Appendix II. The major element composition of sandstones of all the three formations of the Chandarpur Group does not show much variation. In general the SiO_2 concentration is high (avg. 92.96 wt. %) in all the sandstones of the Chandarpur Group and the Tiratgarh Formation. Pettijohn et al. (1972) employed a diagram to classify terrigenous sands on the basis of log (Na_2O/K_2O) vs. log (SiO_2/Al_2O_3) (Fig. 21). According to this classification scheme, the sandstones are mostly sublitharenite, subarkose and arenite. On the log (SiO_2/Al_2O_3) vs. log ($Fe_2O_3^t/K_2O$) diagram (Heron, 1988) (Fig. 22), the sandstones plot in the sublitharenite, subarkose and arenite fields, similar to Figure 21. The sandstones do not show much variation in concentration of major elements, but oxides like SiO_2, Al_2O_3 and K_2O show little variation in their concentration. The Lohardih Formation has slightly higher abundance of Al_2O_3 and K_2O and lower abundance of SiO_2 compared to the Kansapathar Formation. This is corroborated by the observed decrease in unstable components (like K-feldspar and rock fragments) and an increase in mineralogical maturity from the Lohardih Formation to the Kansapathar Formation stratigraphically. When the major element composition of the Tiratgarh Formation of the Indravati Group is compared with all the three formations of the Chandarpur Group, it shows very much similarity with the Lohardih Formation and the Chopardih Formation of the Chandarpur Group in terms of abundance of all the major elements. This is consistent with petrological observations.

The Paleoproterozoic quartzites show large variation in SiO_2 (75.94 - 95.89 %), Al_2O_3 (1.15 - 10.98 %), $Fe_2O_3^t$ (0.09 - 2.22 %), Na_2O (0.05 - 4.79 %) and K_2O (0.25 - 5.09 %). The variation in these major oxides is due to variation in the amount of mica, opaques and quartz as revealed from petrographic studies (Appendix I).

In general, major element abundances of the sandstones and quartzites do not show much difference, except for SiO_2, Al_2O_3, K_2O and Na_2O. Relative to the sandstones, quartzites have higher concentration of Al_2O_3 (6.19 % for the quartzites, 2.5 % for the sandstones), Na_2O (0.07 % for the sandstones, 1.65 % for the quartzites) and K_2O (0.89 % for the sandstones, 2.93 % for the quartzites). The other major elements like $Fe_2O_3^t$, P_2O_5, CaO, MgO, MnO are almost similar, while SiO_2 and TiO_2 show very little difference between the sandstones and quartzites. The higher concentration of Al_2O_3,

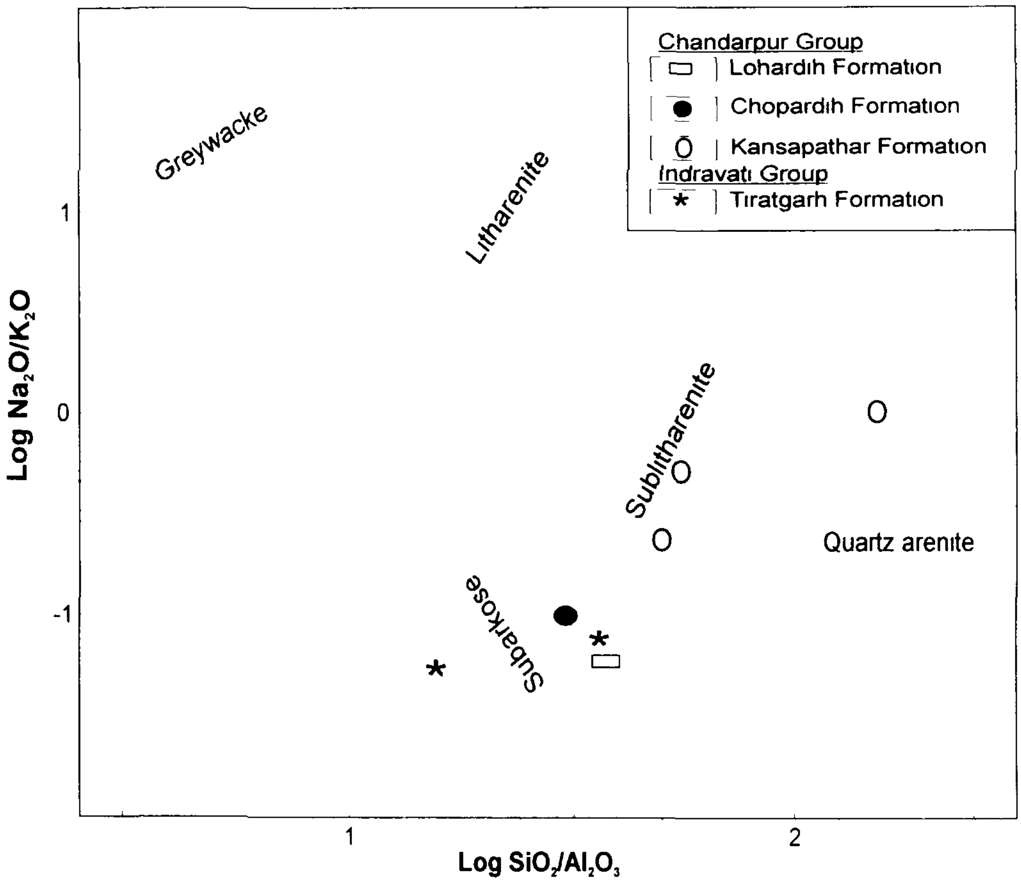

Fig. 21. Geochemical classification of sandstones of the Chandarpur Group and the Tiratgarh Formation using Log (SiO_2/Al_2O_3) vs. Log (Na_2O/K_2O) (Pettijohn et al., 1972).

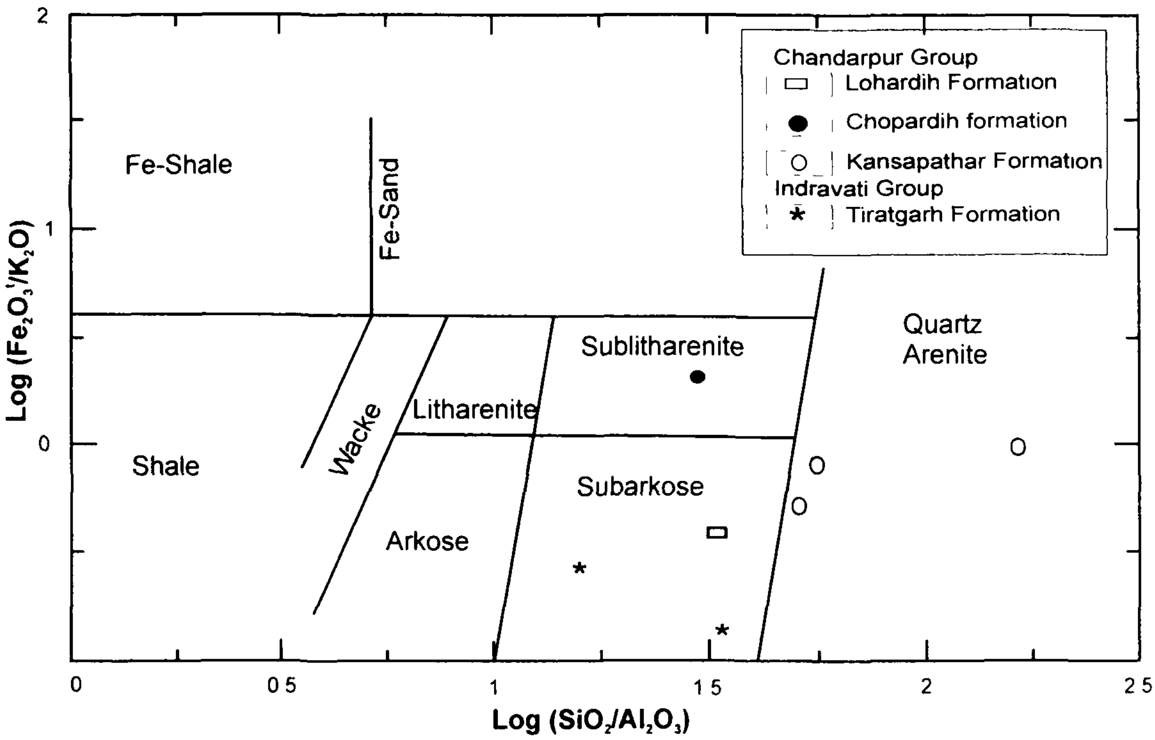

Fig. 22. Geochemical classification of sandstones of the Chandarpur Group and the Tiratgarh Formation using Log (SiO_2/Al_2O_3) vs. Log (Fe_2O_3'/K_2O) (Heron, 1988).

K_2O and Na_2O in the quartzites compared to the sandstones is due to the presence of higher amount of mica in the quartzites than in the sandstones (Appendix II).

Relative to the shales, pelites and NASC, sandstones and quartzites are enriched in SiO_2 and depleted in all other major elements. This is due to higher quartz content and lower abundance of feldspar, mica, rock fragments and absence of clay minerals in the sandstones and quartzites. The major oxides like Al_2O_3, K_2O, TiO_2 and MgO show a negative trend against SiO_2 (Fig. 23). On the other hand Na_2O, CaO, P_2O_5 and MnO do not show any linear trend against SiO_2, Al_2O_3 and K_2O (Figs. 23, 24 and 25). In Figure 24 a linear trend of TiO_2, MgO and K_2O can be observed against Al_2O_3. However, TiO_2 and MgO show a linear trend against K_2O (Fig. 25). The little variation of CaO and Na_2O compared to K_2O against SiO_2 and Al_2O_3, and the strong depletion of CaO and Na_2O indicate absence of plagioclase, which is consistent with petrographic observation of dominance of K-feldspar over plagioclase (palgioclase/K-feldspar ratio <1). The oxides like MnO and P_2O_5 have low concentrations and do not show good positive correlation with Al_2O and K_2O (Figs. 24 and 25). This may suggest that minor accessory minerals like apatite, epidote, sphene contain atleast some of the Mn and P.

4.2.2.2. TRACE ELEMENTS

Trace elements like large ion lithophile elements (LILE) and high field strength elements (HFSE) are incompatible elements and are thus preferentially partitioned into melts during crystallization and as a result these elements are enriched in felsic rather than mafic rocks. Transition elements like Sc, Cr and Ni are compatible elements and therefore get enriched in mafic rocks (Feng and Kerrich, 1990). In Chandarpur Group,

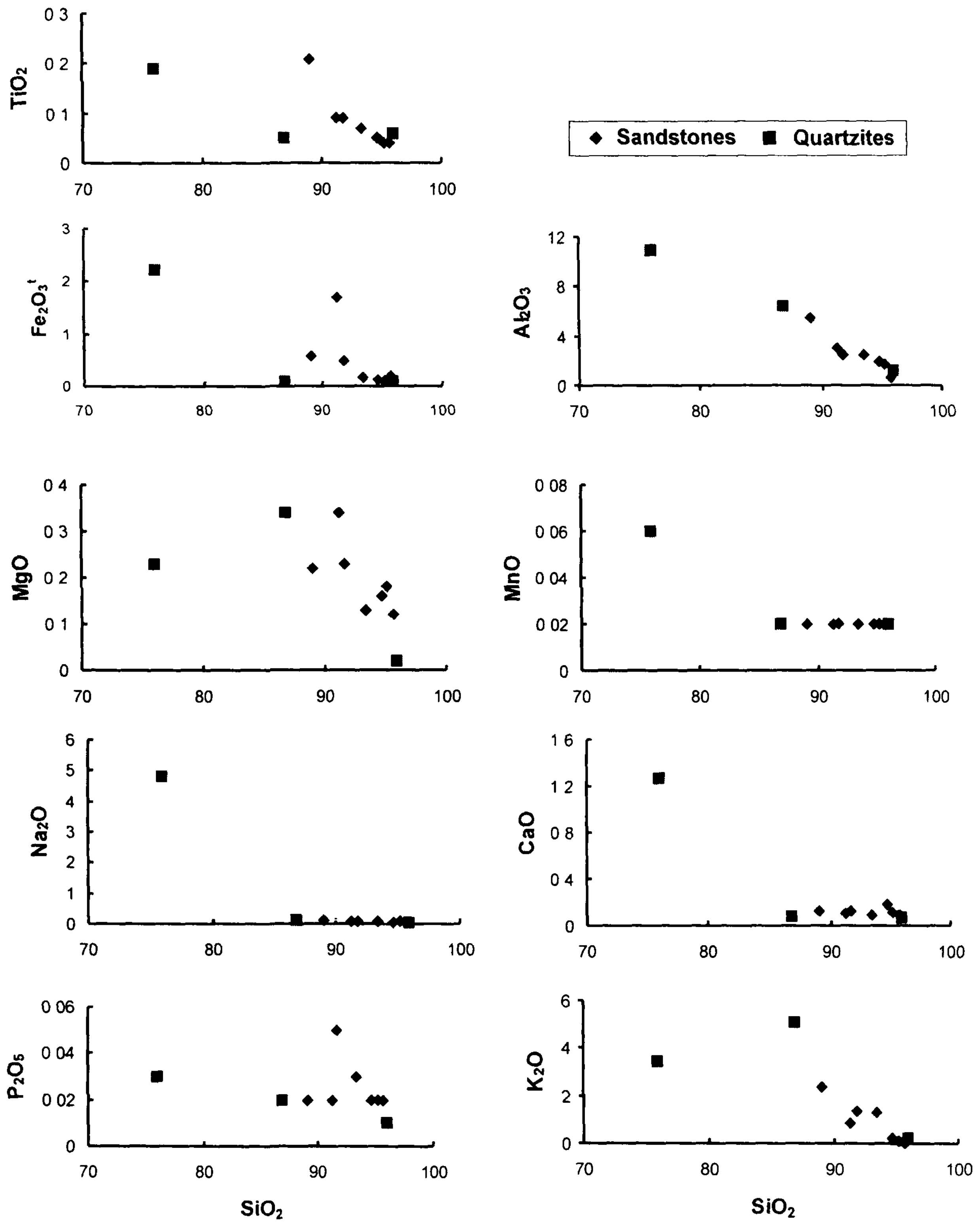

Fig. 23. Major oxides (wt. %) vs. SiO_2 (wt. %) plots for the sandstones of the Neoproterozoic Chhattisgarh and Indravati basins and quartzites of the Paleoproterozoic Sakoli and Sausar basins of the Bastar craton.

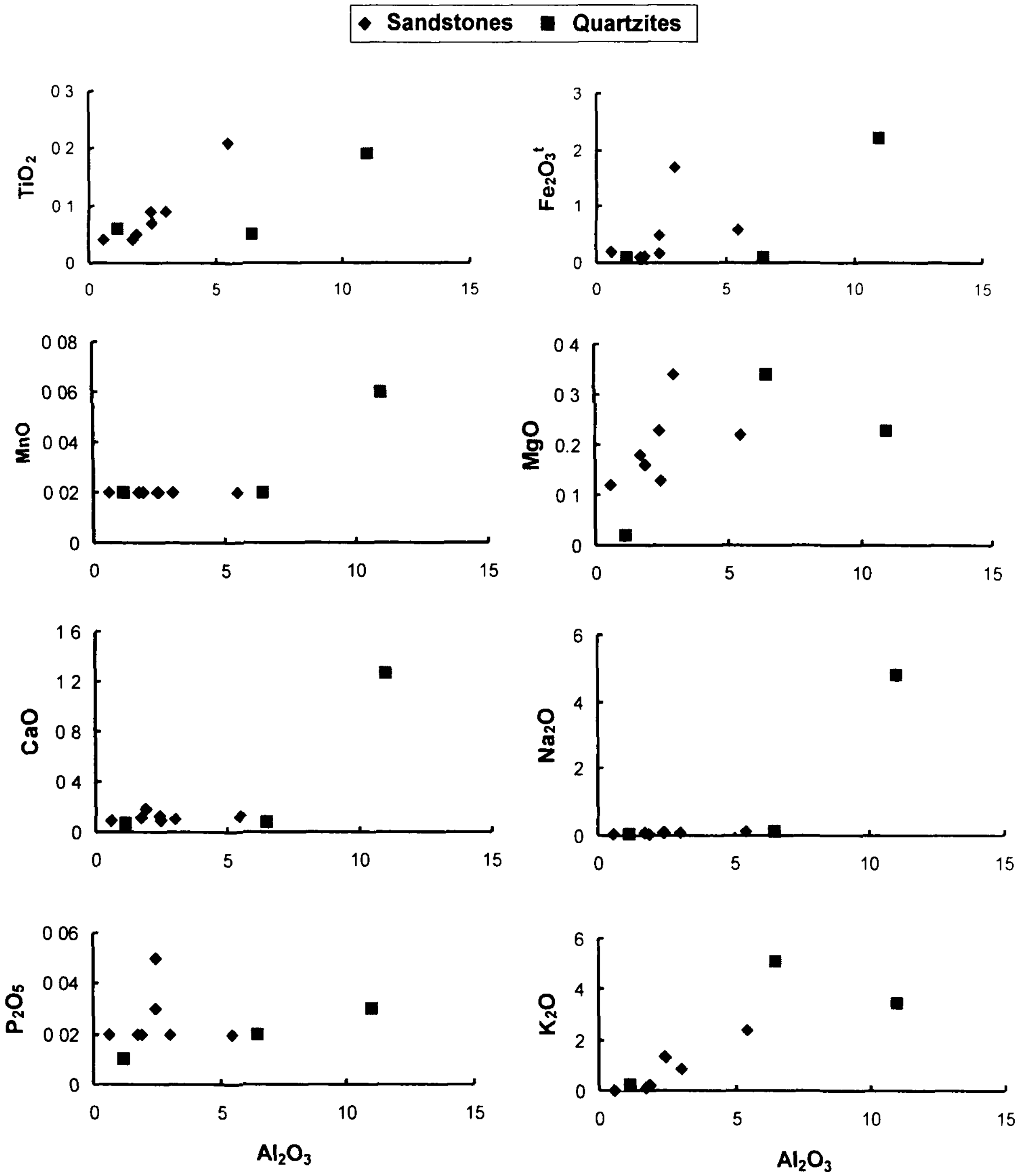

Fig. 24. Major oxides (wt. %) vs. Al_2O_3 (wt. %) plots for sandstones of the Neoproterozoic Chhattisgarh and Indravati basins and quartzites of Paleoproterozoic Sakoli and Sausar basins of the Bastar craton.

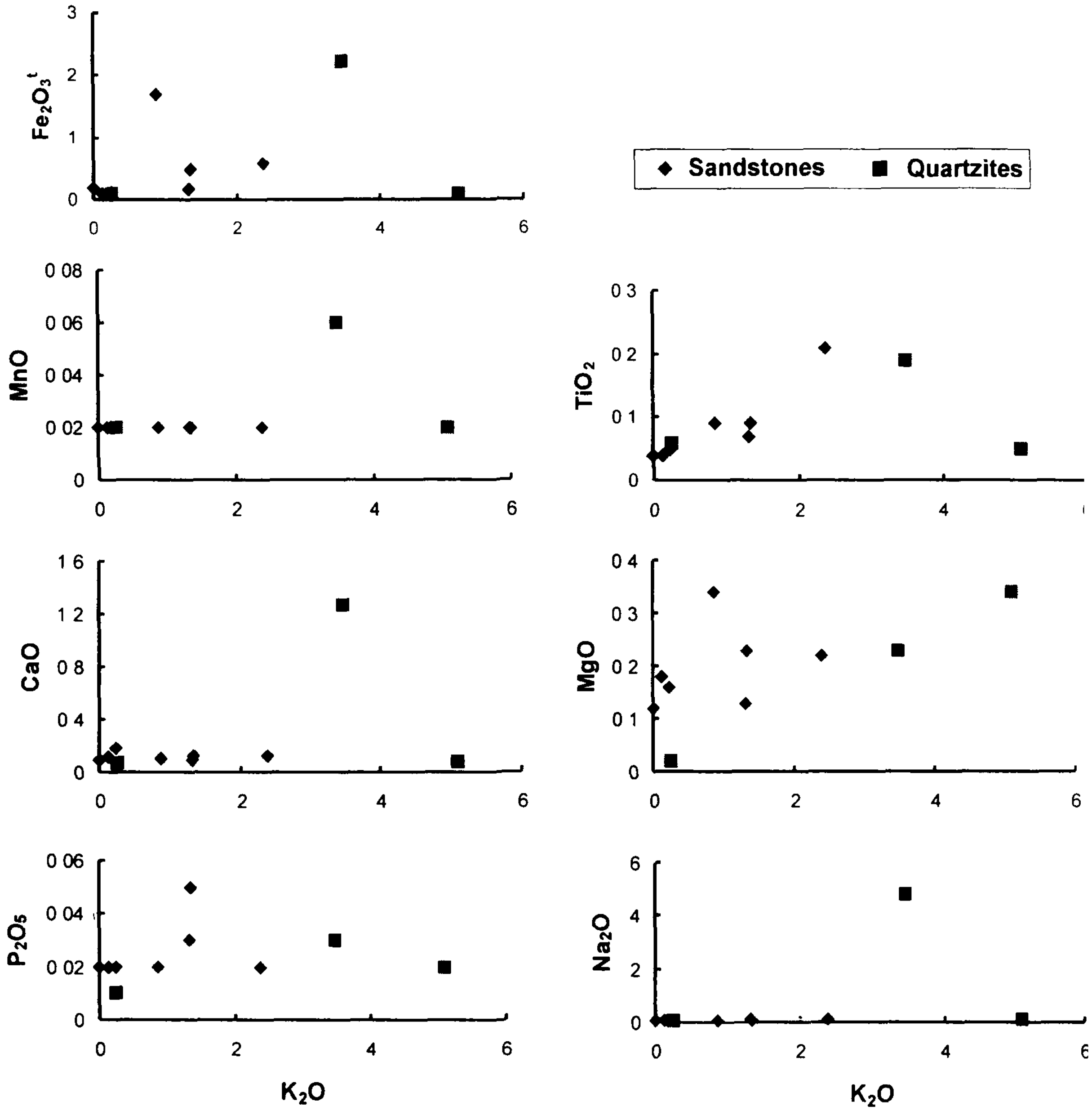

Fig. 25. Major oxides (wt. %) vs. K_2O (wt. %) plots for sandstones of the Neoproterozoic Chhattisgarh and Indravati basins and quartzites of the Paleoproterozoic Sakoli and Sausar basins of the Bastar craton.

abundance of most of the trace elements (e.g. transition elements, LILE and HFSE) decrease from the Lohardih Formation to the Kansapathar Formation stratigraphically, presumably due to decrease in feldspar and rock fragments. In sandstones of the Chandarpur Group and the Tiratgarh Formation, the average contents of transition elements like Ni, Cr, V and Sc, LILEs like Rb (25 ppm), Cs (1 ppm), Sr (16 ppm) and HFSEs like U (0.70 ppm), Th (3.19 ppm), Nb (2.2 ppm), and Y (4.9 ppm) are strongly depleted relative to NASC while trace elements like Co, Zr, Hf and Ta are enriched compared to NASC (Appendix II).

The lower abundances of most of the trace elements in the sandstones may be due to high quartz concentration and low abundances of feldspar, rock fragments and heavy minerals which are consistent with the petrography (Appendix I). Statistically, the Chandarpur Group and the Tiratgarh Formation are indistinguishable in abundance of transition elements, LILE and HFSE except for the higher Ba, Rb,Y, Zr, Th and U contents in the latter (Appendix II).

Relative to the quartzites, the sandstones are slightly depleted in transition elements like Cr, Co and slightly enriched in V and Ni. However, they show similar values for Sc. The LILE and HFSE like Rb, Cs, Sr, Th, U, Nb,Y and Zr are enriched in the quartzites compared to the sandstones. Relative to NASC, the quartzites are depleted in most of the trace elements, while the trace elements like Co, Zr, Hf, Ta, Th and U are enriched in the quartzites relative to NASC. When the average concentration of transition elements, LILE and HFSE of the sandstones and the quartzites are compared with the shales and the pelites, it is observed that the sandstones and the quartzites are strongly depleted in trace elements (except for Co and Zr) (Appendix II). The higher values of trace elements like Co, Zr, Hf, Ta, Th and U in the sandstones and the quartzites relative to the NASC may be due to sedimentary sorting of certain accessory minerals like zircon (for Zr and Hf) and monazite (for Th). The higher value of Zr in sandstones is consistent with petrography which reveals zircon grains in sandstones. Most of the trace elements show good positive correlation between Al_2O_3 and K_2O indicating K-feldspar or mica control on their abundances (Figs. 26, 27 and 28). Plots of transition elements like Sc, Cr, Ni against Al_2O_3 and K_2O yield linear plots for both the sandstones and the quartzites (Fig. 26). The LILE and HFSE like U, Cs, Th, Rb, Ba and Ta show linear trend against Al_2O_3 and K_2O (Figs. 27 and 28). However elements like Zr, Y, Nb do not show linear trend against Al_2O_3 and K_2O (Figs. 27 and 28) indicating some accessory minerals (e.g. allanite for Y, zircon for Zr) other than feldspar and mica to be controlling their abundance in the sandstones and the quartzites.

Overall, the average concentrations of most of the major and trace elements are quite similar in the sandstones and the quartzites. The minor differences in composition are due to the higher concentration of mica and opaque minerals in the quartzites compared to the sandstones.

4.2.2.3. RARE EARTH ELEMENTS (REE)

Total REE concentration in the sandstones of the Chandarpur Group is variable with the highest value in the Chopardih Formation (39 ppm) and the lowest value in the Kansapathar Formation (13 ppm). However, the $\sum$REE concentration of the Tiratgarh Formation of the Indravati Group is higher than all the three formations of the Chandarpur Group (76 ppm). The REE patterns of all the three

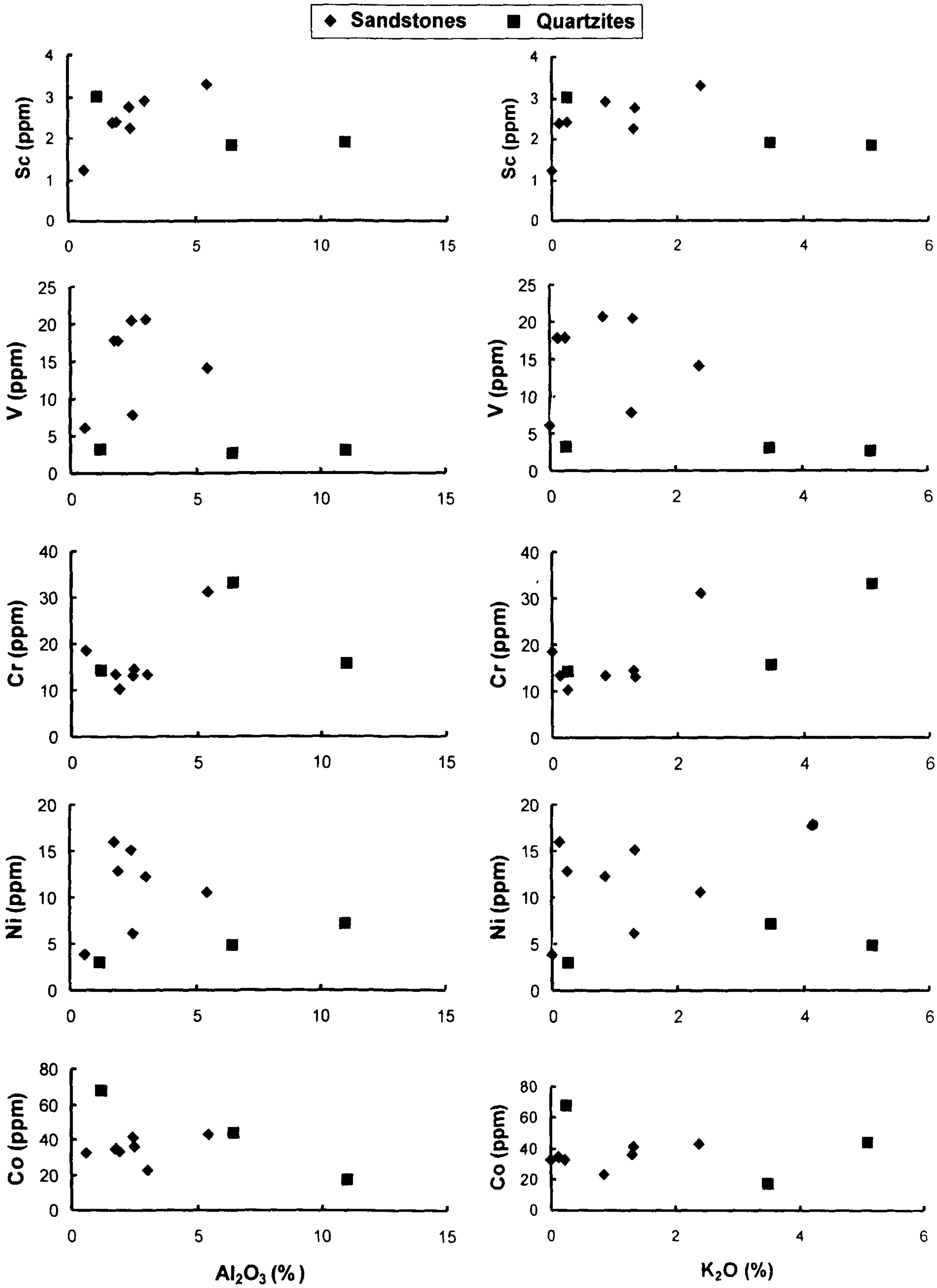

Fig. 26. Plots of transition elements vs. Al_2O_3 and K_2O for the sandstones of the Neoproterozoic Chhattisgarh and Indravati basins and quartzites of the Paleoproterozoic Sakoli and Sausar basins of the Bastar craton.

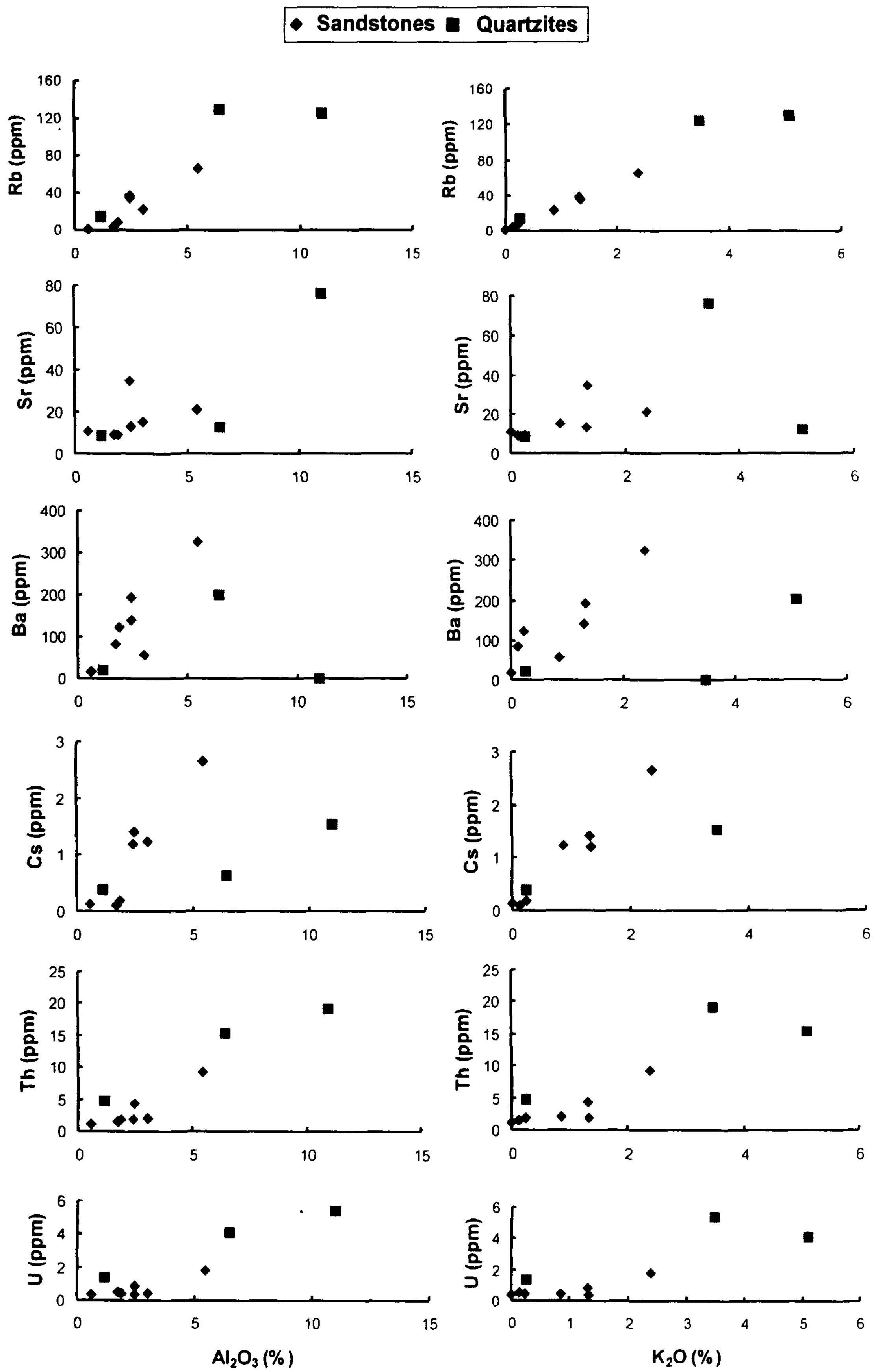

Fig. 27. Plots of large ion lithophile elements (LILE) vs. Al_2O_3 and K_2O for sandstones of the Neoproterozoic Chhattisgarh and Indravati basins and quartzites of the Paleoproterozoic Sakoli and Sausar basins of the Bastar craton.

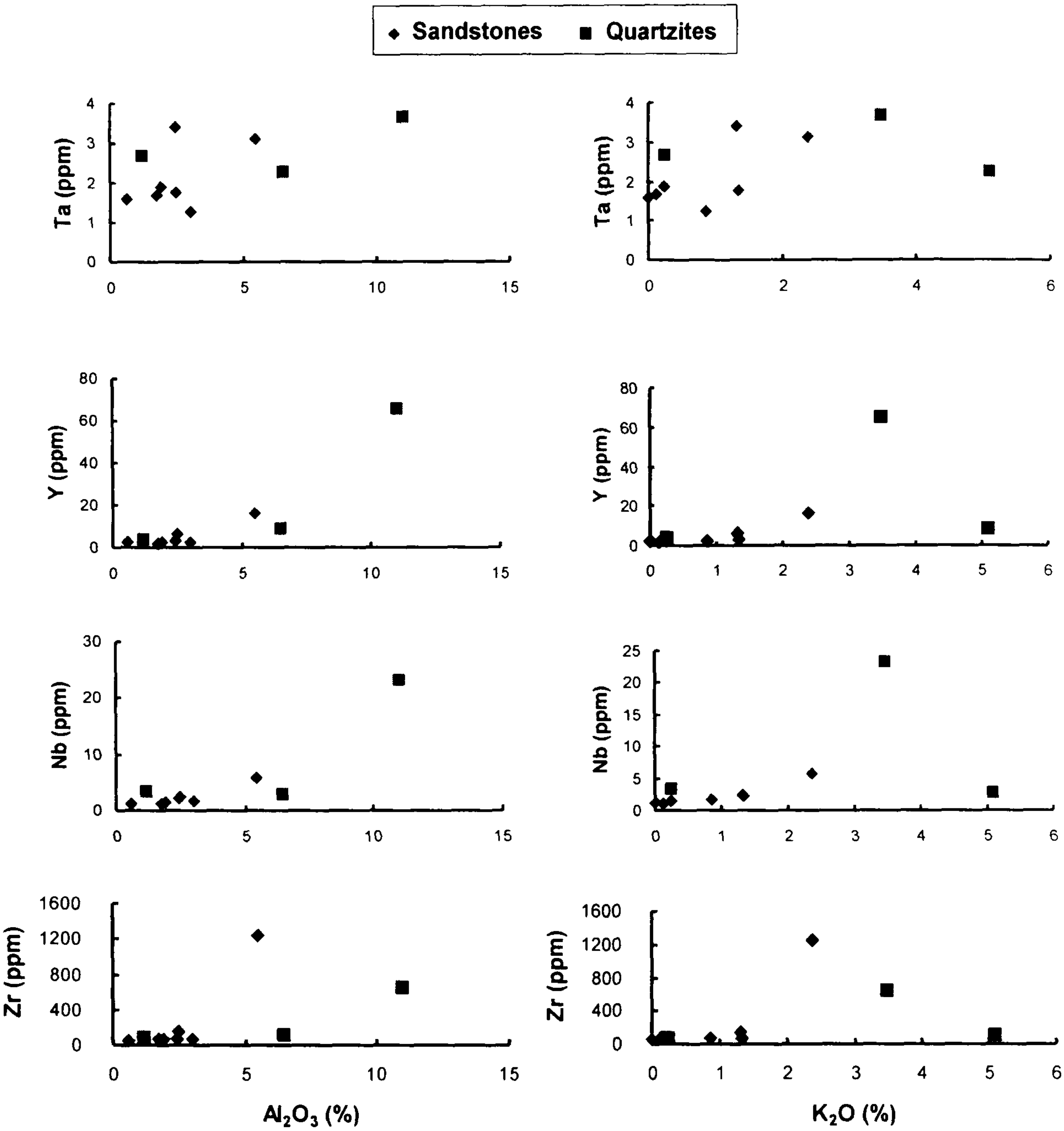

Fig. 28. Plots of high field strength elements (HFSE) vs. Al_2O_3 and K_2O for sandstones of the Neoproterozoic Chhattisgarh and Indravati basins and the quartzites of the Paleoproterozoic Sakoli and Sausar basins of the Bastar craton.

formations of the Chandarpur Group of the Chhattisgarh basin and the Tiratgarh Formation of the Indravati basin are uniform and there are no systematic differences in REE patterns among different formations of the Chandarpur Group and the Tiratgarh Formation (Fig. 29).

When the mean REE concentration of the Paleoproterozoic quartzites are compared with the Neoproterozoic sandstones, it is observed that the quartzites have higher REE mean value (145 ppm) than the sandstones (34 ppm). However, on an average, the sandstones and the quartzites have REE abundances lower than that of the shales and NASC. The REE contents show large variations between the quartzites and the sandstones. It may be due to the reason that REEs are normally reside in fine fraction and it has been inferred that trivalent REEs are readily accommodated in most of the clay-mica minerals (phyllosilicates) enriched with alumina and ferric iron (Cullers et al., 1987; Cullers, 1988). This is also corroborated by the observed positive correlation of REE with Al_2O_3 and K_2O (Fig. 30). Thus, the sandstones with lower mica content have lower REE content, while the quartzites with higher percentage of mica content have higher content of REE than the sandstones (Haskin et al., 1966). Good positive correlation of LREE and HREE with Zr, Th and Y of the sandstones indicate allanite, monazite and zircon control on REE (Fig. 30). In contrast, LREE and HREE in the quartzites do not show good correlation with Zr, Th and Y indicating little or no control of allanite, monazite and zircon on REE in the quartzites (Fig. 30).

In chondrite normalized plot (Sun and McDonough, 1989) both the sandstones and the quartzites show LREE enriched and flat HREE patterns with negative Eu anomalies (Fig. 29). Although there are variations in absolute concentration of REE

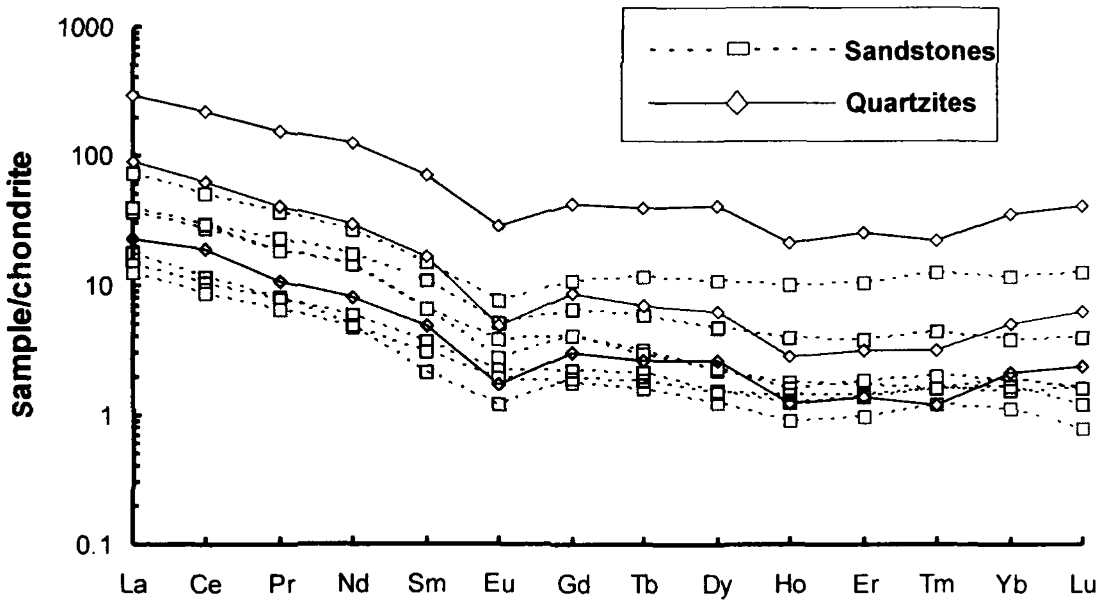

Fig. 29. Chondrite-normailzed REE patterns for sandstones of the Neoproterozoic Chattisgarh and Indravati basins and quartzites of the Paleoproterozoic Sakoli and Sausar basins of the Bastar craton.

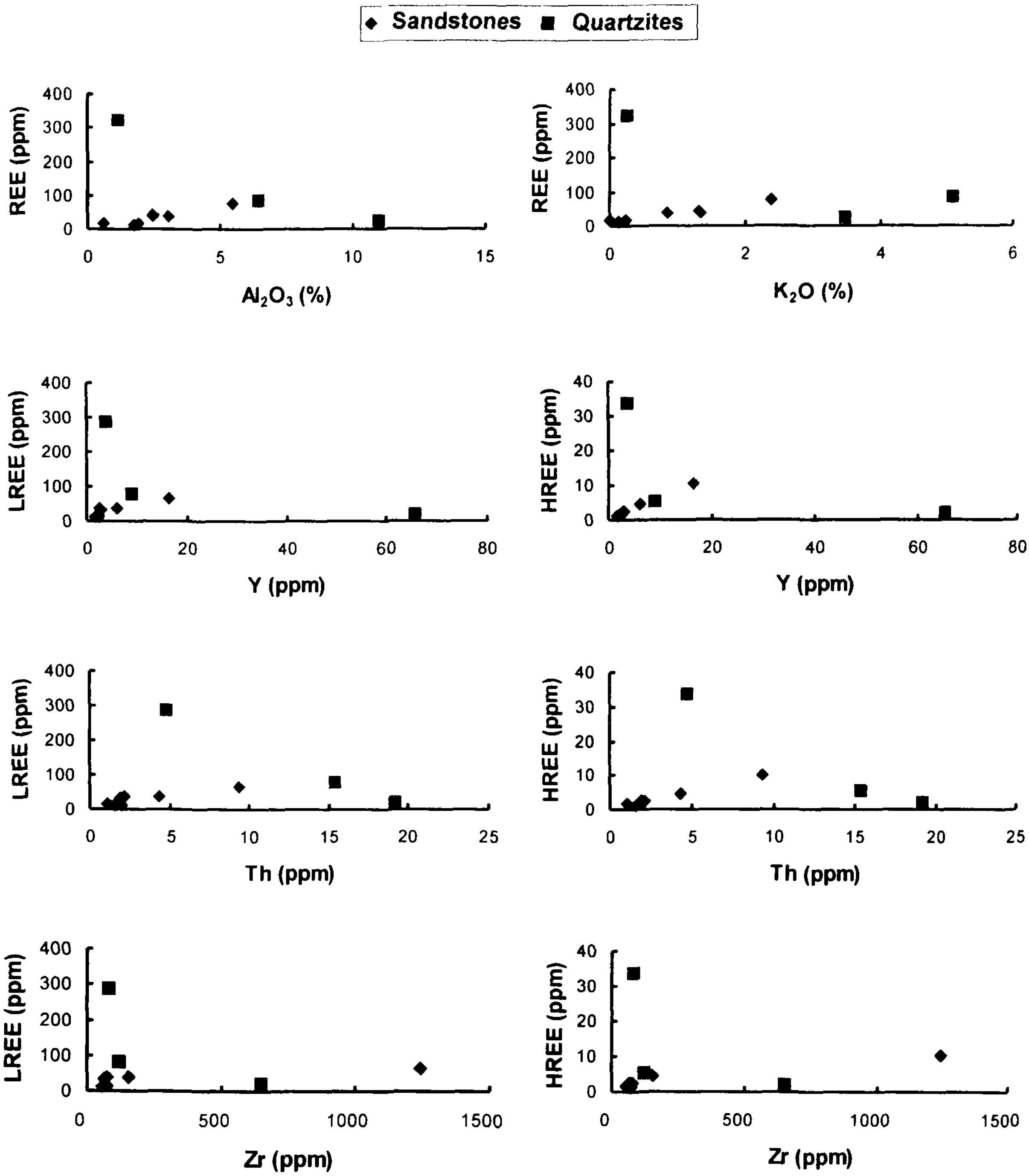

Fig. 30. Plots of REE vs. Al_2O_3 and K_2O and REE vs. Y, Th and Zr for the sandstones of Neoproterozoic Chhattisgarh and Indravati basins and the quartzites of the Paleoproterozoic Sakoli and Sausar basins of the Bastar craton.

between the sandstones and the quartzites, they have almost similar ratios of LREE/HREE (10.50 for the sandstones and 11 for the quartzites). The REE patterns of the sandstones and the quartzites are highly fractionated and uniform with LREE enrichment $(La/Yb)_n$ = 12.5 for the sandstones and 12 for the quartzites, flat HREE $(Gd/Yb)_n$ = 1.56 for the sandstones and 1.42 for the quartzites, and significant Eu anomaly (0.67 for the sandstones and 0.47 for the quartzites). There are no systematic variations in REE patterns between the sandstones and the quartzites (Fig. 29).

Chapter-V

TECTONIC SETTING

5. TECTONIC SETTING

The Bastar craton of the Central Indian shield with Proterozoic supracrustals is very significant with regard to its tectonic evolution. There has not been any significant study on the Proterozoic tectonic evolution of the Paleoproterozoic and Neoproterozoic basins of the Bastar craton. In this chapter an attempt has been made to elucidate the tectonic environment of deposition of the Paleoproterozoic and the Neoproterozoic basins of the Bastar craton employing petrological and geochemical signatures of clastic rocks.

Sandstone petrography is widely considered to be a powerful tool for determining the origin and tectonic reconstructions of ancient terrigenous deposits (Blatt, 1967; Dickinson, 1970; Pettijohn et al., 1972). Sandstone mineralogical characterization of the basin fill is critical to any basin analysis and many studies have pointed to an intimate relationship between detrital sand compositions (i.e. bed rock compositions of sources) and tectonic setting (Ingersoll, 1978; Dickinson and suczek, 1979; Dickinson et al., 1983).

Detrital sandstone compositions have been related to major provenance types such as stable cratons, basement uplifts, magmatic arcs and recycled orogens (Dickinson and Suczek, 1979; Dickinson et al., 1983). To identify the provenances and tectonic setting, the recalculated parameters of Folk (1980) and Dickinson and Suczek (1979) (Table 8) were plotted on standard ternary diagrams given by Dickinson and Suczek (1979) (Figs. 31, 32 and 33). In the QtFL diagram (Fig. 31), where Qt refers to total quartz grains (Qm + Qp) including chert, F refers to total feldspar and L refers to total lithic fragments respectively (Table 7). Most of the sandstones of the Lohardih Formation, the Chopardih

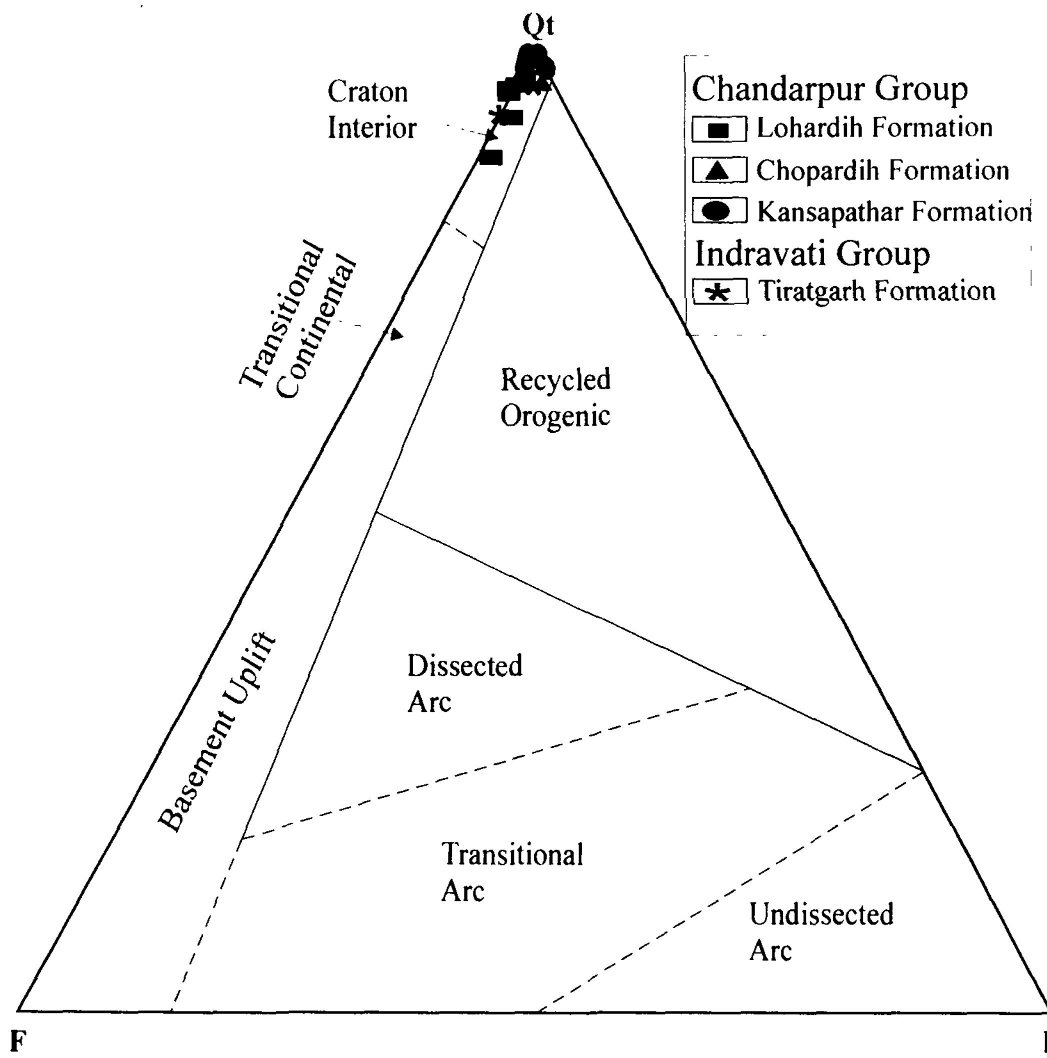

Fig. 31. QtFL discriminant diagram after Dickinson and Suczek (1979) of sandstone samples of the Chandarpur Group of the Chhattisgarh basin and the Tiratgarh Formation of the Indravati basin.

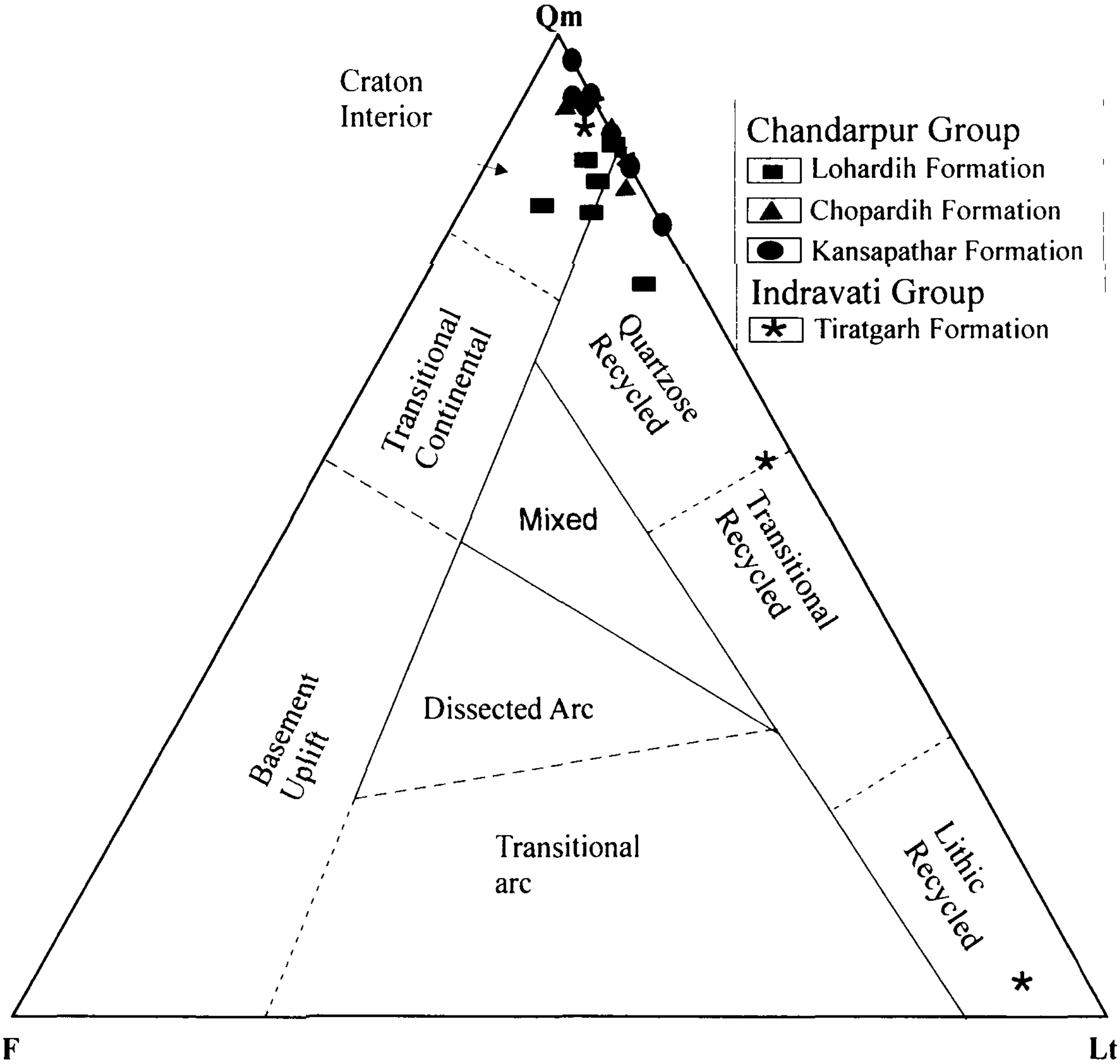

Fig. 32. QmFLt discriminant diagram after Dickinson and Suczek (1979) of sandstone samples of the Chandarpur Group of the Chhattisgarh basin and the Tiratgarh Formation of the Indravati basin.

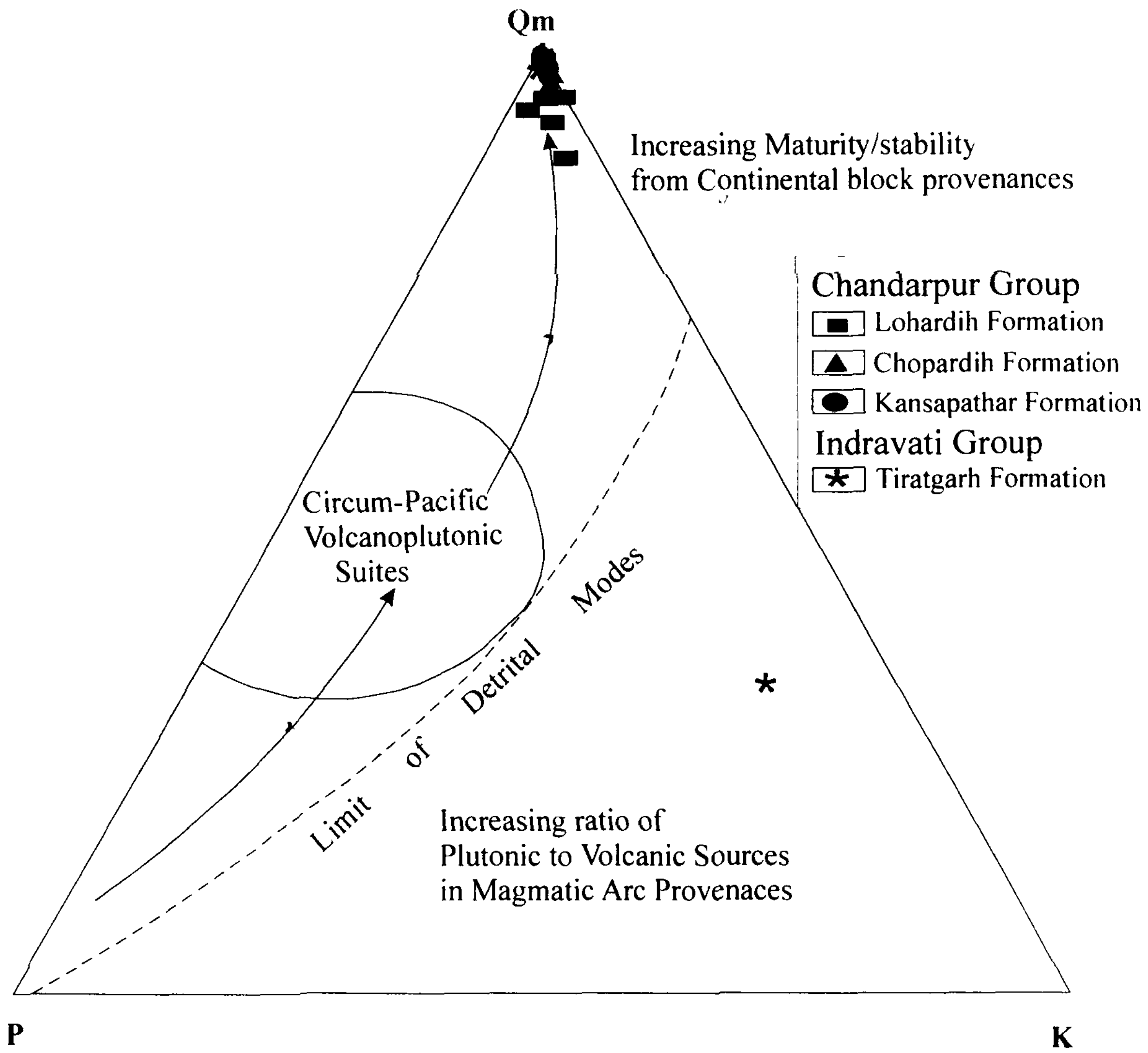

Fig. 33. QmPK discriminant diagram after Dickinson and Suczek (1979) of sandstone samples of the Chandarpur Group of the Chhattisgarh basin and the Tiratgarh Formation of the Indravati basin.

Formation and the Kansapathar Formation of the Chandarpur Group, and the Tiratgarh Formation of the Indravati Group plot in the stable craton field. The mineralogically mature sandstones (arenites) of the Kansapathar Formation of the Chandarpur Group plot very close to Qt pole in the stable cratonic field. In the QmFLt diagram (Fig. 32), where Qm, F and Lt refer to monocrystalline quartz (Qm), total feldspar (P + K) and total lithic fragments including polycrystalline quartz (Qp) respectively (Table 7), the majority of the samples for all the three formations of the Chandarpur Group and the Tiratgarh Formation of the Indravati Group plot in the craton interior provenance field. However, some samples plot on or near the quartzose recycled orogen. Samples have also been plotted on another ternary diagram based on Qm (monocrystalline quartz), P (plagioclase) and K (K-feldspar). On this QmPK diagram (Fig. 33), all the sandstone samples cluster near Qm pole indicating maturity of sandstones and tectonic stability of the provenance.

It is evident from QmFLt, QtFL and QmPK plots, that the sandstone samples from all the three formations of the Chandarpur Group of the Chhattisgarh basin and the Tiratgarh Formation of the Indravati basin plot in intra-cratonic field. In such a tectonic setting, sediments are deposited in plate interiors, away from the plate margins and the sediments were derived from stable continental areas (Roser and Korsch, 1986). Many previous studies on these Neoproterozoic basins of the Bastar craton (the Chhattisgarh and Indravati basins) based on lithology, basin analysis and structural evidence within these sedimentary strata indicate a similar intra-cratonic setting for these supracrustals (Murthi, 1987; Ramakrishnan, 1987; Wani and Mondal, 2007). This study further strengthens the stable intra-cratonic origin for these Neoproterozoic basins. Some earlier workers, however, have suggested continental rift setting for these basins (Chaudhuri et al., 2002; Patrababis Deb, 2004). A continental rift setting for these basins would produce immature clastic sediments from rapid transportation and burial preserving feldspar, particularly plagioclase. The petrographic analysis carried out in this study suggests that all these sandstones are enriched in quartz and poor in feldspar. A continental rift setting should, therefore, have resulted in the associated sandstones plotting in the basement uplift field on QmFLt and QtFL diagram. Hence, the continental rift setting is not consistent with overall petrogrpahic compositions of the sandstones.

The chemical approach is a useful complement to petrographic analysis, and the two methods when combined, become a powerful tool for examination of provenance and determination of tectonic setting. Sedimentologists and geochemists have long endeavored to pursue the relationship between sedimentary rock geochemistry and plate tectonics for recognizing ancient tectonic settings (Armstrong-Altrin and Verma, 2005; Bhatia and Taylor, 1981; Bhatia, 1983, 1985a, b; Bhatia and Crook, 1986; Crook, 1974; Floyd et al., 1991; Gu, 1994; Gu et al., 2002; Maynard et al., 1982; McLennan et al., 1990; Middleton, 1960; Roser and Korsch, 1985, 1986, 1988; Schwab, 1975). Studies in the last decade have shown some complications when composition is related to tectonic setting (Cullers, 1988; McLennan et al., 1990), but such an effort does give insight to the ways in which tectonics and the geochemical processes interact in determining the compositions of sediments.

Some authors have described the usefulness of major element geochemistry of sedimentary rocks to infer tectonic setting based on discrimination diagrams (Bhatia, 1983; Roser and Korsch, 1986), although others have pointed out the difficulties in using geochemistry to interpret tectonic setting (Armstong-Altrin and Verma, 2005;

Milodowski and Zalasiewicz, 1991; Nesbitt and Young, 1989; Van de Kamp and Leake, 1985). The geochemistry of sedimentary rocks is a complex function of the nature of the source rocks, intensity and duration of weathering, sedimentary recyling, diagenesis and sorting (Argast and Donnelly, 1986; Cullers, 2000; McLennan et al., 1993). Furthermore, specific tectonic settings do not necessarily produce rocks with unique geochemical signatures (Banlburg, 1998; McLennan et al., 1990). In some instances, sediments are transported from one tectonic setting into a sedimentary basin having different tectonic environment (McLennan et al., 1990). Inspite of these difficulties, the geochemistry of sedimentary rocks have been used to infer the tectonic setting of ancient sedimentary basins (Burnett and Quirk, 2001; Gu et al., 2002; Kasper-Zubillega et al., 1999).

Roser and Korsch (1986) differentiated the sediments derived from oceanic island arc (Arc according to original authors), active continental margin (ACM) and passive continental margin (PM) using SiO_2 and K_2O/Na_2O ratio (Fig. 34). The fields are based on ancient sandstone-mudstone pairs verified against modern sediments from known tectonic settings. Roser and Korsch (1986) further stated that associated with subduction zones, arc derived material is typical of fore-arc, back-arc and inter-arc basins formed on oceanic crust; whereas ACM derived material occurs in similar settings but on continental crust. PM (passive margin) sediments are derived from stable continental areas and deposited in intra-cratonic basins or passive continental margins. On the SiO_2 vs. K_2O/Na_2O ratio diagram (Fig. 34) of Roser and Korsch (1986), all the Paleoproterozoic pelite and quartzite samples, and the Neoproterozoic sandstone and non-calcareous shale samples plot exclusively in the PM field. According to Roser and Korsch (1986), PM sediments are quartz rich sediments derived from plate interiors or

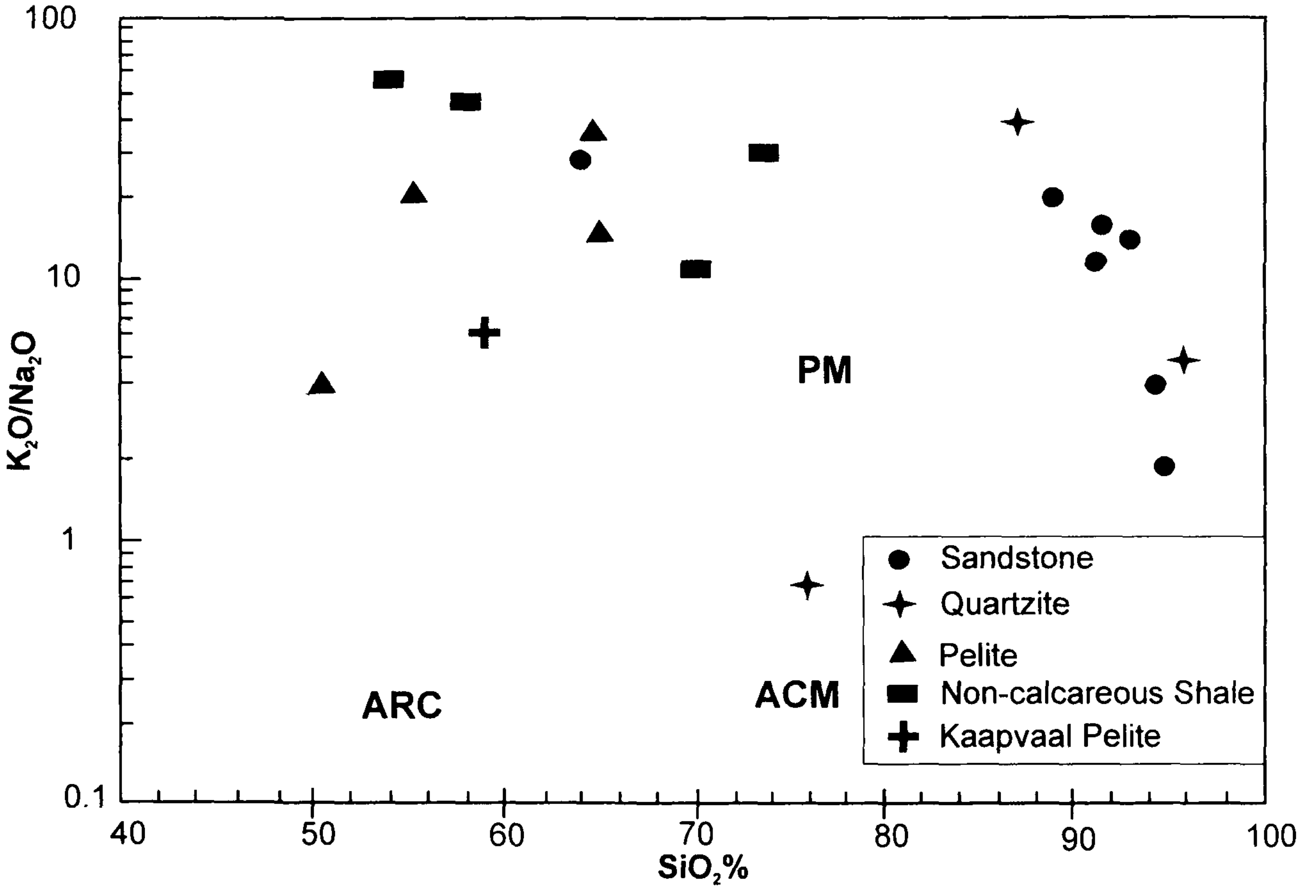

Fig. 34. K_2O/Na_2O - SiO_2 diagram (Roser and Korsch, 1986) showing the distribution of the Paleoproterozoic pelites and quartzites and the Neoproterozoic non-calcareous shales and sandstones of the Bastar craton. PM, passive margin; ACM, active continental margin; ARC, arc.

stable continental areas and deposited in intra-cratonic basins or passive continental margins. The Neoproterozoic calcareous shales (CaO rich) were not plotted on this diagram due to their lower SiO_2 concentration. However, these calcareous shales have high K_2O/Na_2O ratio, indicating their deposition in passive margin tectonic setting (PM). On the SiO_2 vs. K_2O/Na_2O ratio diagram (Fig. 34) of Roser and Korsch (1986), average of the Kaapvaal pelites of the Paleoproterozoic Transvaal and Ventersdrop Groups (Wronkiewicz and Condie, 1990) has also been plotted for comparison because both the Paleoproterozoic pelites of the Transvaal and Ventersdrop Groups of Kaapvaal craton and the Paleoproterozoic Sakoli and Sausar Groups of the Bastar craton have been considered to be formed in passive margin or rift setting (Eriksson et al., 2002; Takashi et al., 2001; Vander Westhuzen et al., 1991). On this diagram the Kaapvaal pelites plot in the passive margin field similar to the Paleoproterozoic pelites of the Sakoli and Sausar Groups.

A similar plot to that of K_2O/Na_2O – SiO_2 (Roser and Korsch, 1986) was used by Maynard et al. (1982) in their study of modern sand. They used SiO_2/Al_2O_3 ratio instead of SiO_2 alone. Higher values of both elemental ratios represent continentally derived material marked by high SiO_2 and low Na_2O, which characterize the passive margin region (PM), whereas lower ratios define the active continental margin (ACM) region. The SiO_2/Al_2O_3 vs. K_2O/Na_2O plot (Maynard et al., 1982) (Fig. 35) for the Paleoproterozoic pelite and quartzite samples, and the Neoproterozoic sandstone, calcareous and non-calcareous shale samples suggest that the sediments were deposited in passive margin setting (except for one pelite sample which falls in continental island arc field (CIA). The Neoproterozoic sandstone samples and two Paleoproterozoic

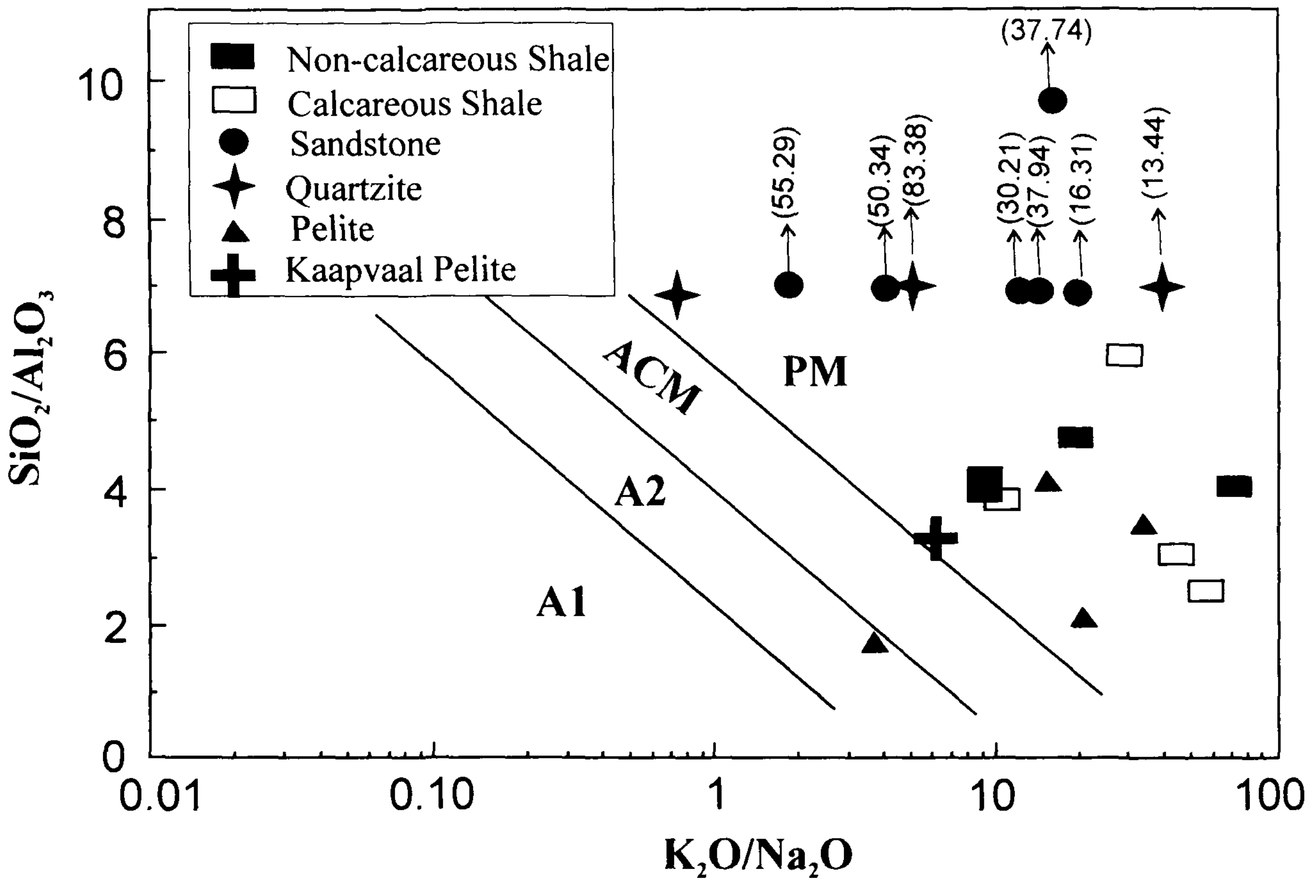

Fig. 35. Tectonic discrimination diagram after Maynard et al. (1982) for the Paleoproterozoic pelites and quartzites, and the Neoprterozoic non-calcareous shales, calcareous shales and sandstones of the Bastar craton. PM - passive margin; ACM - active continental margin; A1 - arc, basaltic and andesitic detritus; A2 - evolved arc setting, felsic plutonic detritus.

quartzite samples due to their considerably higher SiO_2/Al_2O_3 ratio indicate passive margin setting on the SiO_2/Al_2O_3 vs. K_2O/Na_2O diagram (Fig. 35). On this diagram Kaapvaal pelites also plot in passive margin field similar to Paleoproterozoic pelites of the Sakoli and Sausar Groups. This is consistent with the Fig. 34.

Based on nature of Archean crust, Bhatia (1983) divided continental margins and oceanic basins into four tectonic settings viz. oceanic island arcs (OIA), continental island arcs (CIA), active continental margin (ACM) and passive continental margin (PM). He proposed that the most discriminating parameters to decipher different tectonic settings are $Fe_2O_3^t$ + MgO, TiO_2, Al_2O_3/SiO_2, K_2O/Na_2O and Al_2O_3/ (CaO + Na_2O) as shown in Table 9. The geochemical concept behind the discrimination parameters was based on general decrease in $Fe_2O_3^t$ + MgO, TiO_2 and Al_2O_3/SiO_2 and an increase in K_2O/Na_2O and $Al_2O_3/(CaO+Na_2O)$ as the tectonic setting changes in the sequence OIA $\rightarrow$ CIA $\rightarrow$ ACM $\rightarrow$ PM.

It is evident from Table 9 that all the five discriminating parameters $Fe_2O_3^t$ + MgO, TiO_2, Al_2O_3/SiO_2, K_2O/Na_2O and Al_2O_3/ (CaO + Na_2O) of the sandstones and quartzite samples are comparable with that of passive margin (PM) of Bhatia (1983). The higher K_2O/Na_2O and $Al_2O_3/(CaO+Na_2O)$ ratios of the non-calcareous shale and the pelite samples are also comparable with passive margin setting (PM). However, $Fe_2O_3^t$ + MgO, TiO_2 values and Al_2O_3/SiO_2 ratio of the non-calcareous shale and pelite samples are comparable with those of continental island arc and oceanic island arc (Table 9). Average values of these geochemical parameters of Bhatia (1983) for the calcareous shale samples have not been calculated due to their higher CaO content and lower concentration of other major elements due to calcite dilution.

Table 9. Tectonic geochemical discriminating parameters (Bhatia, 1983) compared with th Paleoproterozoic pelites and quartzites, and the Neoproterozoic sandstones and non calcareous shales of the Bastar craton.

Tectonic Discriminating Parameters	OIA	CIA	ACM	PM	Average Sandstone*	Average Quartzite*	Average Non-calcareous Shale*	Averag Pelite*
$Fe_2O_3^t$+MgO (wt%)	11.73	6.79	6.63	2.89	0.67	0.99	8.60	10.41
TiO_2 (wt%)	1.06	0.64	0.46	0.49	0.08	0.10	0.69	0.75
Al_2O_3/SiO_2	0.29	0.20	0.18	0.10	0.02	0.07	0.27	0.38
K_2O/Na_2O	0.39	0.61	0.99	1.60	11.40	1.77	28.16	9.69
$Al_2O_3/(CaO+Na_2O)$	1.72	2.42	2.56	4.15	12.30	14.05	74.44	55.26

OIA – oceanic island arc, CIA – continental island arc, ACM – active continental margin, PM – passive margin, * - this study.

Trace elements, particularly those with relatively low mobility and low residence times in sea water such as Th, Sc, Ti, Nb and Zr are transferred quantitatively into clastic sediments during primary weathering and transportation and are thus useful tool for provenance and tectonic setting discrimination (Bhatia and Crook, 1986; McLennan, 1990; McLennan and Taylor, 1991; Taylor and McLennan, 1985). Bhatia and Crook (1986) use a triangular diagram of Th- Sc- Zr/10 to derive various tectonic provenance fields for Paleozoic turbiditic greywackes in Australia. In this diagram, they distinguish fields for four tectonic environments: oceanic island arcs, continental island arc, active continental margin and passive margin. On this diagram of Th- Sc- Zr/10 (Fig. 36) all the sandstone samples of the Neoproterozoic Chhattisgarh basin and the Indravati basin plot near passive margin while the calcareous and the non-calcareous shale samples of the Chhattisgarh basin and Indravati basin plot near the active continental margin and continental arc fields. The pelite and quartzite samples of the Paleoproterozoic Sakoli and Sausar basins show a lot of scatter between active continental margin (ACM) and continental island arc (CIA). It is to be noted here that none of the samples plot on oceanic island arc field. The shale samples (both the calcareous and non-calcareous), pelite and quartzite samples plot between active continental margin and continental arc field, which is analogous to the results of the major element analysis (Figs. 34 and 35). It should be also emphasized here that the fields on this plot were originally defined for sandstones (Bhatia and Crook, 1986). The wide scattering of the non-calcareous shale, pelite and quartzite samples between active continental margin and continental arc field on the Th-Sc-Zr/10 plot (Fig. 36) may be due effect of sorting. According to Roser and Korch (1986), interpretation of many immobile elements (e.g. Th and Zr), is hampered by

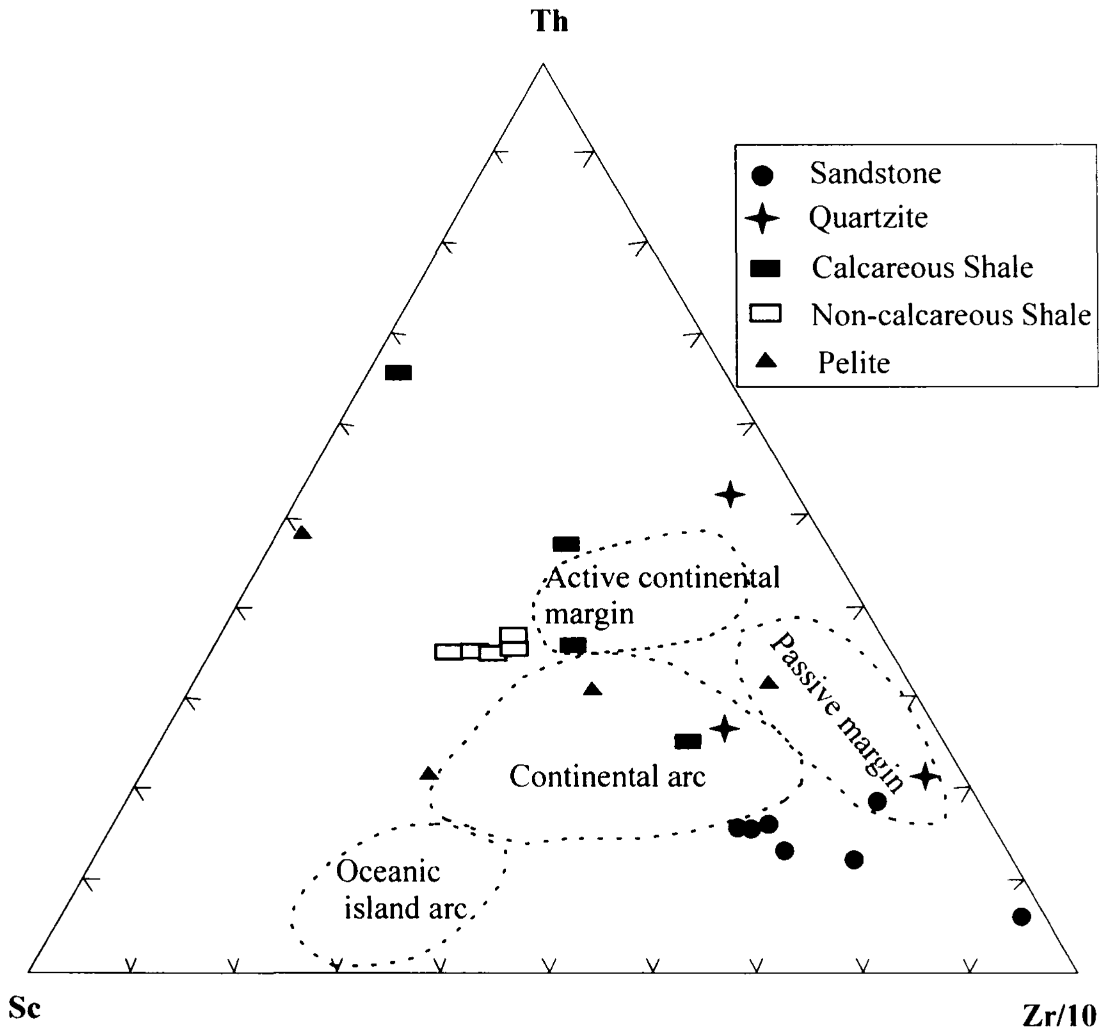

Fig. 36. Th - Sc - Zr/10 tectonic discrimination diagram after Bhatia and Crook (1986) for the Paleoproterozoic pelites and quartzites, and the Neoproterozoic non-calcareous shales, calcareous shales and sandstones of the Bastar craton.

their residence in high density accessory minerals such as zircon and apatite, which may not be necessarily evenly distributed throughout the sediments. So, characteristic geochemical signatures may be difficult to determine (Roser and Korsch, 1986).

Bhatia (1985a, b) opined that the sedimentary rocks deposited on passive margins, platform and cratonic basins are characterized by high enrichment of LREE over HREE and the presence of a pronounced negative Eu anomally on chondrite normalized plots. All the studied Neoproterozoic sandstones and shales, and Paleoproterozoic quartzites and a pelite sample possess similar characteristics as discussed above to that of a passive margin tectonic setting as described by Bhatia (1985a, b). In the present study, the geochemical parameters like $Fe_2O_3^t$ + MgO, TiO_2 (Bhatia, 1983) and Th-Sc-Zr/10 diagram (Bhatia and Crook, 1986) (Fig. 36) suggest active margin or continental island arc setting for the Sakoli and the Sausar pelites. However, Ni and Cr abundances of the pelites are not comparable with the fore-arc setting to the Sakoli and Sausar sediments. The average Ni and Cr content of island arc rocks is 25 ppm and 60 ppm respectively (Gill, 1981; Thrope, 1982). The low Ni and Cr concentration of island arc rocks is due to olivine and spinel fractionation (Taylor, 1977). The Paleoproterozoic pelites of the Bastar craton contain higher Ni and Cr abundances than do the island arc rocks (58 ppm and 189 ppm, respectively) constituting evidence against fore-arc tectonic setting. This observation is consistent with K_2O/Na_2O - SiO_2 and K_2O/Na_2O - SiO_2/Al_2O_3 plots (Figs. 34 and 35) and other geochemical parameters of Bhatia (1983) (Table 9), which suggests passive margin tectonic setting for all the Proterozoic supracrustal rocks of the Bastar craton. The K_2O/Na_2O - SiO_2 plot (Roser and Korch, 1986) (Fig. 34) which suggests passive margin setting for all the Neoproterozoic and Paleoproterozoic samples of the

Bastar craton, is considered to be more suitable than Bhatia's discrimination diagrams (Armstrong-Altrin and Verma, 2005). The extensive field observations conducted by Takashi et al. (2001) also suggest that the sedimentation of the Sakoli Group and Sausar Group took place in the continental shelf or rift-related conditions rather than in the accretionary zone. Therefore, it is inferred that intra-cratonic tectonic setting existed for both the Paleoproterozoic and the Neoproterozoic basins and in other words suggest stability of the Bastar craton during the Paleoproterozoic and the Neoproterozoic time. The petrographic data of the Neoproterozoic sandstones also suggests their cratonic interior tectonic setting or tectonic stability on QtFL, QmFLt and QmPK triangular diagrams of Dickinson and Suczek (1979) (Fig. 31, 32 and 33). This study strengthens the stable intra-cratonic origin of these Paleoproterozoic and Neoproterozoic basins of the Bastar craton using the petrology and geochemistry of the Paleproterozoic and the Neoproterozoic supracrustal rocks of the Bastar craton.

Chapter-VI

PROVENANCE
AND
CRUSTAL EVOLUTION

6. PROVENANCE AND CRUSTAL EVOLUTION

6.1 PALEOWEATHERING CONDITIONS

Chemical weathering has important effects on the composition of siliclastic rocks, where larger cations (e.g. Rb, Ba), remain fixed in the weathered residue, in preference to smaller cations (Na, Ca, Sr) which are selectively leached (Nesbitt et al., 1980). These chemical trends may be transferred to the sedimentary record (Nesbitt and Young, 1982; Wronkiewicz and Condie, 1987), and thus provide a useful tool for monitoring source-area weathering conditions. The enrichment of immobile elements like SiO_2, Al_2O_3, TiO_2, Rb and Ba and depletion of Na_2O, CaO and Sr in the studied samples especially in the Neoproterozoic non-calcareous shales and the Paleoproterozoic pelites suggests strong chemical weathering (Appendix II). Nesbitt and Young (1982) defined a chemical index of alteration (CIA) to quantitatively measure the degree of weathering (in molecular proportions) (Fedo et al., 1995): CIA= $[Al_2O_3/(Al_2O_3+CaO^*+Na_2O+K_2O)]$ x100, where CaO* represents the Ca in the silicate phases. CIA values for average shales range from 70 to 75 (of a possible 100), which reflects the compositions of muscovites, illites and smectites. Intensely weathered rocks yield mineral compositions trending towards kaolinite or gibbsite and a corresponding CIA value approaches 100 (Fedo et al., 1995). In the absence of CO_2 data for the rock samples, correction for Ca in the Neoproterozoic calcareous shales (in which CaO varies from 6.84 % - 35 %) to obtain CaO* was not possible. Therefore, CIA values for the Neoproterozoic calcareous shales have not been calculated. The average CIA values of the Neoproterozoic non-calcareous shales (72.40) and the Paleoproterozoic pelites (79.06) are higher than that of NASC (57.12). The average CIA value of the Paleoproterozoic pelites is also higher than that of typical shale value (75) formed by moderate chemical weathering (Taylor and McLennan, 1985). Thus, CIA values of the Neoproterozoic non-calcareous shales and the Paleoproterozoic pelites suggest moderate to intense chemical weathering for these rock samples. Such an inference is also supported by the average trend of these sediments on A - CN - K diagram (where A, CN and K refers to Al_2O_3, $CaO + Na_2O$ and K_2O respectively) which is defined by the chlorite and muscovite - illite end members (Fig. 37). However, the average CIA values of the Paleoproterozoic quartzites (55.66) and the Neoproterozoic sandstones (67.50) are lower than those of Paleoproterozoic pelites and the Neoproterozoic non-calcareous shales. The average CIA value of the Paleoproterozoic quartzites is very close to that of NASC (57.12); NASC referring to North American Shale Composite. The lower CIA values of the quartzites and sandstones probably do not reflect the general weathering conditions of the source region, but it may be due to sedimentary sorting effect. Physical sorting of sediment during transport and deposition leads to concentration of quartz and feldspar with some heavy minerals in the coarser fraction and secondary and more weatherable minerals in the suspended load sediments (Gu et al., 2002; Wani and Mondal, 2008). Petrographic observations reveal that the sandstones are enriched in quartz and depleted in labile minerals. Therefore, CIA values of the sandstones and the quartzites are less than the Neoproterozoic non-calcareous shales and the Paleoproterozoic pelites. Thus, the lower CIA values of the sandstones and quartzites is due to sorting and as such reflect moderate to intense weathering conditions in the source area as obtained from the shales and pelites (Wani and Mondal, 2008).

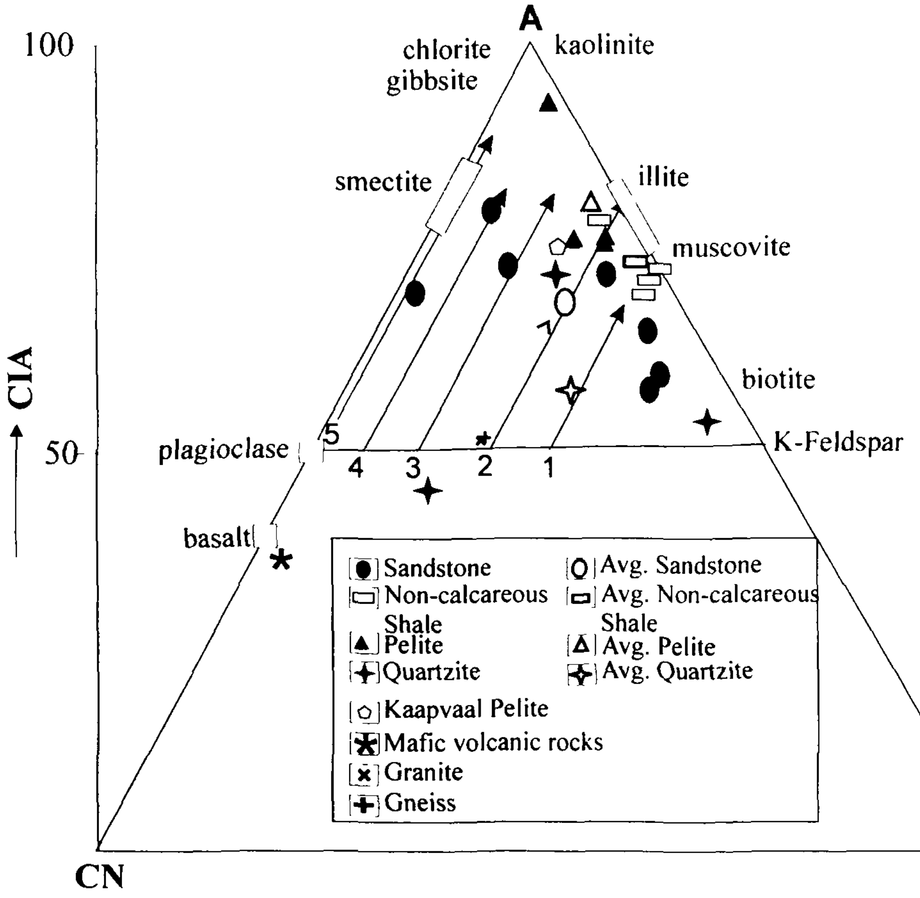

Fig. 37. Al_2O_3 - (CaO^* + Na_2O) - K_2O (A - CN - K) ternary diagram, (Nesbitt and Young, 1982), where CaO^* = CaO in silicate phases showing the plots of the Paleoproterozoic pelites and quartzites, and Neoproterozoic non-calcareous shales and sandstones of the Bastar craton. Average compositions of different rock types of Bastar craton: granite and gneiss of Bastar craton from Mondal et al. (2006), mafic volcanic rocks from Srivastava et al. (2004), Paleoproterozoic pelites of Kaapvaal craton from Wronkiewicz and Condie (1990) have also been plotted for comparison. Numbers 1-5 denote compositional trends of initial weathering profiles of different rocks: 1-gabbro; 2-tonalite; 3-diorite; 4-granodiorite; 5-granite.

Moderate to intense chemical weathering of source rocks of the Paleoproterozoic pelites, and the Neoproterozoic non-calcareous shales and sandstones is also indicated by their high average plagioclase index of alteration values (PIA >80) (Appendix II) calculated following the equation (Fedo et al., 1995): PIA = $[(Al_2O_3 - K_2O)/(Al_2O_3 + CaO^* + Na_2O - K_2O)] \times 100$, where CaO* represents CaO in silicate phases. The Neoproterozoic non-calcareous shales and sandstones, and the Paleoproterozoic pelites have average high PIA values of 95.62, 81.69 and 93.02 respectively indicating near complete alteration of its plagioclase. However, the Paleoproterozoic quartzites have average PIA value (45.70) lower than that of the sandstones, shales and pelites, which is consistent with its lower CIA value. When the average CIA and PIA values of the Paleoproterozoic Kaapvaal pelites of the Kaapvaal craton were calculated (74.36 and 84.93 respectively), they are almost similar to the Paleoproterozoic pelites and the Neoproterozoic non-calcareous shales of the Bastar craton. It is to be noted here that the Paleoproterozoic pelites of the Kaapvaal craton have been suggested to have formed under similar (moderate to intense) weathering conditions (Wronkiewicz and Condie, 1990).

The A – CN - K triangle can also be used to constrain initial compositions of source rocks and to examine their weathering trends because the upper crust is dominated by plagioclase and K-feldspar rich rocks and their weathering products (Fedo et al., 1995; Nesbitt and Young, 1984, 1989). Many weathering profiles show a linear trend subparallel to A - CN join in the A – CN - K triangle (Nesbitt and Young, 1984). In the absence of K-metasomatism, a line extends through the data points intersects the feldspar join at a point that shows the proportion of plagioclase and K-feldspar of the fresh rock.

This proportion yields a good indication of the type of the parent rock. A metasomatised sample suite will typically have a linear trend with a less steep slope, because the amount of K- addition but its intersection with the feldspar join indicates the likely source rock composition (Fedo et al., 1995). The studied samples do not show any linear trend parallel or subparallel to A - CN join except for the non-calcareous shales which plot along granite trend (Fig. 37). The sandstone and quartzite samples show wide scatter on the A – CN - K plot, however, their average value plot between granite and granodiorite trend (Fig. 37). The wide scattering of the sandstone and quartzite samples may be due to dissolution of K-bearing minerals during progressive weathering, which releases K in preference to Al, so the bulk composition trends of the residues are directed towards to the Al_2O_3 apex (Wani and Mondal, 2008). The decrease in the abundance of K-feldspar in sandstones from the Lohardih Formation to the Kansapathar Formation in the Chandarpur Group is consistent with petrographic observations of sandstones which reveals decrease of K-feldspar stratigraphically from bottom to top (Appendix I). The average composition of the Bastar pelites plot between the granodiorite and diorite trend on A- CN -K diagram (Fig. 37). However, when the average composition of the Paleoproterozoic Kaapvaal pelites, which are supposed to be derived from mafic source rocks (Wronkiewicz and Condie, 1990) were plotted for comparison on A- CN -K diagram, it falls on the same trend as that of the Paleoproterozoic pelites Bastar craton which plot between granodiorite and diorite composition. Since the source of the Paleoproterozoic Kaapvaal pelites are considered to be mafic, the source of the Paleoproterozoic pelites of the Bastar craton can also to assumed to be mafic (Fig. 37).

Weathering conditions of the Paleoproterozoic pelites and quartzites, and the Neoproterozoic shales (both calcareous and non-calcareous) and sandstones may also be examined with the K_2O - $Fe_2O_3^t$ - Al_2O_3 ternary diagram of Wronkiewicz and Condie (1989). It is evident from the diagram (Fig. 38), that most of the samples plot near NASC and some samples also plot between NASC and residual clays. The samples on this diagram fall along a trend defined by chlorite – illite and muscovite end members. This is similar to A – CN - K diagram (Fig. 37), where all the samples plot along illite - muscovite trend. It is also clear from the $Fe_2O_3^t$ - K_2O - Al_2O_3 diagram (Fig. 38), that the Paleoproterozoic pelites and the Neoproterozoic shales (both calcareous and non-calcareous) are not much different from NASC. The sandstones and the quartzites show a scatter on the $Fe_2O_3^t$ - K_2O - Al_2O_3 plot (Fig. 38). The scattering may be due to variation in K-feldspar content, and in turn, may be due to variation in K_2O content.

Both the A – CN - K (Fig. 37) and $Fe_2O_3^t$ - K_2O - Al_2O_3 (Fig. 38) plots indicate moderate to intense chemical weathering in the provenance. This is further demonstrated by plots of K vs. Rb (Wronkiewicz and Condie, 1990) (Fig. 39) which indicates that most of the Neoproterozoic calcareous and non-calcareous shale samples, and the Paleoproterozoic pelite samples are depleted in K and have lower K/Rb ratios than a crustal ratio of 230 (Wronkiewicz and Condie, 1990). This can be explained by source area weathering trend, because weathering tends to decrease K relative to Rb in weathering profiles (Nesbitt et al., 1980). The sandstone samples that plot slightly above the K/Rb = 230 line (Fig. 39) is due to presence of K-feldspar (i.e. higher K_2O content) in these sandstones, which is consistent with the petrography.

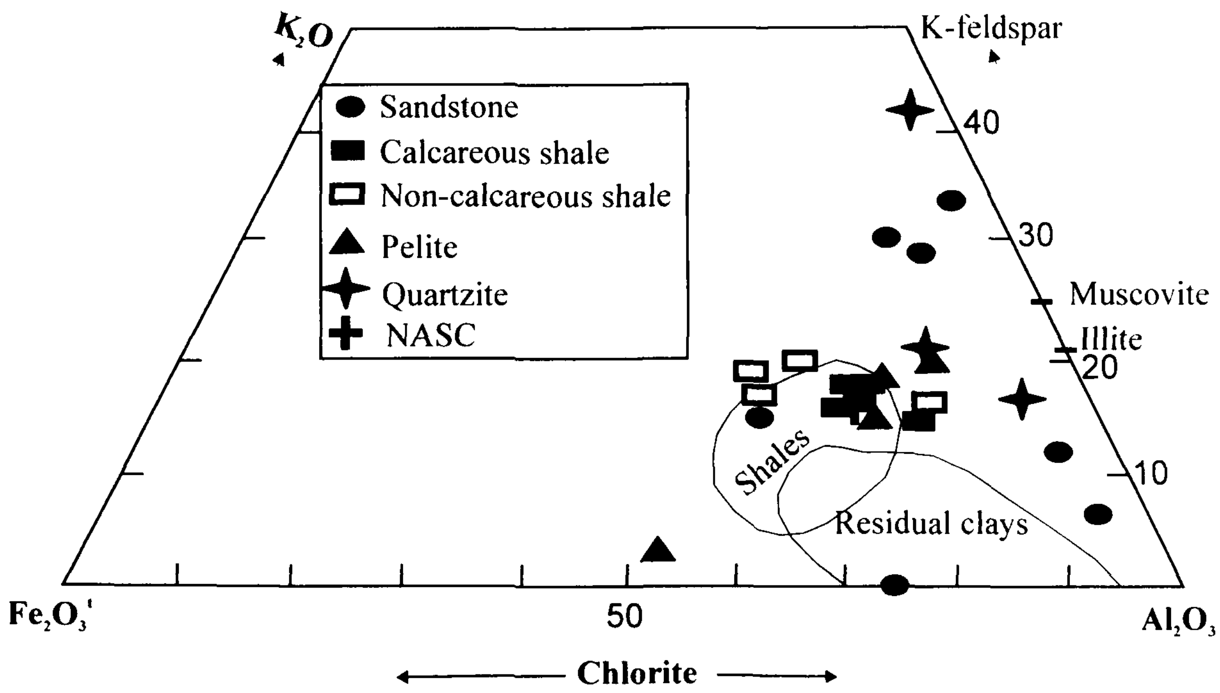

Fig. 38. K_2O - Fe_2O_3t - Al_2O_3 **triangular plot (Wronkiewicz and Condie, 1987) of the Paleoproterozoic pelites and quartzites, and the Neoproterozoic non-calcareous shales, calcareous shales and sandstones of the Bastar craton. NASC indicates North American Shale Composite (value from Gromet et al., 1984).**

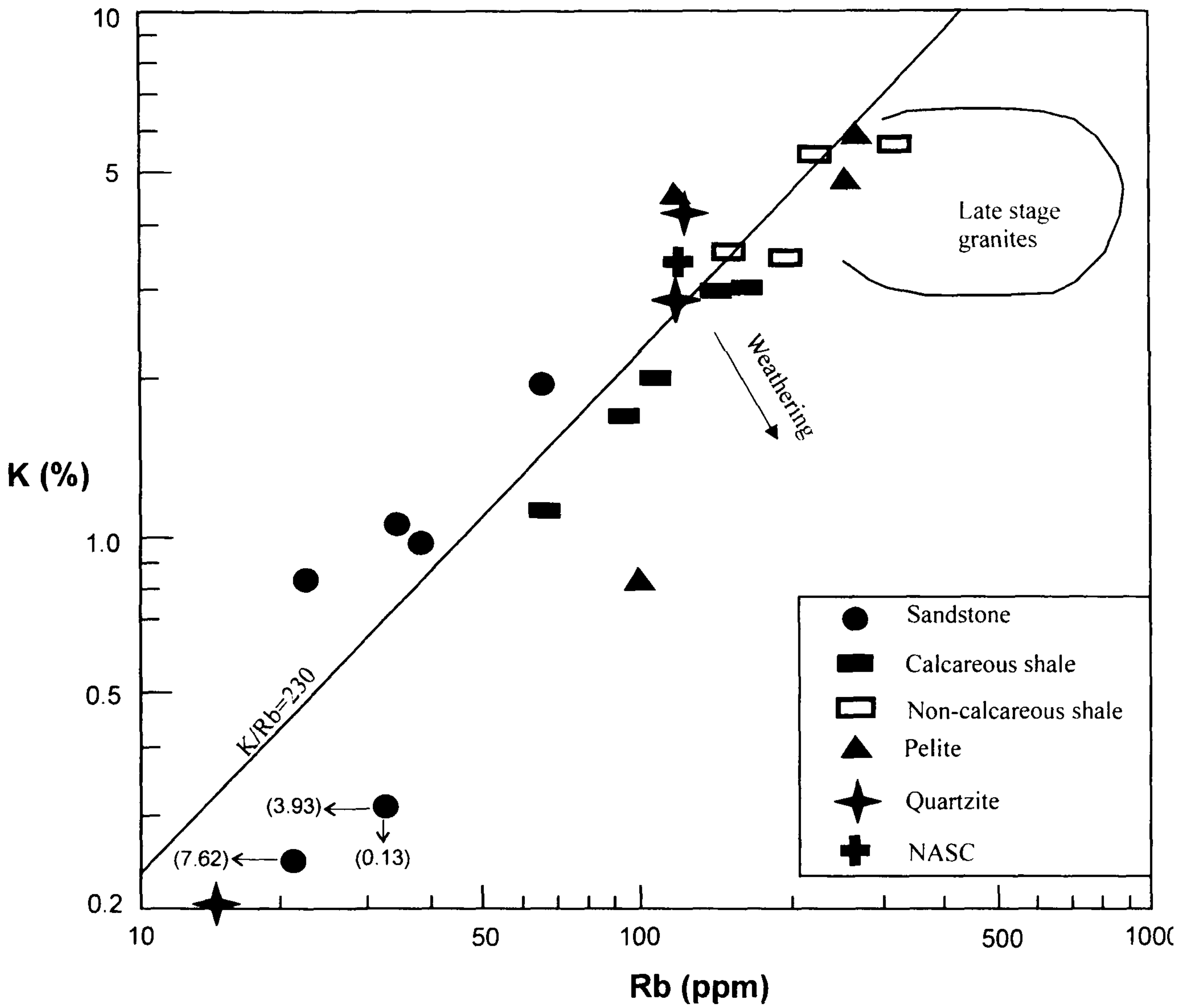

Fig. 39. K vs. Rb diagram (plot adapted from Wronkiewicz and Condie, 1989) for the Paleoproterozoic pelites and quartzites, and the Neoproterozoic non-calcareous shales calcareous shales and sandstones of the Bastar craton. K/Rb =230 line represents the average crustal ratio. NASC indicates North American Shale Composite (value from Gromet et al., 1984).

Th/U ratios are also often used for determining the degree of weathering in ancient sedimentary rocks. The Th/U ratio of sediments and sedimentary rocks is of interest because weathering and recycling are expected to result in oxidation of U^{4+} to the soluble U^{6+} state and subsequently removing it thereby elevating the Th/U ratio (McLennan and Taylor, 1980, 1991; McLennan et al., 1990). Th/U ratios above 4 are thought to be related to weathering history (McLennan et al., 1995). The average Th/U ratios of the sandstones (4.5) and the pelites (4.11) are slightly above Upper Continental Crust (UCC) (Condie, 1993; Taylor and McLennan, 1985) and also above the generally accepted value of 3.8 for bulk earth. However, the quartzites have Th/U ratio (3.6) very close to UCC. The non-calcareous shales (13.98) and the calcareous shales (8) have high average Th/U ratios which is also suggestive of moderate to intense weathering in the source area. The Paleoproterzoic Kaapvąal pelites of Kaapvaal craton have average Th/U value of 3.28.

The relationship among alkali and alkaline earth elements, CIA, PIA, Th/U and K/Rb ratios indicate that the Paleoproterozoic and the Neoproterozoic provenance of the Bastar craton was affected by moderate to intense weathering history. These parameters also give a broad hint of prevailing similar (moderate to intense) weathering conditions in the Bastar craton during the Proterozoic.

6.2 SOURCE ROCK COMPOSITION

The qualitative petrography provides important information on the nature of source rock (Anani, 1999; Critelli and Ingersoll, 1994; Crittelli and Nilsen, 2000; Dickinson and Suczek, 1979; Michaelsen and Henderson, 2000). Petrographic analysis reveals that the main detrital framework mineral grains of the Neoproterozoic sandstones of the Chandarpur Group of the Chhattisgarh basin and the Tiratgarh Formation of the Indravati basin include monocrystalline quartz, polycrystalline quartz, microcline, plagioclase, rock fragments especially chert, mica and heavy minerals. Sandstones of the Chandarpur Group and the Tiratgarh Formation are characterized by abundant quartz grains (82.22 % and 88.16 % on the average, respectively). Feldspar constitutes 1.87 % and 2.02 % on average of the framework grains of the Chandarpur Group and the Tiratgarh Formation respectively, and is dominated by microcline. Heavy minerals are rare and are dominated by zircon (Appendix I).

Overall, the Chandarpur Group of the Chhattisgarh basin shows decrease in feldspar content from the Lohardih Formation (the Lower Formation of the Chandarpur Group) to the Kansapathar Formation (the Upper Formation of the Chandarpur Group) which is accompanied by corresponding increase in the framework quartz grains as well as quartz cement. The increase in quartz and decrease in feldspar content in the Chandarpur Group from the Lohardih Formation to the Kansapathar Formation stratigraphically suggests peneplanation of the stable cratonic provenance. The general petrographic attributes also show similarity between the Lohardih Formation and the Tiratgarh Formation which form the basal part of the Chandarpur Group and the Indravati Group respectively. Overall the little variations in the mineralogy of sandstones of the Chandarpur Group and the Tiratgarh Formation do not reflect any change in the provenance for these sandstones (Wani and Mondal, 2007, 2008). According to Dickinson (1985) the main sources for the craton-derived quartzose sands are low-lying granitic and gneissic exposures, supplemented by recycling of associated flat-lying sediments. The mineralogy of these sandstones is also consistent with their derivation from granitic and gneissic source. The presence of chert, stretched metamorphic polycrystalline quartz grains (subgrains with sutured contacts) (Fig. 11) and lithic fragments in minor amounts in some samples (Fig. 12), and well rounded quartz grains with silica overgrowth floating in calcite cement (Fig. 8) indicates that the minor part of detritus has been derived from an older sedimentary succession in the source area. The northwesterly paleoslopes of the Chandarpur Group of the Chhattisgarh basin, inferred from paleocurrent studies (Datta et al., 1999) indicate that some detritus were derived from the northwestern region of the Chhattisgarh basin. It is interesting to note that the Paleoproterozoic supracrustal rocks like the Sakoli Group and the Sausar Group lie west of the Chhattisgarh basin (Fig. 1). This gives a broad hint that some sediments might have been recycled from these Paleoproterozoic basins.

In the QtFL ternary diagram (Dickinson and Suczek, 1979) (Fig. 31) all the sandstone samples of the Chandarpur Group of the Chhattisgarh basin and the Tiratgarh Formation of the Indravati basin plot in the stable cratonic field. In the QmFLt diagram (Dickinson and Suczek, 1979) (Fig. 32), the population of the samples also suggests the craton interior provenance for the sandstone samples of the Chandarpur Group of the Chhattisgarh basin and the Tiratgarh Formation of the Indravati basin. However, a few samples plot on or near quartzose recycled provenance. The overall petrological evidence indicates that the source rocks of the sandstones are granites, gneisses and low-grade metasedimentary rocks of the Bastar craton (Wani and Mondal, 2007, 2008).

Relative to widely referred NASC (Fig. 40), the Neoproterozoic sandstones and the Paleoproterozoic quartzites are depleted in all major and trace elements except that

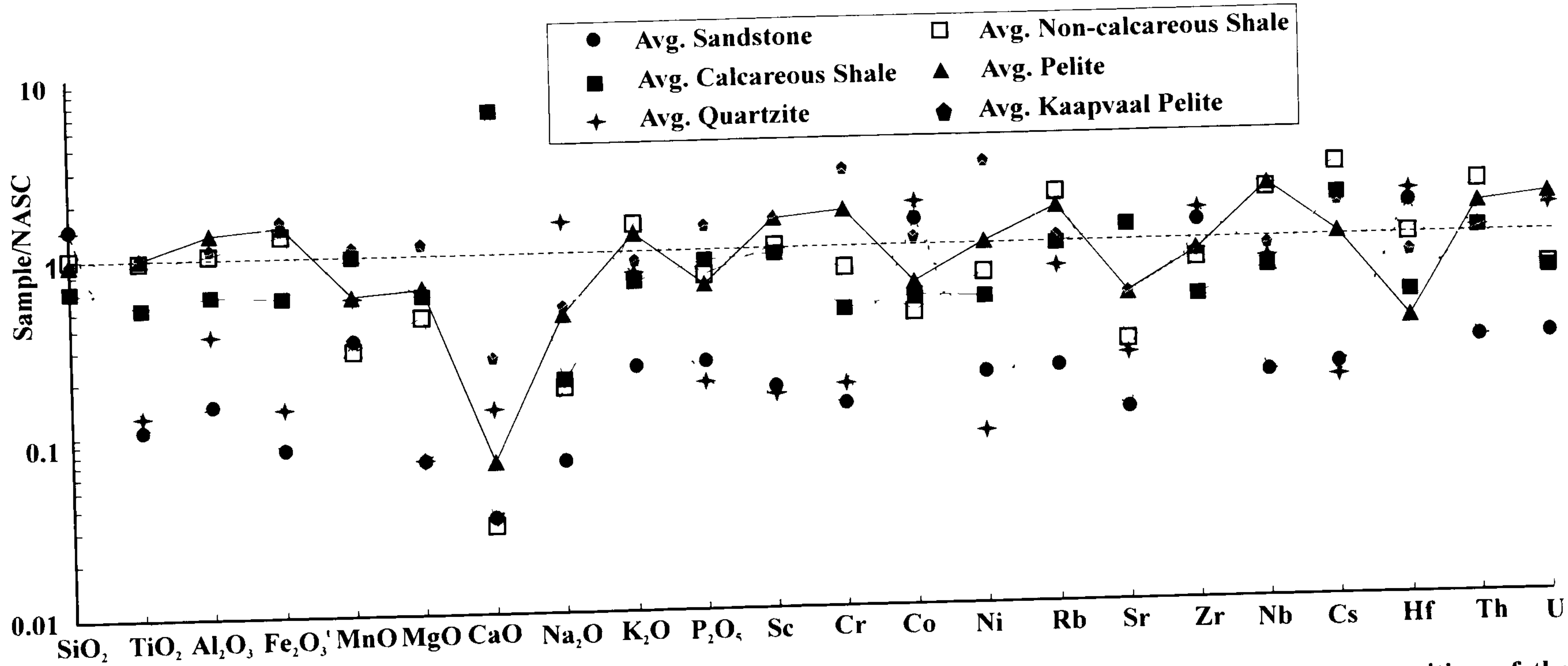

Fig. 40. NASC (North American Shale Composite) normalized average major and trace element composition of the Paleoproterozoic pelites and quartzites, and the Neoproterozoic sandstones and shales of the Bastar craton. Paleoproterozoic Kaapvaal pelites of the Kaapvaal craton (Wronkiewicz and Condie, 1990) are also shown for comparison. NASC values from Gromet et al. (1984)

the sandstones are enriched in SiO_2, Zr and Co, and the quartzites are enriched in SiO_2, Na_2O, Zr and Co (Fig. 40). The enrichment of Co and depletion of all other transition elements like Cr, Sc and Ni in these sandstones and quartzites does not reflect contribution from mafic source and implies that the enrichment of Co may have taken place during sedimentary processes. The quartzites are enriched in Al_2O_3, K_2O and Na_2O compared to sandstones (Fig. 40). It may be due to the presence of mica in the quartzites as revealed from petrographic studies. The difference in the rest of the major elements is not very significant. There is no such systematic difference in transition elements, LILE and HFSE between the sandstones and the quartzites. However, concentration of some elements like Rb, Th, Zr, Sr, Y, Nb are higher in the quartzites compared to the sandstones (Fig. 40).

The Neoproterozoic calcareous and the non-calcareous shales are depleted in most of the major and trace elements relative to the NASC (Fig. 40). The non-calcareous shales are strongly depleted in CaO, MnO, Sr and Ba compared to NASC. They are enriched in Al_2O_3, $Fe_2O_3^t$, K_2O, Rb, Cs, Th, Ta and Nb and have almost similar concentrations of SiO_2, TiO_2, Sc and Hf relative to the NASC. The calcareous shales are, however, enriched in CaO, Sr, Cs, Ba and Th and show similar concentrations of MnO, Sc and Ta relative to the NASC. The higher concentration of Sr is related with CaO in the calcareous shales as supported by the positive correlation between Sr and CaO ($r = 0.82$). The strong enrichment of Th in shales relative to the NASC may be a reflection of Th enriched granitic source for these shales. The granites and gneisses of the Bastar craton are enriched in Th (Appendix II), which suggest that these shales may have been derived from granite and gneiss of the Bastar craton.

The Paleoproterozoic pelites are strongly enriched in $Fe_2O_3^t$ + MgO and Al_2O_3 compared to NASC and the Neoproterozoic shales (both calcareous and non-calcareous shales). The incompatible elements like Rb, Y, Cs, Th, LREE and HREE have lower values for the pelites than those for the shales. However, transition elements e.g. Sc, Ni, Cr (except Co) have higher values in pelites compared to NASC and the shales (both calcareous and non-calcareous shales) (Appendix II). The differences in rest of the major and trace elements are not very significant. Overall, the incompatible elements like LILE (large ion lithophile elements) and HFSE (high field strength elements) e.g. Rb, Sr, Cs, Ba, Ta, Nb and Th which are believed to be enriched in felsic source rocks (Feng and Kerrich, 1990) are enriched in the calcareous and the non-calcareous shales as compared to the NASC and the pelites. However, compatible elements like transition elements (Sc, Ni and Cr) which are believed to be enriched in mafic sources (Feng and Kerrich, 1990) have lower values (except Co) in both the calcareous and the non-calcareous shales compared to NASC and the pelites. This general stratigraphic geochemical trend indicates that mafic source decreased with time during the deposition of the Neoproterozoic sandstones and shales (calcareous and non-calcareous) in the Bastar craton. In the Figure 40, the Neoproterozoic sandstones and shales (calcareous and non-calcareous shales), and the Paleoproterozoic quartzites and pelites have been compared with the Paleoproterozoic pelites of Kaapvaal craton. The Paleoproterozoic Kaapvaal pelites of the Kaapvaal craton are derived from mafic source (Wronkiewicz and Condie, 1990). It is evident from Figure 40, that the sandstones, quartzites and shales (calcareous and non-calcareous shales) of the Bastar craton are depleted in mafic components like Ni, Cr, Sc, $Fe_2O_3^t$, MgO and TiO_2 while the Paleoproterozoic pelites show close similarity in these elements with the Paleoproterozoic Kaapvaal pelites of the Kaapvaal craton (Fig. 40). This comparison further indicates that the pelites were derived from mafic sources and the sandstones, quartzites and shales (calcareous and non-calcareous) were derived from felsic sources.

In general, most of the elemental concentrations of the Neoproterozoic sandstones are lower than those in NASC due to higher quartz content. The elemental concentrations of the Neoproterozoic calcareous shales are also lower than those in NASC due to calcite dilution. So, it is inferred that the elemental concentrations of the quartz rich sandstones and calcareous shales should deviate from the source rock. However, trace elemental ratios in these quartz rich sandstones and in the calcareous shales may be more representative of the source than their elemental concentrations (Cullers, 2000; Cullers and Podkovyrov, 2002). To evaluate the extent to which trace elemental ratios do vary in the calcareous shales and quartz rich sandstones, certain key elemental ratios like Eu/Eu*, Th/Sc, La/Sc, Th/Ni, Th/Cr, La/Ni and La/Cr of the quartz rich sandstones against SiO_2 (wt. %) have been plotted and the calcareous shales against CaO (wt. %) (Fig. 41). It is evident from the Figure 41 that these elemental ratios do not vary much over a range of SiO_2 (wt. %) in sandstones and over a range of CaO (wt. %) in the calcareous shales (Wani and Mondal, 2008). Thus, it indicates that these elemental ratios are not much affected in the calcareous shales by calcite dilution and in sandstones by higher quartz content. Therefore, this study attests the importance of these elemental ratios in determining source rock characteristics.

To know the nature of the provenance of the Paleoproterozoic quartzites and pelites, and the Neoproterozoic shales (calcareous and non-calcareous) and sandstones,

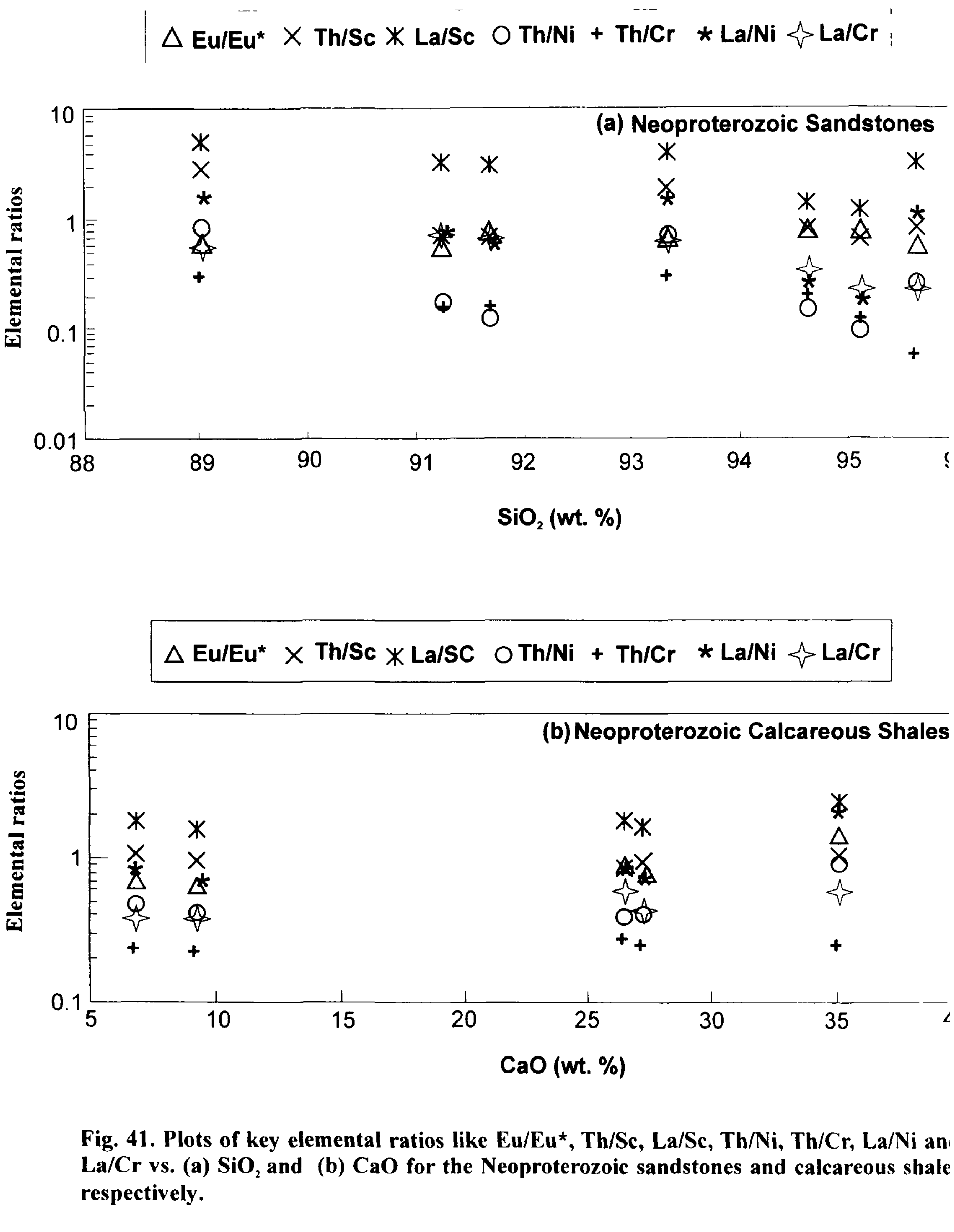

Fig. 41. Plots of key elemental ratios like Eu/Eu*, Th/Sc, La/Sc, Th/Ni, Th/Cr, La/Ni an La/Cr vs. (a) SiO_2 and (b) CaO for the Neoproterozoic sandstones and calcareous shale respectively.

certain key elemental ratios (incompatible/compatible) like Th/Sc, La/Sc, Th/Ni, Th/Cr, La/Ni and La/Cr normalized with respect to upper continental crust (UCC) have been plotted in Figure 42. It is evident from the Figure 42 that all the elemental ratios of the Neoproterozoic sandstones, shales (calcareous and non-calcareous shales) and the Paleoproterozoic quartzites are similar to UCC and show small deviation from UCC, suggesting that all these rocks were derived from sources similar to UCC. However, the Paleoproterozoic pelite sample show strong depletion in La/Sc, Th/Ni, Th/Cr, La/Ni and La/Cr ratios compared to UCC indicating a less differentiated source than UCC for the pelite.

Generally it is believed that post-Archean pelites have less concentration of mafic elements, particularly Ni and Cr, when compared with the Archean pelites. The cause of higher concentrations in Archean pelites has been explained by the presence of an ultramafic/mafic component in the Archean source, whereas the absence or scarcity of ultramafic/mafic component in the post-Archean period have been invoked for the low content of Ni and Cr in the post-Archean pelites (McLennan et al., 1983). On the Ni-Cr diagram (Fig. 43) (Taylor and McLennan, 1985) all the Paleoproterozoic pelite and quartzite samples, and the Neoproterozic shale (calcareous and non-calcareous) and sandstone samples plot along a linear trend. The Paleoproterozoic pelites have higher Ni and Cr concentrations than those of the sandstones, quartzites and shales (calcareous and non-calcareous). The average Ni and Cr concentrations of the pelites of the Bastar craton are similar to typical Neoarchean pelites. Sandstones and quartzites have lower Ni and Cr contents similar to post-Archean pelites, whereas shales (calcareous and non-calcareous) have highly variable Ni and Cr contents that are intermediate between Neoarchean and

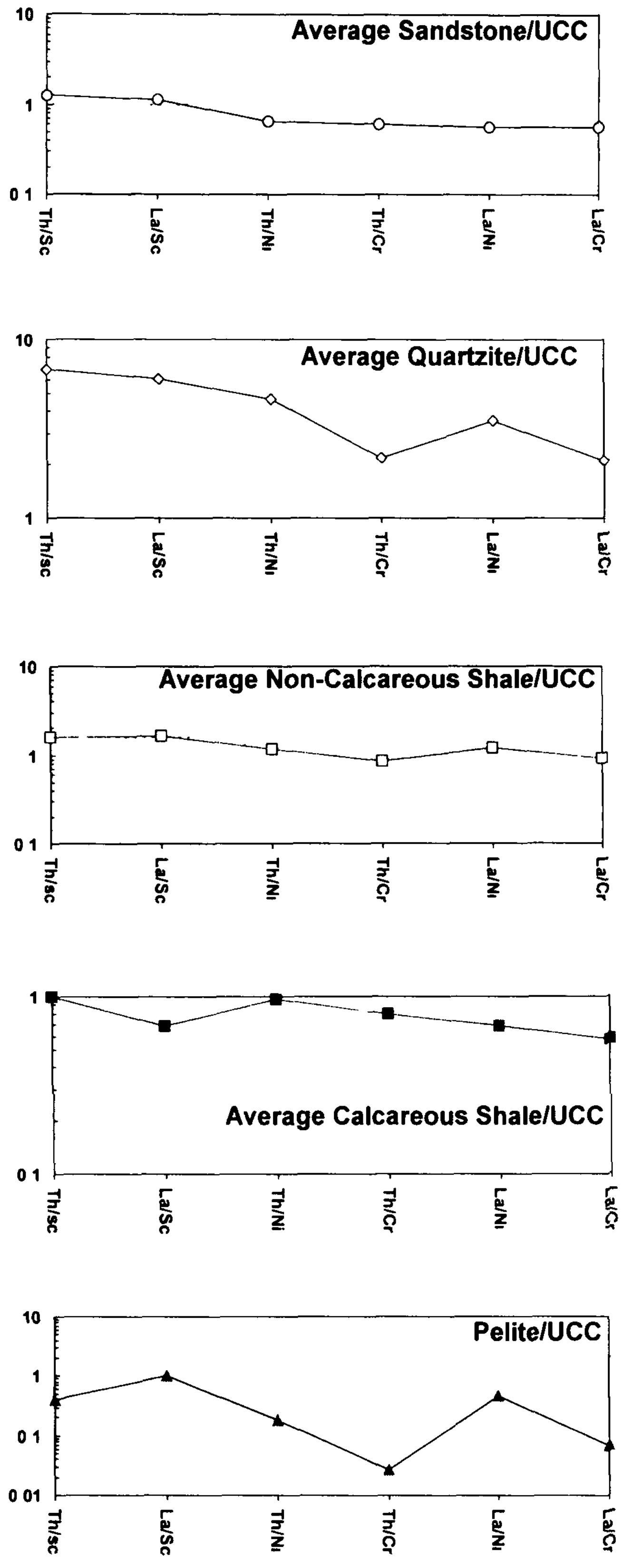

Fig. 42. UCC (Upper Continental Crust) normalised key elemental ratios of the Paleoproterozoic quartzites and a pelite sample and the Neoproterozoic non-calcareous shales, calcareous shales and sandstones of the Bastar craton.

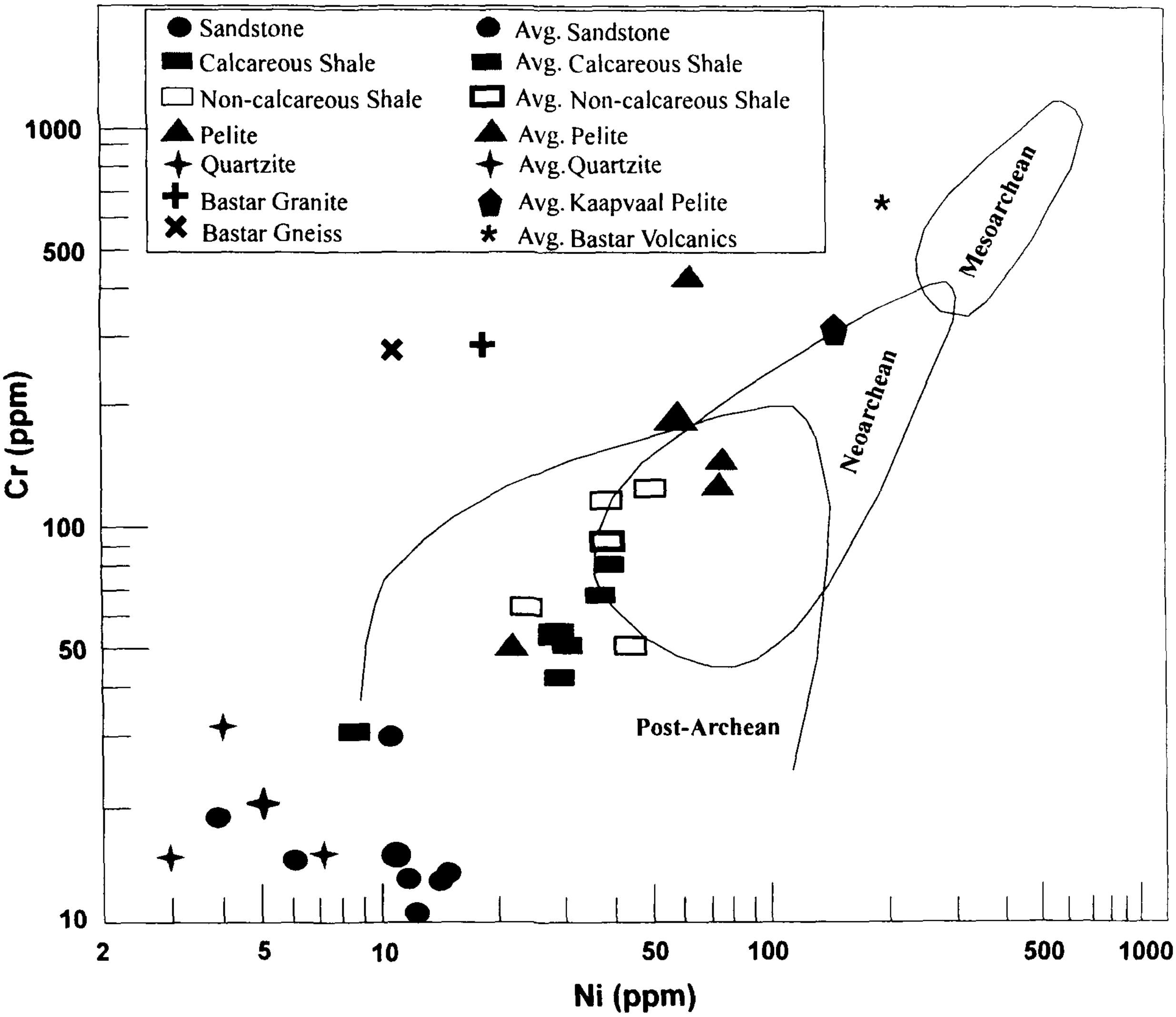

Fig. 43. Distribution of Ni and Cr in the Paleoproterozoic pelites and quartzites, and in the Neoproterozoic sandstones and shales (calcareous and non-calcareous) of the Bastar craton. Different types of rocks are also shown for comparison. Fields after Condie (1993). Data for the granite and gneiss of the Bastar craton from Mondal et al. (2006), mafic volcanic rocks of the Bastar craton from Srivastava et al. (2004) and the Paleoproterozoic pelites of the Kaapvaal craton from Wronkiewicz and Condie (1990).

post-Archean pelites. Data for the granite, gneiss and the mafic volcanic rocks of the Bastar craton, and the Paleoproterozoic pelites of the Kaapvaal craton have also been plotted on this diagram (Fig. 43) for comparison. The Kaapvaal pelites are thought to be derived from mafic rocks (Wronkiewicz and Condie, 1990). It is evident from Figure 43 that granite and gneiss of the Bastar craton are only enriched in Cr and depleted in Ni. Therefore, the sandstones, the quartzites and the shales (calcareous and non-calcareous shales) which fall at lower end of Ni-Cr trend may have been derived from granite and gneiss of the Bastar craton. However, the pelites are enriched in both Ni and Cr compared to the shales, sandstones, quartzites, and granite and gneiss of the Bastar craton but slightly depleted when compared with the Paleoproterozoic pelites of the Kaapvaal craton and mafic volcanic rocks of the Bastar craton. These observations may indicate derivation of the Bastar pelites from mafic sources. It should be noted here that pelites are also enriched in $Fe_2O_3^t$ compared to NASC and the shales (calcareous and non-calcareous shales), which may be another evidence for derivation of the pelites from mafic sources (Appendix II).

The relative contributions of mafic and felsic sources in the pelites should be reflected in the distribution of Zr and Cr in pelites, since these two elements monitor zircon and chromite contents respectively (Wronkiewicz and Condie, 1989). The pelites are enriched in both Cr and Zr (189 ppm and 167 ppm respectively) compared to the Neoproterozoic shales (calcareous and non-calcareous) (Appendix II). Thus, it may indicate presence of both felsic and mafic (granite and basalt) source rocks in the Bastar craton during the Paleoproterozoic. Lower values of Cr and higher values of Zr in the quartzites and the sandstones signify dominance of felsic source relative to mafic source for these rocks. Thus, it is concluded based on Ni-Cr relationship that both mafic and felsic sources shed the detritus were present during the Paleoproterozoic and dominantly felsic rocks acted as source of the sediments during the Neoproterozoic.

Th/Sc - Sc relations have proved to be more robust and are widely used compared to other trace elements/elemental ratios in the characterization of source lithology for clastic sediments (Taylor and McLennan, 1985). So data for the Paleoproterozoic pelites and quartzites, and the Neoproterozoic shales (calcareous and non-calcareous) and sandstones of the Bastar craton using Th/Sc - Sc relations have been plotted (Fig. 44). Data for the granite, gneiss of the Bastar craton, and the Paleoproterozoic Kaapvaal pelites have also been plotted on this diagram (Fig. 44). The granite and gneiss plot on low Sc - high Th/Sc end and the Kaapvaal pelites plotting on the high Sc - low Th/Sc end on this diagram. When the Paleoproterozoic pelites and quartzites, and the Neoproterozoic sandstones and shales (calcareous and non-calcareous shales) are compared to granite and gneiss of the Bastar craton and the Paleoproterozoic Kaapvaal pelite of the Kaapvaal craton, it is observed that the average pelite of the Bastar craton fall near the average Paleoproterozoic Kaapvaal pelite. However, the shales, sandstones and quartzites fall far away from the Paleoproterozoic Kaapvaal pelites and plot near the granite and gneiss fields of the Bastar craton (Fig. 44). These observations point to a felsic source (granitic and gneissic) for the shales, sandstones and the quartzites, and mafic source for the pelites. This conclusion is also consistent with Ni-Cr relations for these sediments (Fig. 43).

Understanding the origin of the depletion of Eu, relative to other chondrite normalized REE in clastic sedimentary rock is fundamental to any interpretation of

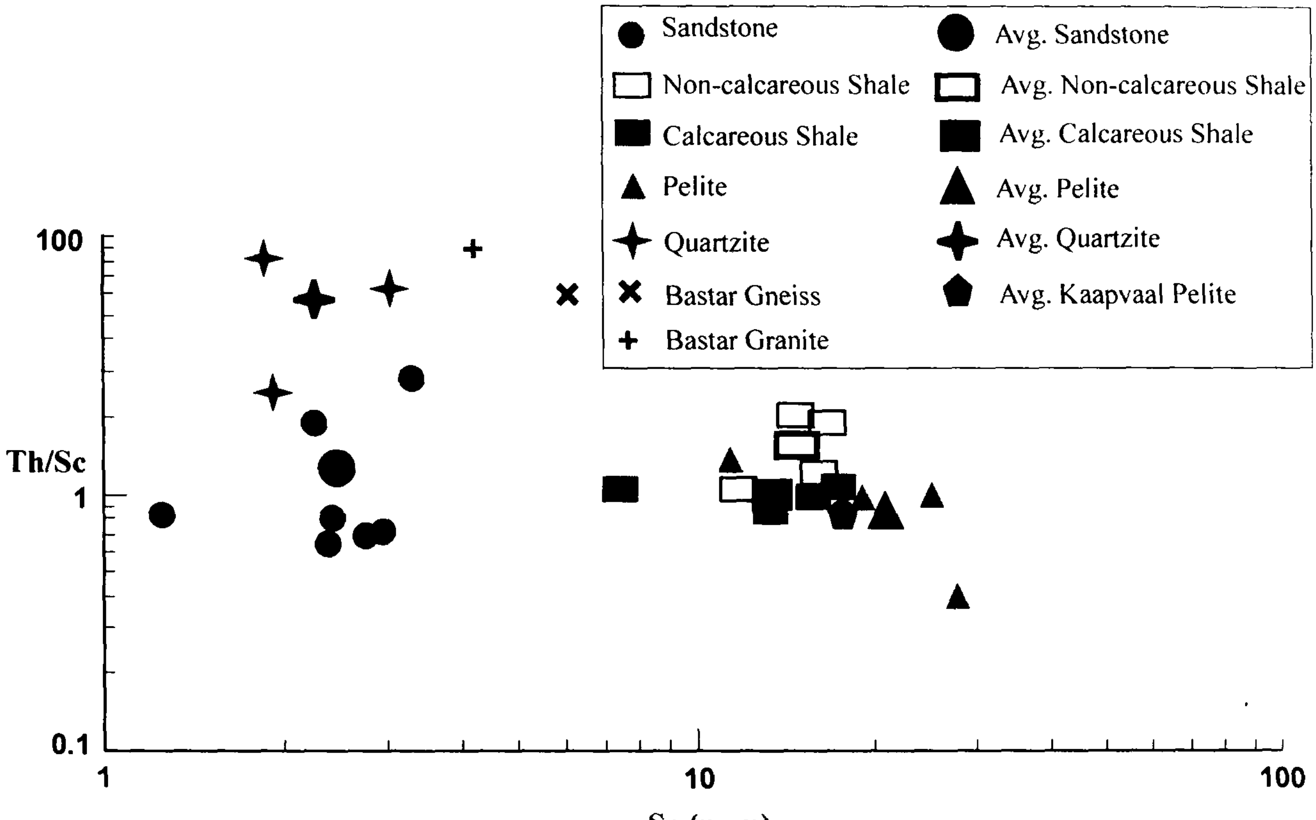

Fig. 44. Th/Sc vs. Sc distributions in the Paleoproterozoic pelites and quartzites, and the Neoproterozoic shales (calcareous and non-calcareous) and sandstones of the Bastar craton. Data for granite and gneiss of Bastar craton from Mondal et al. (2006), Kaapvaal pelite from Wronkiewicz and Condie (1990).

crustal composition and evolution (Taylor and McLennan, 1985). The most significant observation in this regard is that virtually all post-Archean sedimentary rocks are characterized by Eu depletion of approximately comparable magnitude. The most striking evolutionary pattern of sedimentary trace element patterns is for Eu/Eu*. Archean sedimentary rocks are not anomalous or only slightly anomalous with respect to Eu anomaly (Eu/Eu* = 1) but post-Archean sedimentary rocks on average show a significant and constant depletion in Eu (Eu/Eu* = 0.65). This break in composition corresponds to the Archean - Proterozoic boundary (Taylor and McLennan, 1985). It has also been generally observed that contrary to the Archean, post-Archean sedimentary rocks are enriched in LREE, depleted in HREE and having Eu/Eu* <1 and (Gd/Yb)n <2 (McLennan et al., 1993). It is because LREE (La - Sm) are more incompatible in typical igneous differentiation processes than the HREE (Gd - Lu). Therefore, there is a general increase in the LREE/HREE ratio from more mafic to more felsic composition. Archean samples generally fall in the range of LREE/HREE = 6 - 9 and post-Archean samples typically have values in the range of LREE/HREE= 8 - 12 (Taylor and McLennan, 1985). When compared with NASC, the sandstones and the quartzites have lower ∑REE abundances. It may be due to higher quartz concentration and lower amount of heavy minerals which is consistent with petrography. However, when quartzites are compared with sandstones, it is observed that quartzites have higher ∑REE abundances (Appendix II). The sandstones and quartzites show high LREE enrichment with (La/Yb)n ratio (12.5) for sandstones and (12) for the quartzites, similar (Gd/Yb)n ratio for the sandstones (1.56) and for the quartzites (1.42), and a significant Eu anomaly (Eu/Eu* 0.67 and 0.42 for the sandstones and the quartzites, respectively). The Eu/Eu* values for both the sandstones and the quartzites are similar to the Eu/Eu* value of the granite (0.39) and the gneiss (0.65) of the Bastar craton (Appendix II).

Relative to the calcareous shales, the non-calcareous shales have higher ∑REE abundances than do the calcareous shales (Appendix II). The lower ∑REE abundances in the calcareous shales compared to the non-calcareous shales are due to calcite dilution in the calcareous shales. The calcareous and the non-calcareous shales show LREE enrichment with (La/Yb)n ratio higher for the non-calcareous shales (18) compared to the calcareous shales (7), slightly higher (Gd/Yb)n ratio for the non-calcareous shales (1.9) than for the calcareous shales (1.4), and a negative Eu anomally (Eu/Eu* 0.65 for the non-calcareous and 0.8 for the calcareous shales). The Eu/Eu* values of the non-calcareous shales show similarity with the Eu/Eu* value of gneiss (0.65) and granite (0.39) of the Bastar craton and NASC. It is also evident from the chondrite normalized (Sun and McDonough, 1989) REE patterns (Fig. 45) of the sandstones, the quartzites and the shales (calcareous and non-calcareous) that the REE patterns are highly fractionated and there are no systematic variation in the REE patterns of the sandstones, quartzites and shales (calcareous and non-calcareous). The REE patterns of both the calcareous and non-calcareous shales are similar to the granite and the gneiss of the Bastar craton and do not match with the REE patterns of Archean mafic volcanic rocks of the Bastar craton (Fig. 45). This further supports the felsic source for the Neoproterozoic sandstones and shales (calcareous and non-calcareous) of the Bastar craton.

The pelite sample of the Bastar craton have lower REE abundances (124 ppm) and has lower (La/Yb)n ratio 8.86 and (Gd/Yb)n ratio (1.83) than the non-calcareous shales, sandstones and quartzites (Appendix II). In comparison to NASC, the pelite

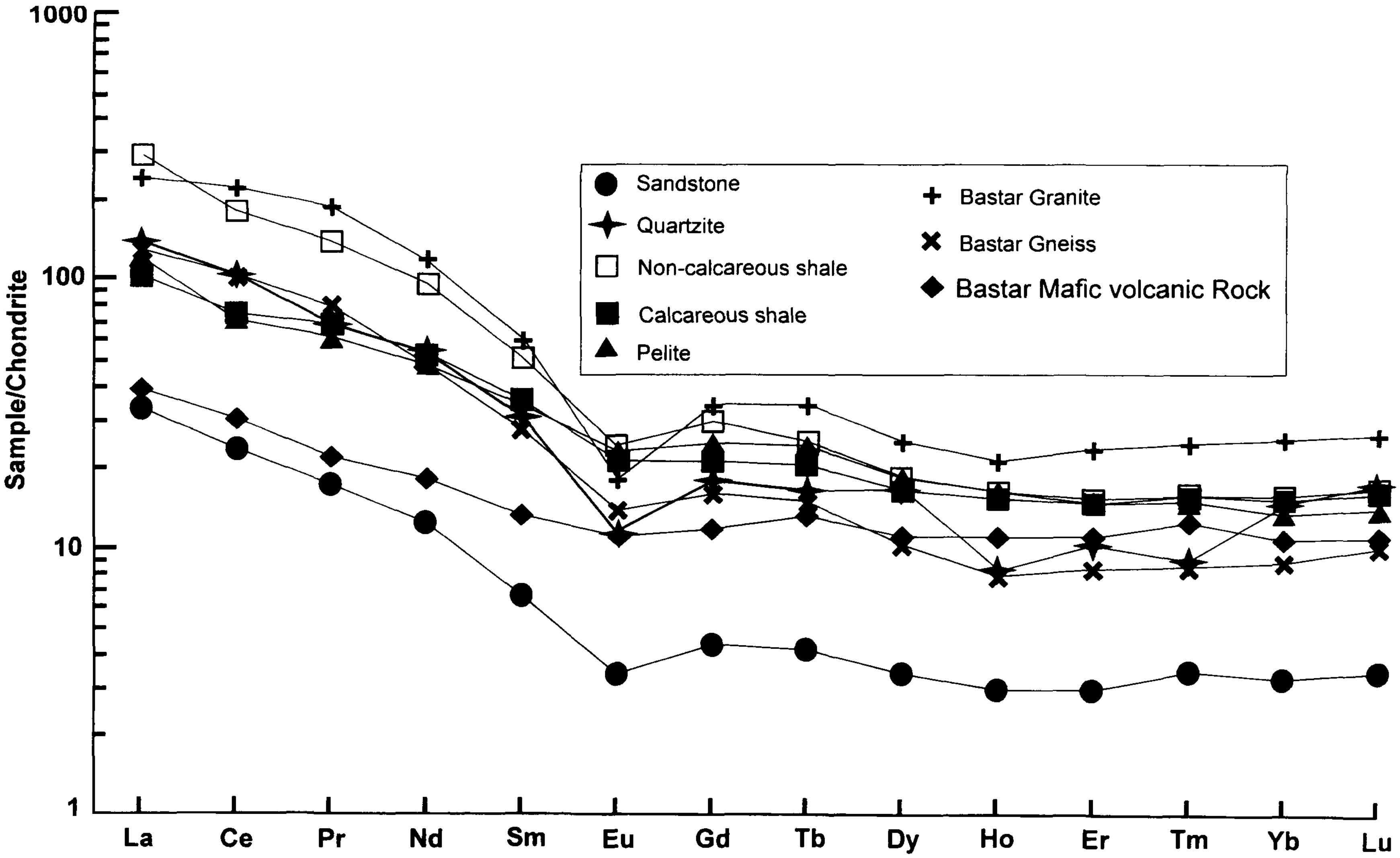

Fig. 45. Chondrite normalized REE patterns of the Paleoproterozoic quartzites and pelite, and the Neoproterozoic non-calcareous, calcareous shales and sandstones of the Bastar craton. Chondrite normalized REE patterns of the granite, gneiss and mafic volcanic rocks of the Bastar craton have been shown for comparison. Data for the granite and gneiss of the Bastar craton from Mondal et al. (2006), mafic volcanic rocks from Srivastava et al. (2004). Chondrite normalization values from Sun and McDonough (1989).

sample has lower REE abundances, and lower (La/Yb)n and (Gd/Yb)n ratios (Appendix II). The REE pattern of the Paleoproterozoic pelite of the Bastar craton is clearly different from the Neoproterozoic sandstones, shales (calcareous and non-calcareous) and the Paleoproterozoic quartzites. The REE pattern of the pelite sample also shows a fractionated trend, but it is less fractionated than that of the sandstones, quartzites and shales (non-calcareous and calcareous) (Fig. 45).

It is also is to be noted that the Paleoproterozoic pelite of the Bastar craton has a small negative Eu anomally (Eu/Eu* = 0.80), which may indicate contribution from mafic source rocks. It should also be taken into consideration that earlier studies (McLennan, 1989) have shown that Eu is not fractionated during weathering or diagenesis relative to other REE. Therefore, size of Eu anomaly in sedimentary rocks reflects input from source rocks. The average Eu/Eu* value of Archean mafic volcanic rocks of the Bastar craton (0.90) is very close to Eu/Eu* value of the Paleoproterozoic pelite of the Bastar craton (0.80) (Appendix II). This may suggest that these mafic volcanic rocks may have contributed detritus for the pelites. This is consistent with high $Fe_2O_3^t$, Ni, Cr, Sc concentrations and low Th/Sc ratio in the Paleoproterozoic pelites of the Bastar craton. However, REE abundances and the LREE fractionated pattern of the pelite indicate contribution from granitoids also, because the REE budget in clastic sedimentary rocks is chiefly controlled by granitoids, which mask the contribution of mafic-ultramafic components (Jahn and Condie, 1995). This conclusion is consistent with the enrichment of both Cr and Zr in pelites (Appendix II).

Like the pelite sample, the calcareous shales have small negative Eu anomaly (Eu/Eu* ratio = 0.8), which is higher than those of the non-calcareous shales (0.65).

granite (0.39) and gneiss (0.65) of the Bastar craton. However, the calcareous shales cannot be considered to be derived from mafic sources as suggested for the pelite, because the calcareous shales are depleted in mafic elements. So enrichment in Eu anomaly alone cannot indicate the derivation of the calcareous shales from the mafic sources (Taylor and McLennan, 1985).

The overall petrological and geochemical evidence indicates source rocks for the Neoproterozoic shales (calcareous and non-calcareous shales) and sandstones, and the Paleoproterozoic quartzites were felsic in nature and the source rocks were identified to be granite and gneiss of the Bastar craton. However, the source rocks for the Paleoproterozoic pelites are mafic in nature and the source rocks are identified to be mafic volcanic rocks of the Bastar craton. The data also show petrological and geochemical similarities between the Neoproterozoic sandstones of the Chandarpur Group of the Chhattisgarh basin and the Tiratgarh Formation of the Indravati basin. The shales of the Chhattisgarh basin and the Indravati basin also show geochemical similarities, thus indicate homogeneity in the source rock composition during the Neoproterozoic time and also indicate that the sediments for the Neoproterozoic Chhattisgarh and Indravati basins have been derived from similar sources i.e. granite and gneiss of the Bastar craton, and minor amount of detritus may have been derived from older sedimentary/metasedimentary successions of the craton which is consistent with petrography and paleocurrent studies. Ramakrishnan (1987) have suggested that the Chhattisgarh and Indravati basins represent the faulted and eroded remnants of a single continuous Bastar-Chhattisgarh superbasin. In the present study, the petrological and geochemical similarities between the Neoproterozoic Chhattisgarh and Indravati basins gives a broad hint that the Chhattisgarh and Indravati basins might have remained once connected.

In contrast, the Paleoproterozoic pelites and quratzites of the Sakoli and Sausar basins suggest heterogeneity in the source area. The Paleoproterozoic pelites of the Sakoli and Sausar Groups are enriched in mafic components while the Paleoproterozoic quartzites from the Sakoli and Sausar Groups are enriched in felsic components. This may be due to hydraulic sorting, as it sorts different source components into different grain size class. Lahtinen (1996) also noticed that a slight grain-size induced preferential separation of felsic source into the psammites and mafic source into the pelites. Thus, this is advantageous to use both pelites/shales and psammites so as to delineate all source end members particularly the mafic end members and felsic end members respectively. It becomes disadvantageous to use only one of these in crustal evolution studies as one of the end members of the mafic and felsic sources will be either overshadowed or underestimated as the case may be. Similar results were also traced out by Lahtinen (2000).

6.3 CRUSTAL EVOLUTION

The petrology of the sandstones, and the geochemistry of the sandstones and shales (calcareous and non-calcareous shales) of the Neoproterozoic Chhattisgarh and Indravati basins, and the pelites and quartzites of the Paleoproterozoic Sakoli and Sausar basins of the Bastar craton have been studied for paleoweathering, tectonic setting and to delineate sediment source components and finally to trace the Proterozoic crustal evolution in the Bastar craton, Central Indian Shield. The petrological evidence indicates that the source rocks of the Neoproterozoic sandstones were dominantly felsic rocks (granites and gneisses) with minor component of the detritus derived from older sedimentary succession in the source area (Wani and Mondal, 2007, 2008). Relative to NASC, the sandstones and the quartzites are depleted in major and trace elements including REE except for SiO_2, Na_2O, Co and Zr. Enrichment of SiO_2 and Zr in the sandstones indicate quartz rich felsic sources for these sediments. The REE patterns of the sandstones and the quartzites are highly fractionated with LREE enrichment and flat HREE. The REE patterns of these sandstones are similar to granite and gneiss of the Bastar craton. The Eu/Eu* values of the sandstones (0.67) and the quartzites (0.47) are also very close to Eu/Eu* values of the granite (0.39) and the gneiss (0.65) of the Bastar craton.

In the Neoproterozoic shales (calcareous and non-calcareous) and in the Paleoproterozoic pelites, large ion lithophile elements (LILE) and high field strength elements (HFSE) tend to increase and the transitional elements like Sc, Ni and Cr tend to decrease from the Paleoproterozoic pelites to the Neoproterozoic shales. This general stratigraphic geochemical trend indicates that felsic source (granitic/gneissic) increased and mafic source decreased with time during the deposition of the Proterozoic supracrustals. When the Neoproterozoic shales (calcareous and non-calcareous shales) and pelites are compared with the Paleoproterozoic pelites (derived from mafic sources) of the Kaapvaal craton, it is observed that the Neoproterozoic shales of the Bastar craton are depleted in mafic components like Ni, Cr, Sc, $Fe_2O_3^t$, MgO and TiO_2 while the Paleoproterozoic pelites show close similarity in these elements with the Kaapvaal pelites. The REE patterns of the shales (calcareous and non-calcareous shales) are similar to the sandstones and the quartzites. On the other hand REE pattern of the pelite sample of the Bastar craton is also fractionated but less fractionated than that of the shales (non-calcareous and calcareous), sandstones and quartzites with LREE enrichment having $(La/Yb)_n = 8.86$, flat HREE with $(Gd/Yb)_n = 1.83$ and slightly small negative Eu anomaly ($Eu/Eu^* = 0.80$). The other geochemical characteristics like UCC (upper continental crust) normalized important elemental ratios e.g. Th/Sc, La/Sc, Th/Ni, Th/Cr, La/Ni and La/Cr of the Paleoproterozoic pelite and quartzites, and the Neoproterozoic sandstones and shales indicate that the Paleoproterozoic quartzites, and the Neoproterozoic shales and the sandstones were derived from a source similar to UCC while the pelites were derived from a less differentiated source than UCC, possibly from a mafic source.

Overall, the present study shows that there is strong evidence to suggest a change in the upper crustal composition during Proterozoic in the Bastar craton and also there is ample evidence to suggest that the Paleoproterozoic exposed crust was less differentiated compared to the Neoproterozoic crust. The decreasing abundance of transition elements and increasing negative Eu anomaly from pelites to shales, accompanied by an increase in LILE suggests partial exposure of granitoids in the Paleoproterozoic and unroofing of the granitoids by the complete removal of mafic rocks in the provenance as the Neoproterozoic sedimentation progressed. The granites of the Bastar craton were emplaced at ~2.6 Ga (Sarkar et al., 1990a). The interval between the granite emplacement and their dominant contribution in the Neoproterozoic indicates slow exposure of granites during the Proterozoic. The overall mineralogical and geochemical characteristics i.e. mixing of two end member source compositions as exhibited by the Paleoproterozoic pelites (more mafic) and quartzites (felsic) relative to total felsic composition of the Neoptoterozoic shales and sandstones suggest that the composition of the source region of the Paleoproterozoic supracrustal rocks represented a transitional stage from mixed (mafic + felsic) in the Paleoproterozoic to entirely felsic in the Neoproterozoic in the unidirectional evolution of the Proterozoic continental crust of the Bastar craton. However, the geochemical characteristics do not indicate any change in tectonic setting from the Paleoproterozoic Sakoli and Sausar basins and the Neoproterozoic Chhattisgarh and Indravati basins of the Bastar craton. It is inferred that the intra-cratonic tectonic setting existed for both the Paleoproterozoic Sakoli and Sausar basins and the Neoproterozoic Chhattisgarh and Indravati basins and in other words suggest stability of the Bastar craton during the Paleoproterozoic and Neoproterozoic time. This study also strengthens the stable intra-cratonic origin of these Paleoproterozoic and Neoproterozoic basins of the Bastar craton using the petrology and geochemistry of the Paleproterozoic and the Neoproterozoic supracrustal rocks of the Bastar craton. The relationship among alkali and alkaline earth elements, CIA, PIA, Th/U and K/Rb ratios indicate that source area in the Bastar craton during the Proterozoic was affected by moderate to intense weathering history.

Chapter-VII

SUMMARY AND CONCLUSION

7. SUMMARY AND CONCLUSION

The geochemical studies of the sedimentary rocks from different parts of the world reveal that the Archean crust was enriched in Mg, Cr, Co and Ni, and depleted in Th, U, Rb and K when compared to the post-Archean crust. Although most of the rare earth element patterns of sedimentary rocks are remarkably uniform with absolute abundances, the LREE enrichment and HREE depletion demarcates the early Archean from the post-Archean (Taylor and McLennan, 1985). Some of these changes observed in the crustal rocks indicate a change in the composition of the upper crustal source from relatively mafic to felsic through time. This change probably marks the Archean - Proterozoic boundary and seems to be related with widespread granitic magmatism during latter periods. However, the geochemical changes during the Proterozoic (Paleoproterozoic - Neoproterozoic boundary) has not been studied to the extent as has been studied for the Archean - Proterozoic boundary. Thus, the present study not only reveals the nature of crust in the Proterozoic but also gives an opportunity to trace the geochemical changes from the Paleoproterozoic to the Neoproterozoic in the Bastar craton, Central Indian Shield.

The Bastar craton which is considered to be of Archean age contains granitoids and gneisses. These granitoids and gneisses form the basement for the Proterozoic supracrustal rocks. The older supracrustals (Paleoproterozoic) like the Sakoli and Sausar Groups that occur in the northern part of the Bastar craton are highly deformed and metamorphosed, while the younger supracrustals (Neoproterozoic) of the Chhattisgarh and Indravati basins of the Bastar craton are undeformed and unmetamorphosed (Naqvi and Rogers, 1987) (Fig. 1). Origin of these Paleoproterozoic and Neoproterozoic cratonic basins, however, is still poorly constrained, though an intracratonic origin or riftogenic origin has been invoked for them (Chaudhuri et al., 2002; Patranabis Deb and Chaudhuri, 2002; Naqvi and Rogers, 1987; Takashi et al., 2001; Wani and Mondal, 2007). Availability of a complete Proterozoic sedimentary record in the Bastar craton from the Paleoproterozoic (e.g. the Sakoli and Sausar Groups) to the Neoproterozoic (e.g. the Chhattisgarh and Indravati Groups) is the unique factor which makes this study very important. The sedimentary record is well preserved and the geological framework of the region has been worked out by earlier workers (e.g. Murthi, 1987; Naqvi and Rogers, 1987; Narayanswami et al., 1963; Ramakrishnan, 1987). The terrain is ideal not only for the studies of provenance, paleoclimate and tectonics but also to decipher the Proterozoic evolutionary history of the Bastar craton.

The petrology and geochemistry of the Neoproterozoic sandstones and shales, and the Paleoproterozoic pelites and quartzites of the Bastar craton have been studied for paleoweathering, tectonic setting and to delineate sediment source components and finally to trace the Proterozoic crustal evolution in the Bastar craton, Central Indian Shield. In the absence of geochemical data of detrital sediments from the Neoproterozoic and the Paleoproterozoic basins of the Bastar craton, a comparison is made against the available geochemical data of NASC (Gromet et al., 1984), UCC (Taylor and McLennan, 1985), granite and gneiss of the Bastar craton (Mondal et al., 2006), Archean mafic volcanics of the Bastar craton (Srivastava et al., 2004) and the Paleoproterozoic pelites of the Kaapvaal craton (Wronkiewicz and Condie, 1990).

The sandstones of the Chandarpur Group of the Neoproterozoic Chhattisgarh basin starts with the subarkosic Lohardih sandstone which becomes more matured

Kansapathar sandstone upwards mineralogically (Fig. 7). When sandstone composition of the Tiratgarh Formation of the Indravati Group is compared with all the three formations of the Chandarpur Group, the sandstone composition of the Tiratgarh Formation shows similarity with that of the Lohardih Formation of the Chandarpur Group. Provenance analysis of the sandstone composition of the Chandarpur Group and the Tiratgarh Formation of the Indravati Group indicate that the sediments were derived from granite and gneiss of the continental block (passive margin) tectonic setting. The presence of chert and stretched polycrystalline quartz grains in minor amounts in some samples and well rounded quartz grains with silica overgrowth floating in calcite cement indicates that the minor part of the detritus has been derived from an older sedimentary succession in the source area (Figs. 8, 9, 11 and 12) (Wani and Mondal, 2007, 2008). This is consistent with paleocurrent studies of Datta et al. (1999), that some detritus were derived from the northwestern region of the Chhattisgarh basin. The Paleoproterozoic Sakoli Group and the Sausar Group lie west of the Chhattisgarh basin (Fig. 1). This indicates that some sediments might have been recycled from these Paleoproterozoic basins.

The geochemical data of the sandstones is consistent with petrographic data which shows that SiO_2 increases through time (from Lohardih Formation to the Kansapather Formation) and all other major oxides decreases progressively. In comparison to NASC, sandstones and quartzites are depleted in major, trace including REE except for SiO_2, Na_2O, Co and Zr (Appendix II). The Neoproterozoic calcareous and the non-calcareous shales are depleted in most of the major and trace elements in comparison to the NASC. The non-calcareous shales are enriched in Al_2O_3, $Fe_2O_3^t$, K_2O, Rb, Cs, Th, Ta and Nb and have almost similar concentrations of SiO_2, TiO_2, Sc and Hf in comparison to the NASC. The calcareous shales are however, enriched in CaO, Sr, Cs, Ba and Th and show similar concentrations of MnO, Sc and Ta in comparison to NASC. The pelites are enriched in $Fe_2O_3^t$, Al_2O_3, K_2O, Ni, Cr, Sc, Nb, Tb and U in comparison to NASC (Appendix II).

The REE patterns of sandstones and quartzites are uniform and are similar to granite and gneiss of the Bastar craton with LREE enrichment and flat HREE (Fig. 45). The average Eu/Eu* values of the sandstones (0.67) and quartzites (0.42) is close to Eu/Eu* value of granite (0.39) and gneiss (0.65) of the Bastar craton. The REE patterns and Eu/Eu* values of the calcareous and the non-calcareous shales are similar to the sandstones and the quartzites (Fig. 45). The difference lies only in that the shales (calcareous and non-calcareous shales) have higher abundance of REE than do the sandstones and quartzites. The REE pattern of pelite sample (Fig. 45) is also fractionated but less fractionated than that of shales (calcareous and non-calcareous shales) with LREE enrichment having $(La/Yb)_n = 8.86$ and flat HREE with $(Gd/Yb)_n = 1.83$ and small negative Eu anomally (Eu/Eu* = 0.80). These geochemical characteristics of the pelites of the Bastar craton and Th/Sc-Sc and Ni-Cr relations (Figs. 43 and 44) indicate that the Paleoproterozoic pelites of the Bastar craton were derived from mafic source, while the shales, sandstones and quartzites were derived from felsic source.

The nature of the provenance for the Paleoproterozoic pelites and quartzites, and the Neoproterozoic shales and sandstones is further revealed by incompatible/compatible elemental ratios (like La/Cr, La/SC, La/Ni, Th/Cr, Th/Sc, Th/Ni) which are thought to be important in source rock determination. These elemental ratios were normalized with UCC (Fig. 42) (Taylor and McLennan, 1985). The elemental ratios of the sandstones, shales and quartzites are almost similar or slightly depleted in comparison to UCC (Upper Continental Crust). The pelite sample shows strong depletion of these elemental ratios than UCC indicating a less differentiated source than UCC. This study also shows that these elemental ratios (La/Cr, La/SC, La/Ni, Th/Cr, Th/Sc, Th/Ni) in quartz rich sandstones and calcite rich shales do not show much variation over a range of SiO_2 and CaO respectively (Fig. 41). This indicates that these elemental ratios are not affected by higher quartz content in the sandstones and higher calcite content in the calcareous shales. Thus, the study attests the significance of these elemental ratios in source rock determination.

The geochemical study of the Paleoproterozoic pelites of the Bastar craton are enriched in mafic elements (like $Fe_2O_3^t$, MgO, Cr, Ni and Sc) and depleted in LILE (like Th) relative to the Neoproterozic shales (Appendix II). The decreasing abundance of transition elements and Eu/Eu* ratio accompanied by an increase in Th from the Paleoproterozoic pelites to the Neoproterozoic shales suggests partial exposure of the granitoids in the Paleoproterozoic and unroofing of the granitoids by the complete removal of mafic rocks in the provenance as the Neoproterozoic sedimentation progressed. The study also reveals that the Paleoproterozoic pelites and quartzites could have been derived from a mixture of two end member source components, one end member being the granite and gneiss of the Bastar craton for the quartzites with lower abundance of mafic elements like $Fe_2O_3^t$, MgO, Ni, Cr, Sc, and Th/Sc and Eu/Eu* ratios similar to sandstones and shales, and the other end member being the mafic source for the pelites with higher $Fe_2O_3^t$, MgO, Ni, Cr, Sc, and lower Th/Sc and small negative Eu/Eu* ratio. The mafic sources are identified to be mafic volcanic rocks of the Bastar craton.

Thus it indicates that dominantly mafic source components were incorporated into the Paleoproterozoic pelites and the dominantly felsic source components into the Paleoproterozoic quartzites due to hydraulic sorting.

The Chemical Index of Alteration (CIA) values of the Neoproterozoic shales (72.40) and the Paleoproterozoic pelites (79.06) are much higher compared to NASC (57.12). The average CIA value of the pelites is similar to the non-calcareous shales and higher than the sandstones (67.50). This suggests that moderate to intense chemical weathering produced the sandstones, shales and pelites. Such moderate to intense chemical weathering of the pelites, sandstones and non-calcareous shales is also indicated by their average Plagioclase Index of Alteration values (PIA >80). The lower CIA and PIA values of the quartzites probably do not reflect the general weathering conditions in the source region. This may be due to sedimentary sorting effect. The other paleoweathering indicators like Th/U and K/Rb ratios, and $Fe_2O_3^t$ - Al_2O_3 - K_2O triangular diagram (Fig. 38) (Wronkiewicz and Condie, 1989) also suggest that the Paleoproterozoic and the Neoproterozoic provenance of the Bastar craton was affected by moderate to intense weathering history (Wani and Mondal, 2008). Thus, the CIA, PIA and, Th/U and K/Rb ratios gives a broad hint of prevalence of similar (moderate to intense) weathering conditions in the Bastar craton throughout the Proterozoic.

The present study further points to the advantageous use of geochemistry of both shales/pelites and sandstone/quartzites in paleoweathering and crustal evolution studies in order to delineate all source end members. All components of the source rocks may not be clearly resolved by the use of only either one of them.

Sandstone detrital modes and QmFLt, QtFL and QmPK tectonic setting discrimination diagrams (Figs. 31, 32 and 33) of Dickinson and Suczek (1979) indicate cratonic interior or passive margin setting for the sandstones of the Neoproterozoic age of the Chhattisgarh and Indravati basins of the Bastar craton. The higher values of elemental ratios of SiO_2/Al_2O_3 and K_2O/SiO_2 and SiO_2 content (Maynard et al., 1982; Roser and Korsch, 1986) indicate passive margin tectonic setting for the Paleoproterozoic pelites and quartzites, and the Neoproterozoic shales and sandstones (Figs. 34 and 35). Geochemical parameters (Bhatia, 1983) for tectonic setting discrimination like K_2O/Na_2O, $Al_2O_3/(CaO+Na_2O)$, $Fe_2O_3^t$, TiO_2, MgO of the Neoproterozoic sandstones and the Paleoproterozoic quartzites are comparable with passive margin tectonic setting (Table 9). The non-calcareous shales and the pelites have K_2O/Na_2O and $Al_2O_3/(CaO+Na_2O)$ ratios comparable with passive margin tectonic setting, the other geochemical parameters of Bhatia (1983) like Al_2O_3/SiO_2 and $Fe_2O_3^t$, TiO_2 and MgO values of the non-calcareous shales and pelites are comparable with those of island arc (Table 9). However, the pelites of the Sakoli and the Sausar basins have higher abundances of Ni and Cr in comparison to island arc rocks (Nance and Taylor, 1977) constituting evidence against island arc tectonic setting. The recent field study conducted by Takashi et al. (2001) also suggests that the sedimentation of the Sakoli and the Sausar supracrustals took place in the continental shelf or rift-related conditions rather than in the accretionary zone.

The overall mineralogical and geochemical characteristics i.e. mixing of two end member source compositions exhibited by the Paleoproterozoic pelites (mafic) and quartzites (felsic) relative to total felsic composition of the Neoptoterozoic shales and sandstones suggest that the composition of the source region of the Paleoproterozoic supracrustal rocks represented a transitional stage from mixed (mafic + felsic) in the Paleoproterozoic to entirely felsic in the Neoproterozoic in the unidirectional evolution of the Proterozoic continental crust of the Bastar craton. The presence of mafic components in the Paleoproterozoic pelites indicate that mafic to felsic transition had not occurred completely at the Archean-Proterozoic boundary in the Bastar craton (Taylor and McLennan, 1985), but this transition seems to occur in between the Paleoproterozoic – Neoproterozoic in the Bastar craton. However, the geochemical characteristics do not indicate any change in tectonic setting from the Paleoproterozoic Sakoli and Sausar basins to the Neoproterozoic Chhattisgarh and Indravati basins of the Bastar craton. The present study indicates that both the Neoproterozoic supracrustals and Paleoproterozoic supracrustals were deposited in plate interiors at continental margins or in passive margin tectonic settings. This conclusion strengthens the intracratonic origin of these basins.

APPENDIX-I

APPENDIX-I

Modal analysis of sandstones of the Chandarpur Group of the Chhattisgarh basin and the Tiratgarh Formation of the Indravati basin of the Bastar craton

Lohardih Formation (Chandarpur Group)

Mineral (%)	RD-406	RD-420	RD-421	RN-438	RD-509	RD-523	Average
Monocrystalline quartz	76.33	37.46	57.64	79.37	85.90	68.36	67.51
Polycrystalline quartz	5.12	0.65	1.05	3.37	4.51	5.68	3.40
K-feldspar	6.18	0.65	1.91	2.52	0.37	3.84	2.60
Plagioclase	3.18	1.60	0.52	1.05	0.00	1.38	1.30
Total feldspar	9.36	2.25	2.43	3.57	0.37	5.22	3.90
Chert	0.00	9.65	4.68	6.53	6.02	3.32	5.02
Glauconite	0.00	0.00	0.00	0.00	0.00	0.00	0.00
Quartz cement	0.55	0.16	0.52	5.06	2.07	0.00	1.39
Calcite cement	6.53	33.44	33.15	0.00	0.00	15.55	14.80
Iron cement	0.70	16.07	0.35	1.05	0.94	0.30	3.20
Rock fragment	1.23	0.00	0.00	0.00	0.00	0.77	0.33
Others (include mica and heavy minerals)	0.18	0.32	0.18	1.05	0.19	0.80	0.45
Total	100	100	100	100	100	100	

Appendix-I (*Continued*)

Chopardih Formation (Chandarpur Group)

Mineral (%)	RD-404	RN-423	RN-425	Average
Monocrystalline quartz	80.47	67.26	82.01	76.59
Polycrystalline quartz	9.19	4.19	1.00	4.80
K-feldspar	1.34	0.00	2.02	1.12
Plagioclase	0.00	0.00	0.86	0.29
Total feldspar	1.34	0.00	2.88	1.40
Chert	2.00	3.07	2.44	2.50
Glauconite	3.01	21.77	9.06	11.28
Quartz cement	0.66	2.09	1.73	1.49
Calcite cement	0.00	0.00	0.00	0.00
Iron cement	0.83	1.45	0.59	0.95
Rock fragment	1.83	0.00	0.00	0.61
Others (include mica and heavy minerals)	0.67	0.17	0.29	0.37
Total	100	100	100	

Appendix-I (*Continued*)

Kansapathar Formation (Chandarpur Group)

Mineral (%)	RD-405	RD-408	RD-409	RD-410	RN-424	RD-510	RD-520	Average
Monocrystalline quartz	87.28	86.76	91.54	80.00	88.89	85.33	93.79	87.70
Polycrystalline quartz	6.66	3.63	4.94	16.50	5.48	7.81	1.77	6.68
K-feldspar	0.00	0.90	0.00	0.00	0.81	0.00	0.00	0.23
Plagioclase	0.00	0.55	0.00	0.00	0.00	0.00	0.00	0.07
Total feldspar	0.00	1.45	0.00	0.00	0.81	0.00	0.00	0.32
Chert	2.37	0.72	0.58	2.17	0.16	2.43	0.00	1.20
Glauconite	0.00	0.00	0.00	0.00	0.00	0.00	0.00	0.00
Quartz cement	2.52	1.99	2.12	0.49	4.02	1.14	4.14	2.34
Calcite cement	0.00	0.00	0.00	0.00	0.00	0.00	0.00	0.00
Iron cement	0.29	5.27	0.23	0.24	0.32	0.72	0.15	1.03
Rock fragment	0.00	0.00	0.36	0.24	0.00	2.28	0.00	0.41
Others (include mica and heavy minerals)	0.88	0.18	0.23	0.36	0.32	0.29	0.15	0.34
Total	100	100	100	100	100	100	100	

Appendix-I (*Continued*)

Tiratgarh Formation (Indravati Group)

Mineral (%)	JC-541	JC-542	JC-543	JT-547	JT-548	Average
Monocrystalline quartz	3.28	79.83	89.79	50.42	86.14	61.89
Polycrystalline quartz	85.80	1.80	5.83	32.10	5.82	26.27
K-feldspar	5.47	0.36	0.00	1.53	0.00	1.47
Plagioclase	1.09	1.26	0.00	0.41	0.00	0.55
Total feldspar	6.56	1.62	0.00	1.94	0.00	2.02
Chert	0.00	3.61	0.00	2.08	5.54	2.24
Glauconite	0.00	0.00	0.00	0.00	0.00	0.00
Quartz cement	0.00	0.36	0.36	0.00	1.25	0.39
Calcite cement	3.83	10.61	3.05	10.42	0.00	5.60
Iron cement	0.18	0.90	0.36	1.12	0.69	0.65
Rock fragment	0.00	0.54	0.48	1.38	0.28	0.54
Others (include mica and heavy minerals)	0.35	0.73	0.13	0.54	0.28	0.40
Total	100	100	100	100	100	

APPENDIX-II

Appendix-II

Major and trace elements including rare earth elements of the Paleoproterozoic and the Neoproterozoic supracrustals of the Bastar craton. Data on different types of rocks have been shown for comparison.

	Sandstones							
	Chhattisgarh Basin					**Indravati Basin**		
Major oxides	**LF (CG)**	**CF (CG)**	**KF (CG)**			**TF (IG)**		
(wt. %)	**RN-438**	**RN-423**	**RD-405**	**RD-409**	**RD-520**	**JC-542**	**JT-547**	**Avg.**
SiO_2	91.71	91.25	94.64	95.11	95.64	89.05	93.34	92.96
TiO_2	0.09	0.09	0.05	0.04	0.04	0.21	0.07	0.08
Al_2O_3	2.43	3.02	1.88	1.72	0.59	5.46	2.46	2.50
$Fe_2O_3^t$	0.48	1.69	0.12	0.10	0.20	0.58	0.16	0.47
MnO	0.02	0.02	0.02	0.02	0.02	0.02	0.02	0.02
MgO	0.23	0.34	0.16	0.18	0.12	0.22	0.13	0.19
CaO	0.13	0.10	0.18	0.11	0.09	0.13	0.09	0.11
Na_2O	0.08	0.07	0.06	0.07	0.06	0.12	0.09	0.07
K_2O	1.34	0.86	0.24	0.13	0.00	2.38	1.32	0.89
P_2O_5	0.05	0.02	0.02	0.02	0.02	0.02	0.03	0.02
LIO	3.42	2.48	2.55	2.44	3.35	1.81	2.35	2.26
Sum	99.98	99.94	99.92	99.94	100.13	100	100.06	99.57
Trace elements including REE (ppm)								
Sc	2.76	2.93	2.42	2.38	1.25	3.3	2.26	2.47
V	20.53	20.7	17.77	17.89	6.06	14.15	7.8	14.98
Cr	13.21	13.3	10.17	13.32	18.52	31.07	14.48	16.3
Co	41.36	22.85	32.9	34.41	32.67	43.35	36.22	34.82
Ni	15.12	12.27	12.86	15.97	3.85	10.62	6.13	10.98
Rb	34.99	23.19	7.62	3.93	1.23	66.1	37.86	25
Sr	34.97	15.21	9.34	9.25	11.07	21.27	13.22	16
Y	2.97	2.67	2.28	1.71	2.4	16.4	6.15	4.9
Zr	65.2	76.35	72.87	71.95	57.34	1243.24	154.76	248.82
Nb	2.29	1.76	1.43	1.12	1.25	5.81	2.32	2.2
Cs	1.21	1.24	0.19	0.1	0.13	2.65	1.42	1
Ba	193.65	57.29	123.16	82.72	16.98	324.92	139.99	134.1
La	8.69	9.46	3.44	2.97	4.18	16.92	9.24	7.84
Ce	16.96	17.87	6.28	5.35	7.04	30.7	18.05	14.61
Pr	1.74	1.77	0.75	0.62	0.77	3.44	2.18	1.61
Nd	6.7	6.69	2.72	2.22	2.28	12.24	8.01	5.84
Sm	1	0.98	0.56	0.47	0.33	2.27	1.64	1.03
Eu	0.22	0.16	0.13	0.11	0.07	0.43	0.29	0.2
Gd	0.83	0.84	0.46	0.37	0.39	2.17	1.32	0.91
Tb	0.12	0.11	0.08	0.06	0.07	0.43	0.22	0.16
Dy	0.56	0.58	0.39	0.31	0.38	2.73	1.18	0.87
Ho	0.1	0.09	0.07	0.05	0.08	0.57	0.22	0.17
Er	0.28	0.3	0.23	0.16	0.24	1.7	0.62	0.5
Tm	0.04	0.05	0.04	0.03	0.04	0.32	0.11	0.09
Yb	0.33	0.32	0.28	0.19	0.26	1.98	0.65	0.57
Lu	0.04	0.04	0.03	0.02	0.04	0.32	0.1	0.09
Hf	1.99	2.17	2.33	2.21	7.43	36.26	11.93	9.19
Ta	1.76	1.26	1.89	1.68	1.6	3.12	3.4	2.1
Th	1.92	2.13	1.97	1.57	1.05	9.34	4.33	3.19
U	0.36	0.45	0.43	0.54	0.4	1.85	0.85	0.7

LF - Lohardih Formation, CF - Choprdih Formation, KF - Kansapathar Formation, TF - Tiratgarh Formation, CG -Chandarpur Group, IG - Indravati Group

Appendix-II (*continued*)

Major Oxides (wt.%)	Non-Calcareous Shales					Calcareous Shale					
	Chhattisgarh Basin		Indravati Basin			Chhattisgarh Basin					
	TF (RG)		JF (IB)			GF (RG)					
	SB-81	SB-83	JC-540	JT-549	Avg.	RD-402	RD-411	RD-412	RD-416	RD-512	Av
SiO_2	73.86	70.05	58	54.07	64	56.71	50.28	37.77	39.93	29.03	.
TiO_2	0.63	0.65	0.74	0.76	0.69	0.6	0.5	0.29	0.36	0.29	(
Al_2O_3	11.93	18.27	18.59	20.04	17	14.23	12.82	8.01	9.37	7	
$Fe_2O_3^t$	6.7	3.89	7.95	11.04	7.39	5.33	4.27	2.59	2.78	1.66	3
MnO	0.02	0.02	0.02	0.01	0.01	0.06	0.06	0.06	0.07	0.04	0.
MgO	1.33	0.86	1.66	1.19	1.26	2.02	2.03	1.44	1.64	1.08	1.
CaO	0.28	0.07	0.04	0.04	0.1	6.84	9.27	26.51	27.25	35	
Na_2O	0.15	0.37	0.14	0.12	0.2	0.34	0.38	0.11	0.26	0.02	0.
K_2O	4.47	4.18	6.51	6.81	5.5	3.72	3.56	2.07	2.48	1.39	2
P_2O_5	0.14	0.04	0.07	0.06	0.07	0.08	0.1	0.12	0.1	0.07	0.
LIO	0.66	1.54	5.56	5.23	3.248	10.06	15.98	20.42	15.34	24.2	17
Sum	100.17	99.94	99.28	99.37	99.47	99.99	99.25	99.39	99.58	99.78	99
Trace elements including REE (ppm)											
Sc	11.72	16.13	14.8	16.72	14.85	17.45	15.73	13.36	13.38	7.36	13.
V	59.47	95.33	80.57	90.76	81.53	96.3	98.32	62.98	69.04	33.16	71.
Cr	50.85	63.32	119.19	134.34	91.92	81.59	67.06	41.76	51.13	31.16	54.
Co	13.42	9.69	14.02	5.41	10.64	16.34	17.34	15.59	12.61	3.29	13.
Ni	43.56	23.08	38.86	50.87	39.09	38.94	36.98	28.83	30.95	8.64	28.
Rb	159.78	198.22	228.13	316.47	225.7	175.9	153.68	93.68	111.32	64.87	119.
Sr	43.02	57.82	22.98	33.5	39.33	89.08	147.56	200.78	211.68	181.55	166.
Y	15.26	30	24.44	21.94	22.91	27.37	26.16	25.13	26	17.9	24.
Zr	240.78	179.61	3.16	189.53	153.3	144.41	118.11	71.37	85.12	54.95	94.
Nb	37.21	17.14	19.65	19.53	23.38	12.95	10.23	6.97	8.21	5.6	8.
Cs	11.88	10.94	12.37	16.41	12.9	13.02	10	6.02	7.82	6.72	8.
Ba	412.71	528.98	495.94	0.93	359.6	2091.31	427.61	4255.73	2515.54	1.4	1858.
La	44.89	56.33	69.94	101.09	68.06	31.51	25.44	24.3	22.4	18.08	24.
Ce	93.88	100.03	112.76	131.2	109.5	63.48	52.85	43.75	43.98	20.5	44.
Pr	9.77	12.67	13.3	16.8	13.13	8.73	7.29	6.29	6.34	3.45	6.
Nd	34.53	45.5	45.53	55.04	45.15	32.35	27.73	24.12	24.82	12.66	24.
Sm	5.79	8.3	7.84	8.91	7.71	6.63	5.82	5.77	5.73	3.5	5.
Eu	1	1.55	1.45	1.54	1.39	1.35	1.11	1.44	1.33	1.02	1.
Gd	4.41	6.55	6.75	6.53	6.06	5.24	4.71	4.42	4.54	2.55	4.
Tb	0.68	1.09	1.06	0.95	0.95	0.92	0.84	0.78	0.79	0.49	0.
Dy	3.36	5.73	5.25	4.47	4.7	4.98	4.59	4.45	4.49	2.82	4.
Ho	0.6	1.19	1.02	0.88	0.92	1	0.94	0.9	0.89	0.63	0.
Er	1.66	3.32	2.76	2.44	2.55	2.85	2.6	2.46	2.42	1.77	2.
Tm	0.25	0.54	0.43	0.4	0.41	0.47	0.43	0.41	0.4	0.3	0.
Yb	1.58	3.57	2.7	2.77	2.66	2.94	2.9	2.52	2.63	1.94	2.
Lu	0.25	0.57	0.43	0.45	0.42	0.47	0.46	0.42	0.42	0.31	0.
Hf	6.5	5.58	6.42	6.25	6.19	4.42	3.57	2.22	2.62	1.79	2.
Ta	2.83	2.07	1.57	1.5	1.99	1.45	1.13	1.46	0.88	0.4	1.
Th	12.31	19.5	29.95	31.57	23.33	18.7	15.15	11.36	12.47	7.8	13.
U	1.1	2.65	1.46	1.45	1.66	2.32	2.15	1.4	1.6	0.67	1.

TF - Tarenga Formation, JF - Jagdalpur Formation, GF- Gunderdehi Formation, RG - Raipur Group, IG - Indravati Group

Appendix-II (*Continued*)

Major Oxides (wt.%)	Pelites					Quartzites			
	Sakoli Basin		Sausar Basin			Sakoli Basin		Sausar Basin	
	BF		JF			PF		JF	
	DS-524	**DS-525**	**ST-528**	**ST-534**	**Avg.**	**DS-526**	**AD-536**	**ST-530**	**Avg.**
SiO_2	65 08	55 7	50 51	64 56	59	95 89	75 94	86 82	86 21
TiO_2	0 85	0 19	0 73	1 26	0 75	0 06	0 19	0 05	0 1
Al_2O_3	15 51	25 81	27 58	19 19	22 02	1 15	10 98	6 46	6 19
$Fe_2O_3^t$	14 33	6 85	8 38	3 24	8 62	0 09	2 22	0 09	0 8
MnO	0 08	0 01	0 04	0 01	0 03	0 02	0 06	0 02	0 03
MgO	0 32	1 49	3 13	2 23	1 79	0 02	0 23	0 34	0 19
CaO	0 07	0 28	0 34	0 28	0 25	0 07	1 27	0 08	0 47
Na_2O	0 06	0 34	1 44	0 15	0 5	0 05	4 79	0 13	1 65
K_2O	1	7 08	5 88	5 33	4 8	0 25	3 47	5 09	2 93
P_2O_5	0 17	0 05	0 03	0 02	0 06	0 01	0 03	0 02	0 02
LIO	2 26	1 68	1 76	3 65	2 3375	2 24	0 62	0 64	1 26
Sum	99 73	99 48	99 82	99 92	97 4	99 85	99 8	99 74	99 85
Trace elements including REE (ppm)									
Sc	27 82	19 28	25 28	11 34	21	3 03	1 91	1 85	2 27
V	83 93	130 6	129 2	55 59	100	3 14	3 08	2 76	2 99
Cr	423 97	154 19	129 24	49 03	189	14 23	15 85	33 26	21 11
Co	9 78	19 69	22 89	9 49	15 46	67 58	17 48	43 82	42 96
Ni	61 9	74 69	73 52	22 08	58	2 96	7 15	4 89	5
Rb	99 81	276 5	264 4	127 15	191 96	14 31	124 88	129 88	89 69
Sr	28 29	58 07	186 67	10 53	70 89	8 78	76 17	12 38	32 44
Y	24 13	0 85	0 35	0 7	6 51	3 76	65 59	8 89	26 08
Zr	141 88	232 79	3 86	290 35	167	80 7	648 89	118 46	282 68
Nb	8 93	35 16	25 66	28 89	24 66	3 32	23 29	2 88	9 83
Cs	0 86	3 25	7 12	9 94	5 29	0 39	1 54	0 64	0 86
Ba	49 31	NA	NA	NA	NA	20 82	0 86	200 11	73 93
La	28 52	NA	NA	NA	NA	5 49	69 76	21 38	32 21
Ce	43 58	NA	NA	NA	NA	11 75	136 57	39	62 44
Pr	5 83	NA	NA	NA	NA	1 01	14 54	3 91	6 48
Nd	22 85	NA	NA	NA	NA	3 79	57 06	13 93	24 92
Sm	5 19	NA	NA	NA	NA	0 74	10 8	2 55	4 7
Eu	1 33	NA	NA	NA	NA	0 1	1 65	0 28	0 67
Gd	5 12	NA	NA	NA	NA	0 62	8 8	1 75	3 73
Tb	0 9	NA	NA	NA	NA	0 1	1 47	0 26	0 61
Dy	4 62	NA	NA	NA	NA	0 66	10 35	1 57	4 19
Ho	0 93	NA	NA	NA	NA	0 07	1 21	0 16	0 48
Er	2 42	NA	NA	NA	NA	0 23	4 28	0 53	1 68
Tm	0 38	NA	NA	NA	NA	0 03	0 57	0 08	0 23
Yb	2 3	NA	NA	NA	NA	0 36	6 08	0 87	2 44
Lu	0 36	NA	NA	NA	NA	0 06	1 03	0 16	0 41
Hf	4 38	1 31	1 06	1 66	2 1	8 31	20 23	4 37	10 97
Ta	0 96	104 32	63 13	86 16	63 64	2 68	3 67	2 27	2 87
Th	11 39	18 86	24 81	15 42	17 62	4 79	19 13	15 36	13 1
U	6 27	3 52	4 13	3 2	4 28	1 37	5 4	4 1	3 62

BF - Bhiwapur Formation, JF - Junewani, PF - Pawni Formation

Appendix-II (*Continued*)

	Bastar Granite*	Bastar Gneiss*	Bastar Volcanics*	NASC*	Kaapvaal Pelite*
SiO_2	71.23	71.47	50.59	64.8	59.29
TiO_2	0.26	0.22	1.25	0.78	0.75
Al_2O_3	14.25	14.25	11.91	16.9	18.22
$Fe_2O_3^t$	2.46	2.35	14.78	5.7	8.8
MnO	0.03	0.03	0.55	0.06	0.06
MgO	0.55	0.49	7.28	2.85	3.16
CaO	1.99	1.52	9.42	3.56	0.9
Na_2O	3.62	4.11	1.89	1.15	0.56
K_2O	4.28	3.61	1.04	3.99	3.42
P_2O_5	0.08	0.04	0.23	0.11	0.14
LIO	NA	NA	NA	NA	NA
Sum	98.78	98.13	98.98	99.9	95.34
Trace elements including REE (ppm)					
Sc	6.14	4.27	NA	14.9	20.83
V	25	13.87	220.83	130	164.16
Cr	283.95	273.2	647.52	124.5	317
Co	32.53	33.47	NA	25.7	27.5
Ni	18.99	11.86	196.82	58	158
Rb	165.13	144.66	26.23	125	130
Sr	278.76	226.62	131.08	142	68
Y	29.75	22.2	16.5	35	NA
Zr	273.53	221.47	66.04	200	168.83
Nb	16.16	16.79	3.64	13	11.63
Cs	NA	NA	NA	5.2	7.85
Ba	827.92	690.42	124.62	636	545.66
La	56.87	29.7	9.23	31.1	37.83
Ce	133.94	61.26	18.57	66.7	72.66
Pr	17.78	7.4	2.06	NA	NA
Nd	55.95	22.52	8.5	NA	NA
Sm	9.23	4.28	2.03	5.59	5.68
Eu	1.04	0.8	0.65	1.18	1.19
Gd	7.07	3.31	2.43	NA	NA
Tb	1.28	0.56	0.5	0.85	0.77
Dy	6.46	2.62	2.79	NA	NA
Ho	1.2	0.45	0.62	NA	NA
Er	3.94	1.4	1.83	NA	NA
Tm	0.63	0.22	0.32	NA	NA
Yb	4.33	1.53	1.83	3.06	2.66
Lu	0.68	0.26	0.28	0.46	0.41
Hf	NA	NA	1.8	6.3	4.96
Ta	NA	NA	0.3	1.1	1.06
Th	34.76	37.58	3.53	12.3	12.58
U	6.7	7.17	0.61	2.66	3.83

	Sandstones							
	RN-438	**RN-423**	**RD-405**	**RD-409**	**RD-520**	**JC-542**	**JT-547**	**Avg.**
CIA	57.19	71.09	73.27	79.04	69.22	64.46	58.56	67.50
PIA	72.69	87.55	79.18	83.36	69.22	86.92	76.79	81.69
K_2O/Na_2O	16.75	12.28	4	1.85	0	19.83	14.66	11.4
SiO_2/Al_2O_3	37.74	30.21	50.34	55.29	162.1	16.3	37.94	55.7
Th/U	5.23	4.66	4.53	2.88	2.63	5.02	5.08	4.50
K/Rb	317.87	307.89	261.45	274.49	0	298.92	289.4	295.71
LREE/HREE	15.05	15.51	8.46	9.47	6.39	8.78	10.45	10.50
(La/Yb)n	18.9	20.62	8.73	11.05	6.13	10.13	12.59	12.50
(Gd/Yb)n	2.08	2.11	1.35	1.61	0.91	1.67	1.62	1.56
Eu/Eu*	0.74	0.55	0.79	0.8	0.59	0.61	0.68	0.67

	Non-calcareous Shales					Calcareous Shales					
	SB-81	**SB-83**	**JC-540**	**JT-549**	**Avg.**	**RD-402**	**RD-411**	**RD-412**	**RD-416**	**RD-512**	**Avg.**
CIA	68.07	77.64	71.66	72.39	72.40	NA	NA	NA	NA	NA	NA
PIA	90.36	94.91	97.44	97.91	95.62	NA	NA	NA	NA	NA	NA
K_2O/Na_2O	29.8	11.29	46.5	56.75	28.16	10.94	9.36	18.81	9.53	69.5	23.62
SiO_2/Al_2O_3	3.2	2.63	0.88	0.64	1.84	3.98	3.92	4.71	4.26	4.14	4.2
Th/U	11.15	7.34	20.45	21.71	13.98	8.03	7.03	8.1	7.78	11.51	8.00
K/Rb	232.26	175.07	236.9	178.65	202.1	175.59	192.34	183.45	184.98	177.89	182.85
LREE/HREE	14.72	9.86	12.21	16.53	13.02	7.54	6.8	6.36	6.21	5.36	6.45
(La/Yb)n	20.29	11.29	18.56	26.14	18	7.66	6.28	6.9	6.09	6.66	7.00
(Gd/Yb)n	2.3	1.51	2.06	1.90	1.9	1.47	1.34	1.44	1.42	1.08	1.4
Eu/Eu*	0.64	0.67	0.64	0.64	0.65	0.7	0.65	0.87	0.8	1.04	0.80
Ce/Ce*	1.09	0.91	0.9	0.78	0.93	0.93	0.95	0.86	0.9	0.63	0.86

	Pelites					Quartzites			
	DS-524	**DS-525**	**ST-528**	**ST-534**	**Avg.**	**DS-526**	**AD-536**	**ST-530**	**Avg.**
CIA	92.22	74.72	74.67	74.62	79.26	70.54	44.05	52.39	55.66
PIA	98.45	94.43	87.65	94.66	93.02	80.75	41.48	72.57	45.70
K_2O/Na_2O	16.66	20.82	4.08	35.53	9.69	5	0.72	39.15	1.77
SiO_2/Al_2O_3	2.67	1.53	2.27	2.61	2.67	83.38	6.91	13.43	34.57
Th/U	1.81	5.35	6	4.81	4.11	3.49	3.54	3.74	3.61
K/Rb	83.17	212.58	184.63	348.01	208.6	145.06	230.72	325.4	271.82
LREE/HREE	6.21	NA	NA	NA	NA	8.53	10.46	14.96	11.00
(La/Yb)n	8.86	NA	NA	NA	NA	8.22	10.76	17.63	12.00
(Gd/Yb)n	1.83	NA	NA	NA	NA	1.19	1.41	1.67	1.42
Eu/Eu*	0.79	NA	NA	NA	NA	0.51	0.46	0.4	0.47

Appendix-II (*Continued*)

	Bastar Granite*	Bastar Gneiss*	Bastar Volcanics*	NASC*	Kaapvaal Pelite*
CIA	50 04	51 43	35 78	57 12	74 36
PIA	50 07	52	34.74	60 06	84 93
K_2O/Na_2O	1 18	0 87	0 55	3 46	6 1
SiO_2/Al_2O_3	4 99	5 01	4 24	3 83	3 25
Th/U	5 18	5 23	5.73	4 62	3 28
K/Rb	215 21	207.2	329.21	265	218 84
LREE/HREE	10 67	12 06	3.8	9 45	NA
(La/Yb)n	9 41	13 9	3 6	9 73	NA
(Gd/Yb)n	1 35	1 78	1.09	1 38	NA
Eu/Eu*	0 39	0 65	0.89	0 65	NA

Bastar Granite*- Average of thirteen granitoids from Mondal et al. (2006), Bastar Gneiss* - Average of Fourteen gneisses from Mondal et al. (2006), Bastar Volcanics*- Average of twenty four mafic volcanic rocks from Srivastava et al. (2004), Kaapvaal pelite* - Average composition of pelites of Transvaal and Ventersdorp Groups of Kaapvaal craton from Wronkiewicz and Condie (1990), $Fe_2O_3^t$- total iron, CIA- Chemical Index of Alteration, PIA-Plagioclase Index of Alteration, NA- Not available, LIO- Loss on ignition

REFERENCES

REFERENCES

Anani C., 1999. Sandstone petrology and provenance of the Neoproterozoic Voltaian Group in the southeastern Voltaian Basin, Ghana. Sed. Geol. 128, 83 - 98.

Argast, S., Donelly, T.W., 1986. Composition and sources of metasediments in the upper Dharwar Supergroup, South India. J. Geol. 94, 215 - 231.

Armstrong-Altrin J.S., Verma S.P., 2005. Critical evaluation of six tectonic setting discrimination diagrams using geochemical data of Neogene sediments from known tectonic settings. Sed. Geol. 177, 115 - 129.

Arora, M., Khan, R.M.K., Naqvi, S.M., 1994. Composition of the middle and late Archean upper continental crust as sampled from the Kaldurga Conglomerate, Dharwar craton, India. Precambrian Res. 70, 93 - 112.

Bahlburg, H., 1998. The Geochemistry and provenance of Ordovician turbidites in the Argentine Puna. Geol. Soc. London, Special Paper 142, 127 - 142.

Balram, V., Ramesh, S.L., Anjaiah, K.V., 1996. New trace and REE data in thirteen GSF refrence samples by ICP-MS. Geostandard. New. Lett. 20, 71 - 78.

Bandyopadhaya, B.K., Roy, A., Huin, A.K., 1995. Structure and tectnonics of a part of the Central Indian Shield. In: S. Sinha Roy and K. R. Gupta (Eds.), Continental Crust of Northwestern and Central India. Geol. Soc. India Mem. 31, 433 - 468.

Bellanca, A., Masetti, D., Neri, R., 1997. Rare earth elements in limestone/marlstone couplets from the Albanian-Cenomanian Cismon section (Venetian region, northern Italy): assessing REE sensitivity to environmental changes. Chem. Geol. 141, 141 - 152.

Bhat, M.I., Ghosh, S.K., 2001. Geochemistry of the 2.51 Ga old Rampur Group pelites, western Himalayas: implications for their provenance and weathering. Precambrian Res. 108, 1 - 16.

Bhatia, M.R., Taylor, S.R., 1981. Trace element geochemistry and sedimentary provinces: A study from the Tasman Geosyncline, Australia. Chem. Geol. 33, 115 - 126.

Bhatia, M.R., 1983. Plate tectonics and geochemical composition of sandstones. J. Geol. 91, 611 - 627.

Bhatia, M.R., 1985a. Rare earth element geochemistry of Australian Paleozoic greywackes and mudrocks: provenance and tectonic control. Sed. Geol. 45, 97 - 113.

Bhatia, M.R., 1985b. Composition and classification of flysch mudrocks of eastern Australia: Implications in provenance and tectonic setting interpretation. Sed. Geol. 41, 249 - 268.

Bhatia, M.R., Crook, K.A.W., 1986. Trace element characteristics of greywackes and tectonic discrimination of sedimentary basins. Contrib. Mineral. Petrol. 92, 181 – 193.

Bhowmik, S.K., Pal, T., Roy A., Chatterjee, K.K., 1997. Penecontemporaneous deformation structures in relation to diagenesis of carbonate-hosted manganese ores: an example from polydeformed and metamorphosed Sausar belt. Indian Mineral. 51, 149 - 164.

Blatt, H., 1967. Provenance determinations and recycling of sediments. J. Sed. Petrol. 37, 1311 - 1320.

Burnett, D.J., Quirk, D.G., 2001. Turbidite provenance in the lower Paleozoic Manx Group, Isle of Man: Implications for the tectonic setting of Eastern Avalonia. J. Geol. Soc. London 45, 411 - 425.

Chakraborthy, P.P., Sarkar, A., Bhattacharya, Sanyal P., 2002. Isotopic and sedimentological clues to productivity change in Late Riphean Sea. A case study from two intracratonic basins of India. Proc. Indian Acad. Science (Earth and Planetary Sciences) 111, 379 - 390.

Chatterjee, A., 1964. Geology, mineralogy and genesis of iron ores of some deposits of the Bailadila range, Bastar District (M.P.). Geol. Min. Metall. Soc. India 36, 57 - 72.

Chatterjee, A., 1969. Mineralogy and stability relations of magnesio-riebeckite amphiboles from metamorphosed iron formation of Bailadila, Bastar District of Madhya Pradesh. Geol. Min. Metall. Soc. India 41, 75 – 96.

Chatterjee, A., 1970. Structure, tectonics and metamorphism in part of the south Bastar (M.P). Geol. Min. Metall. Soc. India 42 (2), 75 - 96.

Chaudhri, S., Cullers, R.L., 1979. The distribution of rare-earth elements in deeply buried gulf coast sediments. Chem. Geol. 24, 327 - 338

Chaudhuri, A.K., Saha, D., Deb, G.K., Deb, S.P., Mukherji, M.K., Ghosh, G., 2002. The Purana basins of southern cratonic province of India- a case for Mesoproterozoic fossil rifts. Gond. Res. 5, 23 - 33.

Condie, K.C., 1982. Early and Middle Proterozoic supracrustal successions and their tectonic settings. American J. Sci. 282, 341 – 357.

Condie, K.C., Wronkiewicz, D.J., 1990. The Cr/Th ratio in Precambrian pelites from Kaapvaal craton as an index of craton evolution. Earth Planet. Sci. Lett. 97, 256 - 267.

Condie, K.C., 1991. Another look at rare earth elements in shales. Geochim. Cosmochim. Acta 55, 2527 - 2531.

Condie, K.C., 1993. Chemical composition and evolution of the upper continental crust; contrasting results from surface samples and shales. Chem. Geol. 104, 1 - 37.

Cox, R., Low, D.R., Cullers, R.L., 1995. The influence of sediment recycling and basement composition on evolution of mudrock chemistry in the southwestern United States. Geochim. Cosmochim. Acta 59, 2919 - 2940.

Critelli, S., Ingersoll, R.V., 1994. Sandstone petrology and provenance of the Siwalik Group (northwestern Pakistan and western-southeastern Nepal). J. Sed. Res. 64 (4), 815 - 823.

Critelli, S., Nilsen, T.H., 2000. Provenance and stratigraphy of the Eocene Tejon Formation, Western Tehachapi Mountains, San Emigdio Mountains, and Southern san Joaquin Basin, California. Sed. Geol. 136, 7 - 27.

Crook, K.A.W., 1974. Lithogenesis and geotectonics: The significance of compositional variations in flysch arenite (graywackes). In R. H. Doot and R.H. Shaver (eds.), Modern and ancient Geosynclinal sedimentation: SEPM Special Pub. 19, 304 - 310.

Crookshank, H., 1963. Geology of southern Bastar and Jeypore from Bailadila range to eastern ghats. Geol. Surv. India, Mem. 87, 96 – 108.

Cullers, R.L., Barrent, T., Carlson, R., Robinson, B., 1987. Rare earth element and mineralogical changes in Holocene soil and stream sediment: a case study in the wet mountains, Colorado, USA. Chem. Geol. 63, 275 – 297.

Cullers, R.L., 1988. Mineralogical and chemical changes of soil and stream sediment formed by intense weathering of the Danberg granite, Georgia, USA. Lithos 21, 301 - 314.

Cullers, R.L., Berendsen, P., 1998. The provenance and chemical variation of sandstones associated with the Mid-continent rift system, USA. Europ. J. Mineral. 10, 987 - 1002.

Cullers, R.L., 2000. The geochemistry of shales, siltstones and sandstones of Pennsylvanian-Permian age, Colorado, USA: implications for provenance and metamorphic studies. Lithos 51, 181 - 203.

Cullers, R.L., Podkovyrov, V.N., 2002. The source and origin of terrigenous sedimentary rocks in the Mesoproterozoic Ui Group, southeastern Russia. Precambrian Res. 117, 157 - 183.

Cullers, R.L., 2002. Implications of elemental concentrations for provenance for provenance, redox conditions, and metamorphic studies of shales and limestones near Pueblo, CO, USA. Chem. Geol. 191, 305-327.

Das D.P., Kundu A., Das N., 1992. Lithostratigraphy and sedimentation of Chhattisgarh basin. Indian Mineral. 46, 271 - 288.

Das, N., Dutta, D.R., Das, D.P., 2001. Proterozoic cover sediments of southeastern Chhattisgarh state and adjoining part of Orissa. Geol. Surv. India, Special Pub. 55, 237 - 262.

Dasgupta, S., Banerjee, H., Majumdar, N., 1984. Contasting trends of mineral reactions during progressive metamorphism in interbanded pelite-magnese oxide sequence: example from Precambrian Sausar Group, India. Neues Jahrb. fur Mineral. Abhandlung. 150, 95 - 102.

Datta, B., 1998. Stratigraphic and sedimentologic evolution of the Proterozoic siliclastics in the southern part of Chhattisgarh and Khariar, Central India. J. Geol. Soc. India 51, 345 - 360.

Datta, B., Sarkar, S., Chaudhri, A.K., 1999. Swaley cross-stratification in medium to coarse sandstone produced by oscillatory and combined flows: examples from the Proterozoic Kansapathar Formation, Chhattisgarh basin, M.P. India. Sed. Geol. 129, 51 - 70.

Dickinson, W.R., 1970. Interpreting detrital modes of greywacke and arkose. J. Sed. Petrol. 40, 695 – 707.

Dickinson, W.R., Suczek, C.A., 1979. Plate tectonics and sandstone compositions. AAPG Bull. 63, 2164 - 2182.

Dickinson, W.R., Beard, L.S., Brakenridge, G.R., Erjavec, J.L., Ferguson, R.C., Inman, K.F., Knepp, R.A., Lindberg, P.T., 1983. Provenance of North American Phanerozoic sandstones in relation to tectonic setting. Geol. Soc. America Bull. 94, 222 - 235.

Dickinson, W.R., 1985. Interpreting provenance reltions from detrital modes of sandstones. In: G .G. Zuffa (eds.) Provenance of Arenites (Dordrecht: D. Reidel publications.co.) pp. 333 - 362.

Drury, S.A., 1984. A Proterzoic intracratonic basin, dyke swarms and thermal evolution in south India. J. Geol. Soc. India 25, 437 - 444.

Dutt, N.V.B.S., 1963. Stratigraphy and correlation of the Indravati series (Purana Group) of Bastar District, Madhya Pradesh. J. Geol. Soc. India 4, 35 - 49.

Dutt, S.M., Mishra, V.P., Dutta, N.K., Pandhare, S.A., 1979. Precambrian Geology of a part of Narainpur and Kondagaon Tahsils, Bastar District, with special reference to Rowghat iron ore deposits. Geol. Surv. India, Special Pub. 3, 55 - 67.

Dutta, S.M., Mishra, V.P., Dutta, N.K., Phadtare, S.A., 1981. Precambrian geology of a part of Narianpur and Kondagaon tehsils, Bastar District, with special reference to Rowghat Iron Ore deposits. In: Archeans of Central India. Geol. Surv. India, Special Pub. 3, 55 - 67.

Elderfield, H., Greaves, M.J., 1982. The rare earth elements in sea-water. Nature 296, 214 - 219.

Engel , A.E.J., Itson, S.P., Engel, C.G., Stickney, D.M., Cray E.J., 1974. Crustal evolution and Global tectonics: A petrogenic view. Geol. Soc. America Bull. 85, 843 - 858.

Erikson, K.A., Taylor, S.R., Korsch. R.J., 1992. Geochemistry of 1.8-1.67 Ga mudstones and siltstones from the mount Isa Inlier, Queensland, Australia: Provenance and tectonic implications. Geochim. Cosmochim. Acta 56, 889 – 909.

Eriksson, P.G., Condie, K.C., Vander, W., Vander, M., DeBruiyn, H., Nelson, D.R., Altermann, W., Catuneanu, O., Bumby. A.J., Lindsay, J., Cunningham, M.J., 2002. Late Archaean superplume events, a Kaapvaal-Pilbara perspective. J. Geodyn. 34, 207 – 247.

Fedo, C.M., Nesbitt, H.W., Young, G.M., 1995. Unraveling the effects of potassium metasomatism in sedimentary rocks and paleosols, with implications for weathering conditions and provenance. Geology 23, 921 - 924.

Fedo, C.M., Young, G.M., Nesbitt, H.W., 1997. Paleoclimatic control on the composition on the Paleoproterozoic Serpent Formation, Huronian Supergroup, Canada: a greenhouse to icehouse transition. Precambrian Res. 86, 211 - 223.

Feng, R., Kerrich, R., 1990. Geochemistry of fine grained clastic sediments in the Archean Abitibi greenstone belt, Canada: Implications for provenance and tectonic setting. Geochim. Cosmochim. Acta 54, 1061 - 1081.

Fermor, L. L., 1936. An attempt at the correlation of ancient schistose formations of peninsular India. Geol. Surv. India, Mem. 70, 1 - 217.

Fermor, L.L., 1909. The manganese ore deposits of India. Geol. Surv. India, Memoir 37, 235 – 364.

Floyd P.A., Leveridge B.E., Franke W., 1991. Geochemistry and provenance of Rhenohercynian synorogenic sandstones: implications for tectonic environment discrimination: In, A.C. Morton, S.P. Todd, and P.D.W. Haughton, (eds). Developments in provenance studies. Geol. Soc. London, Special pub. 57, 173 - 188.

Folk, R.L., 1980. Petrology of sedimentary rocks. Hemphill Publishing Co., Austin, Texas, U.S.A., 182p.

Gazzi, P., 1966. Le arenarie del flysch sopracretaceo dell' Appennino modenese; correlazioni con il flysch di Monghidoro. Mineral. Petrograph. Acta 12, 69 - 97.

German, C.R., Elderfield, H., 1990. Application of the Ce anomaly as a paleoredox indicator: the ground rules. Paleooceanography 5, 823 - 833.

Ghosh, P.K., Prasad, U., Banerjee, A.K., 1977. Geology and mineral occurrences of part of the Abuj Mar area, Bastar District Madhya Pradesh. Geol. Surv. India Rec. 108, 182-188.

Ghosh, P.K., Chandy, K.C., Bishui, P.K., Prasad, R., 1986. Rb-Sr age of granitic gneiss in Malanjkhand area, Balaghat district, Madhya Pradesh. Indian Mineral. 40, 1 - 8.

Gibbs, A.K., Montgomery, C.W., O'Day, P.A., Erislv, E.A., 1986. The Archean – Proterozoic transition: evidence from the geochemistry of metasedimentary rocks from Guyana and Montana. Geochim. Cosmochim. Acta 50, 2125 - 2145.

Gill, J.B., 1981. Orogenic andesites and plate tectonics. Springer-Verlag.

Gromet, L.P., Dymek, R.F., Haskin, L.A., Korotev, R.L., 1984. The North Amarican shale Composite: Its compilation, major and trace element characteristics. Geochim. Cosmochim. Acta 48, 2469 - 2482.

Gu, X.X., 1994, Geochemical characteristics of the Triassic Tethys-turbidites in the north-western Sichuan, China: Implications for provenance and interpretation of the tectonic setting. Geochim. Cosmochim. Acta 58, 4615 - 4631.

Gu, X.X., Liu, J.M., Zheng, M.H., Tang, J.X., Qi, L., 2002. Provenance and tectonic setting of the Proterozoic turbidites in Hunan, South China: Geochemical evidence. J. Sed. Res. 72, 393 - 407.

Gupta, A., 1998. Hummocky cross-stratification in the Chhattisgarh Basin, M.P. and its hydraulic and bathymetric implications. J. Indian Assoc. of Sed. 17, 213 - 224.

Haskin, L.A., Wildeman, T.R., Frey, F.A., Collins, K.A., Keedy, C.R., Haskin, M. A., 1966. Rare earths in sediments. J. Geophys. Res. 71, 6091 - 6105.

Herron, M.M., 1988. Geochemical classification of terrigenous sands and shales from core or log data. J. Sed. Petrol. 58, 820 - 829.

Holland, T.H., 1907. Imperial Gazetteer of India. Government of India Delhi 1, 50 - 103.

Hussain, M. F., Mondal, M.E.A., 2004. Growth of Bastar nucleus, central India via multiphase subduction : evidence from geochemistry of gneisses. Jour. Appl. Geochem. 6, 164 - 176.

Hussain, M. F., Mondal, M.E.A., Ahmad, T., 2004a. Geochemistry of basement gneisses and gneissic enclaves from Bastar craton: geodynamic implications. Curr. Sci. 86, 1543 - 1547.

Hussain, M. F., Mondal, M.E.A., Ahmad, T., 2004b. Geodynamic evolution and crustal growth of the central Indian shield: evidence from geochemistry of gneisses and granitoids. Proc. Indian Acad. Sci. (Earth Planet. Sci.) 113, 699 - 714.

Hussain, M.F., Mondal, M.E.A., Ahmad, T., 2004c. Petrological and geochemical characteristics of Archean gneisses and granitoids from Bastar craton- Implication for subduction related magmatism. Gond. Res. 7, 531 - 537.

Ingersoll, R.V., 1978. Petrofacies and petrologic evolution of late Cretaceous fore-arc basin, northern and central California. J. Geol. 86, 335 - 352.

Ingersoll, R.V., Bullard T.F., Ford, R.L., Grimm, J.P., Pickle, J.D., Sares, S.W., 1984. The effect of grain size on detrital modes: a test of Gazzi-Dickinson point-counting method. J. Sed. Petrol. 54, 103 - 116.

Jahn, B. M., Condie, K. C., 1995. Evolution of the Kaapvaal Craton as viewed from geochemical and Sm-Nd isotopic analyses of intracratonic pelites. Geochim. Cosmochim. Acta 59, 2239 - 2258.

Jairam, R., Banerjee, D.M., 1978. Preliminary studies on the stromatolites from the Raipur area, Chhattisgarh Basin. Proceedings Workshop on Stromatolites. Geol. Surv. India Miscell. Pub. 44, 57 - 67.

Johnsson M.J., Basu A., 1993. Processes controlling the composition of clastic sediments. Geol. Soc. America, Special Paper 285, 354p.

Kasper-Zubillaga, J.J., Carranza-Edwards, A., Rosales-Hoz, L., 1999. Petrography and geochemistry of Holocene sands in the western Gulf of Mexico: implications for provenance and tectonic setting. J. Sed. Res. 69, 1003 - 1010.

Khan, M.W.Y., Mukherjee, A., 1990. Sedimentology and petrography of Chandrapur sandstones, Chhattisgarh Supergroup, around Lohara, Durg District, M.P., Indian J. Earth Sci. 17, 44 - 50.

Klein, G. De. V., 1963. Analysis and review of sandstone classifications in the North American Geological Literature. Geol. Soci. American Bull. 77, 555 - 576.

Klein, G. De.V., Hsui, A.T., 1987. Origin of cratonic basins. Geology 15, 1094 – 1098.

Kruezer, H., Harre, W., Kursten, M., Schinitzer, W.A., Murthi, K.S., Srivastava, N.K., 1977. K/Ar dates of two glauconites from the Chandarpur series (Chhattisgarh/India): on the stratigraphic status of the Late Precambrian Basins in India. Geol. Jharb. Bull. 28, 23 - 36.

Lahtinen, R., 1996. Geochemistry of Paleoproterozoic supracrustal and plutonic rocks in the Tempere-Hameenlinna area. Central Finland. Geol. Surv. Finland Bull. 389, 113p.

Lahtinen, R., 2000. Archean-Proterozoic transition: geochemistry, provenance and tectonic setting of metasedimentary rocks in central Fennoscandian shield, Finland. Precambrian Res. 104, 147 - 174.

Lee, Y.I., 2002. Provenance derived from the geochemistry of late Paleozoic-early Mesozoic mudrocks of the Pyeongan Supergroup, Korea. Sed. Geol. 149, 219 - 235.

Maheshwari, A., Sial, A.N., Guhey, R., Ferreira, V.P., 2005. C-isotope composition of carbonates from Indravati Basin, India: implications for Regional Stratigraphic Correlation. Gond. Res. 8, 603 - 610.

Manikyamba, C., Kerrich, R., Alvarez, I.G., Mathur, R., Khanna, T.C., 2008 Geochemistry of Paleoproterozoic black shales from intracontimental Cuddapah basin, India: implications for provenance, tectonic setting and weathering intensity. Precambrian Res. 162, 424 - 440.

Maynard, J.B., Valloni, R., Yu, H., 1982. Composition of modern deep sea sands from arc-related basins. Geol. Soc. London, Special Pub. 10, 551 - 561.

McLennan, S.M., Taylor, S.R., 1980. Rare earth element-thorium correlations in sedimentary rocks, and the composition of the continental crust. Geochim. Cosmochim. Acta 44, 1833 - 1839.

McLennan, S.M., Taylor, S.R., Eriksson, K.A., 1983. Geochemistry of Archean shales from the Pilbara Supergroup, Western Australia. Geochim. Cosmochim. Acta 47, 1211 - 1222.

McLennan, S.M., 1989. Rare earth elements in sedimentary rocks: influence of provenance and sedimentary process. Review. Mineral. 21, 169 - 200.

McLennan, S.M., Taylor, S.R., McCulloch, M.T., Maynard, J. B., 1990. Geochemical and Nd-Pb isotopic composition of deep sea turbidites: crustal evolution and plate tectonic associations. Geochim. Cosmochim. Acta 54, 2015 - 2050.

McLennan, S.M., Taylor, S.R., 1991. Sedimentary rocks and crustal evolution: Tectonic setting and secular trends. J. Geol. 99, 1 - 21.

McLennan, S.M., Hemming, S., McDaniel, D.K., Hanson, G.N., 1993. Geochemical approaches to sedimentation, provenance and tectonics. Geol. Soc. America, Special Pub. 284, 21 - 40.

McLennan, S.M., Hemming, S., Taylor, S.R., Eriksson, K.A., 1995. Early Proterozoic crustal evolution: Geochemical and Nd-Pb isotopic evidence from metasedimentary rocks, southwestern North America. Geochim. Cosmochim. Acta 59, 1153 - 1177.

McRae, S.G., 1972. Glauconite. Earth Sci. Rev. 8, 397 – 440.

Michaelsen, P., Henderson, R.A., 2000. Sandstone petrofacies expressions of multiphase basinal tectonics and arc magmatism: Permian and Triassic north Bowen Basin, Australia. Sed. Geol. 136, 113 - 136.

Middleton, G.V., 1960. Chemical composition of sandstones. Geol. Soc. America Bull. 71, 1011 – 1026.

Milodowski, A.E., Zalasiewicz, J.A., 1991. Redistribution of rare earth elements during diagenesis of turbidite/hemipelagic mudrock sequences of Landovery age from central Wales. In : A.C. Morton, S.P. Todd, P.D.W. Haughton (eds). Developments in sedimentary provinance studies. Geol. Soc. America, Special Pub. 57, 101 - 124.

Moitra, A. K., 1995. Depositional environmental history of Chhattisgarh Basin, M.P., based on stromatolites and microbiota . J. Geol. Soc. India 46, 359 – 386.

Mondal, M.E.A., 2002. Geochemistry and petrogenesis of the Archean-Proterozoic gneisses and granitoids from central Indian shield. J. Appl. Geochem. 4, 170-182.

Mondal, M.E.A., Hussain, M.F., 2003. Geochemical characteristics of granitoids from Bastar craton, central India. Gond. Geol. Magaz. Special Vol. 7, 193-199.

Mondal, M. E.A., Hussain, M. F., Ahmad, T., 2006. Continental Growth of Bastar Craton, Central Indian Shield during Precambrian via Multiphase Subduction and Lithospheric Extension/Rifting: Evidence from Geochemistry of Gneisses, Granitoids and Mafic dykes. Jour. Geosci. Japan 49, 137-151.

Mondal, M. E.A., Hussain, M. F., Ahmad, T., 2007. Geochemistry and petrogenesis of the Proterozoic mafic dyke swarms of Bastar craton of central Indian shield. Jour. Appl. Geochem. 9, 17 - 27.

Mukharaya, I.L., 1975. Metamorphism and petrogenesis of the Dalli-Rajhara and Ari Dongri Iron formations, Madhya Pradesh. Geol. Soc. India 16, 441 - 449.

Murthi, K. S., Rao, R. U. M., Aswathanarayana, U., 1984. Radioactive elements in the sediments of the Upper Proterozoic Chhattisgarh basin, India, as indicators of palaeoenvironments. Precambrian Res. 25, 325 - 328.

Murthi, K.S., 1987. Stratigraphy and sedimentation in Chhattisgarh Basin. In: Purana basins of peninsular India. Geol. Soc. India, Mem. 6, 239 – 260.

Murthi, K.S., 1996. Geology, sedimentation and economic mineral potential of the south – central part of the Chhattisgarh Basin. Geol. Surv. India, Mem. 125, 139p.

Nance, W.B., Taylor, S.R., 1977. Rare earth element pattern and crustal evolution-II. Archean sedimentary rocks from Kalgoorlie, Australia. Geochim Cosmochim Acta 41, 225p.

Naqvi, S.M., Hussain, S.M., 1972. Petrochemistry of the early Precambrian sediments from the central part of the Chitradurga schist belt, Mysore India. Chem. Geol. 10, 109 -135.

Naqvi, S.M., Rogers, J.J.W., 1987. Precambrian Geology of India. Oxford University Press, New York, U.S.A.

Narayanaswami, S., Chakaravarty, S.C., Vemban, N.A., Shukla, K.D., Subramanyam, M.R., Rao, G.V., Anandalwar, M.A., Nagarajaiah, R.A., 1963. The Geology and the magnese ore deposits of the magnese belt in M.P. and adjoining parts of Maharashtra, Part I, General Introduction. Geol. Surv. India, Bull. Series A 69.

Nesbitt, H.W., Markovics, G., Price, R.C., 1980. Chemical processes affecting alkalies and alkaline earth during continental weathering. Geochim. Cosmochim. Acta 44, 1659 - 1666.

Nesbitt, H.W., Young, G.M., 1982. Early Proterozoic climates and plate motions inferred from major element chemistry of lutites. Nature 54, 2015 - 2050.

Nesbitt, H W., Young, G.M., 1984. Prediction of some weathering trends of plutonic and volcanic rocks based on thermodynamic and kinetic consideration. Geochim. Cosmochim. Acta 48, 1523 - 1534.

Nesbitt, H.W., Young, G.M., 1989. Formation and diagenesis of weathering profiles. J. Geol. 97, 129 - 147.

Ordin, G. S., Morton, A. C., 1988. Authigenic green particles from marine environments. In: G. V. Chilingarian, K. H. Wolf, (Eds). Diagensis II. Developments in Sedimentology, Elsevier, Amsterdam, 43, 213 – 264.

Paikaray S., Banerjee, S., Mukherji., 2007. Geochemistry of shales from the Paleoproterozoic to Neoproterozoic Vindhyan Supergroup: Implications on provenance, tectonics and paleoweathering. J. Asian Earth Sci. 32 (1), 34 - 48.

Parekh, P.P., Moller, P., Dulski, P., 1977, Distribution of trace elements in foraminifera tests. Earth Planet. Sci. Lett. 73, 285 - 298.

Patranabis Deb, S., Chaudhuri, A.K., 2002. Stratigraphic architechture of the Proterozoic sucession in the eastern Chhattisgarh basin: its tectonic implication. Sed. Geol. 147, 105 -125.

Patranabis Deb, S., 2004. Lithostratigraphy of the Neoproterozoic Chhattisgarh sequence, its bearing on the tectonics and paleogeography. Gond. Res. 7, 323 – 337.

Pettijohn, F.J., Potter, P.E., Siever, R., 1972. Sand and sandstone. Berlin, Springer-verlag, 57p.

Pettijohn, F. L., Potter P. E., Siever, R., 1987 Sand and Sandstone. 2nd Edn, New York, Springer-Verlag, 533p.

Prasad, B., 1990. Observations in the Precambrian geology of Central India vis a vis adjoining region. Geol. Surv. India, Special Pub. 28, 181 – 198.

Radhakrishna, B.P., 1987. Introduction. In: Purana basins of peninsular India. Geol. Soc. India, Mem. 6, i-xv.

Radhakrishna B.P., Ramakrishnan M., 1988. Archean-Proterozoic Boundary in India. J. Geol. Soc. India 32, 263 – 278.

Radhakrishna, B.P., Naqvi, S.M., 1986. Precambrian continental crust of India and its evolution. J. Geol. 94, 145 - 166.

Radhakrishna, B. P., 1989. Suspect tectono-stratigraphic terrane elements in the Indian subcontinent. J. Geol. Soc. India 34, 1 - 24.

Ramakrishnan, M., 1987. Stratigraphy, sedimentary environment and evolution of the Late Proterozoic Indravati Basin, Central India. In: B.P. Radhakrishna, (Ed.), Purana basins of peninsular India. Geol. Soc. India Mem. 6, 139 - 160.

Ramakrishnan, M., 1990. Crustal development in Southern Bastar, Central Indian craton. Geol. Surv. India Special Pub. 28, 44 – 66.

Rao, D. V., 1985. Polyphase granites of the Indian shield and Lithosphere evolution. In: S.A. Athens (Ed.), The Crust; The significance of granites-Gneisses in the Lithosphere. Theophrastus Publ. pp.147 - 168.

Rao, V.V.S., Sreenivas.B., Balram, V., Govil, P.K., Srinivasan, R., 1999. The nature of the Archean upper crust as revealed by the geochemistry of the Proterozoic shales of the Kaladgi basin, Karnatka Southern India. Precambrian Res. 98, 53 - 65.

Raza, M., Casshyap, S.M., Khan, M.S., 2002. Proterozoic crust in the northern part of the Indian shield and its tectonic evolution. J. Geol. Soc. India 60, 198 -218.

Reddy A.G.B., Ramakrishna T.S., 1988. Subsurface structure of the shield area of Rajasthan-Gujarat as inferred from Gravity. In: A.B. Roy (Ed.), Precambrian of the Aravalli Mountain, Rajasthan, India.Geol. Soc. India, Mem. 7, 279 – 284.

Roser, B.P., Korsch, R.J., 1985. Plate tectonics and geochemical composition of sandstones: a discussion. J. Geol. 93, 81 - 84.

Roser, B.P., Korsch, R.J., 1986. Determination of tectonic setting of sandstone-mudstone suites using SiO_2 content and K_2O/Na_2O ratio. J. Geol. 94, 635 – 650.

Roser, B.P., Korsch, R.J., 1988. Provenance signatures of sandstone-mudstone suites determined using discriminant function analysis of major-element data. Chem. Geol. 67, 119 - 139.

Roy, A., Bandopadhyay, B.K., 1988. Tectonic significance of ultramafic and associated rocks near Tal in Bijawar belt, Sidhi district, Madhya Pradesh. J. Geol. Soc. India 32, 397 - 410.

Roy, A., Bandyopadhyay, B.K., 1990. Tectonic and structural patterns of the Mahakoshal belt of central India: A discussion. Geol. Surv. India Special Pub. 28, 226 - 240.

Roy, A., Bandyopadhay, B.K., Huin, A.K., 1992. Occurrence and significance of a ductile shear zone near the eastern margin of the Sakoli belt in central India. Indian Mineral. 46, 323 - 336.

Saini, N.K., Mukherjee, P.K., Rathi, M.S., Khanna, P.P., Purohit, K.K., 1998. A new geochemical refrence sample of granite (DG-H) from Dalhousie, Himachal Himalaya. J. Geol. Soc. India 52, 603 - 606.

Sarkar, S.N., Gautam, K.V.V.S., Roy, S., 1977. Structural analysis of a part of Sausar Group rocks in Chikla, Sitekere area, Bhandara District, Maharashtra. Geol. Soc. India 18, 627 -643.

Sarkar, S.N., Gopalan, K., Trivedi, J.R., 1981. New data on the geochronology of the Precambrians of Bhandara-Durg, Central India. Indian J. Earth Sci. 8, 131-151.

Sarkar, S.N., Saha, A.K., 1982. Stucture and tectonics of the Singhbum Orissa Iron Ore craton, Eastern India. Rec. Res. Geol. 10, 1 - 25.

Sarkar, S.N., 1983. Present status of Indian stratigraphy and geochronology of peninsular India- A synopsis. Indian J. Earth Sci. 1, 237 - 268.

Sarkar, A., Gopalan, K., Trivedi, J.R., 1988. Tectonics and geochronology of the Proterozoic rocks of Dongargarh, Sakoli and Sauser areas in Dongargarh-Bhandara-Durg region, Central region, (Abs.) Workshop, Proterozoic Geochem. Calcutta, India pp. 91 - 93.

Sarkar, A., Sarkar, G., Paul, D. K., Mitra, N. D., 1990a. Precambrian Geochronology of the Central Indian Shield – A review. Geol. Soc. India Special Pub. 28, 453 - 482.

Sarkar, G., Paul, D. K., deLaeter, J. R., McNaughton, N. J., Mishra, V. P., 1990b. A geochemical and Pb, Sr isotopic study of the evolution of granite gneisses from the Bastar craton, Central India. J. Geol. Soc. India 35, 480 - 496.

Sarkar, G., Corfu, F., Paul, D.K., McNaughton, N.J., Gupta, S.N., Bishnui, P.K., 1993. Early Archean crust in Bastar craton, Central India- a geochemical and Isotopic study. Precambrian Res. 62, 127 - 137.

Schwab, F.L., 1975. Framework mineralogy and chemical composition of continental margin- type sandstone. Geology 3, 487 - 490.

Sengupta, A., 1965. Some aspects of metamorphism of Sakoli series around Gangajhiri, Bhandara District, Maharashtra. Geol. Soci. India 6, 1 - 17.

Shastry, B.V., Dekate, Y.G., 1984. Petrochemistry of the Sakoli and Sauser metasediments in Southern part of Balaghat district, Madhya Pradesh. Geol. Surv. India, Special Pub. 12, 485 - 490.

Sirivastava, R.K., Singh, R.K., Verma, S.P., 2004. Neoarchean mafic volcanic rocks from the southern Bastar greenstone belt, Central India: petrological and tectonic significance. Precambrian Res. 131, 305 - 322.

Sun, S.S., McDonough, W.F., 1989. Chemical and Isotopic systematics of oceanic basalts: implications for mantle composition and processes. In: A.D. Saunder and M.J Norry (eds.), Magmatism in oceanic basins Geol. Soc. London Special Pub. 42, 313 – 345.

Takashi, K., Yoshida, M., Wada, H., Satish-Kumar, M., Roy A., Bandhopadyay B.K., Khan A.S., Pal, T., Huin, A. K., Bhowmik, S.K., Chattopadhyay, A., 2001. Field studies in the Sakoli Belts of the Central Indian Tectonic Zone. J. Geosci. Osaka City University 44, 17 - 39.

Taylor, S.R., 1977. Island arc models and the composition of the continental crust. AGU Ewing Series I, 325p.

Taylor, S. R., McLennan, S. M., 1981. The composition and evolution of continental crust: Rare earth element evidence from sedimentary rocks. Phil. Trans. Roy. Soc. London A 301, 381 – 399.

Taylor, S.R., McLennan, S.M., 1985. The continental crust: Its composition and evolution, Oxford, Blackwell.

Thorpe, R.S. (ed.), 1982. Orogenic Andesites and Related Rocks. Wiley, New York.

Tripathi, C., Ghosh, P. K., Thambi, P. I., Rao, T. V., Chandra, S., 1981. Elucidation of the stratigraphy and structure of Chilpi group. Geol. Surv. India, Special Pub. 3, 17 – 30.

Van de Kamp, P.C., Leake, B.E., 1985. Petrography and geochemistry of feldspathic and mafic sediments of the northeasetern Pacific margin. Trans. R. Soc. Edinb. Earth Sci. 76, 411 – 449.

Van der Westhuizen, W.A., de Bruiyn, H., Meintjes, P.G., 1991. The Ventersdorp Supergroup: an overview. J. African Earth Sci. 13, 83 – 105.

Walter, M.R., 1976. Stromatolites; Developments in sedimentology. Elsevier, Amsterdam 20, 790p.

Wani, H., Mondal, M.E.A., 2007. Provenance and Tectonic signals of the Neoproterozoic Basins of the Bastar craton: evidence from sandstone petrology and geochemistry. Proceeding. Indian Nation. Sci. Acad. 73, 81 - 90.

Wani, H., Mondal, M.E.A., 2008. Petrochemistry of sandstones from Neoproterozoic basins of the Bastar craton, Central Indian shield: Implications for paleoweathering, provenance and tectonic history. Island Arc (In Press).

Wronkiewicz, D.J., Condie, K.C., 1987. Geochemistry of Archaen shales from the Witwaterstand Supergroup, South Africa, Source area weathering and provenance. Geochim. Cosmochim. Acta 51, 2401 - 2416.

Wronkiewicz, D.J., Condie K.C., 1989. Geochemistry and provenance of sediments from the Pongola Supergroup, South Africa: Evidence from a 3.0 Ga-old continental craton. Geochim. Cosmochim. Acta 53, 1537 - 1549.

Wronkiewicz, D.J., Condie, K.C., 1990. Geochemistry and mineralogy of sediments from the Ventersdorp and Transvaal Supergroups, South Africa: cratonic evolution during the early Proterozoic. Geochim. Cosmochim. Acta 54, 343 - 354.

Yadekar, D. B., Jain, S. C., Nair, K. K. K., Gupta, K. K., 1990. The Central Indian collision suture. Geol. Surv. India, Special Pub. 28, 1 - 43.

Zhang, L., Sun, M.N., Wang, S., Yu, X., 1998. The composition of shales from the Odos basin, China: effects of source weathering and diagenesis. Sed. Geol. 116, 129 - 141.

PUBLICATIONS

LIST OF PUBLICATIONS

Wani, H., Mondal, M.E.A., 2007. Provenance and Tectonic signals of the Neoproterozoic Basins of the Bastar craton: evidence from sandstone petrology and geochemistry. Proc. Indian Nation. Sci. Acad. 73, 81 - 90.

Wani, H., Mondal, M.E.A., 2008. Petrochemistry of sandstones from Neoproterozoic basins of the Bastar craton, Central Indian shield: Implications for paleoweathering, provenance and tectonic history. Island Arc (In Press).

Proc Indian Natn Sci Acad 73 No.2 pp. 81-90 (2007)

Research Paper

Provenance and Tectonic Setting Signals of the Neoproterozoic Basins of the Bastar Craton: Evidence from Sandstone Petrology and Geochemistry

H. WANI[1] and M.E.A. MONDAL*
Department of Geology, Aligarh Muslim University, Aligarh-202 002 (UP)
[1]Department of Geology, Amarsingh College, Srinagar-190 008

(Received 05 February 2007; Accepted 14 May 2007)

The lower parts of the Chattisgarh Basin and the Indravati Basin of Bastar craton start with the sandstone successions as the Chandarpur Group and the Tiratgarh Formation respectively. The sandstones of the Chandarpur Group of the Chattisgarh Supergroup show a broad similarity in composition with sandstones of the Tiratgarh Formation of Indravati Group. Sandstones of the Chandarpur Group display progressive change towards greater mineralogical maturity from base to top of the succession. On average, compositions of Chandarpur Group become mature in Upper Kansapathar Formation. The proportion of framework quartz increases upwards stratigraphically. The chemical data also show that SiO_2 increases and CaO, Na_2O, K_2O decrease through time at the expense of less robust constituents. Provenance of sandstones of the Chandarpur Group and Tiratgarh Formation on QtFL diagram has been established as cratonic interior provenance while on QmFLt diagram, sandstones are considered to have been derived from cratonic interior and quartzose recycled provenance. The overall petrological and geochemical evidence indicate their source rocks were granites, gneisses and metasedimentary rocks, while mineralogical and geochemical maturity of sandstones suggests tectonic stability of the provenance and some contribution from pre-existing sedimentary rocks. Presence of multi-cycle quartz grains, chert and glauconite grains support the above conclusion.

Key Words: Bastar Craton, Chattisgarh Basin, Indravati Basin, Sandstone Petrology, Geochemistry, Provenance, Tectonic Setting

Introduction

The peninsular India preserves an extensive record of Proterozoic successions which display extreme heterogeneity in stratigraphy, sedimentation pattern, metamorphism, deformation and magmatism. Radiometric age data from the mobile belt successions indicate that the history of deformed metasedimentary and metavolcanic successions with multiple episodes of deformation, metamorphism and magmatism extends mainly between 2500-1500Ma, though events reflecting crustal perturbations in the Indian peninsula extended up to 1000Ma and even up to Proterozoic –Phanerozoic boundary. Not withstanding the above, there is evidence of development of cratonic basins during the period between 1700-700Ma on different Paleoproterozoic and Archean basements. The dominance of the orthoquartzite-shale-carbonate rocks (Table1) indicate their generation on stable continental margins or within intracratonic basins [1]. The basal Groups of these basins can be classified as 'Assemblage II' of Condie [1]. This suggests that the early history of these basins involved lithospheric continental rifting (with or without abortive) mantle activation. The basic igneous activity within these sequences and the Paleo- (± Meso-) Proterozoic intrusions in their basements [2,3] testify to similar thermal activity in the crust associated with the development of these basins. Possibly, the Late Archean – Paleoproterozoic granitizataion event in the Peninsular shield [4,5] also have contributed to the generation of these supracrustal intracratonic basins as has been postulated by Klein and Hsui [6].

The Chattisgarh and the Indravati Basins are two major Proterozoic intra-cratonic sedimentary basins of the Bastar craton containing the Neoproterozoic sediments. The basins are similar in their mixed siliclastic-carbonate lithology, absence of metamorphic over-printing and very low tectonic disturbance. These sedimentary successions are believed to be younger than 1600Ma commonly designated as Purana successions in the Indian stratigraphy [7,8]. Origin of these cratonic basins however is still poorly constrained, though a riftogenic origin has been invoked for them [9,10]. The cylothem at the basal part of the Chattisgarh succession has been attributed to active tectonic episodes and rifting of the cratonic basement [11].

The Chattisgarh Basin has been so far studied mainly from the point of view of lithostratigraphy, lithofacies and paleogeography [11-20]. Similar work on Indravati basin has also been carried out by the previous workers [21-25]. The present study is focused on the petrofacies and major element analyses of the Chandarpur Group and Tiratgarh Formation. These two sandstone successions *viz.*, Chandarpur Group and Tiratgarh Formation which form lower parts of sedimentary successions of the Chattisgarh and the Indravati Basins respectively have been taken into account into this study

* *Author for Correspondence: Email: emondal2002@yahoo.co.in*

(Table1). The major emphasis of the present study is directed towards assessment of provenance and tectonic regime by the use of quantitative detrital modes, calculated from point counts of thin sections [26] and major element geochemistry of sandstones. The tectonic setting of the provenance apparently exerts primary control on sandstone compositions [27]. Geochemistry of clastic sedimentary rocks can best be used to determine the compositions of the provenance [28] and tectonic setting of the basin [29-31].

Table 1. Lithostratigraphy of the Indravati Basin and the Chattisgarh Basin after Ramakrishnan et al., [23] and Murthi [12]

Indravati Basin		**Chattisgarh Basin** (Chattisgarh Supergroup) ***Raipur Group***	
Indravati Group		**Chandrapur Group**	
Jagdalpur Formation	Calcareous Shales with Purple & gray Stromatolitic dolomite	Kansapathar Formation	White sandstone
Kanger Limestone	Purple limestone Grey limestone	Chaporadih Formation	Reddish Brown and Olive green sandstone
Cherakur Formation	Purple shale with arkosic sandstone and chert pebble Conglomerate grit	Lohardih Formation	White pebbly sandstone
Tiratgarh Formation	Chitrakot sandstone member Mendri sandstone member		
- - - - - - Unconformity - - - - - -			
Archean granites, gneisses and older supracrustals (Sonakhan greenstone belt)			

Geological Setting

The Bastar craton lies in the southern corner of central Indian shield. Bastar craton is bounded on the east by the high-grade Eastern Ghat Mobile belt and Mahanadi and Godavari rifts in the north and south respectively. Gneisses and granitoids form the basement for the supracrustal rocks (Fig. 1). The younger supracrustal rocks in Bastar craton occur in two major Neoproterozoic intra-cratonic basins: (a) the Chattisgarh Basin and (b) the Indravati Basin as shown in Figure 2.

(a) Chattisgarh Basin

The Chattisgarh Basin occurs within an area of 35,000 km^2, this is the third largest Purana Basin in the peninsular India. The Chattisgarh Supergroup comprises of a thick succession of sandstone, shale and limestone [9,12,-14,16,32]. The lower part of the succession is dominated by sandstone (Chandarpur Group), whereas limestone and shale dominate the upper part (Raipur Group).

The Chandarpur Group comprises of unmetamorphosed and gently dipping subhorizontal beds of sandstone with conglomerate and shale as subordinate constituents. The succession unconformably overlies gneisses, granitoids and the Sonakhan greenstone belt of the Archean basement complex (Table1). The Chandarpur Group is subdivided into three formations viz. Lohardih, Chaporadih and Kansapathar Formations, arranged in ascending order of superposition [16,12]. The rocks of Chandarpur Group were deposited in fan-fan delta, deep water prodelta and storm tide dominated prograding shelf environments [16,33].

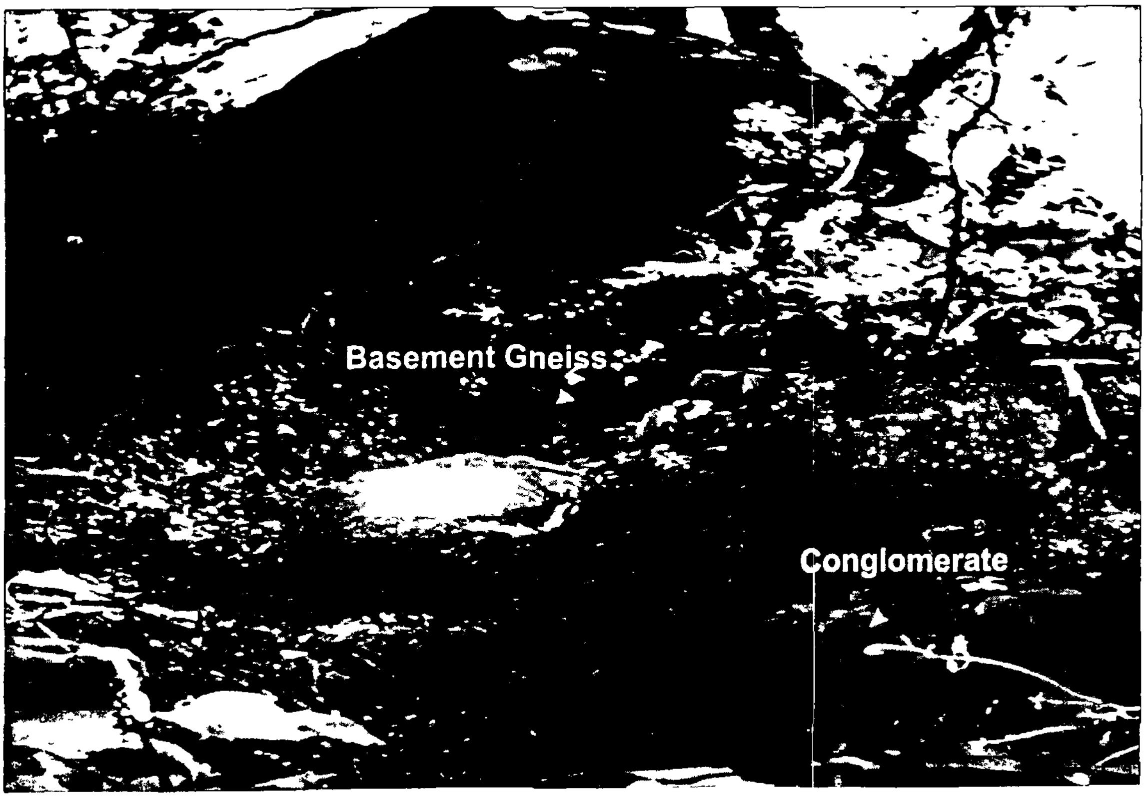

Fig. 1: Field photograph showing contact between Chandarpur conglomerate/sandstone and Archean basement gneiss, Chattisgarh basin

(b) Indravati Basin

The Indravati Group occupies a vast plateau around Jagdalpur, Bastar district of Chattisgarh. The Indravati Basin covers an area of 9000 km^2 in Kanker-Bastar-Dantewara districts of Chattisgarh and Orrisa. The Indravati Group of rocks unconformably overlie the Archean gneissic and granitic rocks. The Indravati Group comprises of basal sandstone (Tiratgarh Formation) grading upwards into a conformable sequence of shale with sandstone (Cherakur Formation), horizontally laminated Kanger limestone and purple shales with stromatolitic dolomite (Jagdalpur Formation) in ascending order. The sediments of the Indravati Basin are considered to have been deposited in shallow marine, near shore tidal flat or lagoonal environment [25].

The generalized stratigraphic succession for the Indravati Group and Chattisgarh Supergroup are shown in Table 1.

(c) Age Considerations

The Chattisgarh and the Indravati Basins of the Bastar craton present considerable problems for intrabasinal correlation of different lithounits because of the paucity of chronostratigraphic and biostratigraphic evidence. On the basis of lithology and cyclic nature of sedimentation, these basins were considered as equivalent to the lower Vindhyans [22,34,12]. The Indravati Basin has been correlated with the Lower Vindhyans and the Kurnool [22]. Later research revealed that the Sandstone Member (Tiratgarh Formation) of the Indravati Basin can be compared with the Chopardih Formation (Chandarpur Group) of the Chattisgarh Supergroup, which gives K-Ar age of 700-750Ma [34]. This age data is also supported by presence of stromatolites in limestones and dolomites of Machkot area, which corresponds to late Riphean age (700-1100 Ma) as suggested by Walter [35]. Recent research revealed that the elevated $\delta^{13}C$ values of the Indravati carbonates and the Chattisgarh carbonates are comparable with the Bhander limestone unit of the Upper Vindhyan [36, 37].

Methodology

Unaltered sandstone samples were collected from the Chandarpur Group and the Tiratgarh Formation of the Indravati Group (Fig. 2). Most of the samples collected from outcrops and mine exposures in the study area. Mineralogical composition of the sandstone was determined by the modal analysis with about 500-1000 points counted for each thin section. After careful examination under microscope representative samples of each Formation of Chandarpur Group and Tiratgarh Formation with little or no carbonate minerals have been analyzed for major element analysis. Major elements were analyzed on WD-XRF (Siemens SRS 3000) at Wadia Institute of Himalayan Geology, Dehradun. The precision of XRF major oxide data is better than 1.5%.

The sandstone classification proposed by Folk [38] has been followed in the present study. The modal analysis data were recalculated on a matrix free basis (Table 2) and was plotted in QFL diagram (Fig. 3). Polycrystalline quartz though not as durable as monocrystalline quartz was placed at Q pole to obviate the problems of distinction between plutonic polycrystalline quartz and metaquartzite fragments. In the triangular diagram constructed for delineating the tectonic setting of the provenance, polycrystalline quartz was placed at rock fragment (RF) pole (in the Lt pole of QmFLt plot of Dickinson and Suczek, [26] and chert was placed at rock fragment (RF) pole as its origin can be unequivocally traced to a sedimentary source, though it was placed at the Q pole by several earlier workers [39,40]. Klein [41] argued that chert is less stable than quartz during transport and placed the chert fragment at the RF pole [38]. The F-pole comprises all types of feldspar grains and granite and gneiss rock fragment. For recognition of source rock lithology and tectonic setting of the provenance, the modal data were plotted on QtFL, QmFLt and QmPK triangular diagrams of Dickinson and Suczek [26] (Fig. 4). In QtFL diagram, all quartzose grains were plotted together; the emphasis was on grain stability and consequently on weathering and relief in the provenance, transport mechanism, as well as composition of the source rock. In QmFLt diagram all lithic fragments were plotted together and emphasis was shifted towards the grain size of the rocks, because finer-grained rocks yield more lithic fragments in the sand-size range.

Sandstone Petrology

Sandstone petrography is widely considered to be a powerful tool for determining the origin and tectonic reconstructions of ancient terrigenous deposits [39,42,43]. Sandstone mineralogical characterization of the basin fill is critical to any basin analysis and many studies have pointed to an intimate relationship between detrital sand compositions (i.e. bed rock compositions of sources) and tectonic setting [26,31,44]. Sand composition which is sensitive to a complex set of factors like climate, relief, transport, diagenesis, etc. provides valuable information for paleoenvironment reconstructions [45].

Modal analysis reveals that the main detrital framework mineral grains of the Chandarpur Group and the Tiratgarh Formation of the Indravati Group include quartz, potash feldspar, plagioclase, rock fragments especially chert, mica and heavy minerals. Sandstones of the Chandarpur Group and the Tiratgarh Formation are characterized by abundant quartz grains (83.15% and 88.19% on average, respectively). According to Folk's classification [38], the sandstones of Chandarpur Group and Tiratgarh Formation are mostly subarkoses, sublitharenites and quartz arenite (Fig. 3). Quartz occurs mainly as monocrystalline quartz. Some of these have undulatory extinction. Polycrystalline quartz represented by recrystallised and stretched metamorphic quartz occurs

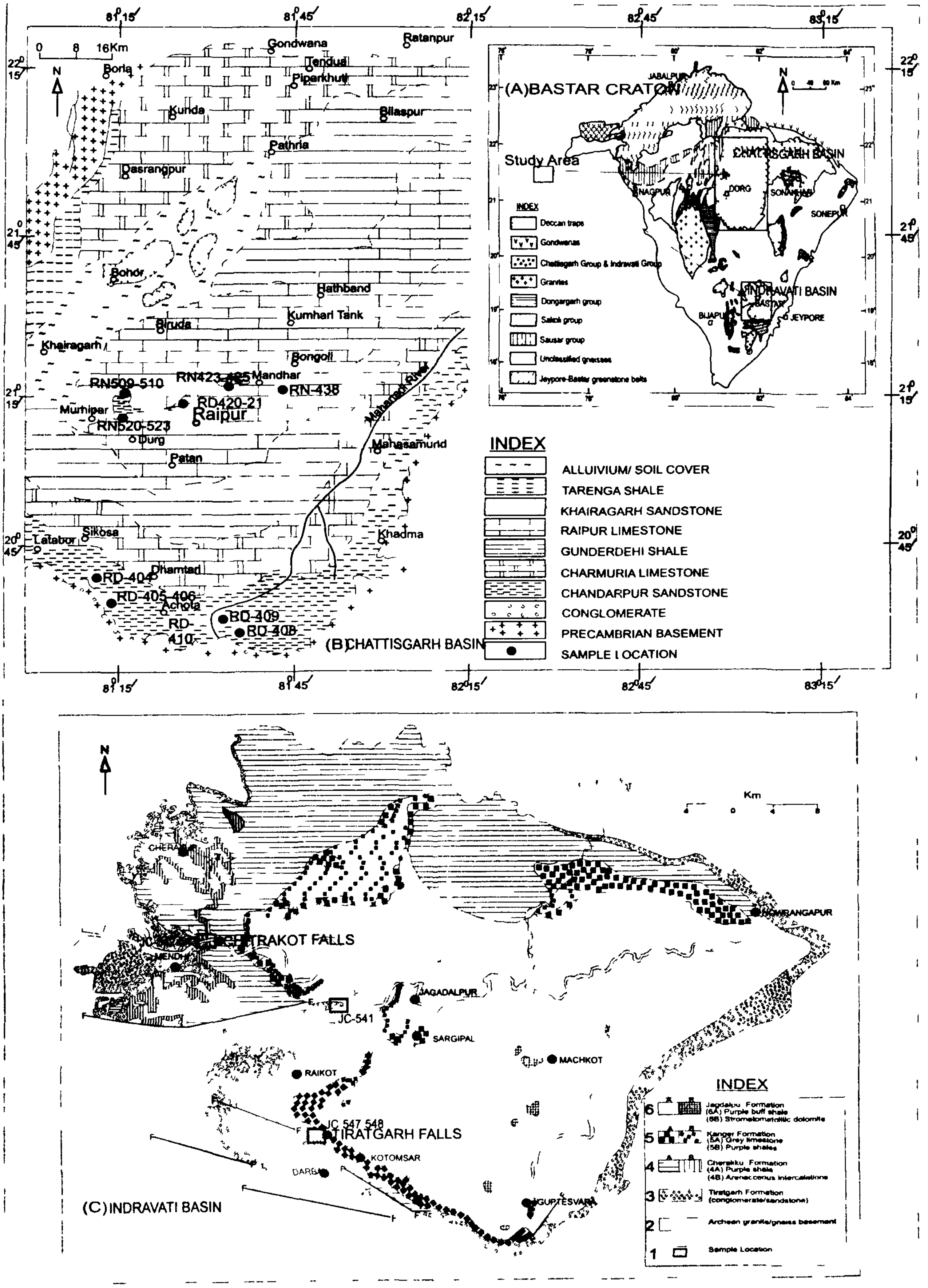

Fig 2 Geological map of the Chattisgarh Basin (B) and Indravati Basin (C) showing the locations of the areas from which samples have been taken Inset Geological map of Bastar craton (A) showing different sedimentary Basins of the craton Numbers indicate sample locations

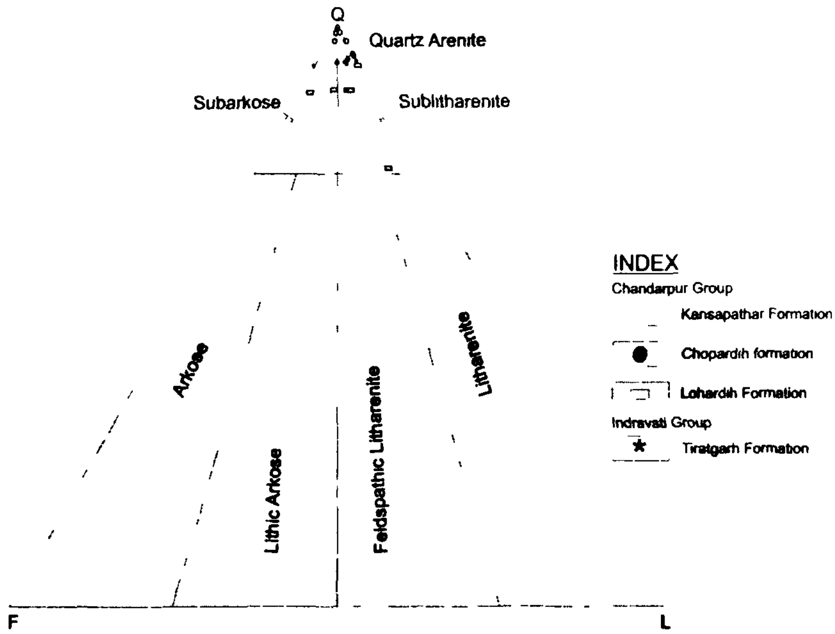

Fig. 3: ***QFL plots of the classification Folk*** **[38]** ***Indravati Basin***

Table 2: Modal analysis of sandstones of Chandarpur Group, Chattisgarh Basin and Tiratgarh Formation of Indravati Basin.

Sample No	Qm %	Qp %	Kfelds-par%	Plagioc lase%	Feldsp-ar total%	Chert %	Glaucon-Ite%	Silica cement%	calcite cement%	Iron cement%	Rock fra-gment%	Others %	Total %
Chandarpur Group													
Lower Lohardih Formation													
RD-406	76 33	5 12	6 18	3 18	9 36	0	0	0 55	6 53	0 7	1 23	0 18	100
RD-420	37 46	0 65	0 65	1 6	2 25	9 65	0	0 16	33 44	16 07	0	0 32	100
RD-421	57 64	1 05	1 91	0 52	2 43	4 68	0	0 52	33 15	0 35	0	0 18	100
RN-438	79 37	3 37	2 52	1 05	3 57	6 53	0	5 06	0	1 05	0	1 05	100
RD-509	85 9	4 51	0 37	0	0 37	6 02	0	2 07	0	0 94	0	0 19	100
RD-523	68 36	5 68	3 84	1 38	5 22	3 32	0	0	15 55	0 3	0 77	0 8	100
Average	67 51	3 4	2 6	1 3	3 9	5 02	0	1 39	14 8	3 2	0 33	0 45	100
Average P/K ratio of Lohardih Formation is 0 5													
Middle Chopardih Formation													
RD-404	80 47	9 19	1 34	0	1 34	2	3 01	0 66	0	0 83	1 83	0 67	100
RN-423	67 26	4 19	0	0	0	3 07	21 77	2 09	0	1 45	0	0 17	100
RN-425	82 01	1	2 02	0 86	2 88	2 44	9 06	1 73	0	0 59	0	0 29	100
Average	76 59	4 8	1 12	0 29	1 4	2 5	11 28	1 49	0	0 95	0 61	0 37	100
Average P/K ratio of Chopardih Formation is 0 25													
Upper Kansapathar Formation													
RD-405	87 28	6 66	0	0	0	2 37	0	2 52	0	0 29	0	0 88	100
RD-408	86 76	3 63	0 9	0 55	1 45	0 72	0	1 99	0	5 27	0	0 18	100
RD-409	91 54	4 94	0	0	0	0 58	0	2 12	0	0 23	0 36	0 23	100
RD-410	80	16 5	0	0	0	2 17	0	0 49	0	0 24	0 24	0 36	100
RN-424	88 89	5 48	0 81	0	0 81	0 16	0	4 02	0	0 32	0	0 32	100
RD-510	85 33	7 81	0	0	0	2 43	0	1 14	0	0 72	2 28	0 29	100
RD-520	93 79	1 77	0	0	0	0	0	4 14	0	0 15	0	0 15	100
Average	87 7	6 68	0 23	0 07	0 32	1 2	0	2 34	0	1 03	0 41	0 34	100
Average P/K ratio of Kansapathar Formation is 0 31													
Average of all the three Formation of Chandarpur Group													
	78 02	5 15	1 28	0 57	1 85	2 87	2 11	1 82	5 55	1 84	0 41	0 38	100
Average P/K ratio of all the three Formations of Chandarpur Group is 0 44													
Indravati Group													
Tiratgarh Formation													
JC 541	3 28	85 8	5 47	1 09	6 56	0	0	0	3 83	0 18	0	0 35	100
JC-542	79 83	1 8	0 36	1 26	1 62	3 61	0	0 36	10 61	0 9	0 54	0 73	100
JC-543	89 79	5 83	0	0	0	0	0	0 36	3 05	0 36	0 48	0 13	100
JT-547	50 42	32 1	1 53	0 41	1 94	2 08	0	0	10 42	1 12	1 38	0 54	100
JT-548	86 14	5 82	0	0	0	5 54	0	1 25	0	0 69	0 28	0 28	100
Average	61 89	26 3	1 47	0 55	2 02	2 24	0	0 39	5 6	0 65	0 54	0 4	100
Average P/K ratio of Tiratgarh Formation is 0 37													

Qm-monocrystalline Quartz, Qp-Polycrystalline Quartz, others include heavy minerals and mica in subordinate proportions (Table 2). In majority of polycrystalline grains, subgrains with both straight and sutured contacts are common. Feldspar constitutes 1.85% and 2.02% on average of the framework grains of the Chandarpur Group and the Tiratgarh Formation respectively, and is dominated by microcline. However, plagioclase (especially albite) is also present in minor quantities in some samples (Table 2). Rock fragments are very few and are dominated by sedimentary lithics especially chert and followed by metamorphic lithics mostly tectonites. Heavy minerals are mainly zircon. These sandstones are generally matrix free. Authigenic quartz, iron oxide and calcite are cementing material. Quartz cement occurs primarily as overgrowth around detrital grains.

Chandarpur Group (Chattisgarh Basin)

(a) Lower Lohardih Formation

Lohardih Formation is dominated by quartz (70% on average). Monocrystalline quartz is dominant type, averages 67.50%. Feldspar content of this formation exceeds that of any other unit documented here and the entire feldspar population averages 3.9 % for the sample set. Microcline dominates over plagioclase (P/K ratio averages 0.5). Most of the samples of the Lohardih Formation show little compaction and framework grains are seen floating in carbonate cement (Fig. 5-I). Some feldspar grains are replaced by carbonate cement through cracks and cleavages (Fig. 5-II). The rock fragments are negligible in these sandstones and are made up of chert and fine grained rock, composed of quartz and mica. This stratigraphic unit has the highest representation of chert grains (5.02% on average).

(b) Middle Chopardih Formation

The Chopardih Formation is characterized high values of quartz (81.39% on average). Quartz strongly dominated by monocrystalline quartz averages 76.59%. Polycrystalline quartz generally constitutes 4.8% of quartz grains. Microcline dominates over plagioclase (P/K ratio averages 0.25) for the sample set. Glauconite pellets are very common in the Chopardih Formation (up to 11.28%). Glauconite pellets commonly occur within interstitial spaces coated with ferrugeneous materials. However well rounded glauconite pellets are also noticed (Fig. 5-III). The cementing material is mostly silica cement (quartz overgrowth).

(c) Upper Kansapathar Formation

This stratigraphic unit has the highest representation of quartz grains (average 94.4%) for the entire basinal infill. The framework grains of Kansapathar Sandstone Formation are composed dominantly of monocrystalline and polycrystalline quartz with insignificant feldspar and rock fragments including chert which accounts 1.2% on average. Stretched metamorphic quartz is very common among the polycrystalline quartz. The intragranular space is entirely filled by the quartz cement which constitutes about 2.39% on average. An interlocking quartz mosaic is developed due to silica overgrowth on the grains (Fig. 5-IV).

Indravati Group

Tiratgarh Formation

The Tiratgarh Formation is dominated by high values of quartz (88.16% on average). Monocrystalline is dominant quartz type (61.79% on average); however, in two samples polycrystalline quartz dominates (Fig. 5-V and 5-VI). K-feldspar dominates over plagioclase except in one sample (P/K ratio averages 0.37%) and the entire feldspar population averages 2.02% for all samples (Table 2). The sandstones are mainly cemented by carbonate cement and silica cement. Some quartz grains are seen floating in carbonate cement. Heavy minerals and opaques are zircon and iron oxides respectively. Quartz cement occurs primarily as overgrowth around quartz detrital grains. Rock fragments are rare and are dominated by chert fragments.

Major Element Geochemistry

In general SiO_2 concentration are higher (average 92.96%) in all sandstone samples (Table 3). The highest SiO_2 concentration and lower Na_2O, K_2O, CaO are in upper Kansapathar Formation than Lower Lohardih Formation and Middle Chopardih Formation of Chandarpur Group and Tiratgarh Formation of Indravati Group (Table 3). It may be due to higher concentration of quartz and trace amount of feldspar and rock fragments in the Kansapathar Formation. K_2O and Na_2O contents and high K_2O/Na_2O ratio is consistent with petrographic observation, according to which K-feldspar dominates over plagioclase feldspar. Correlation between modal abundances and CaO, Na_2O, K_2O indicate that alkalis are mainly controlled by the presence and composition of feldspar.

Provenance and Tectonic Setting

To identify the provenance and tectonic setting, the detritus composition was plotted on standard ternary diagrams of Dickinson and Suczek [26]. In QtFL diagram most of the subarkosic sandstones of the Lohardih Formation and the Chopardih Formation and the Tiratgarh Formation of the Indravati Group plot in stable cratonic field. The mineralogically mature rocks (arenites) of the Upper Kansapathar Formation of the Chandarpur Group also plot in the stable cratonic field very close to Qt pole i.e. craton interior field (Fig. 4A). In the QmFLt diagram (Fig. 4B), the population suggests craton interior provenance for all the three formations of the Chandarpur Group and the Tiratgarh Fornmation of the Indravati Group and a few samples also plot on or near quartzose recycled orogen. Provenances on QmPK diagram (Fig. 4C) samples cluster near Qm pole but are showing a linear trend from the Lower Lohardih to Upper Kansapathar Formation towards increasing maturity from continental provinces.

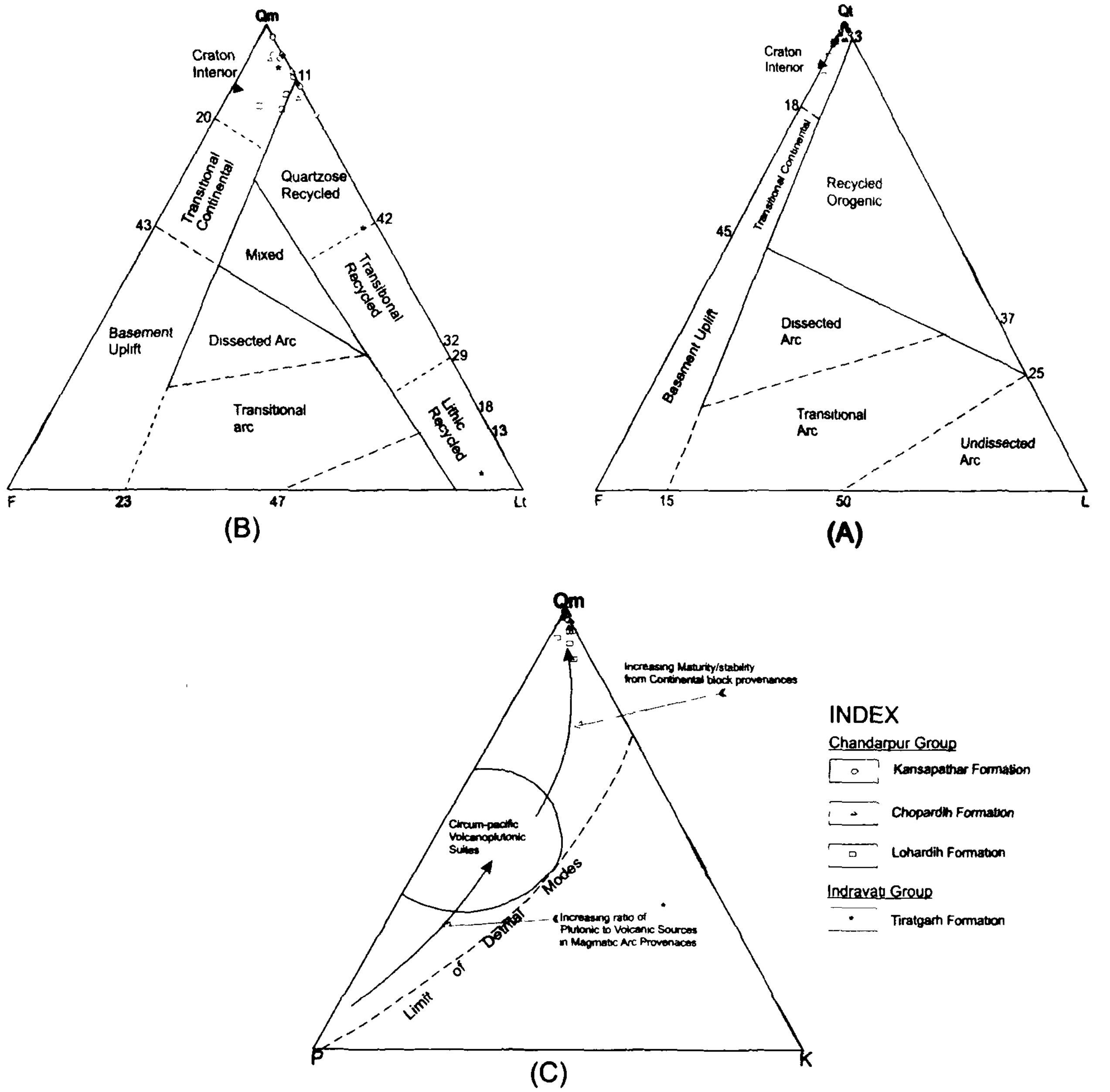

Fig. 4: Provenance discriminant diagrams after Dickinson and Suczek [26] of sandstone samples of the Chandarpur Group, Chattisgarh Basin and the Tiratgarh Formation, Indravati basin

Sedimentologists and geochemists have long endeavored to pursue the relationship between sedimentary rock geochemistry and plate tectonic setting. Roser and Korsh [31] established a discrimination diagram using K_2O/Na_2O vs. SiO_2 to determine the tectonic setting of terrigenous sedimentary rocks. The diagram shows a passive margin setting for all sandstone samples of Chandarpur Group and Tiratgarh Formation of Indravati Group (Fig. 6).

Arora *et al* [46] use a triangular diagram of CaO-Na_2O-K_2O major element data to derive various provenance fields for Archean conglomerate of Dharwar craton. In this diagram they distinguish fields for four provenances: Tholeiita and basaltic komatiite, younger greenstone belts, tonalite-trondhjemite, granite, quartz-monzonite. The compositions of average gneisses, granites, mafic volcanic rocks of Bastar craton [47,48] and UCC [49] are also shown for comparison. The sandstone samples of Lower Lohardih Formation, Middle Chopardih Formation and Tiratgarh Formation fall near the granite-quartz monzonite field and average composition of granites and gneisses of Bastar craton, while sandstone samples of Upper Kansapathar Formation fall above granite-quartz monzonite field and average compostion of granites, gneisses of Bastar craton (Fig. 7). This may be due to the strong depletion of K_2O in the Upper Kansapathar Formation. The depletion can be attributed to the absence of K-feldspar in this sample, which is consistent with the petrographic data.

The general petrographic and geochemical attributes show similarity between the Lower Lohardih Formation and the Tiratgarh Formation which form the basal part of

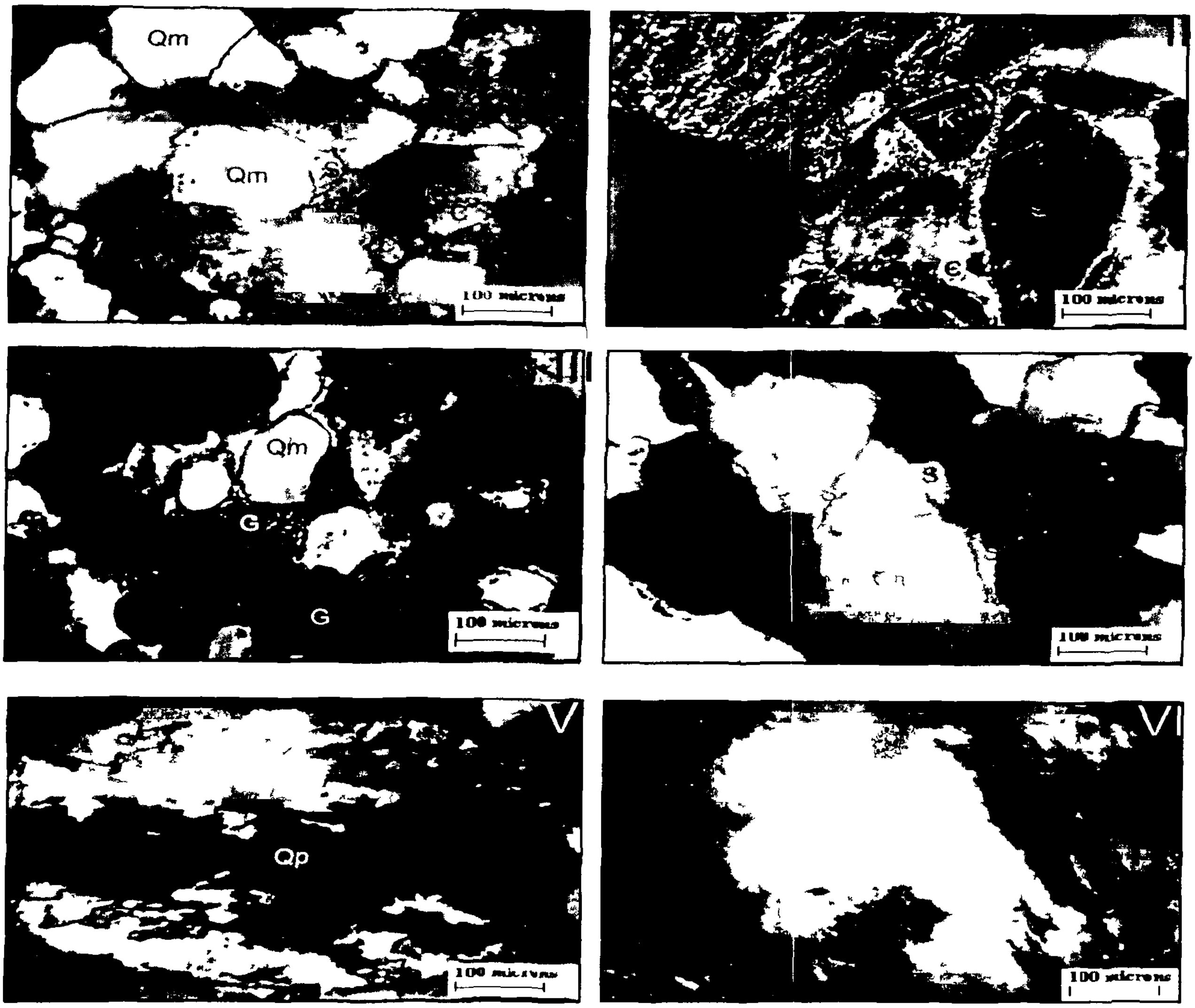

Fig 5 Photomicrographs of sandstones of the Chandarpur Group, Chattisgarh Basin and the Tiratgarh Formation, Indravati basin showing different types of mineral grains present (I) Lower Lohardih Formation showing multicycle quartz grain floating in calcite cement, (II) Lower Lohardih Formation showing microcline replaced by calcite along twinning planes, (III) Middle Chopardih Formation showing multicycle quartz with well rounded glauconite, (IV) Upper Kansapathar Formation showing advance stage of silica overgrowth (V) Tiratgarh Formation showing polycrystalline quartz grain with semicomposite crystals having sutured contacts, (VI) Tiratgarh Formation showing highly stretched polycrystalline quartz grain

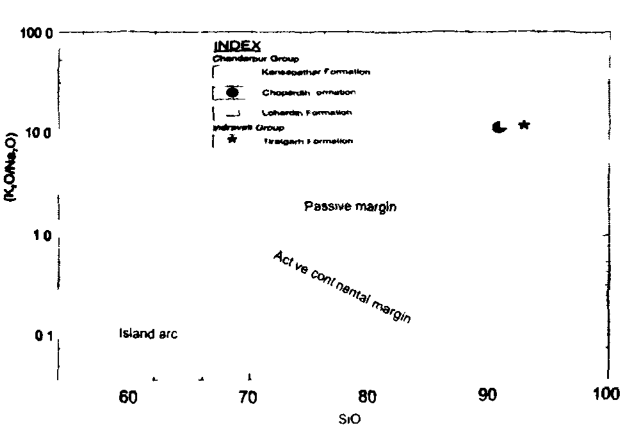

Fig 6 CaO Na_2O K_2O ternary ratio diagram showing the compositional characteristics of sandstones of Chandarpur Group and Tiratgarh Formation Different fields from Arora et al [46] Average data on granite gneiss of Bastar craton from Mondal et al [47] mafic volcanic rocks of Bastar craton from Srivasatava et al [48] and UCC from Taylor and McLennan [49]

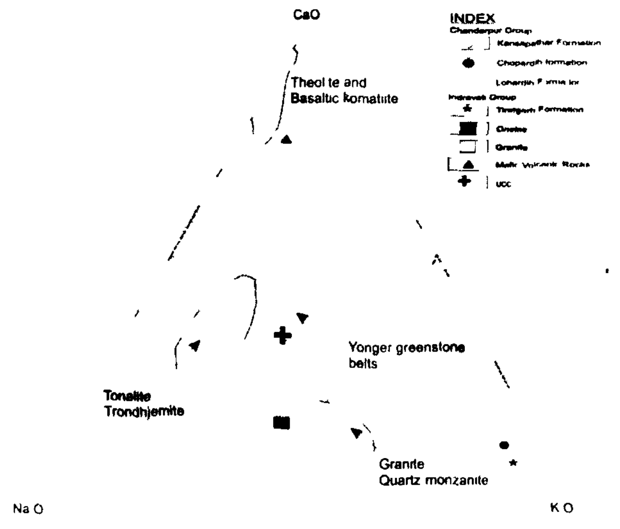

Fig 7 Tectonic discrimination plot of SiO_2 vs K_2O/Na_2O for Chandarpur Group and Tiratgarh Formation Boundary lines from different tectonic setting from Roser and Korch [31]

Table 3: Major element composition of sandstones of Chandarpur Group and Tiratgarh Formation

	Chandarpur Group			Indravati Group
	Lohardih Formation	Chopardih Formation	Kansapathar Formation	Tiratgarh Formation
	RN-438	RN-423	RD-409	JT-547
SiO_2	91.71	91.25	95.11	93.34
Na_2O	0.08	0.07	0.07	0.09
K_2O	1.34	0.86	0.13	1.32
CaO	0.13	0.1	0.11	0.09
K_2O/Na_2O	16.75	12.28	1.85	14.66

the Chandarpur Group and the Indravati Group respectively. These Formations are somewhat feldspathic and comparatively low silica cemented. Most of the samples of Lower Lohardih Formation and Tiratgarh Formation show little compaction and quartz grains are seen floating in the carbonate cement. The decreasing feldspar content at the top of the Chandarpur Group (Kansapathar Formation) is accompanied by corresponding increase in the framework quartz as well as quartz cement. Monocrystalline and polycrystalline varieties exhibit a positive correlation in their concentration. The frequency of feldspar gradually decline while monocrystalline quartz and polycrystalline quartz increases upwards at the top of the Kansapathar Formation and the rock becomes a supermature quartzarenite with high amount of quartz cement up to 2.34%. The occurrence of subarkosic sandstone at the base of the Chandarpur sandstone in the stable cratonic field and decrease of feldspar content suggests peneplanation of stable cratonic provenance, through transition from less mature to mineralogically supermature sandstone.

The little variations in the sandstone mineralogy and geochemistry of the Chandarpur Group and Tiratgarh Formation do not reflect any change in provenance and tectonic setting. The present study suggests that the detritus for Chandarpur and Tiratgarh sandstones were mainly derived from cratonic basement granite/gneiss. Presence of stretched pollycrystalline quartz, microcrystalline chert and multicycle quartz grain floating in calcite cement suggests some minor contribution from preexisting sedimentary and metasedimentary rocks in the source area. The Paleoproterozoic metasedimentary belts such as Sakoli, Sauser, Dongargarh in the northwest of the Chattisgarh basin and Sukma, Bengpal, Bailadila rock belts and Archean greenstone belt in the south of the Bastar craton which were exposed already in Neoproterozoic contain such type of quartz grains and probably might have also shed some detritus to these sandstones. Chert is also present in some metasedimentary belts e.g. Dhabeterki Formation of Sakoli Group [50] which might have contributed some chert to the Chandarpur and Tiratgarh sandstones. The northwesterly paleoslopes of the Chandarpur Group, inferred from the paleocurrent studies [18] indicates that the sediments were mainly derived from the northwest of the Chattisgarh Basin which confirms the above conclusion.

In contrast to certain Paleoproterozoic successions in mobile belts of Bastar craton which show strongly deformed and metamorphosed character, these well developed Neoproterozoic cratonic successions are virtually unmetamorphosed and are mildly deformed. There is a peculiar geographic and structural juxtapositioning of an active mobile belt and Neoproterozoic Basins in the Peninsular India which coexisted adjacently for approximately 1000Ma (~1700Ma- ~700Ma) Kale and Phansalkar [51]. These deformed mobile belts are thrust [52] against or unconformably overlain by these passive un-metamorphosed and sparingly deformed sediments from the Basins of Neoproterozoic age. This represents a significant change in the tectonic styles from active continental margin in the Paleoproterozoic to passive continental margin in the Neoproterozoic.

Conclusion

The siliclastic succession of the Chandarpur Group of the Neoproterozoic Chattisgarh Supergroup starts with the subarkosic Lohardih sandstone and becomes more matured Kansapathar sandstone upwards mineralogically and geochemically. When sandstone composition of the Tiratgarh Formation of the Indravati Group is compared with all the three formations of the Chandarpur Group, the Tiratgarh Formation shows similarity in sandstone composition with the Lower Lohardih Formation. Provenance analysis of the sandstone composition of the Chandarpur Group and the Tiratgarh Formation of the Indravati Group indicate that the sediments were derived from granite/gneisses of continental block (passive) tectonic setting. Dominance of microcline in feldspar population (low average P/K ratio), high SiO_2 and K_2O/Na_2O ratio suggests derivation primarily from a felsic plutonic provenance. $CaO-K_2O-Na_2O$ triangular diagram also suggests derivation from granite gneissic source. The presence of chert and stretched polycrystalline quartz grains in trace amounts in some samples and quartz grains with silica overgrowth floating in calcite cement indicates that the minor part of the detritus has been derived from an older sedimentary succession in the source area. The presence of metamorphic rocks within granite–gneiss provenance (older supracrustal rocks and Achaean Sonakhan greenstone belt) indicates that these older supracrustals might have contributed some detritus to these sandstones. Overall undeformed nature and mineralogically and geochemically highly matured sandstones of the Chandarpur Group and the Tiratgarh Formation may indicate that the Bastar craton might have attained stability during Neoproterozoic. Thus, showing a change in the tectonic style in comparison to Paleoproterozoic to Mesoproterozoic when mobile belts were active.

Acknowledgements

The authors are thankful to the Chairman, Department of Geology, Aligarh Muslim University, Aligarh for providing the facilities to carry out this work and the Principal, Govt. Amarsingh College, Srinagar for encouragement and help during this work. The author Dr H Wani also thankfully acknowledges the Fellowship of CSIR, Govt. of India. Suggestions of an anonymous reviewer greatly helped to improve the manuscript.

References

1. K C Condie *Am J.Sci* **282** (1982) 341
2. S A Drury *Jour Geol Soc India* **25** (1984) 437
3. N S Reddy *Jour Geol Soc India* **32** (1988) 65
4. V Divakara Rao *The Crust, The significance of granites-gneisses in the Lithosphere* Theophrastus Publ S A Athens (1985)147
5. B P Radhakrishna and M Ramakrishnan *J Geol Soc India* **32** (1988) 263
6. G DE V Klein and A T Hsui *Geology* **15** (1987) 1094
7. T H Holland *Imperial Gazetteer of India* Government of India Delhi **1** (1907) 50
8. B P Radhakrishna *Mem Geol Soc India* **6** (1987) 618
9. S M Naqvi and J J W Rogers *Precambrian Geology of India* Oxford University Press New York USA (1987) pp223
10. A K Chaudhuri, D Saha, G K Deb, S P Deb, M K Mukherji and G Ghosh *Gondwana Res* **5** (2002) 23
11. S P Deb and A K Chaudhuri *Sed. Geol* **147** (2002) 105
12. K S Murthi *Purana basins of peninsular India* Mem Geol Soc India Banglore (1987) pp239
13. K S Murthi *Mem Geol Surv India* (1996) 139
14. D P Das, A Kundu, N Das, D R Dutta, K Kumaran, S Ramamurthy, C Thanavelu and V Rajaiya *Indian Min* **46** (1992) 271
15. A K Moitra *Jour Geol Soc India* **46** (1995) 359
16. B Datta *J Geol Soc India* **51** (1998) 345
17. A Gupta *J Ind Assoc Sed* **17** (1998) 213
18. B Datta, S Sarkar, and A K Chaudhuri *Sedimentary Geology* **129** (1999) 51
19. R Jairam and D M Banerjee *Geol Surv India Misc publ* **44** (1978) 57
20. M W Y Khan and A Mukherjee *Indian Jour Earth Sciences* **17** (1990) 44
21. H Crookshank *Mem Geol Surv India* **87** (1963)
22. N V B S Dutt *J Geol Soc India* **4** (1963) 35
23. M Ramakrishnan, S V G Krishna Rao and S M Dutta *Proc Symp on Purana Formations of Peninsula India* Univ of Sauger (1978) 260
24. K S Murthi, R U M Rao and U Aswathanarayana *Precambrian research* **25** (1984) 325
25. M Ramakrishnan *Mem Geol Soc India* **6** (1987) 139
26. W R Dickinson and C A Suczek *Am Ass Petroleum Geol Bull* **63** (1979) 2164
27. W R Dickinson, L S Beard, G R Brakenridge, J L Erjavec, R C Ferguson, K F Inman, R A Knepp, F A Lindbergand and P T Ryberg *Geol Soc Am. Bull* **94** (1983) 222
28. S M McLennan, S Hemming, D K McDaniel and G N Hanson *Geol Soc Am Spl Pap* **284** (1993) 21
29. M R Bhatia *Journal of Geology* **91** (1983) 611
30. M R Bhatia and K A W Crook *Contributions to Mineralogy and Petrology* **92** (1986) 181
31. B P Roser and R J Korsch *Journal of Geology* **94** (1986) 635
32. N Das, D R Dutta and D P Das *Geol Surv Ind Spec Publ* **55** (2001) 237
33. S P Deb *Gondwana Res* **7** (2003) 323
34. H Kreuzer, W Harre, M Kursten, W A Schnitzer, K S Murthi and N K Srivastava *Geol Jb* **28** (1977) 23
35. M R Walter *Stromatolites* Elsevier Amsterdam (1976) pp790
36. Anil Maheshwari, A N Sial, Rajeev Guhey and V P Ferreira *Gondwana Res* **8** (2005) 603
37. P P Chakraborthy, A Sarkar, Bhattacharya and P Sanyal *Earth Planet Sci* Proc Indian Acad Sci **111** (2002) 379
38. R L Folk *Petrology of sedimentary rocks* Hemphill Publishing Co Austin Texas USA (1980) pp182
39. H Blatt *J Sedim Petrol* **37** (1967) 1311
40. F L Pettijohn, P E Potter and R Siever *Sand and Sandstone* 2nd edn New York Springer-Verlag (1987) pp533
41. G De V Klein *Geol Soc Am Bull* **77** (1963) 555
42. W R Dickinson *J Sedimem Petrol* **40** (1970) 695
43. F J Pettijohn, P E Potter and R Siever *Sand and Sandstone* Berlin Springer-Verlag (1972) 618
44. R V Ingersoll *Journal of Geology* **86** (1978) 335
45. M J Johnsson and A Basu *Geological Society of Amarica Special Paper* **285** (1993) 354
46. M Arora, R M K Khan and S M Naqvi *Precambrian Research* **70** (1994) 93
47. M E A Mondal, M F Hussain and T Ahmad *Jour of Geosciences, Osaka City University* **49** (2006) 137
48. R K Srivastava, R K Singh and S P Verma *Precambrian Research* **131** (2004) 305
49. S R Taylor, S M McLennan *The Continental Crust its composition and evolution* Blackwell Press, Oxford (1985) pp312
50. B K Bandyopadhyay, Roy Abhinaba and A Huin *Mem Geol Surv India* **31** (1995) 433
51. V S Kale and V G Phansalkar *Basin Research* **3** (1991) 1
52. K L Kaila, P R Reddy, M M Dixit and P K Rao *Jour Geol Soc India* **26** (1985) 465

Author Acceptance Letter

執筆者承認通知レター

Dear Author,

執筆者の皆様

Thank you for submitting your article to our journal. We are pleased to inform you that your article has been accepted for publication. I would like to take this opportunity to explain our recently launched functions to assist authors with tracking their manuscripts through the production process

この度は弊社ジャーナルへご投稿頂き、誠にありがとうございます。

貴論文が採択されましたことをご報告いたします。

貴論文が出版製作過程に入ってからの状況については、以下に説明いたしますAuthor Serviceサイトを使ってご自身で確認していただくことができます。ぜひご利用ください。

To minimise publication time of your manuscript it is important that all electronic artwork is supplied to the editorial office in the correct format and resolution I recommend that you consult the **Illustration guidelines** at http //www blackwellpublishing com/bauthor/digill asp if you need advice on any aspect of preparing your artwork

貴論文を迅速に出版するためには、全ての図版の電子ファイルを適切な保存形式と解像度にて編集事務局へ提出して頂くことが重要です。図版の準備に関連する詳しい説明は、

http //www blackwellpublishing com/bauthor/digill asp 内のイラストレーションガイドラインをご参照下さい。

Author Services - Production status tracking - You can now track your article via the publisher's Author Services. Once your paper is with the Production Editor, you will receive an e-mail with a unique code that automatically adds your article to the system when you register With Author Services you can check the status of your article online and choose to receive automated e-mails at key stages of production Therefore, please ensure that we have your complete e-mail address There may be a short delay whilst the article is sent to the Production Editor and logged into the production tracking system Additional services will be added to the website soon

Author Services - Production status tracking - 弊社ホームページ上のAuthor Serviceを利用して、貴論文の出版製作状況を確認することができます。採択後の論文が出版製作に入り次第、論文のコレスポンディング著者にEメールでuser name、Passwordなどサイトにアクセスするための情報が送信されます。Author Serviceサイトでは、オンラインにて論文の出版製作状況を確認できるとともに、ご希望により校正やオンライン出版のタイミングなど主要段階での進捗状況を自動送信メールで受信できるよう設定可能です。ご投稿に際しては、連絡可能な最新のメールアドレスをお知らせ下さいますようお願いいたします。なお、貴論文採択後Author Serviceのご連絡をEメールで差し上げるまでに、多少の時間差が生じることがございますので予めご了承下さい。今後も、サイト上に著者に有益な情報や追加サービスが追加されていく予定です。

Proofing your manuscript – *Island Arc* is included in a new electronic service, "e-proofing" You will receive an e-mail from the typesetter when your article is ready for proofing You'll receive instructions about how to download your paper and how to return your corrections Your e-mail address is needed for this vital step, too When you download your paper, you will also be able to download an offprint order form if this available for your article type

Proofing your manuscript – *Island Arc* はE-proofingサイトを利用した校正システムを採用しています。貴論文の校正紙が整った時点で、担当者より校正紙のダウンロード方法と校正手順などをEメールにて送付いたします。ご自身でE-proofingサイトにアクセスして、校正紙やその他の書類をダウンロードし

てください。抜き刷りのご注文についても、校正のときにご案内致します。貴論文採択後に連絡先が変更となった場合には、必ず貴誌プロダクション担当者まで最新のEメールアドレスをお知らせください。

OnlineEarly – *Island Arc* operates a system called OnlineEarly, whereby articles are published online ahead of assignment to an issue and publication in print If your article is eligible for this service you can track the progress of your article and learn when it is published online by registering for Author Services Please note that in order to publish your article as quickly as possible, and if your article is received very close to the copy deadline for an issue, it may be incorporated directly into that issue without first appearing OnlineEarly The Blackwell Synergy Website for journal is http //www blackwell-synergy com/loi/iar If you register in Author Services you will receive free access to your article

OnlineEarly – *Island Arc* は OnlineEarly を採用しており、貴論文は紙面出版に先駆け、著者校正後論文単位でオンライン出版されます。貴論文に OnlineEarly が適用される場合には、Author Service を使って OnlineEarly 適用時の出版時期を確認することも可能です。又、Author Service へのご登録により、オンライン出版された貴論文へ自由にアクセスして頂く事ができます。
但し、出版スケジュールの都合上、当該号の締め切り直前に提出された論文では OnlineEarly が適用されず、当該号の正規スケジュールにて出版される場合がありますのでご了承下さい。
貴誌のオンライン版は、http //www blackwell-synergy com/loi/iar より閲覧いただけます。

Reprints and Offprints - You will receive instructions for ordering offprints when you are notified that your proofs are ready for review
Reprints and Offprints - 別刷り・抜き刷りのご注文については、貴論文校正紙と一緒に案内書を送付いたします。
Production queries – Please note that now your paper has been accepted, all queries related to the production of your paper may be directed to the Production Office at Blackwell [IAR@blackwellpublishing com]

Production queries –ご投稿頂きました貴論文は採択後、出版製作段階に進んでいます。今後の出版製作過程におけるご質問は、出版社のプロダクションオフィス[IAR@blackwellpublishing com] まで直接ご連絡下さい。

Petrochemistry of sandstones from Neoproterozoic basins of the Bastar craton, Central Indian Shield: Implications for paleoweathering, provenance and tectonic history

Journal:	*Island Arc*
Manuscript ID:	IAR-08-0009.R5
Manuscript Type:	Research Article
Date Submitted by the Author:	20-Oct-2008
Complete List of Authors:	Wani, Hamiduulah; AMU Aligarh, Geology; Amarsing College Srinagar, Geology Mondal, M; A M U Aligarh, Geology
Key words:	Bastar craton, Neoproterozoic sandstones, Paleoproterozioc Sakoli schists, Petrochemistry, Weathering, Provenance, Tectonic history

Petrochemistry of sandstones from Neoproterozoic basins of the Bastar craton, Central Indian Shield: Implications for paleoweathering, provenance and tectonic history

H. WANI[1*] AND M. E. A. MONDAL

Department of Geology, AMU, Aligarh-202002, India

[1]Present address: Department of Geology, Amar Singh College, Srinagar-190008, India

[*]Corresponding author (E Mail: hamid79@rediffmail.com)

Abstract: Petrographic analysis, and chemical analysis of major and trace elements including rare earth elements of the Neoproterozoic sandstones from the Chandarpur Group and the Tiratgarh Formation have been carried out to determine their provenance, tectonic setting and weathering conditions. All sandstone samples are highly enriched in quartz but very poor in feldspar and lithic fragments. Petrographically and geochemically these sandstones are classified as subarkose, sublitharenite and arenite. The Chemical Index of Alteration (CIA mean 68) and Th/U ratios (mean 4.2) for these sandstones suggest their moderate weathering nature. Generally, all sandstone samples are strongly depleted in major elements (except SiO_2), trace elements (except Zr) and REE in comparison with PAAS and UCC. Their mineralogy and mean of elemental ratios suitable for determination of provenance and tectonic setting, e.g. Al_2O_3/SiO_2 (0.02), K_2O/Na_2O (10), Eu/Eu* (0.67), (La/Lu)n (10.4), La/Sc (3), Th/Sc (1.2), La/Co (0.22), Th/Co (0.08) and Cr/Th (7.2), support a felsic source and passive margin tectonic setting for these sandstones. Also these key elemental ratios do not show much variation over a range of SiO_2. Thus we attest their significance in determining source rock characteristics of quartz rich sandstones. Chondrite-normalized REE patterns with LREE enrichment and strong negative Eu anomaly are also attributed to felsic source rock characteristics for these sandstones. The source rocks identified are granite and gneiss of the Bastar craton. Minor amounts may have been derived from older supracrustals of the Bastar craton. However, the major element data of the Paleoproterozoic Sakoli schists when compared with those of the Neoproterozoic sandstones indicate that the schists were derived from mafic source and deposited in an active continental margin tectonic setting. There is, however, little difference in CIA values between the Paleoproterozoic Sakoli

schists and Neoproterozoic sandstones, indicating prevailing of similar (moderate-intense) weathering conditions throughout the Proterozoic in the Bastar craton. Our study also suggests a change in provenance and tectonic setting of deposition of sediments from dominantly mafic source and active continental margin in the Paleoproterozoic to dominantly granite and gneiss (felsic source) and passive continental margin in the Neoproterozoic in the Bastar craton.

Keywords: Bastar craton, Neoproterozoic sandstones, Paleoproterozoic Sakoli schists, Petrochemistry, Weathering, Provenance, Tectonic history.

INTRODUCTION

The Indian peninsular shield preserves an extensive record of Proterozoic successions which display extreme heterogeneity in stratigraphy, sedimentation pattern, metamorphism, deformation and magmatism. Radiometric age data from the mobile belt successions indicate that the history of deformed metasedimentary and metavolcanic successions with multiple episodes of deformation, metamorphism and magmatism extends mainly between 2500 - 1500 Ma, though events reflecting crustal perturbations in the Indian peninsular shield extended up to 1000 Ma and even up to Proterozoic – Phanerozoic boundary. Not withstanding the above, there is evidence of development of cratonic basins during the period between 1700 Ma - 700 Ma on different Paleoproterozoic and Archean basements. The dominance of the orthoquartzite - shale - limestone suites indicates their generation on stable continental margins or within intracratonic basins (Condie 1982). The basal groups of these basins can be classified as 'Assemblage II' of Condie (1982). This suggests that the early history of these basins involved lithospheric continental rifting with or without mantle activation. The basic igneous activity within these sequences and the Paleoproterozoic or Mesoproterozoic intrusions in their basements (Drury 1984, Reddy & Ramakrishna 1988) testify to similar thermal activity in the crust associated with the development of these basins Possibly, the Late Archean – Paleoproterozoic granitization event in the Peninsular shield (Rao 1985, Radhakrishna & Ramakrishnan 1988) also has contributed to the generation of these supracrustal intracratonic basins as has been postulated by Klein and Hsui (1987) Therefore, Precambrian supracrustal sequences are important for understanding the origin and evolution of the continental crust Clastic sedimentary rocks are the main sources of information regarding past geological conditions prevailed on the earth's surface They may preserve detritus from the orogenic settings, which may be later obscured by tectonic overprinting or even eroded. In many cases, the clastic rocks provide the big clue of long eroded or obscured source rocks

Sandstone petrography is widely considered to be a powerful tool for determining the origin and tectonic reconstructions of ancient terrigenous deposits (Blatt 1967, Dickinson 1970, Pettijohn *et al* 1972) Mineralogical characterizations of sandstone of the basin fill are critical to any basin analysis and many studies have pointed to an intimate relationship between detrital sand compositions (i e bedrock compositions of sources) and tectonic setting (Ingersoll 1978, Dickinson & Suczek 1979, Dickinson *et al* 1983, Dickinson 1985) Sand composition is also sensitive to a complex set of factors involved in the clastic sediment system (e g climate, relief, transport, diagenesis) which provide valuable information for paleoecological reconstructions (Johnson & Basu 1993)

Geochemistry of clastic sedimentary rocks can best be used to determine the compositions of the provenance (McLennan *et al* 1993), to evaluate weathering processes and paleoclimate (Nesbitt & Young 1982; Fedo *et al.* 1995), to qualify the secondary processes such as hydraulic sorting (McLennan *et al.* 1993), to model the tectonic setting of the basin (Bhatia 1983; Bhatia & Crook 1986; Naqvi *et al.* 1988) and finally to trace the evolutionary history of mantle and crust (Condie 1993).

Several trace elements like Y, Th, Zr, Hf, Nb, Sc and rare earth elements are most suitable for discriminations of provenance and tectonic setting because of their relatively low mobility during sedimentary processes and their short residence times in seawater (Taylor & McLennan 1985). These elements probably are transferred quantitatively into clastic sediments during weathering and transportation, reflecting the signature of the parent materials and hence are expected to be more useful in discriminating tectonic environments and source rock compositions (Bhatia & Crook 1986; McLennan 1989; Condie 1993).

The Bastar craton which is considered to be of Archean age contains granitoids and gneisses. These granitoids and gneisses form the basement for supracrustal rocks. The older (Paleoproterozoic) supracrustals like the Sakoli, Sausar and Dongargarh occur in the northern part of the Bastar craton in the proximity of Central Indian Suture Zone (CITZ) and are highly deformed and metamorphosed. The Sakoli and Sausar sediments show metamorphism of greenschist to lower amphibolite facies (Shastry & Dekate 1984) while the younger (Neoproterozoic) supracrustals like the Chattisgarh and Indravati basins are undeformed and unmetamorphosed. Origin of these Neoproterozoic cratonic basins, however, is still poorly constrained, though a riftogenic origin has been invoked for them (Naqvi & Rogers 1987; Chaudhuri *et al.* 2002). The cylothem at the basal part of the Chattisgarh succession has been attributed to active tectonic episodes and rifting of the cratonic basement (Deb & Chaudhuri 2002)

Extensive work has been carried out on geochemistry of granites and gneisses of the Bastar craton (Mondal *et al* 2006, Hussain *et al* 2004, Sarkar et al 1993) but the geochemistry of overlying supracrustals of the craton has not been given due attention In the present study, petrographic, major elements and trace elements including REE analysis of the sandstones from the Chandarpur Group and the Tiratgarh Formation which form lower parts of the Chattisgarh and Indravati basins respectively (Table1) have been carried out to determine their provenance, tectonic setting and weathering conditions Comparison of our data is made with the available geochemical data of PAAS, UCC (Taylor & McLennan 1985), granite and gneiss of the Bastar craton (Mondal *et al* 2006), Archean mafic volcanics of the Bastar craton (Srivastava *et al* 2004) and the Paleoproterozoic Sakoli schists (Shastry & Dekate 1984) Although the trace and REE data for these Paleoproterozoic Sakoli schists are not available, their available major element data have been compared with these Neoproterozoic sandstones of the Chandarpur Group and the Tiratgarh Formation

GEOLOGICAL SETTING

The Bastar craton lies in the southern corner of the central Indian shield The Bastar craton is bounded on the east by the high-grade Eastern Ghat Mobile belt and Mahanadi and Godavari rifts in the north and south respectively Gneisses and granitoids form the basement for the supracrustal rocks. The older supracrustals consist of (i) the Sakoli Group, (ii) the Dongargarh Supergroup, and (iii) the Sausar Group in the northern part of the craton (Naqvi & Rogers, 1987) and (iv) the Bailadila Group, (v) the Bengpal Group and (vi) the Sukma Group (Crookshank 1963) in the southern part of the craton The Paleoproterozoic Sakoli basin that occurs in the northern part of the Bastar craton (Naqvi & Rogers 1987) in the proximity of the Central Indian Tectonic Zone (CITZ) is highly deformed and metamorphosed The rocks of the Sakoli Group show metamorphism of greenschist - lower amphibolite facies (Shastry & Dekate 1984, Shastry 1976) The Paleoproterozoic Sakoli Group consists of supracrustal sequences and reworked basement of gneissic complex and form an integral part of the central portion of the Central Indian Tectonic Zone The Sakoli Group is composed of supracrustal rocks including mostly metapelite and quartzite with basalt and rhyolite The younger undeformed and unmetamorphosed supracrustals of the Bastar craton occur in two major Neoproterozoic intra-cratonic basins the Chattisgarh basin and the Indravati basin as shown in Fig 1.

CHATTISGARH BASIN

The Chattisgarh basin occurs over an area of 35,000 km^2, this is the third largest Purana basin in the peninsular India The Chattisgarh Supergroup comprises a thick succession of sandstone, shale and limestone (Naqvi & Rogers 1987, Murthi 1987, 1996, Das *et al* 1992; Das *et al.* 2001, Datta 1998) The lower part of the succession is dominated by sandstone (Chandarpur Group), whereas limestone and shale dominate the upper part (Raipur Group).

The Chandarpur Group consists of unmetamorphosed and gently dipping subhorizontal beds of sandstone with conglomerate and shale as subordinate constituents The succession unconformably overlies gneisses, granitoids and the Sonakhan greenstone belt of the Archean basement complex (Table 1) The Chandarpur Group is subdivided into three formations viz. Lohardih, Chaporadih and Kansapathar Formations, arranged in ascending order of superposition (Datta 1998; Murthi 1987). The rocks of the Chandarpur Group were deposited in fan-fan delta, deep water prodelta and storm tide dominated prograding shelf environments (Datta 1998; Deb 2003).

INDRAVATI BASIN

The Indravati Group occupies a vast plateau around Jagdalpur, Bastar district of Chattisgarh. The Indravati basin covers an area of 9000 km^2 in Kanker-Bastar-Dantewara districts of Chattisgarh and Orrisa. The Indravati Group of rocks unconformably overlies the Archean gneissic and granitic rocks. The Indravati Group comprises basal sandstone (Tiratgarh Formation) grading upwards into a conformable sequence of shale with sandstone (Cherakur Formation), horizontally laminated Kanger limestone and purple shales with stromatolitic dolomite (Jagdalpur Formation) in ascending order. The sediments of the Indravati basin are considered to have been deposited in shallow marine, near shore tidal flat or lagoonal environment (Ramakrishnan 1987). The generalized stratigraphic succession for the Indravati Group and the Chattisgarh Supergroup are shown in Table 1.

The Chattisgarh and Indravati basins of the Bastar craton were considered as equivalent to the lower Vindhyans (Dutt 1963; Kruezer *et al.* 1977; Murthi 1987). Later research revealed that the Chitrakot sandstone member (Tiratgarh Formation) of the Indravati basin can be compared with the Chopardih Formation (Chandarpur Group) of the Chattisgarh Supergroup, which gives K-Ar age of 700-750 Ma (Kruezer *et al.* 1977). These age data are also supported by presence of stromatolites in limestones and dolomites of Machkot area, and corresponds to late Riphean age (700-1100 Ma) as suggested by Walter (1976). Recent research revealed that the elevated $\delta^{13}C$ values of the Indravati carbonates and the Chattisgarh carbonates are comparable with the Bander limestone unit of the upper Vindhyan Supergroup (Maheshwari *et al.* 2005; Chakraborthy *et al.* 2002).

METHODOLOGY

A large number of fresh sandstone samples were collected from outcrops and mine exposures in the study area. The samples were washed thoroughly to remove dust contamination. Thin sections were prepared for detailed petrography. Mineralogical composition of the sandstone was determined by the modal analysis with >500 points counted for each thin section. The point counts were done using Gazzi-Dickinson method (Gazzi 1966; Dickinson 1970). The modal analysis data were recalculated on a matrix free basis (Table 2) and was plotted in different ternary diagrams of Dickinson and Suczek (1979). After careful examination under microscope, representative samples of each lithounit of the Chandarpur Group and the Tiratgarh Formation with no or little carbonate minerals have been analyzed for major, trace elements and REE. Major elements were analyzed on WD-XRF (Siemens SRS 3000) at Wadia Institute of Himalayan Geology (WIHG), Dehradun. The precision of XRF major oxide data is better than 1.5 %. Details of the analytic techniques, precision and accuracy of the machine are described by Saini *et al.* (1998). Trace elements and REE were analyzed on ICPMS (Perkin Elmer Sciex ELAN DRC II) at National Geophysical Research Institute (NGRI), Hyderabad. The precision of ICPMS trace elements and REE data is better than 5 %. Details of the analytic techniques, accuracy and precision of the instrument are described by Balram *et al.* (1996).

RESULTS

SANDSTONE PETROLOGY

Modal analysis reveals that the main detrital framework mineral grains of the Chandarpur Group and the Tiratgarh Formation of the Indravati Group include quartz, potash feldspar, plagioclase, rock fragments (mainly chert), mica and heavy minerals. Sandstones of the Chandarpur Group and the Tiratgarh Formation of Indravati Group are characterized by abundant quartz grains (83.15 % and 88.19 % on average, respectively). According to Folk's classification (Folk 1980), the sandstones of the Chandarpur Group and the Tiratgarh Formation are mostly subarkoses, sublitharenites and quartzarenite (Fig. 2). Quartz occurs mainly as monocrystalline quartz. Some of these have undulatory extinction. Polycrystalline quartz represented by recrystallized and stretched metamorphic quartz occurs in subordinate proportions (Table 2). In majority of polycrystalline grains, subgrains with both straight and sutured contacts are common. Feldspar constitutes 1.85 % and 2.02 % on average of the framework grains of the Chandarpur Group and the Tiratgarh Formation respectively, and is dominated by microcline. However, plagioclase (mainly albite) is also present in minor quantities in some samples (Table 2). Rock fragments are very few and are dominated by sedimentary lithics (mainly chert). Heavy minerals are rare and are dominated by zircon. These sandstones are generally matrix free. Authigenic quartz, iron oxide and calcite are dominantly cementing material. Quartz cement occurs primarily as overgrowth around detrital grains.

CHANDARPUR GROUP (CHATTISGARH BASIN)

LOHARDIH FORMATION

Sandstones occupied exclusively by the Lohardih Formation are dominated by quartz (70 % on average). Monocrystalline quartz is a dominant type, averages 67.51 %. Feldspar content of this formation exceeds that of any other unit documented here and the entire feldspar population averages 3.9 % for the sample set. Microcline dominates over plagioclase. The P/K ratio (plagioclase/K-feldspar ratio) averages 0.5. Most of the samples of the Lohardih Formation show little compaction and framework grains are seen floating in carbonate cement (Fig. 3a). Some feldspar grains are replaced by carbonate cement through cracks and cleavages (Fig. 3b). The rock fragments in these sandstones are made up of chert and this stratigraphic unit has the highest representation of chert grains (5.02 % on average).

CHOPARDIH FORMATION

Sandstones of the Chopardih Formation are characterized by high values of quartz (81.39 % on average). Quartz is strongly dominated by monocrystalline quartz, averages 76.59 %. Polycrystalline quartz generally constitutes 4.8 % of quartz grains. Microcline dominates over plagioclase (P/K ratio averages 0.25). Glauconite pellets are very common in the Chopardih Formation (up to 11.28 %). Glauconite pellets commonly occur within interstitial spaces coated with ferrugeneous materials. However, well rounded glauconite pellets are also noticed (Fig. 3c). The cementing material is mostly silica cement (quartz overgrowth).

KANSAPATHAR FORMATION

Sandstones of this stratigraphic unit have the highest representation of quartz grains (average 94.38 %) for the entire basinal infill. The framework grains of sandstones of the Kansapathar Formation are composed dominantly of monocrystalline and polycrystalline quartz with insignificant feldspar and rock fragments including chert which counts 1.2 % on average. Stretched metamorphic quartz is very common among the polycrystalline quartz. The intragranular space is entirely filled by the quartz cement which constitutes about 2.34 % on average. An interlocking quartz mosaic is developed due to silica overgrowth on the grains (Fig. 3d).

INDRAVATI GROUP

TIRATGARH FORMATION

Sandstones of the Tiratgarh Formation of the Indravati Group are also dominated by quartz (88.16 % on average). Monocrystalline is the dominant quartz type (61.89 % on average), however, in two samples polycrystalline quartz dominates (Fig. 3e & 3f). K-feldspar dominates over plagioclase except in one sample (P/K ratio averages 0.37) and the entire feldspar population averages 2.02 % for all samples (Table 2). The sandstones are mainly cemented by carbonate and silica minerals. Some quartz grains are seen floating in carbonate cement. Heavy minerals and opaques are rare and are dominated by zircon and iron oxides respectively. Quartz cement occurs primarily as overgrowth around quartz detrital grains. Rock fragments are rare and are dominated by chert fragments.

The general petrographic attributes show similarity between the Lohardih Formation and the Tiratgarh Formation which form the basal part of the Chandarpur Group and the Indravati Group respectively. These formations are somewhat feldspathic and low quartz cemented. Most of the sandstone samples of the Lohardih and Tiratgarh Formations show little compaction and quartz grains are seen floating in the carbonate cement. The decreasing feldspar content at the top of the Chandarpur Group

(Kansapathar Formation) is accompanied by corresponding increase in the framework quartz as well as quartz cement. Monocrystalline and polycrystalline varieties exhibit a positive correlation in their concentrations. The frequency of feldspar gradually declines while monocrystalline quartz and polycrystalline quartz increase upwards at the top of the Kansapathar Formation and the rock becomes a supermature quartzarenite with high amounts of quartz cement up to 2.34 %

GEOCHEMISTRY

MAJOR ELEMENTS

In general the SiO_2 concentrations are high (avg. 92.96 wt.%) in all sandstones of the Chandarpur Group and the Tiratgarh Formation. Pettijohn *et al.* (1973) employed a diagram to classify terrigenous sands based on of log (Na_2O/K_2O) vs. log (SiO_2/Al_2O_3). According to this classification (Fig. 4) these sandstones are mostly sublitharenite, subarkose and arenite. The petrological and geochemical classification of these sandstones shows very similar features. The Kansapathar Formation has higher SiO_2 and lower TiO_2, CaO, Al_2O_3, MgO, Fe_2O_3, K_2O and Na_2O contents than the Lohardih Formation of the Chandarpur Group and the Tiratgarh Formation of the Indravati Group (Table 3). It is due to the high quartz concentration and absence of both feldspar and rock fragments in the Kansapathar Formation of the Chandarpur Group. As expected from petrography, there is strong negative correlation between SiO_2 and Al_2O_3 (r = -0.93), SiO_2 and K_2O (r = -0.91) and SiO_2 and TiO_2 (r = -0.91). Other major oxides like MnO, MgO, CaO and P_2O_5 do not vary systematically with SiO_2. The depletion of Na_2O (<0.1 %) in all sandstones can be attributed to absence of Na-rich plagioclase in them.

TRACE ELEMENTS

Trace elements like LILE and HFSE are incompatible elements and are thus preferentially partitioned into melts during crystallization (Feng & Kerrich 1990). As a result these elements are enriched in felsic rather than mafic rocks. In the sandstones of the Chandarpur Group and the Tiratgarh Formation, the average contents of LILEs like Rb (~25 ppm), Cs (~1 ppm), Sr (~16 ppm) and HFSEs like Th (~3.1 ppm), U (~0.70 ppm), Nb (~2.2 ppm), Hf (~9.1 ppm) and Y (~4.9 ppm) are strongly depleted in comparison with PAAS and UCC (Taylor & McLennan 1985). However, these sandstones have average value of Zr (~248 ppm) higher than the PAAS and UCC (Table 3). The lower abundances of trace elements may be due to higher quartz concentration and low abundances of feldspar, rock fragments and heavy minerals which are consistent with the petrography (Table 2). Statistically, the Chandarpur Group and the Tiratgarh Formation are indistinguishable in abundance of LILE and HFSE except for the higher Ba, Rb,Y, Zr, Th, U contents of the latter (Table 3). Strong positive correlations exist between K-Rb (r = 0.99) and K-Cs (r = 0.98), indicating that K-feldspar control the abundances of these elements (McLennan *et al.* 1983; Feng & Kerrich 1990).

The average concentrations of compatible elements like Co (~35), Cr (~16), Ni (~11) and Sc (~2.5) are strongly depleted in comparison with PAAS and UCC, but are similar to the granite and gneiss of the Bastar craton. However, the ratios like Ni/Co (~0.32), Sc/Ni (~0.25) and Sc/Cr (~0.16) are similar to PAAS, UCC, and granite and gneiss of the Bastar craton.

RARE EARTH ELEMENTS (REE)

The chondrite normalized patterns of REE for the studied sandstones are shown in Fig. 5. Total REE concentration is variable with the highest mean value in the Tiratgarh

Formation (~76 ppm) and the lowest value in the Kansapathar Formation (~13). All analyzed sandstone samples have REE abundances lower than the PAAS and UCC. The REE patterns, however, are uniform and relatively similar to UCC, PASS, and granite and gneiss of the Bastar craton. The REE patterns of sandstones are highly fractionated with LREE enrichment $(La/Yb)_n$ ~12 and $\sum LREE/\sum HREE$ ~10, flat HREE $(Gd/Yb)_n$ ~1.5 and significant negative Eu-anomalies (average Eu/Eu* ~0.67). There is no systematic difference in REE patterns among formations of the Chandarpur Group and the Tiratgarh Formation.

DISCUSSION

PALEOWEATHERING AND RECYCLING

Nesbitt and Young (1982) defined a chemical index of alteration (CIA) to quantitatively measure the degree of weathering (in molecular proportions): CIA= $[Al_2O_3/(Al_2O_3+CaO^*+Na_2O+K_2O)] \times 100$, where CaO* represents the Ca in the silicate fraction only (Fedo *et al.* 1995). CIA values for average shales range from 70-75 (of a possible 100), which reflects the compositions of muscovites, illites and smectites. Intensely weathered rock yields mineral compositions trending towards kaolinite or gibbsite and a corresponding CIA that approaches 100. The CIA of sandstone samples ranges from 57 for the Lohardih Formation to 69 for the Kansapathar Formation (Table 3). The average CIA value for all sandstones is 67.5 and that of the Sakoli schists is 74.6. Both the values are close to typical shale values (~75) formed by moderate chemical weathering (Taylor & McLennan 1985). This suggests that moderate chemical weathering produced these sandstones and the Sakoli schists. However, the average lower CIA value of the sandstones (67.5) than the Sakoli schists (74.6) probably does not reflect the general weathering conditions in the source region. The lower CIA value of sandstones (67.5) may be due to sedimentary sorting effect. Physical sorting of sediment during transport and deposition leads to concentration of quartz and feldspar with some heavy minerals in the coarser fraction and secondary and more weatherable minerals in the suspended load sediments (Gu *et al.* 2002). This is consistent with petrography that these sandstones are enriched in quartz and depleted in labile minerals. Thus, the CIA values of these sandstones should be less than the schists. Therefore, lower CIA values of sandstones suggest stronger (moderate – intense) weathering conditions in the source area. Furthermore, small difference in CIA values between the Sakoli schists (Paleoproterozoic) and the sandstones (Neoproterozoic) indicates that similar (moderate - intense) weathering conditions prevailed throughout the Proterozoic in the Bastar craton.

The molar ratios of Al_2O_3 - ($CaO+Na_2O$) - K_2O were plotted in triangular A- CN - K diagram to distinguish chemical weathering, K-metasomatism and source rock compositions (Fedo *et al.* 1995, 1996, 1997). Sandstone may have two extreme paths of K-metasomatism (Fedo *et al.* 1995). In one path, the Al rich minerals like kaolinite may be converted to illite so that samples move to K-rich compositions. In second process, plagioclase may be converted to authigenic alkali feldspar to move the compositions of the sandstone to more K - rich compositions. Sandstone samples on A- CN - K plot (Fig. 6) show a lot of scatter. The wide scattering of sandstone samples may be due to dissolution of K-bearing minerals during progressive weathering, which releases K in preference to Al, so the bulk composition trends of the residues are directed towards to the Al_2O_3 apex. The decrease in the abundance of K-feldspar in sandstones from the Lohardih Formation to the Kansapathar Formation in the Chandarpur Group is consistent with petrography of the sandstones that K-feldspar decreases stratigraphically from bottom to top of the Chandarpur Group However, average composition of all sandstone samples plots on granodiorite trend, the average compositions of the Sakoli schists fall in between diorite and granodiorite trends and the average compositions of granites and gneisses of the Bastar craton plot very near to granodiorite field on CN-K line This indicates that the source of these sandstones were granites and gneisses of the Bastar craton, and is consistent with petrographic observations of the sandstones Thus, the overall trend suggests that the Neoproterozoic sandstones could have been derived from granite and gneiss while the Paleoproterozoic Sakoli schists might have been derived from granodiorite - diorite sources.

The Index of Compositional Variability (ICV= Fe_2O_3 + K_2O + Na_2O + CaO + MgO + TiO_2)/(Al_2O_3) is used to assess the original composition of these sandstones and the Sakoli schists (Cox *et al* 1995) The non clayey minerals in the original rocks have higher values of ICV than do the clayey minerals Therefore, sandstones with abundant clay minerals tend to have ICV <1 and form in areas of minimal uplift and are associated with extensive chemical weathering Sands deposited in such areas attain quartzarenite in composition (Cox *et al* 1995) Thus sandstones with ICV >1 are mostly first cycle sediments and those with ICV <1 may be recycled or intensely weathered first cycle sediment (Cox *et al* 1995) The ICV values of the sandstones and the Sakoli schists have been calculated and are shown in Table 3 The sandstones have ICV values with average close to 0 7, while the Sakoli schists average the value close to 0 8 (Table 3) So it is concluded that the sandstones and the Sakoli schists with ICV <1 are mostly recycled sediments or intensely weathered first cycle sediment However, the petrographic features like the presence of chert, stretched polycrystalline quartz grains in trace amounts in some samples and monocrystalline quartz grains with silica overgrowth floating in calcite cement (Fig. 3) favor that the minor part of the detritus has been recycled from an older sedimentary succession in the source area. The northwesterly paleoslopes of the Chandarpur Group, Chattisgarh basin, inferred from paleocurrent studies (Datta *et al.* 1999) indicate that the sediments were mainly derived from the northwest of the Chattisgarh basin. It is here intresting to note that Paleoproterozoic supracrustal rocks like the Sakoli and Sausar Groups lies west of the Chattisgarh basin (Fig. 1) thus gives a broad hint that some sediment may have been recycled during Neoproterozoic from these Paleoproterozoic basins.

Th/U ratios are often used for determining the degree of weathering in ancient sedimentary rocks. The Th/U ratio of sediments and sedimentary rocks is of interest because weathering and recycling are expected to result in oxidation of U^{4+} to the soluble U^{6+} state and its removal subsequently elevating the Th/U ratio (McLennan & Taylor 1980; McLennan *et al.* 1990; McLennan & Taylor 1991). Th/U ratios above 4 are thought to be related to weathering history (McLennan *et al.* 1995). The average Th/U ratio of sandstones (~ 4.2) is suggestive of moderate-intense weathering conditions.

PROVENANCE AND TECTONIC SETTING

To identify the provenance and tectonic setting, the detritus composition was plotted on standard ternary diagrams given by Dickinson & Suczek (1979). In QtFL diagram most of the subarkosic sandstones of the Lohardih Formation and the Chopardih Formation of the Chandarpur Group, and the Tiratgarh Formation of the Indravati Group plot in stable cratonic field. The minerologically mature rocks (arenites) of the Kansapathar Formation of the Chandarpur Group also plot in the stable cratonic field very close to Qt pole i.e. craton interior field (Fig. 7a). In the QmFLt diagram (Fig. 7b), the population suggests craton interior provenance for all the three formations of the Chandarpur Group and the Tiratgarh Formation of the Indravati Group. However, a few samples also plot on or near quartzose recycled orogen. On average, compositions of the Chandarpur Group become more mature in the Kansapathar Formation. The proportion of framework quartz increases through time at the expense of less robust constituents. The chemical data show that SiO_2 increases through time and all major oxides decreases progressively. Correlations between modal abundances and CaO, Na_2O, K_2O indicate that alkalis are mainly controlled by the abundance and composition of feldspars. The sandstones are mature because of their low feldspar and negligible lithic fragment content. This is also manifested by their high SiO_2/Al_2O_3 ratio. The K_2O and Na_2O values and their ratios in the sandstones indicate that K-feldspar dominates over plagioclase feldspar, which is consistent with petrographic data.

The overall petrological evidence indicates their source rocks of the sandstones were granites, gneisses and low-grade metasedimentary rocks, while mineralogical maturity of sandstones suggests tectonic stability of the provenance and some contribution from pre-existing sedimentary rocks. Arora *et al.* (1994) use a triangular diagram of CaO-Mg-Al_2O_3 major element data to derive various provenance fields for Archean conglomerate of the Dharwar craton, India. The sandstone samples of all the three formations of the Chandarpur Group and the Tiratgarh Formation of the Indravati Group on this diagram (Fig. 8) fall near the granite-quartz monzonite field and average composition fields of granites and gneisses of the Bastar craton, while the average of the

Paleoproterozoic Sakoli schists of the Bastar craton fall between tonalite-trondhjemite and younger greenstone belt fields and fall away from granite-quartz monzonite field, and granite and gneiss of the Bastar craton.

Trace element plots using ratios of compatible elements enriched in mafic rocks (e.g. Ti, Cr, Sc, Co) to incompatible elements enriched in felsic rocks (e.g. Zr, La, Y, Th) are more reliable indicators for provenance and tectonic setting discrimination due to their low residence times in seawater and insolubility during weathering and alteration (Roser 2000; Taylor & McLennan 1985; McLennan *et al.* 1990; McLennan & Taylor 1991; Bhatia & Crook 1986). It is evident from the petrography that these sandstones are enriched in quartz and depleted in feldspar, rock fragments and heavy minerals (Table 2). Therefore, these quartz rich sandstones are more depleted in most elemental concentrations than PAAS and UCC, presumably due to removal of labile minerals. Hence, the elemental concentrations of these sandstones should deviate most from the source rock. However, the elemental ratios of some trace elements in these quartzes rich sandstones may be more representative of the source than the elemental concentrations (Cullers 2000; Cullers & Podkovyrov 2002). The extent to which these elemental ratios are preserved in these sandstones, we normalized different elemental ratios of these sandstones e.g. compatible to incompatible $(La/Yb)_n$, ∑LREE/∑HREE, La/Sc, Th/Sc, La/Co, Th/Co), compatible to compatible (Sc/Cr, Sc/Ni, $(Gd/Yb)_n$), incompatible to incompatible (K/Th, Th/U, Zr/Hf, Zr/Th, La/Th) and also Eu anomaly (Eu/Eu*) with those of UCC and PAAS. It is evident from Figure 9a & 9b, that most of the key elemental ratios which are thought to be characteristic for determining provenance are almost similar to those of PAAS and UCC with slight deviation, suggesting that these sandstones were derived from mostly granitoid sources. In figure 9a & 9b, there are some trends that cannot be explained by source rock variation e.g. Zr/Th, La/Co and Th/Co. The enrichment of Zr/Th ratio could be presence of zircon in these sandstones, which is consistent with petrography. However, depletion of La/Co and Th/Co of these sandstones relative to UCC and PAAS is due to enrichment of Co in these sandstones. The enrichment of Co and depletion of all other transition elements like Cr, Sc and Ni in these sandstones does not reflect contribution from any mafic source and imply that the enrichment of Co may have taken place during sedimentary processes. Thus, this study reveals that elemental ratios like Th/Sc, Th/Co, Th/Cr, Ni/Cr La/Sc and La/Co are most suitable for provenance determination as these ratios do not show much variation over a range of SiO_2 in these sandstones (Fig.10a & 10b) Therefore, the study attests the importance of elemental ratios in determining source rock characteristics in quartz rich sandstones, which are strongly depleted in most of the trace elements.

Certain immobile elements in sedimentary systems such as REE, Th, Sc or elemental ratios of these elements have been used to infer source rock compositions as these elements differ in concentration in silicic and basic sources (Cullers *et al.* 2002; Ronov *et al.* 1972; Wronkiewicz & Condie 1990). A good tracer of mafic source components is the compatible element Sc, particularly when compared with Th which is incompatible and thus enriched in felsic rocks. Thus Th/Sc is considered to be the robust provenance indicator (Taylor & McLennan 1985; McLennan *et al.* 1990). In the Chandarpur Group, the Th/Sc ratios increase from 0.69 in the Lohardih Formation to 0.83 in the Kansapathar Formation with an average of 0.75, close to average PAAS values (0.91) and UCC value (0.79) while the average Th/Sc ratio of the Tiratgarh Formation is

2.37, well above the UCC and PAAS values. Thus, Th/Sc ratios for all the sandstones are likely due to influx of highly differentiated source rocks. On Th/Sc - Zr/Sc element ratios diagram (McLennan *et al.* 1993) the data for all the studied formations cluster almost exclusively in the UCC compositional field which indicates homogeneity in the source rock composition (Fig. 11). Other trace element characteristics of sedimentary rocks also place some constraints on the nature of the source. On TiO_2 - Ni diagram (Fig. 12) (Floyd *et al.* 1991) most of the sandstone samples cluster around the average composition of granite and gneiss of the Bastar craton.

All the sandstone samples show Eu/Eu* in a narrow range with an average of 0.67, that is very close to that of PAAS (0.66) and identical to that of the UCC (0.65) and granite of the Bastar craton (0.65). Eu is not fractionated during weathering or digenesis relative to other REE (McLennan 1989). Therefore increasing size of Eu anomaly in those samples reflects input from source rocks with an increasingly large Eu anomaly. There is no systematic difference in REE patterns among different stratigraphic units because of common heavy minerals like zircon and garnet (Taylor & McLennan 1985). The average $(Gd/Yb)_n$ of sandstones is 1.53 and the ratio is close to UCC and PAAS. Therefore, we assume that these sandstones were derived from source rocks similar to UCC. Average ∑HREE (~4.5) of sandstone shows a strong depletion of ∑HREE relative to UCC which may be due to lesser concentration of heavy minerals, especially zircon, which has a high concentration of ∑HREE. Low amounts of heavy minerals are consistent with petrography. All these sandstone samples have $(Gd/Yb)_n$ ratio of 1.53 suggesting that these sediments were derived from sources having somewhat depleted ∑HREE. The general shapes of REE patterns for sandstones are similar to the granite/gneiss of the Bastar craton (Fig. 5). This suggests that sandstones could have been derived by the contributions from nearby gneisses and granites of the Bastar craton. Furthermore, $(Gd/Yb)_n$ and Eu/Eu* ratios of granite and gneiss of the Bastar craton overlap with the respective ratios of sandstone samples again suggesting that granite, gneiss could have been the source rocks for these sandstones.

Roser and Korsch (1986) defined three broad tectonic categories: Passive margin, active continental margin and oceanic island arc on a bivariate K_2O/Na_2O-SiO_2 plot (Fig. 13a). On this diagram all the sandstone samples plot in passive margin while the Paleoproterozoic Sakoli schists plot in active continental margin. Based on the nature of the Archean crust, Bhatia (1983) divided continental margins and oceanic basins into four tectonic settings viz. Oceanic island arc, continental island arc, active continental margin and passive margin. He proposed that most discriminating parameters to decipher different tectonic settings are $Fe_2O_3^*$ + MgO %, TiO_2 %, Al_2O_3/SiO_2, K_2O/Na_2O and $Al_2O_3/CaO+Na_2O$. On the $Fe_2O_3^*$ + MgO % vs. Al_2O_3/SiO_2 and TiO_2 diagrams (Bhatia 1983) (Fig.13b & 13c) all the sandstone samples plot near passive margin, whereas the Paleoproterozoic Sakoli schists fall near continental island arc in Al_2O_3/SiO_2 vs. $Fe_2O_3^*$ + MgO diagram and fall in between continental island arc and oceanic island arc in Al_2O_3/SiO_2 vs.TiO_2 diagram. It is interesting to note that earlier workers like Yedekar *et al.* (1990) has also established forearc to back-arc tectonic setting for the Paleoproterozoic Sakoli schists. Bhatia and Crook (1986) use a triangular diagram of Th - Sc - Zr/10 to derive various tectonic provenances for Paleozoic turbiditic greywackes in Australia. On this diagram they distinguish fields for four environments: oceanic island arc, continental island arc, active continental margin and passive margin. The sandstones from both the Chandarpur Group and the Tiratgarh Formation fall near passive margin on this diagram (Fig. 14).

Among the most sensitive tectonic setting discriminators, values of Zr/Nb, Sc/Ni, ∑LREE/∑HREE, Zr/Th, K/Th, Zr/Hf, La/Th, , Th/Sc, Ti/Zr, La/Sc, Eu/Eu*, La/Yb, (La/Yb)n and (Gd/Yb)n of sandstones of the Chandarpur Group and the Tiratgarh Formation are comparable with sediments from Passive tectonic setting greywacke values of Bhatia and Crook (1986). Thus, it again indicates passive margin tectonic setting for these sandstones.

CONCLUSION

The petrological and geochemical similarities indicate that Neoproterozoic sandstones of the Chandarpur Group and the Tiratgarh Formation have been derived from granites and gneisses of the Bastar craton and minor part may have been derived from older metasedimentary successions of the craton. The results are consistent with petrography. The REE patterns and Eu* anomaly of these sandstones are almost similar to those of granite and gneiss of the Bastar craton. The tectonic discriminant diagrams like $Fe_2O_3^*$ + MgO vs. TiO_2, $Fe_2O_3^*$ + MgO vs. Al_2O_3/SiO_2 and K_2O/Na_2O vs. SiO_2 and Th-Sc-Zr/10 diagram suggest their deposition in passive margin tectonic setting. Major elements and trace elements abundances and elemental ratios critical to provenance (e.g. high SiO_2/Al_2O_3, K_2O/NaO_2, La/Sc, Zr/Sc, Th/Sc, La/Yb, and low Cr/Th and Eu/Eu*) suggest that the source of these sandstones was felsic in nature. Furthermore, these ratios are not variable over a range of SiO_2, thus attest their significance in provenance determination. The nature of the provenance of these quartz rich sandstones is further revealed, when some elemental ratios which are thought to be important in source determination were normalized with PAAS and UCC. These normalized elemental ratios were almost similar to UCC and PAAS thus gives a broad hint of a felsic source similar to PAAS and UCC. TiO_2-Ni relationship also points to the felsic source.

Overall, petrographic and geochemical evidence does not support any change in provenance and tectonic setting in the sandstones of the Chandarpur Group of the Chattisgarh basin and the Tiratgarh Formation of the Indravati basin. Major element data of the Paleoproterozoic Sakoli schists, however, point to their derivation from dominantly mafic sources and an active continental margin setting or forearc to back-arc tectonic setting for their deposition, which is also consistent with earlier studies. Thus, it appears that there was a change in the composition of the provenance of the sedimentary rocks from dominantly mafic in the Paleoproterozoic to dominantly felsic in the Neoproterozoic time in the Bastar craton. The study also reveals that there was a change in the tectonic style during Proterozoic in the Bastar craton from active continental margin tectonic setting in the Paleoproterozoic to passive continental margin tectonic setting in the Neoproterozoic. CIA values of the sandstones and the Sakoli schists indicate prevalence of moderate-intense weathering conditions. Also small difference in CIA values of the Paleoproterozoic Sakoli schists and Neoproterozoic sandstones indicate similar weathering conditions prevailed throughout the Proterozoic in the Bastar craton.

ACKNOWLEDGEMENTS

The authors are thankful to the Chairman Department of Geology, AMU, Aligarh for providing the facilities to carry out this work. HW thanks the Principal, Govt. Amar Singh College, Srinagar for encouragement and help during this work and thankfully acknowledges the Fellowship of CSIR, Govt. of India. We also thank Dr. Maekawa

Hirokazu for editorial handling and two anonymous reviewers for their suggestions and constructive comments on the manuscript.

REFERENCES

ARORA M., KHAN R.M.K. & NAQVI S.M. 1994. Composition of the middle and late Archean upper continental crust as sampled from the Kaldurga Conglomerate, Dharwar craton, India. *Precambrian Research* **70**, 93-112.

BALRAM V., RAMESH S.L. & ANJAIAH K.V. 1996. New trace and REE data in thirteen GSF refrence samples by ICP-MS. *Geostandards News Letter* **20**, 78.

BHATIA M.R. 1983. Plate tectonics and geochemical composition of sandstones. *Journal of Geology* **91**, 611-627.

BHATIA M.R. & CROOK K.A.W. 1986. Trace element characteristics of greywackes and tectonic discrimination of sedimentary basins. *Contributions to Mineralogy and Petrology* **92**, 181-193.

BLATT H. 1967. Provenance determinations and recycling of sediments. *Journal of Sedimentary Petrology* **37**, 1311-1320.

CHAKRABORTHY P.P., SARKAR A., BHATTACHARYA & SANYAL P. 2002. Isotopic and sedimentological clues to productivity change in Late Riphean Sea; A case study from two intracratonic basins of India. *Proceedings of Indian Academy of Science (Earth and planetary sciences)* **111**, No.4, 379-390.

CHAUDHURI A.K., SAHA D., DEB G.K., DEB S.P., MUKHERJI M.K. & GHOSH G. 2002. The purana basins of southern cratonic province of India- a case for Mesoproterozoic fossil rifts. *Gondwana Research* **5**, 23-33.

CONDIE K.C. 1982. Early and Middle Proterozoic supracrustal successions and their tectonic settings. *American Journal of Science* **282**, 341-357.

CONDIE K.C. 1993. Chemical composition and evolution of the upper continental crust; contrasting results from surface samples and shales. *Chemical Geology* **104**, 1-37.

COX R., LOW D.R. & CULLERS R.L. 1995. The influence of sediment recycling and basement composition on evolution of mudrock chemistry in the southwestern United States. *Geochemica et Cosmochemica Acta* **59**, 2919-2940.

CROOKSHANK H. 1963. Geology of southern Bastar and Jeypore from Bailadila range to eastern ghats. *Geological Survey of India, Memoir* **87**.

CULLERS R.L., 2000. The geochemistry of shales, siltstones and sandstones of Pennsylvanian-Permian age, Colorado, USA: implications for provenance and metamorphic studies. *Lithos* **51**, 181-203.

CULLERS R.L. & PODKOVYROV V.N. 2002. The source and origin of terrigenous sedimentary rocks in the Mesoproterozoic Ui group, southeastern Russia. *Precambrian Research* **117**, 157-183.

DAS D.P., KUNDU A. & DAS N. 1992. Lithostratigraphy and sedimentation of Chattisgarh basin. *Indian Minerals* **46**, 271-288.

DAS N., DUTTA D.R. & DAS D.P. 2001. Proterozoic cover sediments of southeastern Chattisgarh state and adjoining part of Orissa. *Geological Survey of India, Special Publication* **55**, 237-262.

DATTA B. 1998. Stratigraphic and sedimentologic evolution of the Proterozoic siliclastics in the southern part of Chattisgarh and Khariar, Central India. *Journal of Geological Society of India* **51**, 345-360.

DATTA B., SARKAR S. & CHAUDRI A. K. 1999. Swaley cross-stratification in medium to coarse sandstone produced by oscillatory and combined flows: examples from the Proterozoic Kansapathar Formation, Chattisgarh basin, M.P. India. *Sedimentary Geology* **129**, 51-70.

DEB S.P. & CHAUDRI A.K. 2002. Stratigraphic architechture of the Proterozoic sucession in the eastern Chattisgarh basin: its tectonic implication. *Sedimentary Geology* **147**, 105-125.

DEB S.P. 2003. Lithostratigraphy of the Neoproterozoic Chattisgarh sequence, its bearing on the tectonics and paleogeography. *Gondwana Research* **7**, 323-337.

DICKINSON W.R. 1970. Interpreting detrital modes of greywacke and arkose. *Journal of sedimentary Petrology* **40**, 695-707.

DICKINSON W.R. & SUCZEK C.A. 1979. Plate tectonics and sandstone compositions. *American Association of Petroleum Geology, Bulletin* **63**, 2164-2182.

DICKINSON W.R. 1985. *Interpreting provenance relations from detrital modes of sandstones*; In: Provenance of Arenites (ed.) G G Zuffa (Dordrecht: D. Reidel publications.co.333-362

DICKINSON W. R., BEARD L. S. & BRAKENRIDGE G .R. *et al* 1983. Provenance of North American Phanerozoic sandstones in relation to tectonic setting. *Geological Society of America Bulletin* **94**, 222-235.

DRURY S.A. 1984. A Proterzoic intracratonic basin, dyke swarms and thermal evolution in south India. *Journal of Geological Society of India* **25**, 437-444.

DUTT N.V.B.S. 1963. Stratigraphy and correlation of the Indravati series (Purana Group) of Bastar District, Madhya Pradesh. *Journal of Geological Society of India* **4**, 35-49.

FEDO C.M., NESBITT H.W. & YOUNG G.M. 1995. Unraveling the effects of potassium metasomatism in sedimentary rocks and paleosols, with implications for weathering conditions and provenance. *Geology* **23**, 921-924.

FEDO C.M., ERIKSSON K.A. & KROGSTAD E.J. 1996. Geochemistry of shales from the Archean (~3Ga) Buhwa Greenstone Belt, Zimbabwe: Implications for provenance and source area weathering. *Geochemica et Cosmochemica Acta* **60**, 1751-1763.

FEDO C.M., YOUNG G.M., & NESBITT H.W. 1997. Paleoclimatic controle on the composition on the Paleoproterozoic Serpent formation, Huronian supergroup, Canada: a greenhouse to icehouse transition. *Precambrian Research* **86**, 211-223.

FENG R. & KERRICH R. 1990. Geochemistry of fine grained clastic sediments in the Archean Abitibi greenstone belt, Canada: Implications for provenance and tectonic setting. *Geochimica et Cosmochimica Acta* **54**, 1061-1081.

FLOYD P.A., WINCHESTER J.A. & PARK R.G. 1989. Geochemistry and tectonic setting of Lewsian clastic metasediments from early Proterozoic Loch Maree Group of Gairloch N.W. Scotland. *Precambrian Research* **45**, 203-214.

FLOYD P.A., LEVERIDGE B.E. & FRANKE W. 1991. Geochemistry and provenance of Rhenohercynian synorogenic sandstones: implications for tectonic environment discrimination, in Morton, A.C., Todd, S.P.., and Haughton, P.D.W., ed. Developments in provenance studies. *Geological Society of London, Special publication* **57**, 173-188.

FOLK R. L. 1980. *Petrology of sedimentary rocks*; Hemphill Publishing Co., Austin, Texas, U.S.A., 182.

GAZZI P. 1966. Le arenarie del flysch sopracretaceo dell' Appennino modenese; correlazioni con il flysch di Monghidoro. *Mineralogica et Petrographica Acta* **12**, 69-97.

. GU X.X., LIU J.M., ZHENG M.H., TANG J.X. & QI L. 2002. Provenance and tectonic setting of the Proterozoic turbidites in Hunan, South China: Geochemical evidence. *Journal of Sedimentary Research* **72**, 393-407.

HUSSAIN M.F., MONDAL M.E.A. & AHMAD T. 2004. Petrological and geochemical characteristics of Archean gneisses and granitoids from Bastar craton- Implication for subduction related magmatism. *Gondwana Research* **7**, 531-537.

INGERSOLL R.V. 1978. Petrofacies and petrologic evolution of late Cretaceous fore-arc basin, northern and central California. *Journal of Geology* **86**, 335-352.

JOHNSSON M.J. & BASU A. 1993. Processes controlling the composition of clastic sediments. *Geological Society of America, Special Paper* **285,** 354.

KLEIN G. DE.V. & HSUI A.T. 1987. Origin of cratonic basins. *Geology* **15**, 1094-1098.

KRUEZER H., HARRE W., KURSTEN M., SCHINITZER W.A., MURTHI K.S. & SRIVASTAVA N.K. 1977. K/Ar dates of two gluconites from the chandarpur series (Chattisgarh/India): on the stratigraphic status of the Late Precambrian Basins in India. *Geological Jharbuch Bulletin* **28**, 23-36.

MAHESHWARI A., SIAL A.N., GUHEY R & FERREIRA V.P. 2005. C-isotope composition of carbonates from Indravati Basin, India: implications for Regional Stratigraphic Correlation. *Gondwana Research* **8**, 603-610.

MCLENNAN S.M. & TAYLOR S.R. 1980. Rare earth element-thorium correlations in sedimentary rocks, and the composition of the continental crust: *Geochimica et Cosmochimica Acta* **44**, 1833-1839.

MCLENNAN S.M., TAYLOR S.R. & ERIKSSON K.A. 1983. Geochemistry of Archean shales from the Pilbara Supergroup, western Australia. *Geochimica et Cosmochimica Acta* **47**, 1211-1222.

MCLENNAN S.M. 1989. Rare earth elements in sedimentary rocks: influence of provenance and sedimentary process. *Reviews in Mineralogy* **21**, 169-200.

MCLENNAN S.M., TAYLOR S.R., MCCULLOCH M.T. & MAYNARD J. B. 1990. Geochemical and Nd-Pb isotopic composition of deep sea turbidites: crustal evolution and plate tectonic associations. *Geochimica et Cosmochimica Acta* **54**, 2015-2050.

MCLENNAN S.M. & TAYLOR S.R. 1991. Sedimentary rocks and crustal evolution: Tectonic setting and secular trends. *Journal of Geology* **99**, 1-21.

MCLENNAN S.M., HEMMING S., MCDANIEL D.K. & HANSON G.N. 1993. Geochemical approaches to sedimentation, provenance and tectonics. *Geological Society of America, Special Paper* **284**, 21-40.

MCLENNAN S.M., HEMMING S., TAYLOR S.R. & ERIKSSON K.A. 1995. Early Proterozoic crustal evolution: Geochemical and Nd-Pb isotopic evidence from metasedimentary rocks, southwestern North America. *Geochimica et Cosmochimica Acta* **59**, 1153-1177.

MONDAL M.E.A., HUSSAIN M.F. & AHMAD T. 2006. Continental growth of Bastar craton, central Indian shield during Precambrian via multiphase subduction and lithospheric extention/rifting: evidence from geochemistry of gneisses, granitoids and mafic dykes. *Journal of Geosciences, Osaka City University* **49**, 137-151.

MURTHI K.S. 1987. Stratigraphy and sedimentation in Chattisgarh Basin; In:Purana basins of peninsular India. *Geological Society of India, Memoir* **6**, 239-260.

MURTHI K.S. 1996. Geology, sedimentation and economic mineral potential of the south – central part of the Chattisgarh Basin. *Geological Survey of India, Memoir* **125**, 139.

NAQVI S.M. & ROGERS J.J.W. 1987. *Precambrian Geology of India*. Oxford University Press, New York, U.S.A., 223.

NAQVI S.M., SAWKAR R.H., RAO S.D.V., GOVIL P.K. & GNANESHWAR R.T. 1988. Geology, geochemistry and tectonic setting of Archean greywackes from Karnatka nucleus, India. *Precambrian Research* **39**, 193-216.

NESBITT H W. & YOUNG G.M. 1982. Early proterozoic cliimates and plate motions inferred from major element chemistry of lutites. *Nature* **54**, 2015-2050

PETTIJOHN F.J., POTTER P.E. & SIEVER R. 1972. *Sand and sandstone*: Berlin, Springer_verlag 618.

PETTIJOHN F.J., POTTER P.E., & SIEVER R. 1973. *Sand and sandstone*: New York, Springer Verlag 618.

RADHAKRISHNA B.P. & RAMAKRISHNAN M. 1988. Archean-Proterozoic Boundary in India. *Journal of Geological Society of India* **32**, 263-278.

RAMAKRISHNAN M. 1987. Stratigraphy, sedimentary environment and evolution of the Late Proterozoic Indravati Basin, Central India. In: Radhakrishna, B.P (Ed.) Purana basins of peninsular India. *Geological Society of India, Memoir* **6**, 139-160.

RAO D.V. 1985. Polyphase granites of the Indian shield and Lithosphere evolution. In: *The Crust; The significance of granites-Gneisses in the Lithosphere*. Theophrastus Publ. S.A., Athens147-168.

REDDY A.G.B. & RAMAKRISHNA T.S. 1988. Subsurface structure of the shield area of Rajasthan-Gujarat as inferred from Gravity. In: Precambrian of the Aravalli Mountain, Rajasthan, India (Ed. by A.B. Roy).*Geological Society of India, Memoir* **7**, 279-284

RONOV A.B., BALASHOV Y.A., GIRINY.P., BRATISHKO R.K. & KAZAKOV G.A. 1972. Trends in rare-earth distribution in the sedimentary shell in the earth's crust. *Geochemistry International* **9**, 987-1016.

ROSER B.P. & KORSCH R.J. 1986. Determination of tectonic setting of sandstone-mudstone suites using SiO_2 content and K_2O/Na_2O ratio. *Journal of Geology* **94**, 635-650.

ROSER B.P. 2000. Whole rock geochemical studies of clastic sedimentary suites. *Geological Society of Japan, Memoirs* **57**, 73-89.

SAINI N.K., MUKHERJEE P.K., RATHI M.S., KHANNA P.P. & PUROHIT K.K. 1998. A new geochemical refrence sample of granite (DG-H) from Dalhousie, Himachal Himalaya. *Journal Geological Society of India* **52**, 603-606.

SARKAR G., CORFU F., PAUL D.K., MCNAUGHTON N.J., GUPTA S.N. & BISHNUI P.K. 1993. Early Archean crust in Bastar craton, Central India- a geochemical and Isotopic study. *Precambrian Research* **62**, 127-137.

SHASTRY B.V. 1976. Petrology and petrochemistry of rocks of south of Wainganga valley in Balaghat district. *Unpublished PhD. Thesis, Nagpur University, India.*

SHASTRY B.V. & DEKATE Y.G. 1984. Petrochemistry of the Sakoli and Sausar metasediments in Southern part of Balaghat district, Madhya Pradesh. *Geological Survey of India, Special publication* **12,** 485-490.

SRIVASTAVA R.K., SINGH R.K. & VERMA S.P. 2004. Neoarchean mafic volcanic rocks from the southern Bastar greenstone belt, Central India: petrological and tectonic significance. *Precambrian Research* **131**, 305-322.

TAYLOR S.R. & MCLENNAN S.M. 1985. *The continental crust. Its composition and evolution*; Oxford, Blackwell 312

YEDEKAR D.B., JAIN S.C., NAIR K.K.K & DUTTA K.K.1990. The Central Indian Collision Suture. *Geological Survey of India, Special Publication* **28**, 1-43.

WALTER M.R. 1976. *Stromatolites*. Developments in sedimentology. Elsevier, Amsterdam **20**, 790

WRONKIEWICZ D.J. & CONDIE K.C. 1990. Geochemistry and mineralogy of sediments from the Ventersdorp and Transvaal Supergroups, South Africa: cratonic evolution during the early Proterozoic. *Geochimica et Cosmochimica Acta* **54,** 343-354.

List of Figures and Tables

Fig. 1 Geological map of (a) the Chattisgarh basin and (b) the Indravati basin showing the locations of the areas from which samples have been taken. Inset: (c) Geological map of the Bastar craton showing Paleoproterozoic and Neoproterozoic sedimentary basins. Numbers indicate sample locations.

Fig. 2 QFL plots of the classification of sandstone samples from the Chandarpur Group, Chattisgarh basin, and the Tiratgarh Formation, Indravati basin (classification after Folk 1980).

Fig. 3 Photomicrographs of sandstones of the Chandarpur Group, Chattisgarh basin, and the Tiratgarh Formation, Indravati basin, showing different types of mineral grains present. Qm-monocrystalline quartz, Qp-pollycrystalline quartz, K- K-feldspar, G-glauconite, S-silica overgrowth, C-calcite cement. (a) Lohardih Formation showing multicycle quartz grain floating in calcite cement (b) Lohardih Formation showing microcline replaced by calcite along twinning planes (c) Chopardih Formation showing multicycle quartz with well rounded glauconite, (d) Kansapathar Formation showing advance stage of silica overgrowth (e) Tiratgarh Formation showing polycrystalline quartz grain with semicomposite crystals having sutured contacts (f) Tiratgarh Formation showing highly stretched polycrystalline quartz grain.

Fig. 4 Geochemical classification of sandstones of the Chandarpur Group and the Tiratgarh Formation using Log (Na_2O/K_2O) vs. Log (SiO_2/Al_2O_3) (after Pettijohn *et al.* 1973). The sandstones fall into sublitharenite, subarkose and arenite fields.

Fig. 5 Chondrite - normalized REE patterns for the sandstone samples of the Chandarpur Group and the Tiratgarh Formation, compared with granite and gneiss of the Bastar craton (Mondal *et al.* 2006), PAAS and UCC (Taylor & McLennan 1985). Note that the REE patterns of sandstones are similar to the UCC, PAAS, and granite and gneiss of the Bastar craton.

Fig. 6 Al_2O_3 - (CaO^* + Na_2O) - K_2O (A - CN - K) ternary plot, after Nesbitt and Young (1982) (CaO^* = CaO in silicate phase) showing sandstones of the Chandarpur Group and the Tiratgarh Formation. The diagram also shows average compositions of different rock types of the Bastar craton: Sakoli schists from Shastry and Dekate (1984); granite and gneiss of the Bastar craton from Mondal *et al.* (2006), mafic volcanic rocks of the Bastar craton from Srivasatava *et al.* (2004). Numbers 1-5 denote compositional trends of initial weathering profiles of different rocks. 1-gabbro; 2-tonalite; 3-diorite; 4-granodiorite; 5-granite.

Fig. 7 Provenance discriminant diagrams after Dickinson and Suczek (1979) of sandstone samples of the Chandarpur Group, Chattisgarh basin and the Tiratgarh Formation, Indravati basin of the Bastar craton.

Fig. 8 CaO - MgO - Al_2O_3 ternary ratio diagram showing the compositional characteristics of sandstones of the Chandarpur Group and the Tiratgarh Formation. Different fields from Arora *et al.* (1994). Note that all the sandstone samples plot near granite quartz-mozanite field, and granite and gneiss of the Bastar craton, while average of the Sakoli schists plot near tonalite trondhjemite field. Data for the Sakoli schists from Shastry and Dekate (1984); granite and gneiss of the Bastar craton from Mondal *et al.* (2006); mafic volcanic rocks of the Bastar craton from Srivasatava *et al.* (2004).

Fig. 9a & b The elemental ratios of the sandstones of the Chandarpur Group and the Tiratgarh Formation are compared with those of the UCC and PAAS. Note that most of the elemental ratios of sandstones are similar to PAAS and UCC.

Fig. 10a & b Plots of SiO_2 vs. different important elemental ratios for sandstones of the Chandarpur Group and the Tiratgarh Formation. Note that most of the elemental ratios show almost flat trend with increase of SiO_2 content.

Fig. 11 Th/Sc - Zr/SC plot (McLennan *et al.* 1993) for the sandstones of the Chandarpur Group and the Tiratgarh Formation. Note that all the sandstone samples cluster around upper continental crust (UCC).

Fig. 12 TiO_2 - Ni plot for the discrimination of source rocks of the sandstones of the Chandarpur Group and the Tiratgarh Formation. The samples reflect a derivation from predominantly acidic precursors of magmatic origin and also fall very near to granite and gneiss of the Bastar craton. Data for granite and gneiss from Mondal *et al.* (2006). Acidic and basic fields and trends from common mature recycled sediments from Floyd *et al.* (1989).

Fig. 13 Tectonic setting discrimination diagrams for the sandstones of the Chandarpur Group and the Tiratgarh Formation. Data for the Sakoli schists (after Shastry & Dekate 1984) have also been shown for comparison. The tectonic settings are named in each plot. (a) SiO_2 vs. K_2O/Na_2O (after Roser & Korsch 1986); (b) $Fe_2O_3^*$+ MgO vs. Al_2O_3/SiO_2 (after Bhatia 1983); and (c) $Fe_2O_3^*$+ MgO vs.TiO_2 (after Bhatia 1983). ($Fe_2O_3^*$= total iron).

Fig. 14 Th - Sc - Zr/10 plot for the sandstones of the Chandarpur Group and the Tiratgarh Formation for tectonic setting discrimination (Bhatia & Crook 1986). Note that all the sandstone samples plot near passive margin tectonic setting.

Table 1 Lithostratigraphy of the Indravati and Chattisgarh basins (after Ramakrishnan 1987 & Murthi 1987).

Table 2 Modal analysis of sandstones of the Chandarpur Group, Chattisgarh basin and the Tiratgarh Formation of the Indravati basin.

Table 3 Whole rock geochemical analysis of Neoproterozoic sandstones of the Chandarpur Group and the Tiratgarh Formation and their comparison with different rock types of the Bastar craton.

Table 1 Lithostratigraphy of the Indravati and Chattisgarh basins (after Ramakrishnan 1987 & Murthi 1987).

Indravati Basin		**Chattisgarh Basin** (Chattisgarh Supergroup)	
		Raipur Group (Thickness 1770m)	
		...............?....................................	
Indravati Group		**Chandrapur Group**	
Jagdalpur Formation (Thickness 200-250m)	Calcareous shales with purple and gray stromatolitic dolomite	Kansapathar Formation (Thickness 125m)	White sandstone
Kanger Limestone (Thickness 150-200m)	Purple limestone Grey limestone	Chopardih Formation (Thickness 15m)	Reddish brown and olive green sandstone
Cherakur Formation (Thickness 50-60m)	Purple shale with arkosic sandstone and chert pebble conglomerate grit	Lohardih Formation (Thickness 240m)	White pebbly sandstone
Tiratgarh Formation (Thickness 50-60m)	Chitrakot sandstone member (quartz arenite) Mendri sandstone member (subarkose and conglomerate)		

---------------------- Unconformity ----------------------

Archean granites, gneisses and older supracrustals (Sakoli, Sausar, Dongargarh, Sukma, Bengpal, and Bailadila Groups of rocks and Archean Sonakhan greenstone belt)

Table 2 Modal analysıs of sandstones of the Chandarpur Group, Chattısgarh basın and the Tıratgarh Formatıon of the Indravatı basın

Sample NO	Qm%	Qp%	Kfs %	Pl %	Ft %	Chert %	Glt %	Qtz cement %	Cal cement %	Iron cement %	Rf %	Others %	Total %
Chandarpur Group													
Lohardıh Formatıon													
RD-406	76 33	5 12	6 18	3 18	9 36	0 00	0 00	0 55	6 53	0 70	1 23	0 18	100
RD-420	37 46	0 65	0 65	1 60	2 25	9 65	0 00	0 16	33 44	16 07	0 00	0 32	100
RD-421	57 64	1 05	1 91	0 52	2 43	4 68	0 00	0 52	33 15	0 35	0 00	0 18	100
RN-438	79 37	3 37	2 52	1 05	3 57	6 53	0 00	5 06	0 00	1 05	0 00	1 05	100
RD-509	85 90	4 51	0 37	0 00	0 37	6 02	0 00	2 07	0 00	0 94	0 00	0 19	100
RD-523	68 36	5 68	3 84	1 38	5 22	3 32	0 00	0 00	15 55	0 30	0 77	0 80	100
Average	67 51	3 40	2 60	1 30	3 90	5 02	0 00	1 39	14 80	3 20	0 33	0 45	100
Average plagıoclase/k-feldspar ratıo (P/K ratıo) of Lohardıh Formatıon ıs 0 5													
Chopardıh Formatıon													
RD-404	80 47	9 19	1 34	0 00	1 34	2 00	3 01	0 66	0 00	0 83	1 83	0 67	100
RN-423	67 26	4 19	0 00	0 00	0 00	3 07	21 77	2 09	0 00	1 45	0 00	0 17	100
RN-425	82 01	1 00	2 02	0 86	2 88	2 44	9 06	1 73	0 00	0 59	0 00	0 29	100
Average	76 59	4 80	1 12	0 29	1 40	2 50	11 28	1 49	0 00	0 95	0 61	0 37	100
Average plagıoclase/K-feldspar ratıo (P/K ratıo) of Chopardıh Formatıon ıs 0 25													
Kansapathar Formatıon													
RD-405	87 28	6 66	0 00	0 00	0 00	2 37	0 00	2 52	0 00	0 29	0 00	0 88	100
RD-408	86 76	3 63	0 90	0 55	1 45	0 72	0 00	1 99	0 00	5 27	0 00	0 18	100
RD-409	91 54	4 94	0 00	0 00	0 00	0 58	0 00	2 12	0 00	0 23	0 36	0 23	100
RD-410	80 00	16 50	0 00	0 00	0 00	2 17	0 00	0 49	0 00	0 24	0 24	0 36	100
RN-424	88 89	5 48	0 81	0 00	0 81	0 16	0 00	4 02	0 00	0 32	0 00	0 32	100
RD-510	85 33	7 81	0 00	0 00	0 00	2 43	0 00	1 14	0 00	0 72	2 28	0 29	100
RD-520	93 79	1 77	0 00	0 00	0 00	0 00	0 00	4 14	0 00	0 15	0 00	0 15	100
Average	87 70	6 68	0 23	0 07	0 32	1 20	0 00	2 34	0 00	1 03	0 41	0 34	100
Average plagıoclase/k-feldspar ratıo (P/K ratıo) of Kansapathar Formatıon ıs 0 31													
Average of all the three Formatıon of Chandarpur Group													
	78 02	5 15	1 28	0 57	1 85	2 87	2 11	1 82	5 55	1 84	0 41	0 38	100
Average plagıoclase/k-feldspar ratıo (P/K ratıo) of all the three Formatıons of Chandarpur Group ıs 0 44													
Indravati Group													
Tıratgarh Formatıon													
JC-541	3 28	85 80	5 47	1 09	6 56	0 00	0 00	0 00	3 83	0 18	0 00	0 35	100
JC-542	79 83	1 80	0 36	1 26	1 62	3 61	0 00	0 36	10 61	0 90	0 54	0 73	100
JC-543	89 79	5 83	0 00	0 00	0 00	0 00	0 00	0 36	3 05	0 36	0 48	0 13	100
JT-547	50 42	32 10	1 53	0 41	1 94	2 08	0 00	0 00	10 42	1 12	1 38	0 54	100
JT-548	86 14	5 82	0 00	0 00	0 00	5 54	0 00	1 25	0 00	0 69	0 28	0 28	100
Average	61 89	26 27	1 47	0 55	2 02	2 24	0 00	0 39	5 60	0 65	0 54	0 40	100
Average plagıoclase/k-feldspar ratıo (P/K ratıo) of Tıratgarh Formatıon ıs 0 37													

Qm, monocrystallıne quartz, Qp,Polycrystallıne quartz, Kfs, K-feldspar, Pl, plagıoclase, Ft total feldspar Glt, glauconıte, Cal calcıte Rf rock fragment others, ınclude mıca and heavy mınerals

Table 3 Whole rock geochemical analysis of Neoproterozoic sandstones of the Chandarpur Group and the Tiratgarh Formation and their comparison with different rock types of the Bastar craton

	Chandarpur Group					Indravati Group					Different types of Bastar rocks			
	LF	CF	KF			TF		Average			Sakoli	Bastar	Bastar	Bastar
	RN438	RN423	RD405	RD409	RD520	JC-542	JT547	sandstone	PAAS	UCC	schist	Granite	Gneiss	volcanics
Major elements (wt%)														
SiO_2	91 71	91 25	94 64	95 11	95 64	89 05	93 34	92 96	62 80	66 00	68 02	71 47	71 23	50 59
TiO_2	0 09	0 09	0 05	0 04	0 04	0 21	0 07	0 08	1 00	0 50	0 76	0 22	0 26	1 25
Al_2O_3	2 43	3 02	1 88	1 72	0 59	5 46	2 46	2 50	18 90	15 20	14 04	14 25	14 25	11 91
$Fe_2O_3^*$	0 48	1 69	0 12	0 10	0 20	0 58	0 16	0 47	6 30	5 00	5 52	2 35	2 46	14 78
MnO	0 02	0 02	0 02	0 02	0 02	0 02	0 02	0 02	0 11	0 08	0 10	0 03	0 03	0 55
MgO	0 23	0 34	0 16	0 18	0 12	0 22	0 13	0 19	2 20	2 02	2 08	0 49	0 55	7 28
CaO	0 13	0 10	0 18	0 11	0 09	0 13	0 09	0 11	1 30	4 20	0 70	1 52	1 99	9 42
Na_2O	0 08	0 07	0 06	0 07	0 06	0 12	0 09	0 07	1 20	3 90	0 92	4 11	3 62	1 89
K_2O	1 34	0 86	0 24	0 13	0 00	2 38	1 32	0 89	3 70	3 40	1 82	3 61	4 28	1 04
P_2O_5	0 05	0 02	0 02	0 02	0 02	0 02	0 03	0 02	0 16		0 07	0 04	0 08	0 23
Sum	96 56	97 46	97 37	97 50	96 78	98 19	97 71	97 36	97 67	–	94 03	98 13	98 78	98 98
CIA	57 19	71 09	73 27	79 04	69 22	64 46	58 56	67 54	69 37	–	74 60			
ICV	0 97	1 04	0 44	0 37	0 89	0 67	0 76	0 73	–		0 84			
K_2O/Na_2O	16 75	12 28	4 00	1 85	0 00	19 83	14 66	9 91	3 08	–	1 97		–	
Al_2O_3/SiO_2	0 02	0 03	0 02	0 01	0 01	0 06	0 02	0 02	0 30	–	0 20	–	–	
Trace and REE (ppm)														
Sc	2 76	2 93	2 42	2 38	1 25	3 30	2 26	2 47	16 00	11 00	NA	6 14	4 27	NA
V	20 53	20 70	17 77	17 89	6 06	14 15	7 80	14 98	150 00	60 00	NA	25 00	13 87	220 83
Cr	13 21	13 30	10 17	13 32	18 52	31 07	14 48	16 30	110 00	35 00	NA	283 95	273 20	647 52
Co	41 36	22 85	32 90	34 41	32 67	43 35	36 22	34 82	23 00	10 00	NA	32 53	33 47	NA
Ni	15 12	12 27	12 86	15 97	3 85	10 62	6 13	10 98	55 00	20 00	NA	18 99	11 86	196 82
Cu	5 78	6 75	6 11	6 91	5 75	20 77	9 16	8 75	50 00	25 00	NA	10 64	18 02	NA
Rb	34 99	23 19	7 62	3 93	1 23	66 10	37 86	24 99	160 00	112 00	NA	165 13	144 66	26 23
Sr	34 97	15 21	9 34	9 25	11 07	21 27	13 22	16 33	200 00	350 00	NA	278 76	226 62	131 08
Y	2 97	2 67	2 28	1 71	2 40	16 40	6 15	4 94	27 00	22 00	NA	29 75	22 20	16 50
Zr	65 22	76 35	72 87	71 95	57 34	1243 24	154 76	248 80	210 00	190 00	NA	273 53	221 47	66 04
Nb	2 29	1 76	1 43	1 12	1 25	5 81	2 32	2 28	19 00	25 00	NA	16 16	16 79	3 64
Cs	1 21	1 24	0 19	0 10	0 13	2 65	1 42	0 99	NA	3 70	NA	NA	NA	NA
Ba	193 65	57 29	123 20	82 72	16 98	324 92	139 99	134 10	650 00	550 00	NA	827 92	690 42	124 62
La	8 69	9 46	3 44	2 97	4 18	16 92	9 24	7 84	38 00	30 00	NA	56 87	29 70	9 23
Ce	16 96	17 87	6 28	5 35	7 04	30 70	18 05	14 61	80 00	64 00	NA	133 94	61 26	18 57
Pr	1 74	1 77	0 75	0 62	0 77	3 44	2 18	1 61	9 00	7 10	NA	17 78	7 40	2 06
Nd	6 70	6 69	2 72	2 22	2 28	12 24	8 01	5 84	34 00	26 00	NA	55 95	22 52	8 50
Sm	1 00	0 98	0 56	0 47	0 33	2 27	1 64	1 03	5 55	4 50	NA	9 23	4 28	2 03
Eu	0 22	0 16	0 13	0 11	0 07	0 43	0 29	0 20	1 08	0 90	NA	1 04	0 80	0 65
Gd	0 83	0 84	0 46	0 37	0 39	2 17	1 32	0 91	4 66	3 80	NA	7 07	3 31	2 43
Tb	0 12	0 11	0 08	0 06	0 07	0 43	0 22	0 16	0 77	0 64	NA	1 28	0 56	0 50
Dy	0 56	0 58	0 39	0 31	0 38	2 73	1 18	0 87	4 68	3 50	NA	6 46	2 62	2 79
Ho	0 10	0 09	0 07	0 05	0 08	0 57	0 22	0 17	0 99	0 80	NA	1 20	0 45	0 62
Er	0 28	0 30	0 23	0 16	0 24	1 70	0 62	0 50	2 85	2 30	NA	3 94	1 40	1 83
Tm	0 04	0 05	0 04	0 03	0 04	0 32	0 11	0 09	0 41	0 33	NA	0 63	0 22	0 32
Yb	0 33	0 32	0 28	0 19	0 26	1 98	0 65	0 57	2 82	2 20	NA	4 33	1 53	1 83
Lu	0 04	0 04	0 03	0 02	0 04	0 32	0 10	0 09	0 43	0 30	NA	0 68	0 26	0 28
Hf	1 99	2 17	2 33	2 21	7 43	36 26	11 93	9 19	5 00	5 80	NA	NA	NA	1 80
Ta	1 76	1 26	1 89	1 68	1 60	3 12	3 40	2 10	1 50	2 20	NA	NA	NA	0 30
Th	1 92	2 13	1 97	1 57	1 05	9 34	4 33	3 19	14 60	10 70	NA	34 76	37 58	3 53
U	0 36	0 45	0 43	0 54	0 40	1 85	0 85	0 70	3 10	2 80	NA	6 70	7 17	0 61

Table 3 (*Continued*)

∑REE	37 67	39 31	15 52	13 00	16 22	76 28	43 90	34 56	185 00	146 37	NA	300 47	136 37	51 69
Eu/Eu*	0 74	0 55	0 79	0 80	0 60	0 59	0 61	0 67	0 66	0 65	NA	0 39	0 65	0 89
La/Yb	26 36	28 75	12 17	15 41	15 84	8 54	14 13	17 31	13 50	13 63	NA	13 12	19 38	5 02
(La/Yb)n	17 81	19 43	8 22	10 41	10 70	5 77	9 55	11 70	9 20	9 20	NA	8 87	13 09	3 39
(Gd/Yb)n	2 04	2 06	1 32	1 58	1 21	0 89	1 63	1 53	1 36	1 40	NA	1 32	1 75	1 07
∑LREE/∑HREE	15 05	15 51	8 46	9 47	9 49	6 39	8 78	10 45	9 45	9 47	NA	10 67	12 06	3 80
K/Th	5784 36	3346 86	1008 70	686 90	0 00	2113 90	2525 30	2209 00	2103 00	2607 00	NA	1022 97	797 79	2463 30
TH/U	5 23	4 66	4 53	2 88	2 63	5 02	5 08	4 29	4 70	3 80	NA	5 18	5 23	5 73
Zr/Hf	32 66	35 15	31 15	32 52	7 71	34 28	12 96	26 63	42 00	32 76	NA	NA	NA	36 68
Zr/Th	33 91	35 79	36 86	45 80	54 30	133 02	35 66	53 62	14 40	17 76	NA	7 86	5 89	18 68
La/Th	4 52	4 43	1 74	1 89	3 96	1 81	2 13	2 92	2 60	2 80	NA	1 63	0 79	2 61
La/Sc	3 15	3 21	1 42	1 24	3 32	5 11	4 08	3 08	2 38	2 73	NA	9 25	6 95	NA
Th/SC	0 69	0 72	0 81	0 65	0 83	2 82	1 91	1 21	0 91	0 97	NA	5 65	8 80	NA
Sc/Nı	0 18	0 23	0 18	0 14	0 32	0 31	0 36	0 25	0 29	0 55	NA	0 32	0 36	NA
Sc/Cr	0 20	0 22	0 23	0 17	0 06	0 10	0 15	0 16	0 14	0 31	NA	0 02	0 01	NA
Nı/Co	0 36	0 53	0 39	0 46	0 11	0 24	0 16	0 32	2 39	2 00	NA	0 58	0 35	NA
La/Co	0 21	0 41	0 10	0 08	0 12	0 39	0 25	0 22	1 65	3 00	NA	1 74	0 88	NA
Th/Co	0 04	0 09	0 06	0 04	0 03	0 21	0 11	0 08	0 63	1 07	NA	1 06	1 12	NA
Cr/Th	6 87	6 23	5 14	8 47	17 54	3 32	3 33	7 27	7 53	3 27	NA	8 16	7 26	183 16
Zr/Sc	23 62	25 98	30 07	30 22	45 58	375 83	68 32	85 66	1 68	17 27	NA	44 52	51 86	NA

Fe_2O_3*, total ıron, NA, not avaıluable, LF, Lohardıh Formatıon, CF,Chopardıh Formatıon, KF, Kansapathar Formatıon, TF, Tıratgarh Formatıon, Chondrıte normalızıng factors from Taylor and McLennan (1985), Data for granıte and gneıss from Mondal *et al* (2006), Sakolı schısts from Shastry and Dekate (1984), mafıc volcanıc rocks from Srıvastava *et al* (2004)

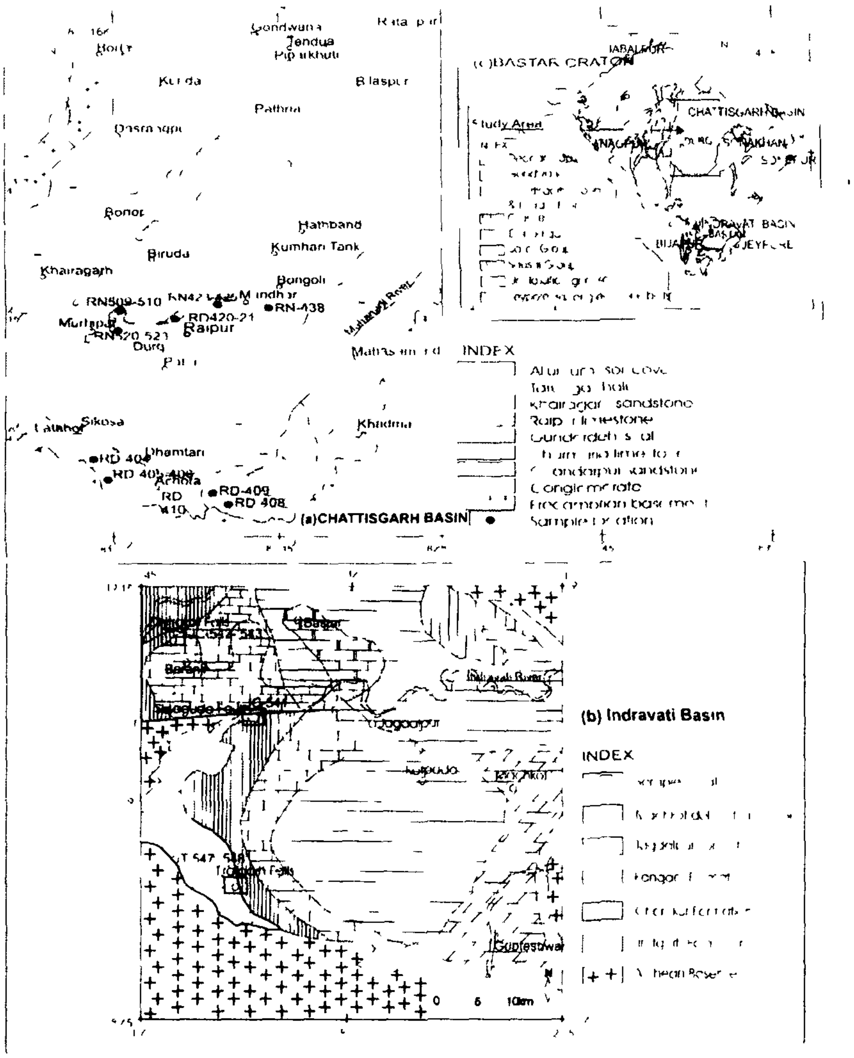

Fig 1 Geological map of (a) the Chattisgarh basin and (b) the Indravati basin showing the locations of the areas from which samples have been taken Inset (c) Geological map of the Bastar craton showing Paleoproterozoic and Neoproterozoic sedimentary basins Numbers indicate sample locations

Fig.1 Geological map of (a) the Chattisgarh basin and (b) the Indravati basin showing the locations of the areas from which samples have been taken. Inset: (c) Geological map of the Bastar craton showing Paleoproterozoic and Neoproterozoic sedimentary basins. Numbers indicate sample locations

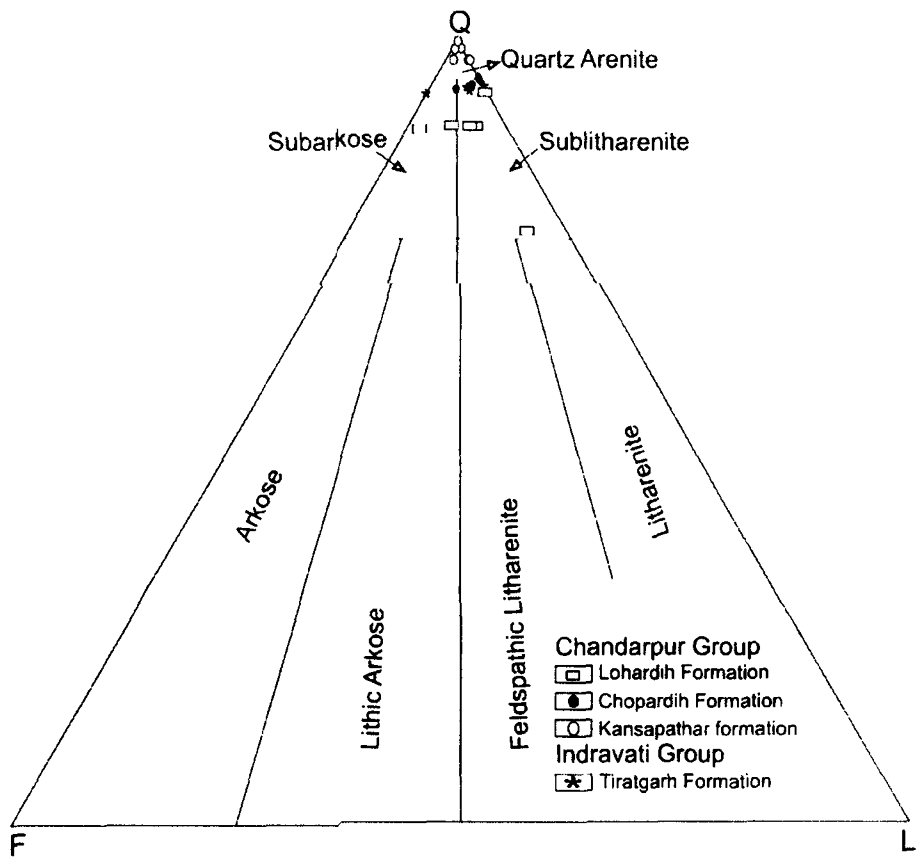

Fig. 2 QFL plots of the classification of sandstone samples from the Chandarpur Group, Chattisgarh basin, and the Tiratgarh Formation, Indravati basin (classification after Folk 1980).

Fig.2 QFL plots of the classification of sandstone samples from the Chandarpur Group, Chattisgarh basin, and the Tiratgarh Formation, Indravati basin (classification after Folk 1980).

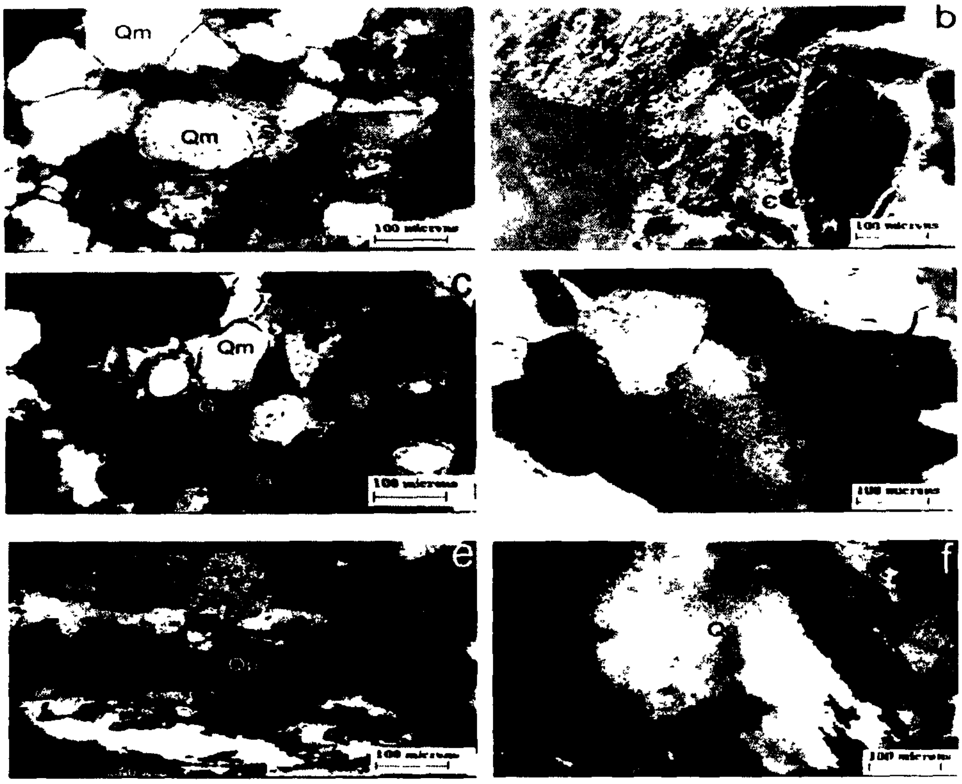

Fig.3 Photomicrographs of sandstones of the Chandarpur Group Chattisgarh basin, and the Tiratgarh Formation Indravati basin showing different types of mineral grains present Qm-monocrystalline quartz, Qp-pollycrystalline quartz K- K-feldspar, G-glauconite, S-silica overgrowth, C-calcite cement (a) Lohardih Formation, showing multicycle quartz grain floatinq in calcite cement (b) Lohardih Formation showing microcline replaced by calcite along twinning planes (c) Chopardih Formation showing multicycle quartz with well rounded glauconite (d) Kansapathar Formation showing advance stage of silica overgrowth (e) Tiratgarh Formation showing polycrystalline quartz grain with semicomposite crystals having sutured contacts (f) Tiratgarh Formation showing highly stretched polycrystalline quartz grain

Fig.3 Photomicrographs of sandstones of the Chandarpur Group, Chattisgarh basin, and the Tiratgarh Formation, Indravati basin, showing different types of mineral grains present. Qm-monocrystalline quartz, Qp-pollycrystalline quartz, K- K-feldspar, G-glauconite, S-silica overgrowth, C-calcite cement. (a) Lohardih Formation showing multicycle quartz grain floating in calcite cement (b) Lohardih Formation showing microcline replaced by calcite along twinning planes (c) Chopardih Formation showing multicycle quartz with well rounded glauconite, (d) Kansapathar Formation showing advance stage of silica overgrowth (e) Tiratgarh Formation showing polycrystalline quartz grain with semicomposite crystals having sutured contacts (f) Tiratgarh Formation showing highly stretched polycrystalline quartz grain.

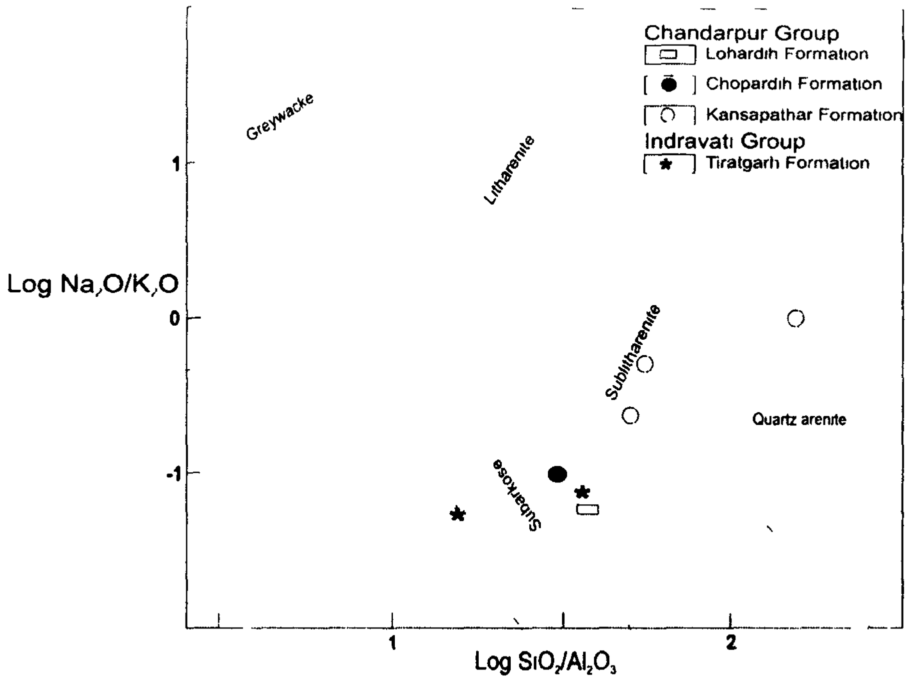

Fig.4 Geochemical classification of sandstones of the Chandarpur Group and the Tiratgarh Formation using log (Na_2O/K_2O) vs Log (SiO_2/Al_2O_3) (after Pettijohn *et al* 1973) The sandstones fall into the sublitharenite, subarkose and arenite fields

Fig 4 Geochemical classification of sandstones of the Chandarpur Group and the Tiratgarh Formation using Log (Na2O/K2O) vs Log (SiO2/Al2O3) (after Pettijohn et al 1973) The sandstones fall into sublitharenite subarkose and arenite fields

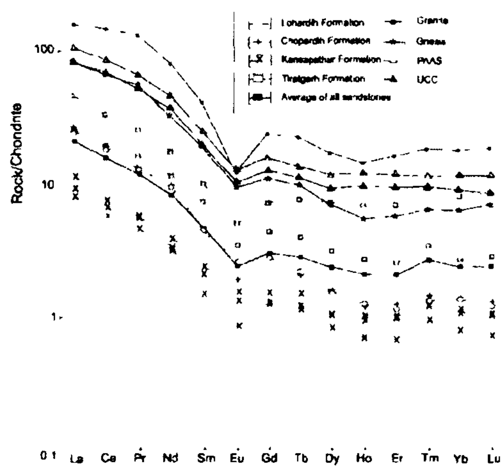

Fig 5 Chondrite normalized REE patterns for the sandstone samples of the Chandarpur Group and the Tiratgarh Formation compared with granite and gneiss of the Bastar craton (Mondal et al 2006), PAAS and UCC (Taylor & McLennan 1985)) Note that the REE patterns of sandstones are similar to the UCC, PAAS, and granite and gneiss of the Bastar craton.

Fig.5 Chondrite - normalized REE patterns for the sandstone samples of the Chandarpur Group and the Tiratgarh Formation, compared with granite and gneiss of the Bastar craton (Mondal et al. 2006), PAAS and UCC (Taylor & McLennan 1985). Note that the REE patterns of sandstones are similar to the UCC, PAAS, and granite and gneiss of the Bastar craton.

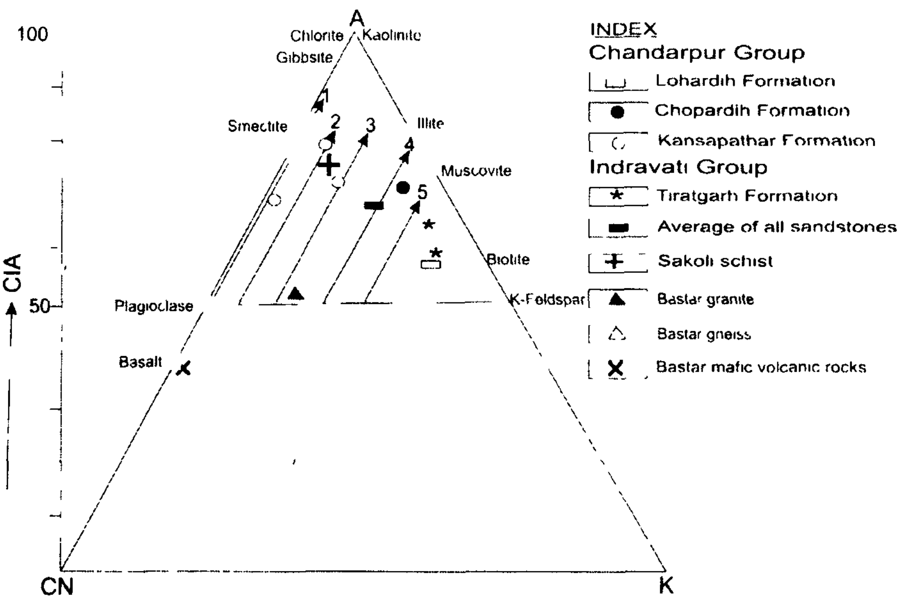

Fig.6 Al_2O_3-(CaO^*+Na_2O)-K_2O (A-CN-K) ternary plot, after Nesbitt and Young (1982) (CaO^* = CaO in silicate phase) showing sandstones of the Chandarpur Group and the Tiratgarh Formation The diagram also showing average compositions of different rock types of the Bastar craton. Sakoli schists from Shastri and Dekate (1984) granite and gneiss of the Bastar craton from Mondal *et al* (2006), mafic volcanic rocks of the Bastar craton from Srivastava *et al* (2004) Numbers 1-5 denote compositional trends of initial weathering profiles of different rocks 1-gabbro, 2-tonalite, 3-diorite, 4-granodiorite, 5-granite

Fig.6 Al2O3 - (CaO* + Na2O) - K2O (A - CN - K) ternary plot, after Nesbitt and Young (1982) (CaO* = CaO in silicate phase) showing sandstones of the Chandarpur Group and the Tiratgarh Formation. The diagram also shows average compositions of different rock types of the Bastar craton: Sakoli schists from Shastry and Dekate (1984); granite and gneiss of the Bastar craton from Mondal et al. (2006), mafic volcanic rocks of the Bastar craton from Srivasatava et al. (2004). Numbers 1-5 denote compositional trends of initial weathering profiles of different rocks. 1-gabbro; 2-tonalite; 3-diorite; 4-granodiorite; 5-granite.

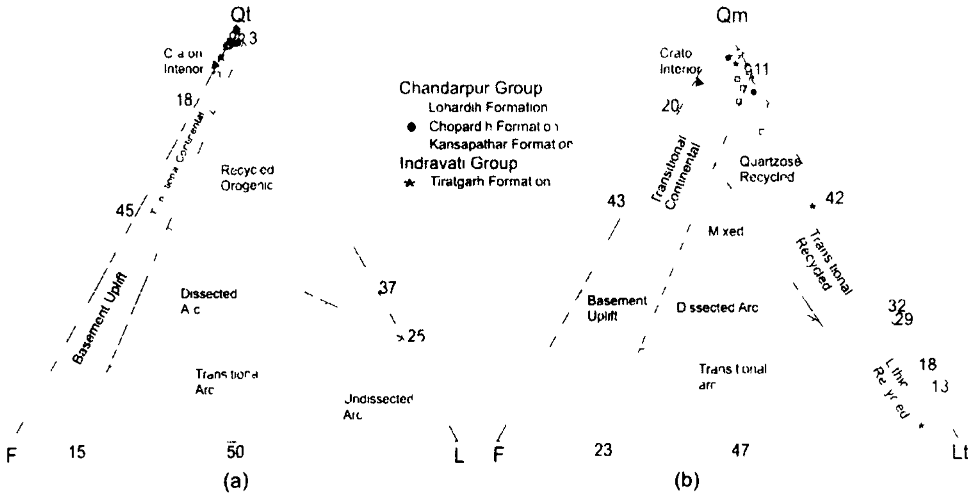

Fig 7 Provenance discriminant diagrams after Dickinson and Suczek (1979) of sandstone samples of the Chandarpur Group Chattisgarh basin and the Tiratgarh Formation Indravati basin of the Bastar craton

Fig.7 Provenance discriminant diagrams after Dickinson and Suczek (1979) of sandstone samples of the Chandarpur Group, Chattisgarh basin and the Tiratgarh Formation, Indravati basin of the Bastar craton.

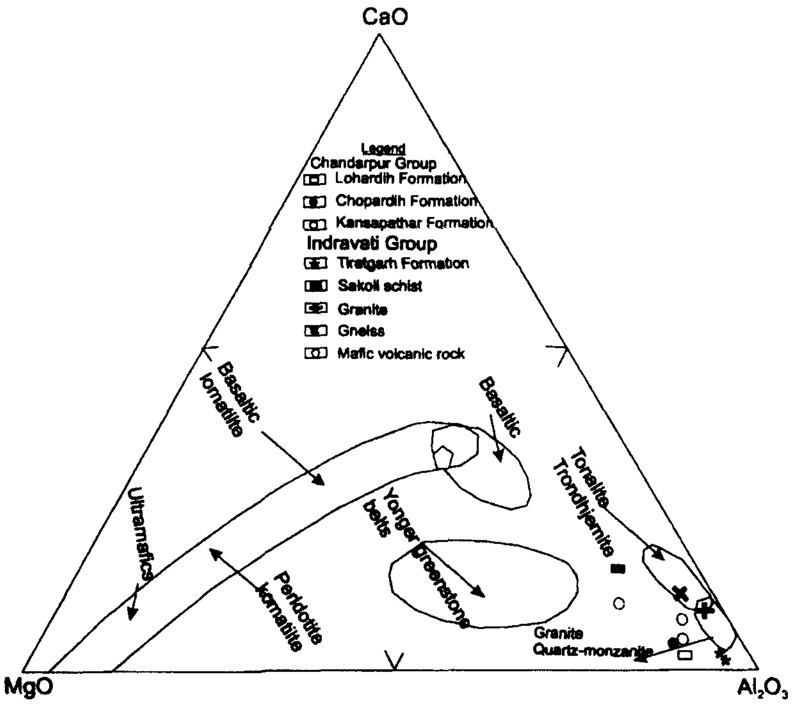

Fig.8 CaO - MgO - Al_2O_3 ternary ratio diagram showing the compositional characteristics of the sandstones of the Chandarpur Group and the Tiratgarh Formation.Different fields from Arora *et al.* (1994). Note that all the sandstone samples plot near granite quartz-monzanite field, and granite and gneiss of the Bastar craton, while average of the Sakoli schists plot near tonalite trondhjemite field. Data for the Sakoli schists from Shastry and Dekate (1984); granite and gneiss of the Bastar craton from Mondal *et al.* (2006); mafic volcanic rocks of the Bastar craton from Srivastava *et al.* (2004).

Fig.8 CaO - MgO - Al2O3 ternary ratio diagram showing the compositional characteristics of sandstones of the Chandarpur Group and the Tiratgarh Formation. Different fields from Arora et al. (1994). Note that all the sandstone samples plot near granite quartz-mozanite field, and granite and gneiss of the Bastar craton, while average of the Sakoli schists plot near tonalite trondhjemite field. Data for the Sakoli schists from Shastry and Dekate (1984); granite and gneiss of the Bastar craton from Mondal et al. (2006); mafic volcanic rocks of the Bastar craton from Srivasatava et al. (2004).

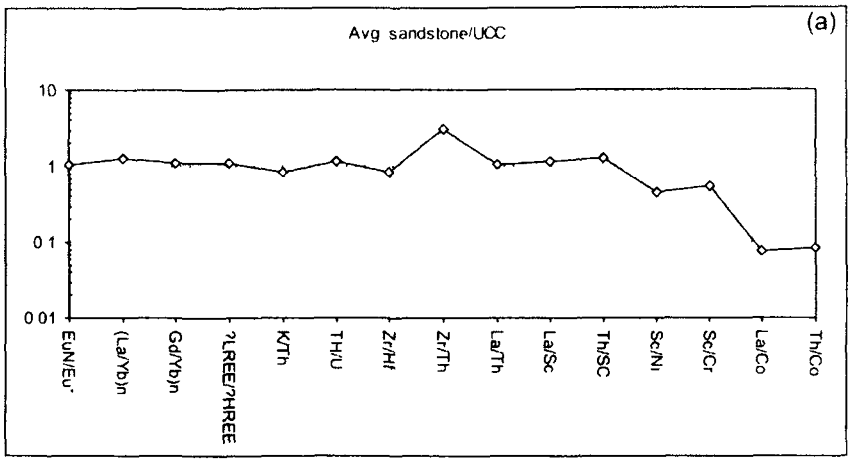

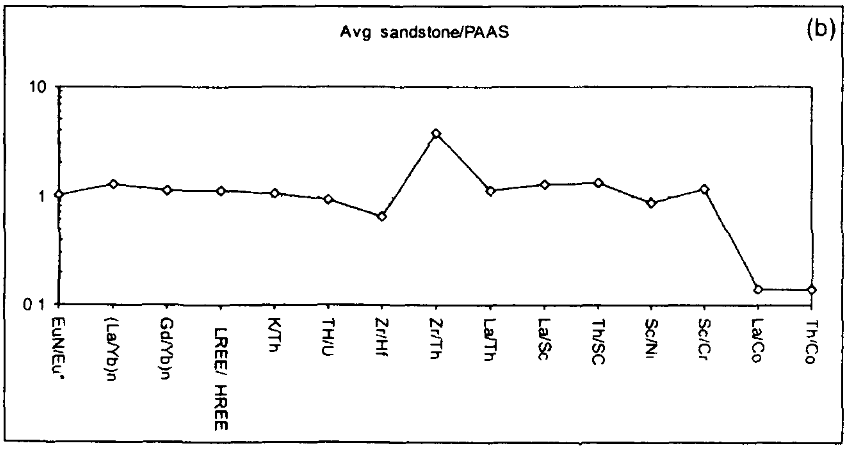

Fig. 9a & b The elemental ratios of sandstones of the Chandarpur Group and the Tiratgarh Formation are compared to those of the UCC and PAAS Note that most of the elemental ratios of sandstones are similar to PAAS and UCC

Fig 9a & b The elemental ratios of the sandstones of the Chandarpur Group and the Tiratgarh Formation are compared with those of the UCC and PAAS Note that most of the elemental ratios of sandstones are similar to PAAS and UCC

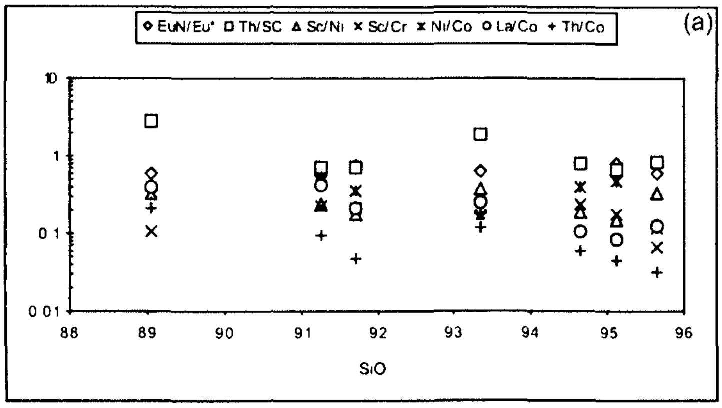

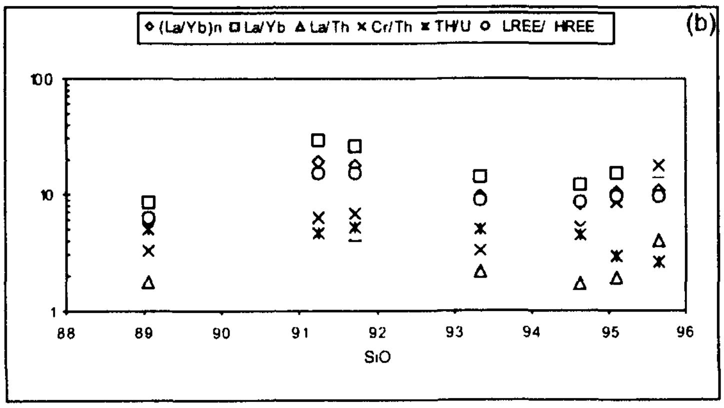

Fig 10 a & b Plots of SiO_2 vs. different important elemental ratios for sandstones of the Chandarpur Group and the Tiratgarh Formation. Note that most of the elemental ratios show almost flat trend with the increase of SiO_2 content

Fig.10a & b Plots of SiO2 vs. different important elemental ratios for sandstones of the Chandarpur Group and the Tiratgarh Formation. Note that most of the elemental ratios show almost flat trend with increase of SiO2 content.

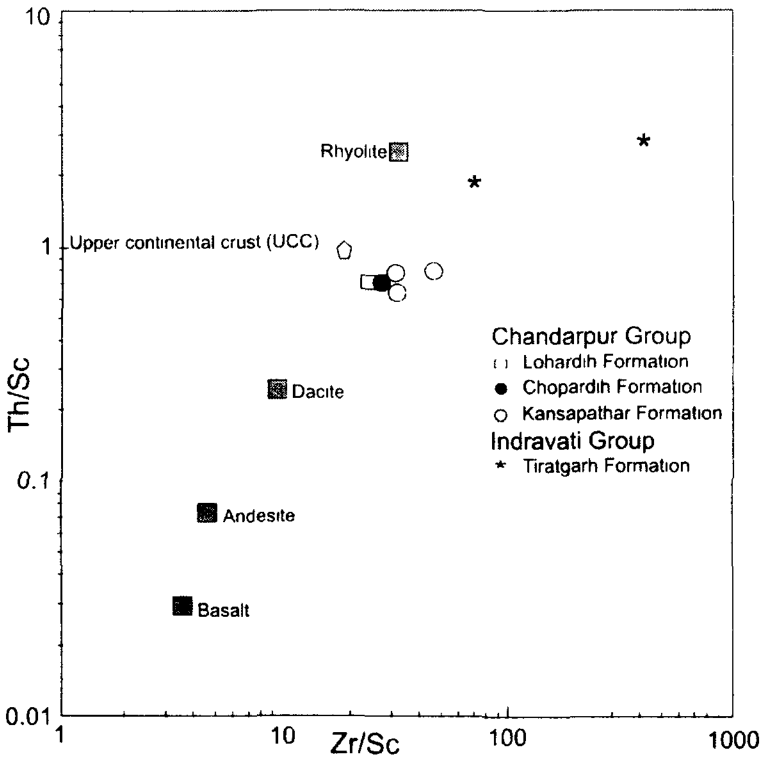

Fig.11 Th/Sc - Zr/Sc plot (McLennan *et al.* 1993) for the sandstones of the Chandarpur Group and the Tiratgarh Formation. Note that all the sandstone samples cluster around upper continental crust (UCC).

Fig.11 Th/Sc - Zr/SC plot (McLennan et al. 1993) for the sandstones of the Chandarpur Group and the Tiratgarh Formation. Note that all the sandstone samples cluster around upper continental crust (UCC).

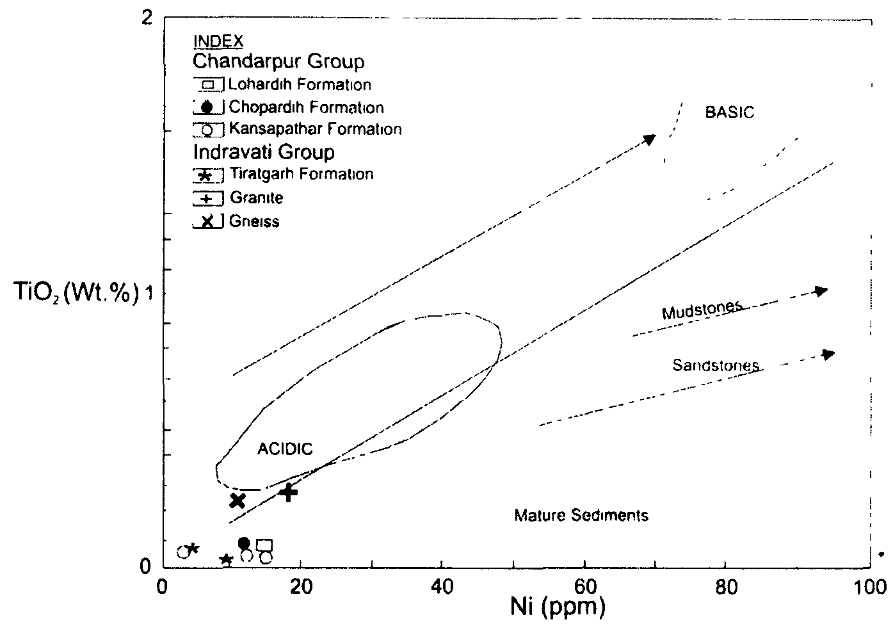

Fig.12 TiO_2 - Ni plot for the discrimination of source rocks of the sandstones of the Chandarpur Group and the Tiratgarh Formation The samples reflect a derivation from predominantly acidic precursors of magmatic origin and also fall very near to granite and gneiss of the Bastar craton Data for granite and gneiss from Mondal *et al.* (2006) Acidic and basic fields. and trends for common mature recycled sediments from Floyd *et al.* (1989).

Fig.12 TiO2 - Ni plot for the discrimination of source rocks of the sandstones of the Chandarpur Group and the Tiratgarh Formation. The samples reflect a derivation from predominantly acidic precursors of magmatic origin and also fall very near to granite and gneiss of the Bastar craton. Data for granite and gneiss from Mondal et al. (2006). Acidic and basic fields and trends from common mature recycled sediments from Floyd et al (1989).

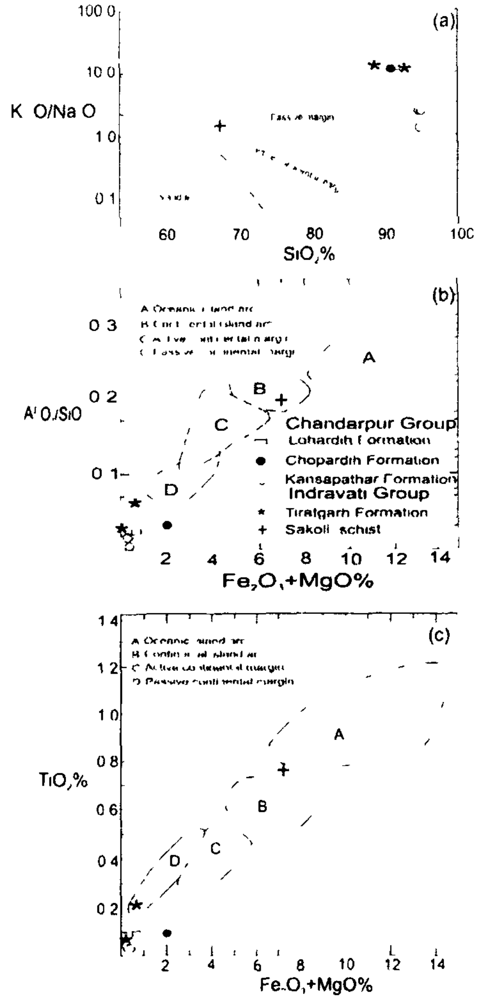

Fig 13 Tectonic setting discrimination diagrams for the sandstones of the Chandarpur Group and the Tiratgarh Formation Data for the Sakoli schists (after Shastry & Dekate 1984) have also been shown for comparison The tectonic settings are named in each plot (a) SiO_2 vs (K_2O/Na_2O) (after Roser & Korsch 1986) (b) $Fe_2O_3^*$+MgO vs Al_2O_3/SiO_2 (after Bhatia 1983) and (c) $Fe_2O_3^*$+MgO vs TiO_2 (after Bhatia 1983) ($Fe_2O_3^*$ = total iron)

Fig.13 Tectonic setting discrimination diagrams for the sandstones of the Chandarpur Group and the Tiratgarh Formation Data for the Sakoli schists (after Shastry & Dekate 1984) have also been shown for comparison The tectonic settings are named in each plot (a) SiO2 vs K2O/Na2O (after Roser & Korsch 1986), (b) Fe2O3*+ MgO vs Al2O3/SiO2 (after Bhatia 1983), and (c) Fe2O3*+ MgO vs TiO2 (after Bhatia 1983) (Fe2O3*= total iron)

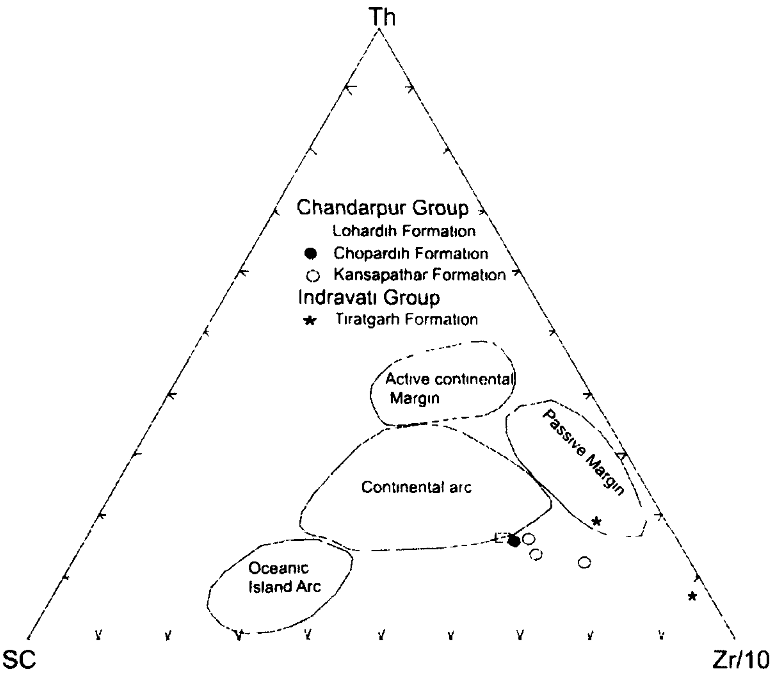

Fig.14 Th - Sc - Zr/10 plot for the sandstones of the Chandarpur Group and the Tiratgarh Formation for tectonic setting discrimination (Bhatia & Crook 1986). Note that all the sandstone samples plot near passive margin tectonic setting

Fig.14 Th - Sc - Zr/10 plot for the sandstones of the Chandarpur Group and the Tiratgarh Formation for tectonic setting discrimination (Bhatia & Crook 1986). Note that all the sandstone samples plot near passive margin tectonic setting.